STRUCTURE-PROPERTY STUDIES OF ION-CONTAINING POLYMERS

Richard Swee-Chye Yeo

B. Sc., Ngee Ann Technical College, Republic of Singapore

M. Sc., St. Francis Xavier University, Nova Scotia, Canada

A thesis submitted to the Faculty of Graduate Studies and Research in partial fulfilment of the requirements for the degree of Doctor of Philosophy

Department of Chemistry
McGill University
Montreal, Quebec
Canada, H3C 3G1

February, 1976

Ph. D. CHEMISTRY

Richard Swee-Chye Yeo

STRUCTURE-PROPERTY STUDIES OF ION-CONTAINING POLYMERS

Abstract

In an investigation of general structure-property relationships in ion-containing polymers, four materials differing in structure, position of ion, and type of ion were studied. The materials were "Nafion", dimethyl diallyl ammonium chloride, 3-acrylamido-3-methylbutyl trimethyl ammonium chloride and sodium-2-acrylamido-2-methylpropanesulfonate, but only "Nafion" was studied in great detail.

The ions in "Nafion", as in many other ionomers, are clustered. The glass transition temperature and water diffusion coefficient were all found to be unusual compared with other ionomers. Neutralization, absorbed water and degradation drastically influenced the mechanical properties of "Nafion".

The other three polymers were studied mostly in highly concentrated solution. The glass transition temperature strongly depends on the coulomb force of the ionic groups and is higher for the polyanionic materials than for the polycationic materials. The mechanical

properties and the glass transitions are greatly modified by plasticizers. In general, the properties of these materials show strong similarities to highly polar but non-ionic polymers.

RELATIONS ENTRE PROPRIETES ET STRUCTURE DE POLYMERES A IONS PIEGES

Résumé

Dans le cadre d'une recherche des relations générales entre les propriétés et la structure de polymères à ions piégés, nous avons étudié quatre échantillons différant par leur structure ainsi que par la nature et la position de l'ion dans le réseau de polymère. Ces échantillons sont le "Nafion", le chlorure de diméthyle diallyl ammonium, le chlorure de 3-acrylamido-3-méthylbutyle triméthyle ammonium et le 2-acrylamido-2-méthylpropanesulfonate de sodium. Cependant, notre étude a principalement porté sur le "Nafion".

Les ions dans le "Nafion", comme dans tout ionomère, se trouvent par agrégats. Nous trouvons que la température de transition vitreuse et le coefficient de diffusion de l'eau sont inhabituels comparés aux valeurs connues pour d'autres ionomères. La neutralisation, la dégradation et le contenu d'eau du "Nafion" influencent fortement ses propriétés mécaniques.

Nous avons étudié les trois autres polymères principalement en solution très concentrée. La température de transition vitreuse dépend fortement des forces de coulomb entre les groupes ioniques et est plus élevée pour les polyanions que pour les polycations. Les propriétés mécaniques et la température de transition vitreuse sont fortement modifiés par l'addition de plastifiants. En général les

propriétés de ces polymères montrent de grandes ressemblances avec les polymères fortement polaires mais non-ioniques.

To

My family

whose love, understanding, and encouragement
transformed work into play, and discovery to joy

TABLE OF CONTENTS

ACKNOWLEDGEMENTS

The author would like to express his appreciation and gratitude to Professor A. Eisenberg for his constant encouragement and counsel throughout the investigation and preparation of this thesis.

Thanks are also due to :

Professor E. A. Secco, the author's M. Sc. degree thesis supervisor, for initiating the author in the field of diffusion research which has been applied to part of this study.

Professor D. J. Simkin for his generous assistance and suggestions in the Mossbauer effect study.

Dr. R. St. John Manley of the Pulp and Paper Research Institute of Canada for use of the X-ray diffraction equipment. Mr. L. Marcotte for assistance with taking X-ray pictures.

The staffs of the Chemistry Department, Miss Renée Charron, Miss Patricia Dawson, Mrs. Barbara Macrotte, Mr. Roland Gamlin, Mr. Fred Kluck and Mr. Georges Kopp are particularly thanked in this regard.

Dr. Ian Hodge, Mr. Chong Seng Su, Mr. Pierre Tancrède and Mr. John Williams for the help they have given in preparing this thesis. Miss Shelley Katz and Mrs. Sandra Yip

for part of the drawing. Mrs. Elizabeth Wong for the typing. Mr. Kook Joe Shin for part of the measurements.

Dr. Toshiaki Takamatsu, Dr. H. Yoon, Mr. Jack Lobos, Mr. Hiroshi Matsuura, Mr. Teng Jiam Liak, Mr. Juei Mao Yang, Mr. John Williams and Mr. Ung-In Cho for their constant encouragement and helpful discussions.

Colleagues and friends who have been helpful in many ways.

McGill University, Defence Research Board and the National Research Council of Canada for financial assistance. E. I. du Pont de Nemours & Company who kindly supplied the materials.

Finally, I thank my wife and all the members in the family for their understanding and patience they have shown at all times.

LIST OF TABLES

LIST OF FIGURES

GLOSSARY OF SYMBOLS

a : line shape exponent

a_T : shift factor

erf : error function

erfc : error function complement, 1 - erf

f : stress

g : gravity constant

h : sample thickness

ierfc : intergral of error function complement

k : Boltzman's constant

l : sample length

n : positive integer

rff : recoilfree fraction

t : time

tanδ : loss tangent

t_r : reduced time

v : velocity

v_o : peak position (Mössbauer effect)

w : sample width

A_1 : amplitude of 1^{st} vibration

A_n : amplitude of n^{th} vibration

AMBTAC : 3-acrylamido-3-methylbutyl trimethylammonium chloride

AMPS : sodium 2-acrylamido-2-methylpropanesulfonate

B : shape factor

C_x : capacitance

D : diffusion coefficient

DMDAAC : dimethyl diallyl ammonium chloride

DSC : differential scanning calorimetry

E(t) : time-dependent Young's modulus

$E_r(t)$: reduced Young's modulus

E(10) : 10-second modulus

EG : ethylene glycol

EW : equivalent weight

G(t) : time-dependent shear modulus

G' : storage shear modulus

G" : loss shear modulus

GL : glycerine

G_x : conductance

$H(\tau)$: distribution of relaxation times

I : intensity

LVDT : linear variable differential transformer

M : moment of inertia

M_t : weight gain at time t

M_∞ : weight gain at equilibrium

"Nafion" : perfluorosulfonated membrane

PNaA : polysodium acrylate

R : universl gas constant

SAXS :	small angle x-ray scattering
T :	temperature
T_g :	glass transition temperature
T_o :	reference temperature
β :	assymetric factor
δ :	phase angle (mechanical or dielectric studies) isomer shift (Mossbauer effect)
μ :	numerical factor ($2.249 < \bar{\mu} > 5.333$)
ν :	frequency
ν_o :	natural frequency of the wire
σ :	compliance of force transducer
$\sigma(\nu)$:	absorption cross-section
σ_o :	maximum absorption cross-section
Δ :	logarithmic decrement (mechanical studies) quadrupole splitting (Mossbauer effect)
Δl :	deformation of sample
$\Delta\nu$:	line-width (mechanical studies)
ρ :	density at temperature T
ρ_o :	density at temperature T_o
τ :	time
π :	3.1416
Γ :	line-width (Mossbauer effect)
χ^2 :	chi square

GENERAL INTRODUCTION

An understanding of the relationships between bulk properties and molecular architecture is the major goal of polymer science research. Chemical modification of a polymer has been a powerful tool for making novel polymeric materials. Many varieties of organic ions can be incorporated into polymers, either as part of the backbone or on a side chain, imparting a wide range of properties to the resultant materials, which have been recently termed as ion-containing polymers or, in some cases, ionomers.

In recent studies on ion-containing polymers, two areas have received considerable attention. One is the field of polyelectrolyte solutions, which has yielded not only a very large number of publications, but also two monographs[1,2]. The other area comprises the solid state properties of ionomers, i.e. thermoplastic copolymers of non-ionics containing small amounts of ionic species. The latter have been the subject of several symposia[3-6], and two books[7,8]. Several additional families of materials have been explored, especially as they are related to industrial applications; e.g. membranes[9,10] and ion exchange resins[11]. By contrast, several areas of ion-containing polymers have received only scant attention. Among these may be mentioned the solid state properties of polyelectrolytes, where the high glass transitions make a thorough study very difficult[12]. Also, the organic ionomers which have been studied to date are based on materials which have a narrow range of dielectric constant or cohesive energy density values. They have similar structures and also similar ionic (e.g. carboxyl) groups placed on or near the backbone.

It was therefore of considerable interest to ascertain to what extent the properties of ion-containing polymers, either in highly concentrated solutions or in bulk, are a function of the type and structure of polymer and ion involved, or whether the fact that the polymers contain ions is of predominant importance. For this purpose, four polymers were selected, differing widely in structure and type of ion. These materials were "Nafion", dimethyl diallyl ammonium chloride, 3-acrylamido-3-methylbutyl trimethylammonium chloride and sodium 2-acrylamido-2-methylpropanesulfonate. (The chemical structures of these are presented later).

Due to the great interest in "Nafion", this material was investigated more extensively than the others, and is described in the first part of this thesis. The "Nafions" represents an excellent choice for investigation: the materials are based on completely fluorinated polymers, and also the ion is placed at the end of a rather long side chain. Furthermore, while most of the mechanical studies of copolymers have been performed on materials containing metal carboxylate ions, the "Nafions" contain the sulfonic acid group.

The results of the other three polymers are described in the second part of the thesis. In contrast to "Nafion", these three polymers contain high concentrations of ionic groups, and are water soluble. Also, the type of ions and the molecular environment of the ions in these polymers are totally different from one other.

REFERENCES

1. S. A. Rice and M. Nagasawa, "Polyelectrolyte Solutions", Academic Press, New York, (1961).
2. F. Oosawa, "Polyelectrolytes", Dekker, New York, (1971).
3. N. M. Bikales, ed., "Water-Soluble Polymers", Plenum Press, New York, (1973).
4. A. Rembaum, ed., "Polyelectrolytes and Their Applications", to be published.
5. A. Eisenberg, ed., "Ion-Containing Polymers", J. Polym. Sci., Polym. Symp., 45 (1974).
6. IUPAC 25th International Congress, Jerusalem, Israel, July, 1975.
7. L. Holliday, ed., "Ionic Polymers", Applied Sci. Publishers, London, (1975).
8. A. Eisenberg and M. King, "Physical Properties and Structures of Ion-Containing Polymers", Academic Press, (1977).
9. H. Z. Friedlander, "Membranes", Encycl. Polym. Sci. Tech., Vol. 8, pp. 620 (1968).
10. G. Eisenman, ed., "Membranes: A Series of Advances", Vol. 1, Dekker, New York, (1971).
11. J. A. Marinsky, ed., "Ion Exchange: A Series of Advances", Vols. 1 and 2, Dekker, New York, (1966-1969).
12. W. E. Fitzgerald and L. E. Nielsen, Proc. Roy. Soc., A282, 137 (1964).

PART ONE

PHYSICAL PROPERTIES AND SUPERMOLECULAR STRUCTURE OF "NAFION"

1. INTRODUCTION

An ideal structural material should strike a good balance between rigidity and toughness, a high softening temperature, high stability, satisfactory weatherability, good flame resistance, and easy processability. However, the more common plastic materials suffer serious deficiencies in some of these characteristics. To achieve the rigidity of conventional structural materials such as glasses and metals, the moduli of most organic polymers would have to be increased by a factor of about 10 to 100 times while the softening temperature would have to be increased to at least 300°C.

A new class of polymers known as ionomers fulfill some of these requirements much better than most normal polymers. Subtle structural changes involving the ionic nature of polymeric systems can produce profound physical and chemical property changes. Ionomers are also aptly described as "Thermoplastic-Thermoset Materials"[1] due to the fact that these polymers can not only be molded by conventional methods as can the thermoplastics, but they also achieve thermosetting properties. The applications of these materials continue to grow since they combine many of the best features of both thermoplastic and thermoset materials[2].

1.1 Previous Studies on Ionomers

A series of recent studies has been devoted to elucidating the effect of ions on the visoelastic properties and structures of ionomers[3-27]. The bulk of the evidence, from small angle x-ray scattering, water uptake, glass transition, rheological and mechanical measurements, suggests that at low ion concentration, the ions are present as multiplets,

acting as simple crosslinks, whereas above a critical ion concentration more extensive aggregation is encountered, leading to the formation of clusters which contain not only ionic material, but also a considerable portion of the organic polymer[4,6,25,27]. In general, these ionic clusters act as a reinforcing filler or crystallite, giving the sample some of the properties of phase separated systems such as are encountered in some block copolymers[28-30] or partly crystalline materials[31]. The ion concentration at the onset of clustering differs from material to material, occurring, for example, at < 1 mol% of ions in polyethylene[7,32], at ca. 5 mol% in polystyrene[15], at ca. 12-15 mol% in ethyl acrylate based materials[33,34], and not at all in the linear polyphosphates[24].

The physical properties of only very few ionic copolymers have been studied in some detail. Except for the polyphosphates, these are all hydrocarbon based materials and include polyethylene[3-11], polystyrene[12-17], polybutadiene[18-22], as well as some polar polymers containing low molecular weight salts[23]; the phenomena which arise due to the presence of ions are quite similar in all these materials.

It is completely beyond the scope of this introduction to review the literature on the physical properties of ionomers. Only a very brief summary will be given here, and only those properties which have a direct bearing on the present work will be summarized.

For most ionomers, it has been found that the glass transition temperature (as determined, for example, by DSC) increases with increasing ion content. At low concentrations, this increase is linear, but as the concentration increases through the clustering region, the rate of increase also rises[23,34]. Loss tangent measurements in the glass transition region generally reveal two peaks. At low ion concentrations this correlates with the DSC value of glass transition, but at high ion contents deviations may appear. Usually, the lower loss tangent peak is due to the glass transition of the ion-poor material, while the peak at higher temperatures is due to the ionic regions.

Stress relaxation studies of non-crystalline ionomers reveal that for systems which are clustered, time-temperature superposition fails, reflecting the existence of a secondary relaxation mechanism[35]. This secondary mechanism is associated with the clustered ionic regions. If the ions are present in low enough concentrations so that they do not cluster but act as multiplets (or crosslinks), no deviation from time-temperature superposition is observed.

In all the materials in which clustering of ions is encountered, this clustering also manifests itself as a small angle x-ray scattering peak. The Bragg distances involved are usually of the order of 50 Å, although smaller distances have been found in some systems.

1.2 Previous Studies on "Nafions"

"Nafion", a perfluorosulfonic acid membrane, was developed recently by du Pont[36].

1.2.1 Composition

This novel material is a copolymer of tetrafluoroethylene and a perfluoroethylenically unsaturated monomer containing a sulfonic acid group, and can be represented by:

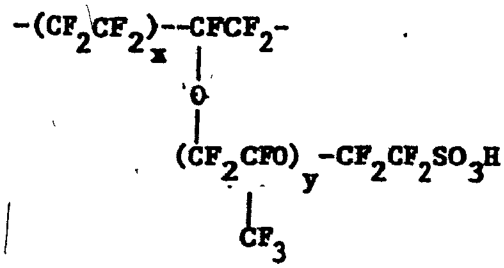

$x = 5 - 12 \qquad y = 1 - 3$

The method of synthesis is described in several U.S. patents[37–42]. "Nafion" is first prepared as a copolymer with the sulfonic acid group in some precursor form such as sulfonyl fluoride[37]. This is a remarkably stable product which can be fabricated easily into various forms. These sulfonyl fluoride groups can then be converted to the corresponding sulfonate salt by reacting the copolymer with aqueous base, such as NaOH, and to the acid form by reacting the salt with a strong inorganic acid such as H_2SO_4[39]. The salt and free acid forms are essentially infusible.

$$\text{Z-SO}_2\text{F} \xrightarrow{\text{NaOH}} \text{Z-SO}_3\text{Na} \xrightarrow{\text{H}_2\text{SO}_4} \text{Z-SO}_3\text{H}$$

Sulfonyl fluoride form	Na salt form	Free acid form

where Z represents the organic portion of the polymer.

1.2.2 Physical Properties

Since a number of physical properties relevant to the proposed commercial applications have been summarized recently[43-45], only those which are concerned with this work are presented below.

The copolymer composition is usually expressed in terms of equivalent weight, EW, which is defined as the weight of polymer in grams which will neutralize one equivalent of base. The equivalent weight of the polymer is solely determined by the ratio of the two monomers. Copolymers of commercial interest have equivalent weights in the range 1000 - 2000.

The swelling of "Nafion" is controlled by the ratio of the two monomers, in contrast to that of conventional ion exchange resins in which it depends on the degree of crosslinking. The higher the equivalent weight of "Nafion", i.e. the higher the TFE content, the less extensive the swelling will be. Generally, the polymers with an EW below 1000, become too weak for use in the swollen form (they may, in fact, be soluble) and those with an EW above 2000 have too few ionic groups. It has been suggested that[46] only the sulfonic acid group of "Nafion" shows an affinity for swelling agents such as water, the remainder of the polymer remaining inert to the swelling agent. The capacity of the polymer to absorb water is thus determined by the EW[43,45].

A reproducible absorptivity can result when "Nafion"-H is boiled for 30 minutes in water. Consequently, this treatment is considered as a standard for the purpose of comparison. The water absorbed under these conditions is called the "Standard Water Absorption". It is also reported[43,45] that the water absorptivity is decreased if the H^+

ions are exchanged for metal ions.

"Nafion" is expected to possess outstanding properties by virtue of its chemical structure. Apart from the desired hydrophilicity and reactivity of the sulfonic acid groups, the remainder of the polymer has the chemical inertness characteristic of fluorocarbon polymers containing no carbon-hydrogen bonds. It absorbs water rapidly even at room temperature, but the reinforced membrane swells only with small and predictable dimensional and rigidity changes. It is thus possible to combine good selectivity with low resistance to ion transportation, high physical strength and long service life by tailoring the polymer structure and by special techniques of fabricating and reinforcing the membrane.

1.2.3 Applications

As a result of its extraordinary properties, "Nafion" membranes have found application as unique, long-life separators in electrochemical[47-54] and chemical processes, such as the new "Chloromat" process, for producing sodium hypochlorite from salt water. "Nafion" is also used in place of the conventional asbestos in chlor-alkali diaphragm cells. Because of potential reductions in energy cost in other processes, "Nafion" membrane technology will also benefit other industrial processes. "Nafion" is viewed as a new electrochemical permselective barrier. In dialysis, it serves as a wettable, permselective reactor. Many other potential uses for "Nafion" are under development.

2. EXPERIMENTAL

Polymer samples were kindly supplied by Dr. W. Grot of E.I. Du Pont de Nemours & Company, in the form of 1.3 mm thick sheets, of equivalent weight of 1155 or 1365. Unless specified, all measurements were performed on the sample with an equivalent weight of 1365.

2.1 Sample Preparation

"Nafion"-Na, "Nafion"-K and "Nafion"-Li were prepared by immersing the "Nafion"-H in the appropriate hydroxide solution, and "Nafion"-Cs was prepared by immersing it in a CsCl solution. The "Nafion"-Fe used for the Mossbauer effect study was prepared by immersing "Nafion"-H in a $Fe_2(SO_4)_3$- H_2SO_4 (2:1) solution. H_2SO_4 was added in order to prevent the formation of hydroxide complexes.

2.2 Drying and Thermal Stability

A sample (ca. 1 gm.) which had been stored at ca. 40% relative humidity and which had absorbed ca. 6 wt% water (based on a method of determining the dry weight to be described below), was placed under vacuum at 25°C for several days until there was no further weight loss (<0.1 mg.), and its weight was determined. Subsequently, the same sample was replaced in the vacuum system, this time at a higher temperature, again for another few days until another constant weight has been reached. The procedure was repeated for temperatures up to 210°C for the acid form and 330°C for the potassium salt. The results are shown in Fig. 1, and will be described more fully below.

An inflection point is evident at ca. 170°C for the acid form; this point was taken as the optimum drying temperature since a sample of maximum modulus is obtained at this temperature (see Fig. 20 below). It is quite possible that some residual water remains in this sample, but no means were available for determining that amount. Subsequently, samples dried at 170°C for periods of over 24 hrs. will be referred to as "dry" samples. It is interesting to note that, below 170°C, water is absorbed and desorbed reversibly, while, above 170°C, the process is irreversible, possibly due to the inception of degradation.

For the salt samples, a drying temperature anywhere from 90°C to ca. 240°C yields identical results; all the salt samples were dried at their glass transition temperatures, T_g, for a period of 24 hrs. or more.

2.3 Water Diffusion

A sample of dry film, ca. 1 mm thick, was immersed in water in a constant-temperature bath. After a certain time, the sample was removed from the water, the surface dried, and the weight gain (M_t) was determined. The same sample was then replaced in the bath at the same temperature for a second time period, and the weight was re-determined. The procedure was repeated until there was no further weight gain; the total weight gain is referred to as the equilibrium sorption, M_∞. All the weighing procedures were done in less than 10 sec.

2.4 Glass Transition Temperature

The glass transition temperatures were measured by the following techniques.

2.4.1 Dynamic Mechanical Method

The T_g was determined by the tan δ maximum obtained on a free-

FIGURE 1.

Drying and thermal stability curves for

"Nafion"-H and "Nafion"-K.

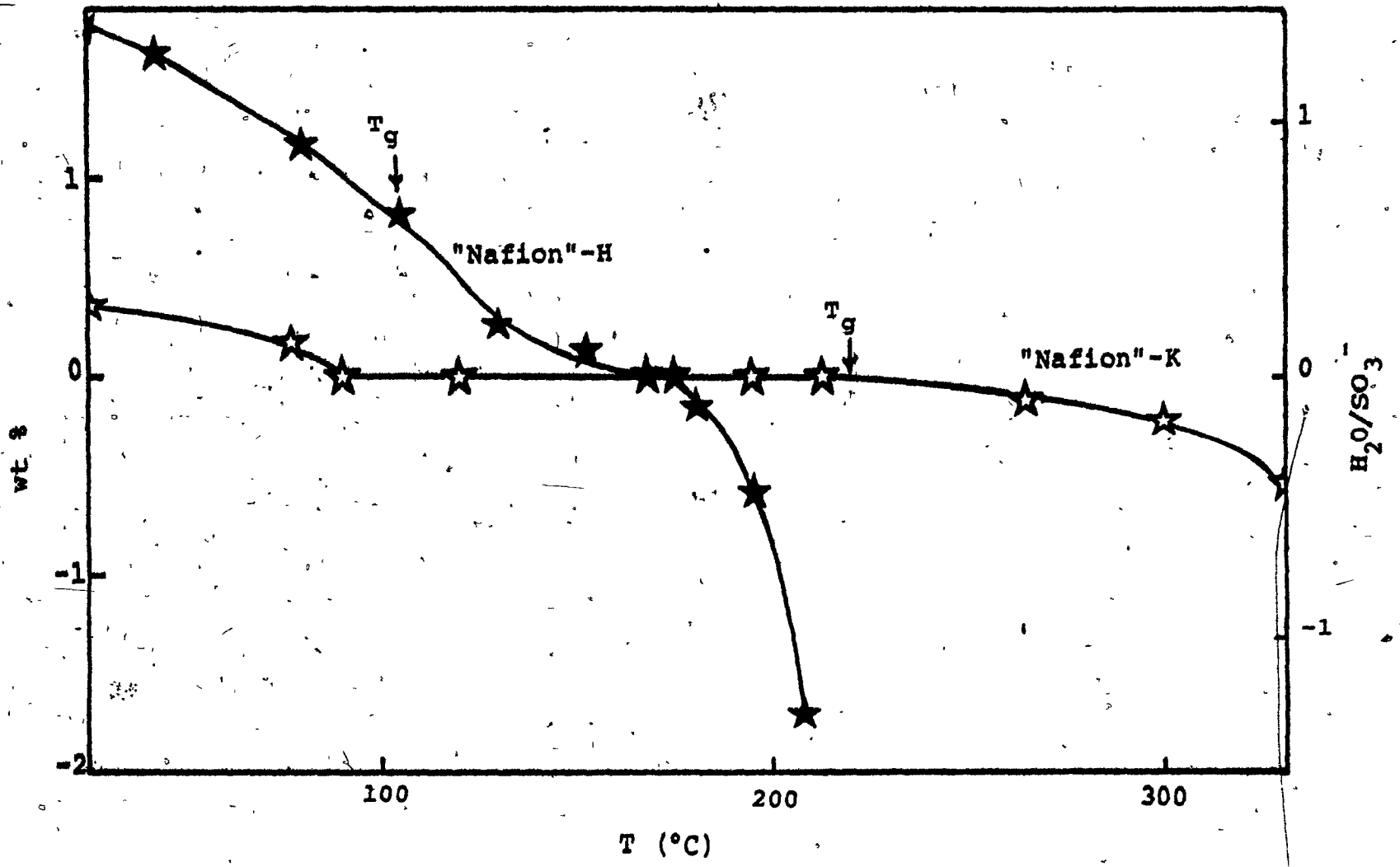
"Nafion"-H
"Nafion"-K
T_g
T_g
wt %
H_2O/SO_3
T (°C)
1
0
-1
-2
100
200
300

vibration torsional pendulum (to be described in Section 2.6.1) at a frequency of ca. 1 Hz. A heating rate of less than 1°C per min. was used.

2.4.2 Calorimetric Method

Calorimetric studies were performed by using a Perkin Elmer Differential Scanning Calorimetor (Model DSC-1), employing a heating rate of 10°C per min. The temperature at which the slope of the lines changed (as determined by the intersection of the extrapolated straight line segments) was taken as the position of the transition.

2.4.3 Dilatometric Method

The linear variable differential transformer (LVDT) method[55] was employed. The sample was placed in a quartz tube with a quartz rod resting on top of the sample. The outer tube was connected to the outer part of the LVDT, while the inner rod was connected to the core. By heating the sample, the core was moved relative to the transformer thus changing the electrical characteristics of the unit and allowing the measurement of the expansion of the sample with temperature by use of the appropriate electronics. A heating rate of ca. 1°C per min. was utilized. The expansion coefficients of the sample above and below T_g were measured. T_g was determined as described in Section 2.4.2.

2.5 Stress Relaxation

One of the most interesting features of high polymers is that a given polymer can display all the features of a glassy solid or an elastic rubber or a viscous liquid depending on the temperature and time (or frequency) scale of the measurement. Thus, polymers are usually described

as viscoelastic materials. They show creep under load and stress relaxation under strain.

The stress relaxometer used in this study is similar to that described previously[56]. The temperature variation during any one run was held below ± 0.1°C. The sample, of thickness 1.2 mm, was deformed to a fixed strain as rapidly as possible (in a stepwise fashion), and the stress decayed monotonically with time.

Rapid deformation will cause local heating in a sample, resulting in an increase in temperature[57]. Because of this drawback, the deformation of the sample was accomplished in a short time, generally 0.3 sec. Making use of the "factor of ten rule"[58], stress readings were taken only after 3 sec, thereby minimizing the effect of the finite deformation time. Most of the runs were done with ca. 4% deformation (in the region of non-linear viscoelasticity) because smaller deformations on such thin samples (1.2 mm) could not produce accurate data, due to the small forces involved.

In the strain region employed here, the deviations from linear viscoelasticity are very small. For example, log E values at 10 secs. for strains of 1.5% and 4.4% are 9.80 and 9.82. Furthermore, the shapes of the curves are identical, except for this small vertical shift. Since all the stress relaxation results were obtained using only a very small range of strains near ca. 4%, the data are believed to be internally self-consistent. As will be seen later, the small deviations from linear viscoelasticity are certainly not responsible for the failure of time-temperature superposition which is observed in some of the "Nafions".

Measurements of high modulus were made in the bending mode, while

those at lower moduli (below ca. 5×10^8 dyn/cm^2) were done in stretching, since bending measurements could not be made accurately in that region again due to the small forces produced. The sources of error in stress relaxation measurements have been treated by Cayrol[59].

The Young's modulus, E(t), can be calculated by the following formulae[60].

$$E(t) = g\ B\ f\ /\ (\Delta l - \sigma f)$$

where Δl is the deformation, f is the stress (in grams), σ is a correction factor for the compliance of the force transducer, g is the acceleration of gravity and B is the appropriate shape factor defined below.

For bending:

$$B = \frac{4\ l^3\ \beta^3\ (1 - \beta)}{w\ h^3}$$

where w and h are the width and thickness of the sample respectively;

$\beta = l_1/(l_1 + l_2)$, $l = l_1 + l_2$ and $l_1 < l_2$, where l_1 and l_2 are the distances between the point of deformation and the edges of the supporting clamp.

For stretching:

$$B = l/w\ h$$

where w and h are defined above and l is the distance between the clamps.

For samples for which the principle of time-temperature superposition of viscoelastic data is valid, master curves of reduced modulus versus reduced time can be prepared by shifting the curves of modulus versus time so that the overlap between successive curves is maximized[61]. The first shift is vertical (in modulus) with the next horizontal (in time).

Shifts are done according to the reduction parameters

$$E_r(t) = \frac{T_o \rho_o}{T \rho} E(t)$$

$$t_r = t/a_T$$

The reference point for the measurement of T_o and ρ_o is normally taken as T_g. a_T, the shift factor, is obtained by determining the horizontal shift between two successive curves, after the vertical reduction parameters have been applied.

In some ionomers, for cases where time-temperature superposition does not hold, the overlap is maximized in the short time region, so that pronounced deviations appear at long times[35]. This shifting procedure results in a pseudo master curve, rather than a true master curve. Modulus-temperature curves can be derived directly from stress relaxation data using the 10 sec modulus for each temperature. The distributions of relaxation times are calculated by the second approximation method of Schwarzl and Staverman[62].

$$H(\tau) = -\frac{dG(t)}{d(\ln t)} + \frac{d^2G(t)}{d(\ln t)^2}\Bigg|_{t=2\tau}$$

or in terms of log-log plots,

$$H(\tau) = -G(t)\{d \log G(t)/d \log t - (d \log G(t)/d \log t)^2 - (1/2.303\, d^2 \log G(t)/d(\log t)^2\}\Big|_{t=2\tau}$$

The computer program for the calculation is presented in Appendix I.

2.6 Dynamic Mechanical Studies

Since polymers are viscoelastic materials, stress and strain are not in phase in dynamic (oscillatory) mechanical measurement. Dynamic mechanical tests make it possible to calculate the real component of the elastic modulus, as well as the imaginary component which determines the dissipation of energy as heat. Furthermore, in dynamic tests the observed responses, especially damping, are much more sensitive to the polymer constitution than in step-function experiments, such as stress relaxation. Greater resolution is achieved at lower frequencies than at higher frequencies (a consequence of the different activation energies of the thermally active underlying mechanisms in the solid state: the lower activation energies are associated with the lower temperature damping peaks).

2.6.1 Infrasonic Frequency (0.1 - 3 Hz)

One of the most versatile and well-known techniques for making low frequency (infrasonic) dynamic mechanical measurements, especially over a wide temperature range, is the torsional pendulum. The one used in these studies has been described in detail elsewhere[59]. Heating rates were less than 1°C per min. to reduce thermo-hysteresis effects due to the poor heat conductivity of polymers.

A rectangular sample was clamped to a rigid supporting rod at the bottom end, and at the top end to the oscillating part of the apparatus, which consists of a torsional wire, an inertial system and a mobile rod. The sample was set into free torsional oscillations by an initial torsional displacement of low deformation (less than 2.5 deg/cm of specimen length). Therefore, the sample was under a sinusoidal strain

and it continued oscillating freely with a constant frequency, ν, and a gradually decreasing amplitude (i.e. a damped sine wave). The viscoelastic parameters can be calculated from the frequency and the amplitude decay of the damped sinusoidal oscillation as follows:

(i) shear storage modulus, G'

$$G' = \frac{4\pi^2 M}{B} \left(\nu^2 - \nu_o^2 + \frac{\nu^2 \Delta^2}{4\pi^2}\right)$$

where ν_o is the natural frequency of the supporting wire and inertial system without the sample, and M is the moment of inertia, B is the shape factor (defined below), and Δ is the logarithmic decrement (also defined below).

(ii) shear loss modulus, G"

$$G'' = \frac{4\pi M}{B} \nu^2$$

(iii) loss tangent, tan δ

$$\tan \delta = G''/G'$$

Δ is defined as $\Delta = 1/n \ln(A_1/A_n)$

where A_1 and A_n are the amplitudes of the 1^{st} and n^{th} oscillation. The shape factor for a torsion of bar with a rectangular cross-section is given by[61]

$$B = w h^3 \mu / 16 l$$

where μ is a numerical factor dependent on the ratio of the thickness to the width of the sample[63], and l, w, and h are the length, width and thickness of the sample, respectively.

2.6.2 Sonic Frequency (100 - 10,000 Hz)

For this frequency range, a vibrating reed was used. Since it will be described fully elsewhere[64], only a brief description is presented here.

Each polymer sample, previously cut into a small rectangular beam of approximate dimensions of 1.5 x 0.1 x 0.5 cm. was mounted vertically in the apparatus by a clamp at its upper end so that it was stressed as a cantilever. The polymer beam was vibrated by energizing a coil with a soft-iron core adjacent to a small iron clip attached to the free end of the specimen.

A complete treatment of the viscoelastic behaviour of the vibrating reed has been given by Bland and Lee[65]. The tan δ value can be calculated from the amplitude versus frequency plot, by using the following formula [66].

$$\tan \delta = \frac{\Delta \nu}{\sqrt{3}\, \nu_o}$$

where ν_o and $\Delta\nu$ are the resonance frequency and line-width at half maximum, respectively.

2.7 Dielectric Experiments

Dielectric measurements were carried out on a General Radio Precision Capacitance bridge (Type 1616) using a three-terminal cell of a type previously employed by McCammon and Work[67]. Measurements were made over the temperature range -190°C to ca. 150°C and at frequencies from 40 Hz to 10kHz. Heating rates of less than 1°C per min. were employed. Due to the ease of water desorption, three frequencies were measured in one single experiment to ensure the same experimental conditions at each frequency.

The dielectric polymer sample can be regarded as being electrically equivalent to a capacitance, C_x, in parallel with a resistance, R_x, at a given frequency. The dissipation factor, tan δ, of the sample is given directly from the bridge readings by measuring the disk capacitance, C_x and resistance, R_x. The relation is:

$$\tan \delta = \frac{1}{2\pi \nu C_x R_x}$$

where ν is the measured frequency.

2.8 Small Angle X-ray Scattering (SAXS)

X-ray diffraction patterns were obtained at room temperature using a Kiessig vacuum camera with Nickel-filtered CuK_α (1.54 Å) radiation (40kV, 20mA). The exposure times were of the order of 100 hr. The photographs were analysed with a Joyce, Loebl double-beam recording microdensitometer.

2.9 Mossbauer Effect Studies

Mossbauer effect spectra were taken at room temperature on a constant-acceleration spectrometer with a multichannel pulse-height analyzer. A 10 mC source of Co^{57} in Cu and a standard metallic iron absorber were obtained from New England Nuclear Corporation and National Bureau of Standard of U.S.A. respectively. The samples prepared have thickness of ca. 12 mg Fe^{57}/cm^2.

The data were recorded as counts per channel vs channel number (up to 512 in the present case). The latter was converted into a velocity

scale by determining the hyperfine structure of the standard metallic iron absorber (as described by Shechter et al[68]. Positive velocity corresponds to the source moving toward the absorber. The total number of counts accumulated per velocity point was $6-7 \times 10^5$. The reproducibility of the spectra was about ± 1 channel (or ± 0.0173 mm/sec).

The resulting spectra were analyzed using a computer program written by Professor D. C. Price, University of Manitoba. The program is a least-square fit to the generalized equation as follows:

$$\sigma\ (v) = \frac{\sigma_o}{1 + (\frac{v - v_o}{\Gamma})^{\alpha}}$$

where v_o and Γ are the peak position and line-width respectively, and α the line shape exponent with $\alpha = 2.0$ for Lorentzian shape. σ (v) and σ_o are the absorption cross-section and the maximum absorption cross-section respectively.

The value of χ^2 (the sum of the squares of the deviations from the fitted curve, divided by the variance of a single count) was used as a criterion for determining optimal fitting. For the fit to be acceptable, it was required that the value of χ^2 be between the 1 and 99% points of the χ^2 distribution; that is, between (ξ + 2.2 - 3.3 ξ) and (ξ + 2.2 + 3.3 ξ) approximately, where ξ, the number of degrees of freedom, is the number of channels used in fitting the spectrum, less the number of adjustable parameters in the fitted curve.

The Mossbauer parameters, namely isomer shift (distance between the center of the line or doublet to that of metallic iron), quadruple splitting (distance between peaks of the doublet), intensity and line-width (at half intensity) were evaluated totally by the computer program.

The peak area was then calculated as:

$$\text{Area} = (\pi/2) \times \Gamma \times I$$

where I is the intensity. The recoil-free fraction, in turn, was calculated by using the Area method[69].

It has been shown[70-75] that the isomer shift measures the electron density at the iron nucleus, and the quadrupole splitting arises from the interaction of the excited Fe^{57} nucleus with the electric field gradient about it.

3. RESULTS

3.1 Desorption of Water and Thermal Stability

Figure 1 shows the desorption of water with increasing temperature presented both as the number of water molecules per sulfonic group (H_2O/SO_3H), and as wt%. For the sake of comparison, the weight loss in the degradation region is also described in the same terms. These plots are discussed in Section 2.2. It is evident that the incorporation of ions into the polymer improves its thermal stability.

Some features of the degradation process are noteworthy: When "Nafion"-H is heated above 170°C, i.e. when degradation commences, HF is evolved. This is indicated by the fact that a glass holder in contact with "Nafion"-H during degradation turns cloudy; if a steel holder is used instead, it is also corroded. Natural "Nafion"-H is transparent and slightly yellow. It turns white if it is bleached by either H_2O_2 or HNO_3. It becomes black when the absorbed water is completely lost and degradation starts, but it turns white again after 7 wt% degradation. Furthermore, the "Standard Water Absorption"[43] goes down drastically as the sample is degraded: A 10 wt% degraded sample can absorb only 2 wt% of water while the undegraded sample can absorbed 24 wt% of water. Some of these facts suggest that the ionic groups of "Nafion"-H are destroyed during degradation.

3.2 Diffusion of Water

The diffusion equation of interest in this case is one in which an infinite sheet of material of uniform thickness. It is bathed in an atmosphere containing the diffusant. For the case of a lamina over a

short time period, the solution to the problem is given by Crank[76,77] as:

$$\frac{M_t}{M_\infty} = 4\left(\frac{Dt}{h^2}\right)^{\frac{1}{2}}\left\{\pi^{-\frac{1}{2}} + 2\sum_{n=0}^{\infty}(-1)^n \text{ ierfc}\frac{nh}{2(Dt)^{\frac{1}{2}}}\right\}$$

where D = diffusion coefficient

M_t = amount of diffusant taken up by the sheet at time, t

M_∞ = amount of diffusant taken up by the sheet at equilibrium

$\text{ierfc } x = \int_x^\infty \text{erfc } y \, dy = \pi^{-\frac{1}{2}} \exp(-x^2) - x \text{ erfc } x$

$\text{erfc } x = 1 - \text{erf } x$ = error function complement

$\text{erf } x = 2\pi^{-\frac{1}{2}} \int_0^x \exp(-y^2)\, dy$ = error function

n = positive integer.

Fig. 2 shows the typical sorption curves at several temperatures. The linearity of the plots below $M_t/M_\infty = \frac{1}{2}$ suggests that the diffusion is Fickian and that a constant diffusion coefficient is operative. The values of D were calculated from the initial slope of the plots, i.e. by setting the second term in the bracket equal to zero[78]. The induction time is estimated to be 3 sec.

Fig. 3 shows a plot of log D vs 1/T. The behaviour is of the Arrhenius type, leading to an expression:

$$D = 6.0 \times 10^{-3} \exp(-4.8 \text{ kcal/RT}) \text{ cm}^2\text{sec}^{-1}$$

3.3 Glass Transition and Dilatometry

Table 1 shows the glass transition temperatures of "Nafions" with different counterions, and also that of polytetrafluoroethylene (PTFE)[79] for comparison. The β peak positions, which are also listed, will be described below. The incorporation of ions into the polymer extends the glassy state to a higher temperature. Except for lithium, the increase in glass transition temperature is inversely proportional to the ionic size. The addition of 3 H_2O/SO_3H has a negligible effect on the glass transition of the acid sample.

Fig. 4 shows a linear dilatometric measurement for "Nafion"-H. The T_g was determined to be 122 ± 11°C from a series of 4 measurements.

3.4 Stress Relaxation

3.4.1 Acid and Salts

The results of the stress relaxation runs are shown in Figs. 5, 6,7 and 9 in which the master curves were plotted with $T = T_g$ as the reference temperature. Fig. 5 also shows the stress relaxation master curves for styrene and for two styrene ionomers[15] for the sake of comparison. The latter are labelled by giving the mol% of methacrylic acid followed by letters in parentheses indicating the counterions followed by a letter indicating the molecular weight range.

3.4.2 Effect of Water

In contrast to the behaviour of the thermorheologically simple dry acid, seen in Fig. 5, time-temperature superposition breaks down with the addition of 0.5 H_2O/SO_3H as shown in Fig. 6. Since the overlap was maximized in the short time region, pronounced deviations appeared

TABLE I

GLASS TRANSITION (α) AND (β) DISPERSION DETERMINED BY VARIOUS TECHNIQUES

	Dynamic Studies (ca. 1 Hz)		Calorimetric Studies		Dilatometric Studies
	T_α (°C)	T_β (°C)	T_α (°C)	T_β (°C)	T_α (°C)
PTFE[79]	ca. 127	18 to 53			
"Nafion"-H (0 H_2O/SO_3H)	111	23	104 ± 1		122 ± 11
(3 H_2O/SO_3H)	109	-62			
"Nafion"-Cs	211	160	212 ± 15	116	
"Nafion"-K	225	150	213 ± 20	109 ± 22	
"Nafion"-Na	235	140	238 ± 25	132 ± 15	
"Nafion"-Li	217	147	212 ± 18	120 ± 9	

at long times. This shifting procedure results in a pseudo master curve, rather than a true master curve which was obtained for the dry acid. It can be seen that the rate of stress relaxation is enhanced by the presence of water. This contrasts with the behaviour of an ethylene ionomer containing 8% acidic groups (47% of which were neutralized with Na)[80], for which water slowed down the rate of stress decay.

3.4.3 Effect of Neutralization

Fig. 7 shows the stress relaxation data of "Nafion"-K (100% neutralized). It is evident that below 180°C, time-temperature superposition is not applicable, whereas above 180°C, it is re-established. Some other features are noteworthy: The stress relaxation is slowed down by neutralization, so that a broadening in the distribution of relaxation times results, as shown in Fig. 8. Again, data for styrene and a styrene ionomer[15] are shown for comparison. The rubbery region for the "Nafion"-K is more pronounced than that in "Nafion"-H. Distinct viscous flow is observed at high temperatures.

3.4.4 Effect on Degradation

Fig. 9 shows the stress relaxation data of the degraded "Nafion"-H, while Fig. 10 compares the master curves for a degraded and an un-degraded sample. The glassy modulus decreases after degradation whereas that in the rubbery region increases, revealing a conversion from a plastic-like material to a more rubber-like one as degradation takes place. Possibly some crosslinking also occurs with increasing degradation, and time-temperature superposition remains applicable. An inflection point is observed at log E' equal to about 7.5 indicating some type of

crosslink structure in the polymer.

The most significant change observed in the master curve is the decrease in the slope of the transition region as a result of degradation. These results are similar to those for plasticized poly (vinyl chloride)[81] in which micro-crystalline regions were found to be important.

3.5 Modulus-Temperature Curves

The simplest way of characterizing the elastic properties of a polymer is to measure its elastic modulus as a function of temperature. Since polymers are viscoelastic, even at low stress levels, the mechanical behavior of polymers is often time dependent. Therefore, in summarizing behavior over a wide range of temperatures, it is convenient to use a standardized test and to report the behavior at a definite time, say 10 seconds. The 10 sec. modulus is plotted vs temperature in Fig. 11 for both the acid and the potassium salt. Curves for styrene and two styrene ionomers[15] are also shown for the sake of comparison. Arrows indicate the glass transition for each material.

3.6 Dynamic Mechanical Studies

3.6.1 Acid and Salts

Figs. 12 - 15 present the loss tangent over the temperature range of -150°C to ca. 250°C for the dry acid and the salts at ca. 1 Hz. It is clear that three relaxation regions are discernible for all the undegraded samples studied. They are labeled as α, β and γ relaxations in order of decreasing peak temperatures. The α relaxation is characterized by tan δ values in the range of 0.5 to 0.6. The β region

manifests itself as a shoulder or a small peak with tan δ values of 0.03 to 0.06 above background (shown also after subtraction from background as a dashed line). The γ region occurs at the same temperature as that of poly(tetrafluoroethylene).

3.6.2 Effect of Water

Fig. 16 shows the loss tangent (at ca. 1 Hz) for "Nafion"-H with various water contents as a function of temperature in the β and γ regions; the β peak, as can be seen, shifts to lower temperatures with the addition of water, and finally merges with the γ peak. For three of the samples, the shear storage and loss moduli, G' and G", are shown in Fig. 17. It can be seen that G' decreases as the water content increases.

3.6.3 Effect of Degradation

In Fig. 18, the loss tangent of "Nafion"-H with different degrees of degradation (defined as % weight loss) is plotted as a function of temperature. It is evident that the β peak is not present in the degraded samples. The shear storage and loss moduli are shown in Fig. 19. The storage modulus decreases as degradation increases.

Fig. 20 shows the storage modulus at 0°C determined at ca. 1 Hz, for samples with differing water contents and various degrees of degradation. It can be seen that G' increases with decreasing water content, and that a maximum G' value is reached as all the water is removed. Beyond this point, G' decreases again as a result of degradation. The position of this maximum was taken as an indication of dryness.

3.6.4 Effect of Counterions

In the presence of water the β dispersion, which in the salt is usually present as a shoulder, becomes a peak (tan $\delta \approx 0.1$) which moves

to lower temperatures with increasing water content. Eventually (at ca. 3 H_2O/SO_3^-) the β peak merges with the γ peak to yield a single dispersion. This is illustrated in Figs. 21 and 22 for the "Nafion"-Li and "Nafion"-Na respectively. The positions of the β peaks at ca. 1 Hz for the dry polymers are also listed in Table 1. Fig. 23 compares the γ relaxation of the dry "Nafion" with different counterions. It is clear that the peak height is inversely proportional to the cation size, except for the acid.

A plot of log ν vs 1/T for the γ peak of "Nafion"-H and PTFE is shown in Fig. 24. The activation energy for "Nafion"-H evaluated from this plot is ca. 13 kcal/mole, and is close to the value for PTFE. The dashed line (for PTFE) was drawn by McCrum[79] for the data from references 82, 83 and 84; only the points of Sauer et al[83] and Schmieder et al[84] are not consistent with that line.

3.7 Dielectric Studies

Figs. 25 - 30 present the dielectric results of "Nafion"-H with various water contents at frequencies of 100 Hz, 1kHz and 10kHz. A major peak with a minor peak adjacent to it are observed in the β relaxation region, while the γ relaxation is dielectrically inactive, as expected. The α relaxation is difficult to observe due to the fast desorption rate of water above room temperature. The β relaxation region at 100 Hz as a function of water content is shown in Fig. 31. It can be seen that the β relaxation shifts to lower temperatures as the water content increases. For water contents less than 1.7 H_2O/SO_3H, the minor peak appears at temperatures lower than the major peak while above 1.7 H_2O/SO_3H water content, the reverse occurs. The variation

of the major dielectric peak positions with water content, and the corresponding variation of the mechanical peak positions, are summarized in Fig. 32.

Fig. 33 shows log ν vs 1/T plots for the major peaks, for varying water contents. The minor peak is not well separated from the major peak in the region of 0.7 to 2.1 H_2O/SO_3H. The activation energies are given in Table 2.

Figs. 34 - 35 show the dielectric results of "Nafion"-K with various water contents at frequencies of 100 Hz, 1kHz and 10kHz, while the loss tangent at 100 Hz as a function of water content is shown in Fig. 36. Again, the β relaxation shifts to lower temperature as the water content increases.

3.8 Small Angle X-ray Scattering Studies

Several diffuse halos were seen in the range $1^\circ<2\theta<40^\circ$. The results are listed in Table 3, along with those for styrene and several styrene ionomers[17] for comparison. No evidence of crystallinity was found.

3.9 Mossbauer Effect Studies

Mossbauer effect spectra of the ferric salt of "Nafion" of two different equivalent weights are shown in Figs. 37 and 38. The parameters of the Mossbauer spectra obtained are summarized in Table 4. The isomer shifts given are relative to metallic iron. It is clear that the isomer shifts are the same for both equivalent weights. The experimental data are well fitted by a broad singlet peak. Nevertheless,

TABLE 2

ACTIVATION ENERGY OF DIELECTRIC RELAXATION FOR "NAFION"-H

Water Content (H_2O/SO_3H)	E_a, Major Peak (Kcal/mole)	E_a, Minor Peak (Kcal/mole)
0.4	25.4	
0.7	27.7	ca. 16
1.4	25.0	ca. 16
1.7	ca. 26	
3.0	25.3	16.2
4.1	29.6	14.9
15.0	22.7	

a doublet gave a better fit to the experimental points (Fig. 39) for an equivalent weight of 1365, though the quadrupole splitting is rather small (which is characteristic of distorted Fe^{3+} ion).

For both equivalent weights, the peak area, and therefore recoil-free fraction as well, are the same, but the height and linewidth differ somewhat. The observed linewidths are considerably greater than the natural linewidth of 0.19 mm/sec.

TABLE 3

X-RAY DIFFRACTION DATA FOR "NAFION"-H, "NAFION"-Cs, POLYSTYRENE AND THREE STYRENE IONOMERS

Samples	Bragg angle (2θ)		
"Nafion"-Cs	1°43'	9°16'	32°20'
"Nafion"-H (Dried)	3°9'(a)	9°26'	
"Nafion"-H (degraded)		9°22'	27°48'
Polystyrene		9°32'	18°38'
PS 3.8 (Cs)h	4°40'	9°32'	18°38'
PS 7.9 (Cs)l	1°28'	9°32'	18°38'
PS 9.7 (Cs)h	1°34'	9°32'	18°38'

(a) This value is in close agreement with the one communicated to Dr. A. Eisenberg privately by Dr. W. Grot of Du Pont.

TABLE 4

MÖSSBAUER PARAMETERS OF NAFION-FE

EW — 1155

	δ (mm/sec)	Δ (mm/sec)	Γ (mm/sec)	I (%)	rff
Singlet (Lorentzian)	0.444		1.34	1.02	0.06
Singlet (a — 1.57)	0.444		1.34	1.17	0.07
Doublet (Lorentzian)	0.436	0.017	1.30	0.51	0.06

EW — 1365

Singlet (Lorentzian)	0.447		0.98	1.32	0.06
Singlet (a — 2.12)	0.448		0.99	1.29	0.06
Doublet (Lorentzian)	0.449	0.381	0.70	0.78	0.05
Doublet (Assymmetric)	0.416	0.367	0.60 0.83	0.63 0.91	0.05

FIGURE 2.

Water sorption curves of "Nafion"-H (EW = 1155).

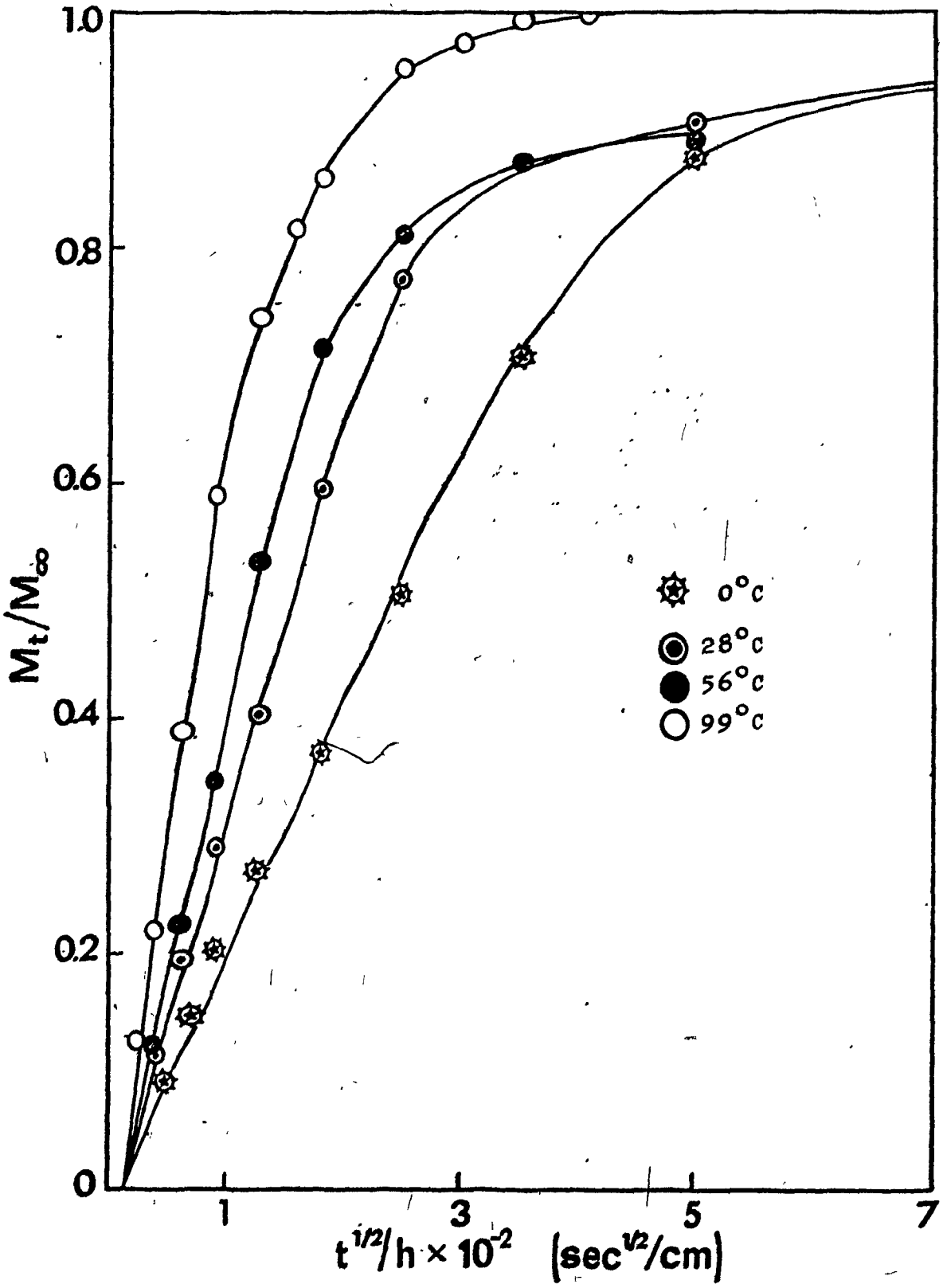
1.0
0.8
0.6
0.4
0.2
0
M_t/M_∞
0°c
28°c
56°c
99°c
1
3
5
7
$t^{1/2}/h \times 10^{-2}$ (sec$^{1/2}$/cm)

FIGURE 3.

Plot of log D vs. 1/T for "Nafion"-H (EW = 1155).

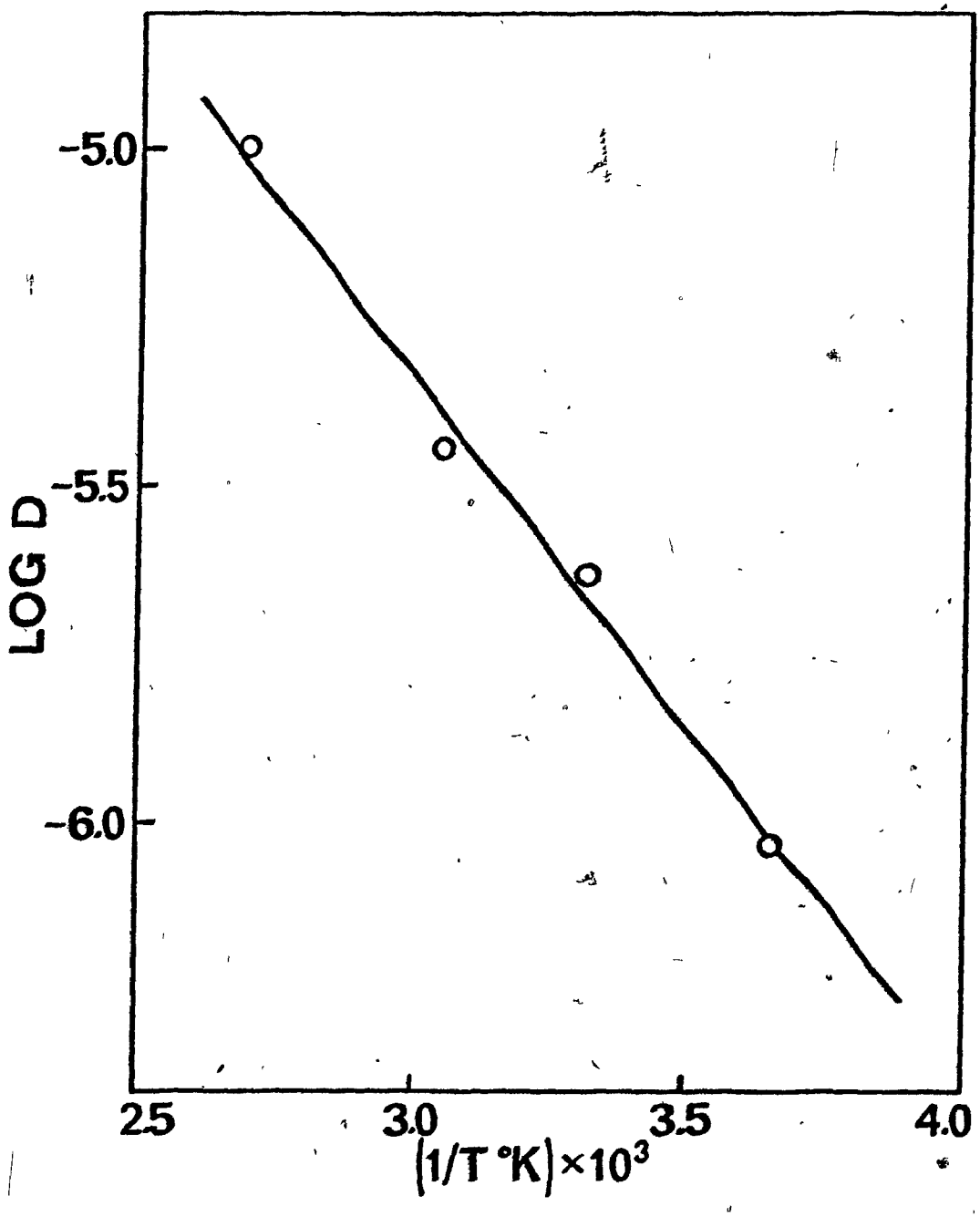
-5.0
-5.5
-6.0
LOG D
2.5
3.0
3.5
4.0
(1/T °K) × 10³

FIGURE 4.

Linear expansion coefficient as a function of temperature for "Nafion"-H.

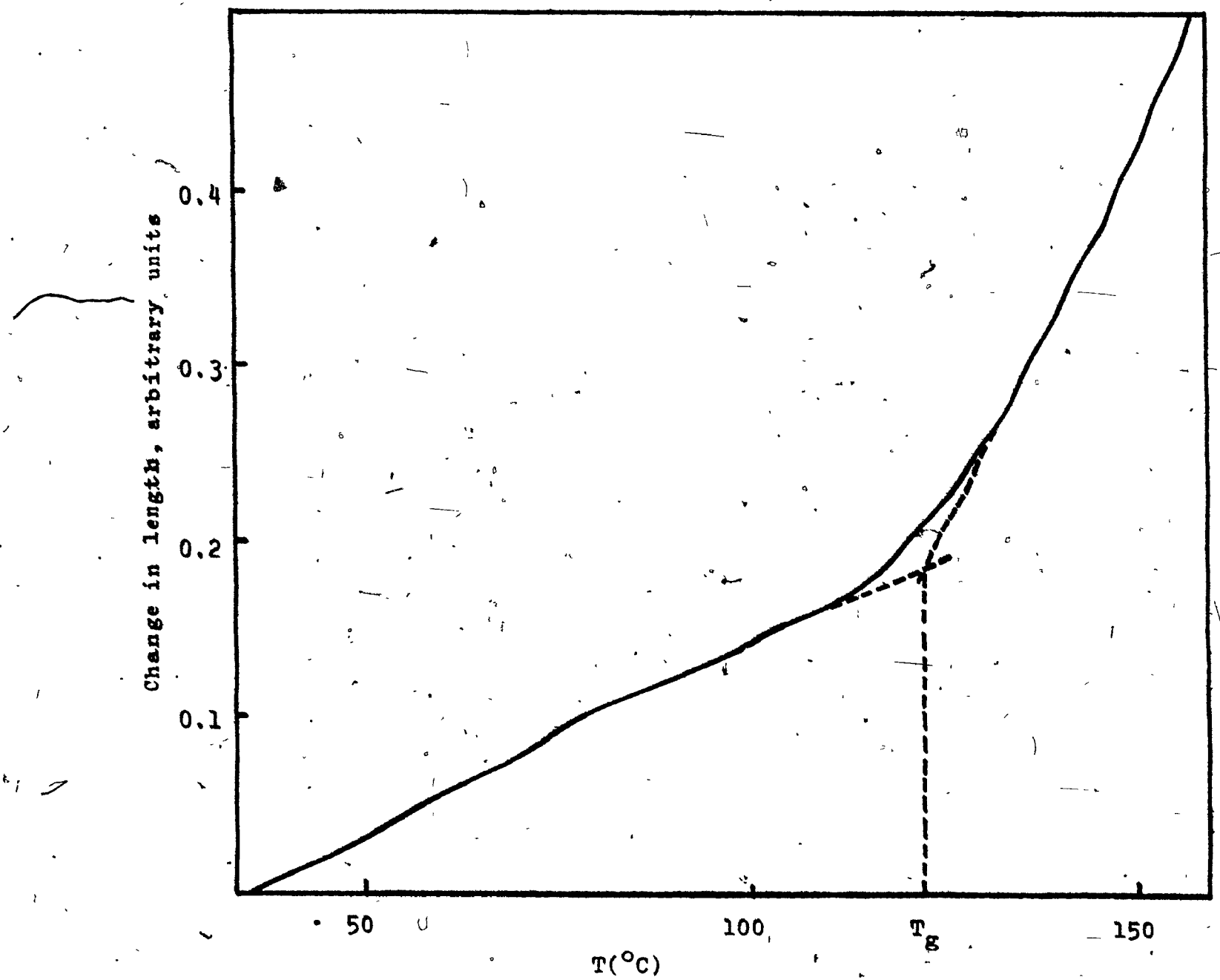
Change in length, arbitrary units
0.4
0.3
0.2
0.1
50
100
T_g
150
T(°C)

FIGURE 5.

Original stress relaxation curves and master curve for "Nafion"-H as well as master curves for polystyrene PS and two styrene ionomers PS 3.8 (Na)h, and PS 7.9 (Na)ℓ. $T_o = T_g$.

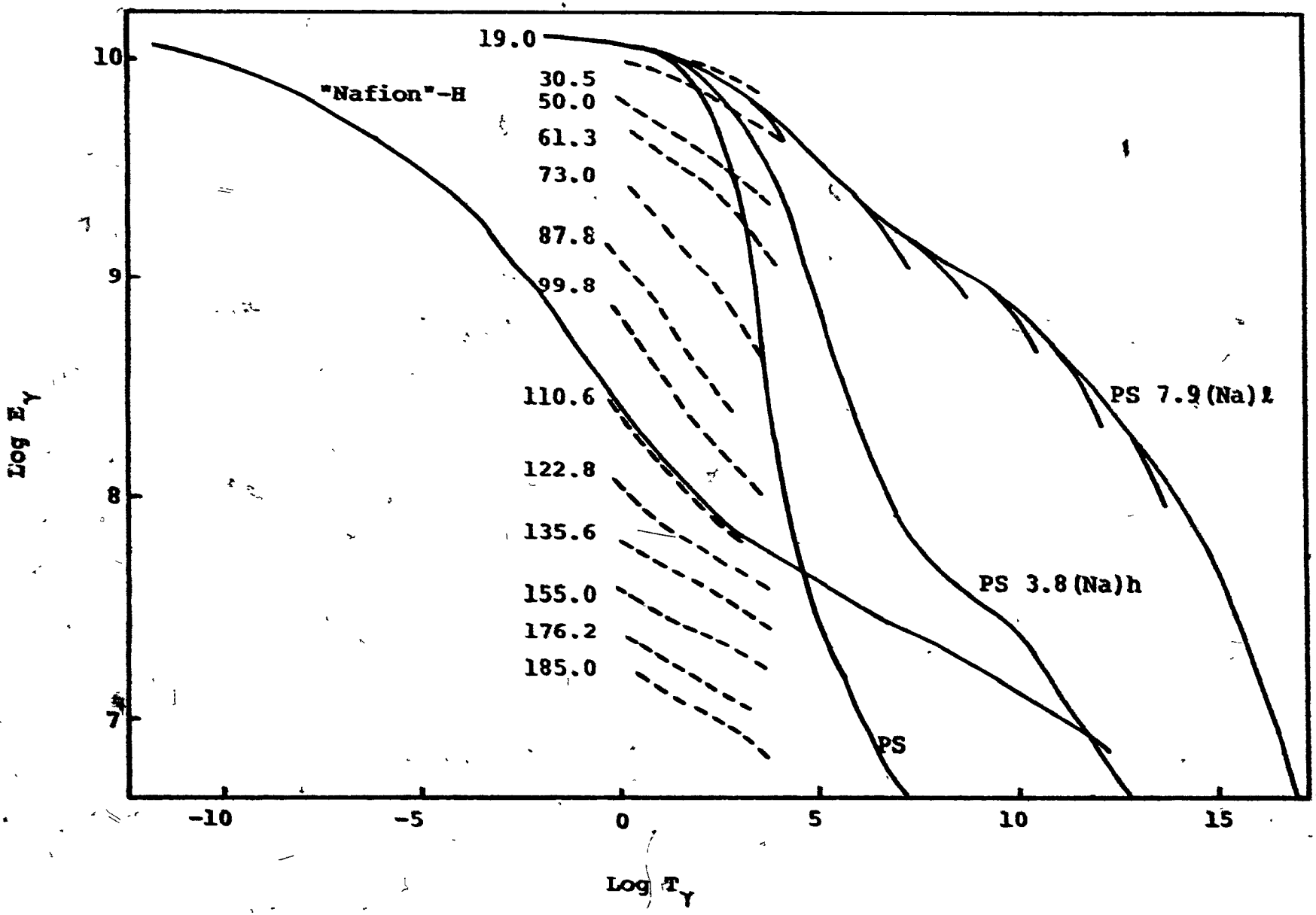
19.0
30.5
50.0
61.3
73.0
87.8
99.8
110.6
122.8
135.6
155.0
176.2
185.0
"Nafion"-H
PS 7.9(Na)l
PS 3.8(Na)h
PS
10
9
8
7
-10
-5
0
5
10
15
Log E_γ
Log T_γ

FIGURE 6.

Original stress relaxation curves and pseudo master curve for "Nafion"-H with 0.5 H_2O/SO_3H. $T_o = T_g$.

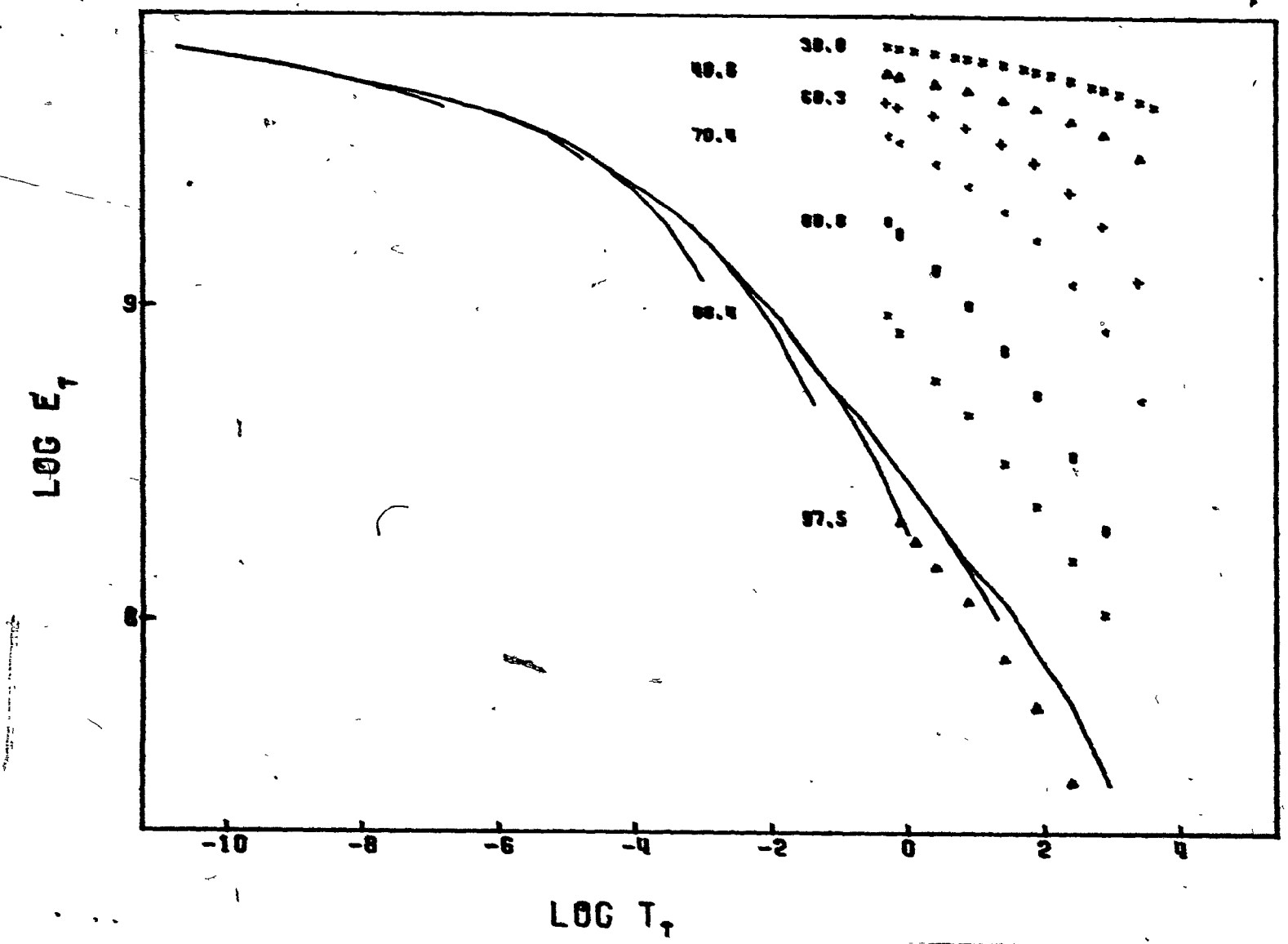
38.8
48.8
58.3
70.4
88.8
96.4
97.5
9
8
-10
-8
-6
-4
-2
0
2
4
LOG E_r
LOG T_r

FIGURE 7.

Original stress relaxation curves and pseudo master curve for "Nafion"-K. $T_o = Tg$.

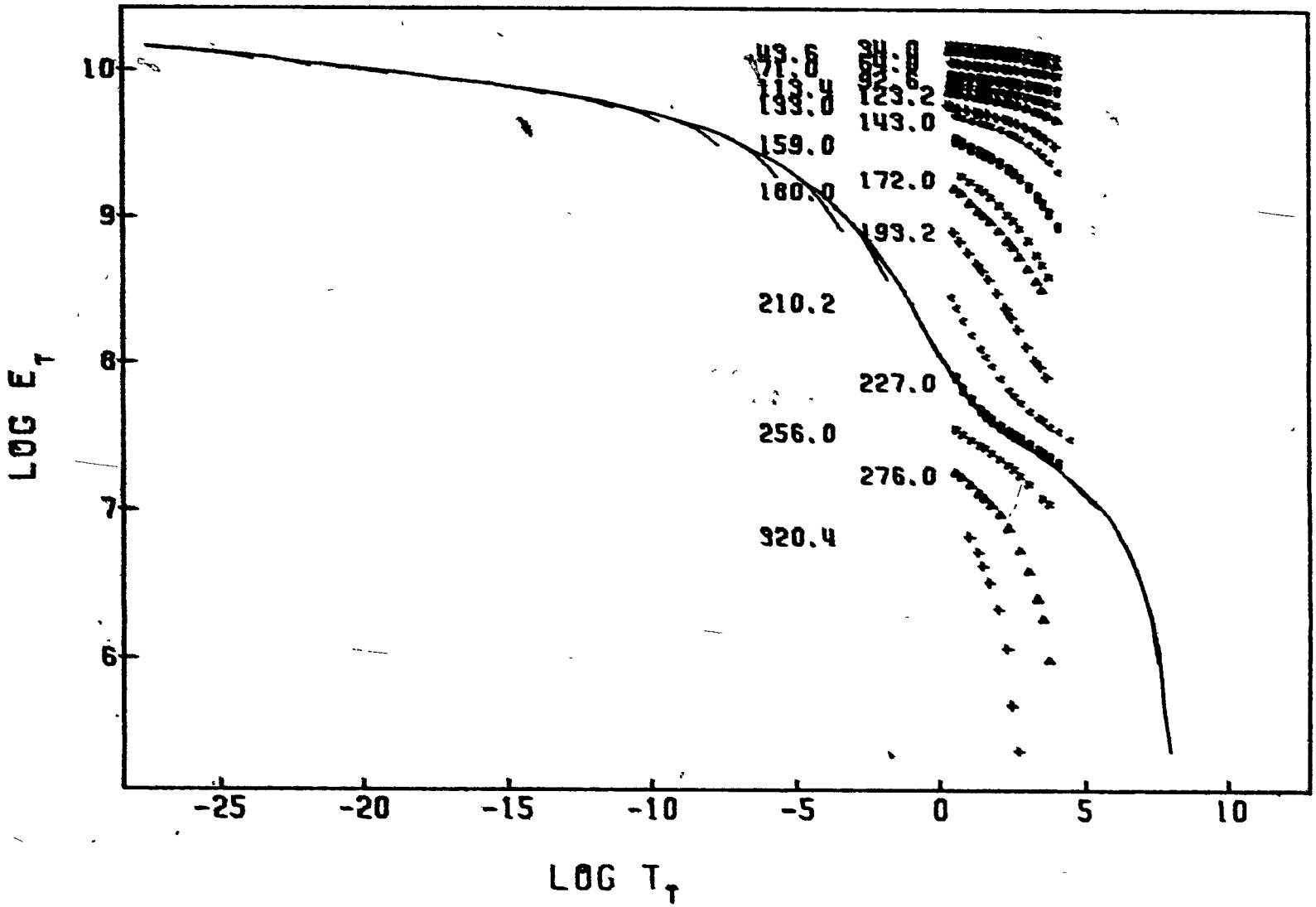
LOG E_T
LOG T_T
10
9
8
7
6
-25
-20
-15
-10
-5
0
5
10
159.0
210.2
227.0
256.0
276.0
320.4

FIGURE 8.

Distribution of relaxation times for "Nafion"-H, "Nafion"-K, PS and PS 3.8 (Na)h. $T_o = 25^oC$.

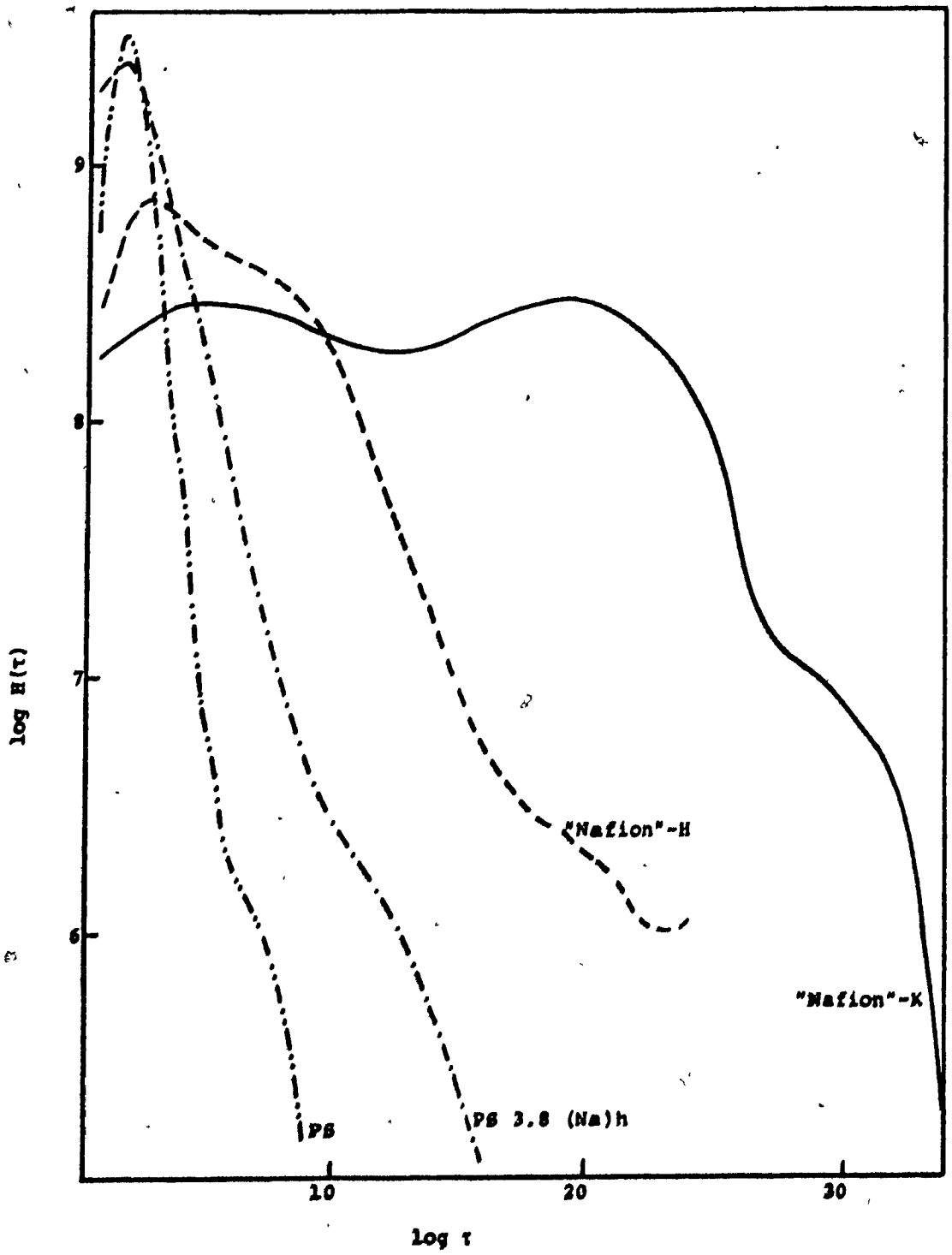
9
8
7
6
log E(τ)
"Nafion"-H
"Nafion"-K
PS
PS 3.8 (Na)h
10
20
30
log τ

FIGURE 9.

Original stress relaxation curves and master curve for degraded "Nafion"-H. $T_o = T_g$.

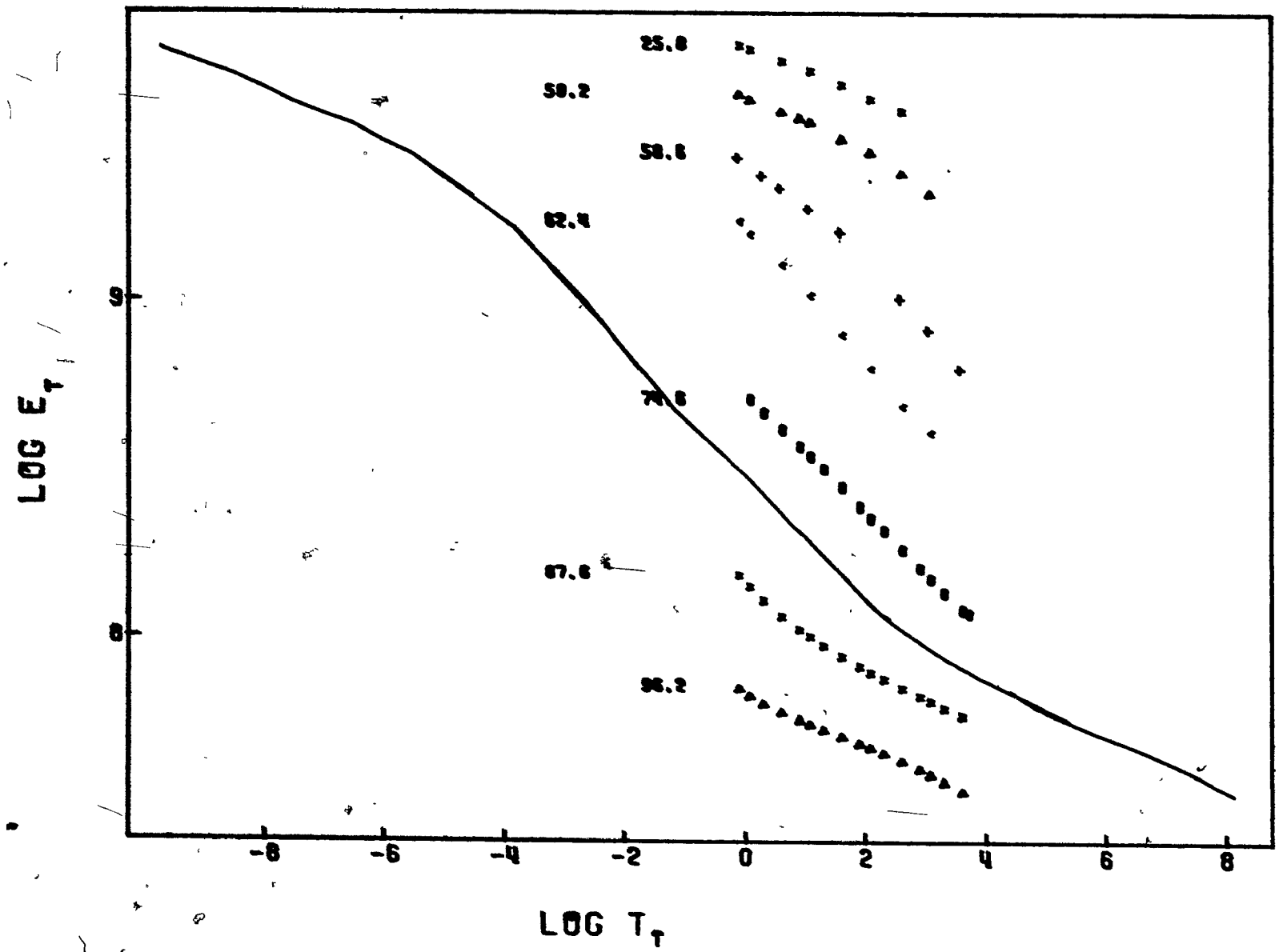
25.8
59.2
58.8
62.4
74.8
87.6
96.2
LOG E_T
LOG T_T
-8
-6
-4
-2
0
2
4
6
8

FIGURE 10.

Stress relaxation master curves for degraded and undegraded "Nafion"-H. $T_o = T_g$.

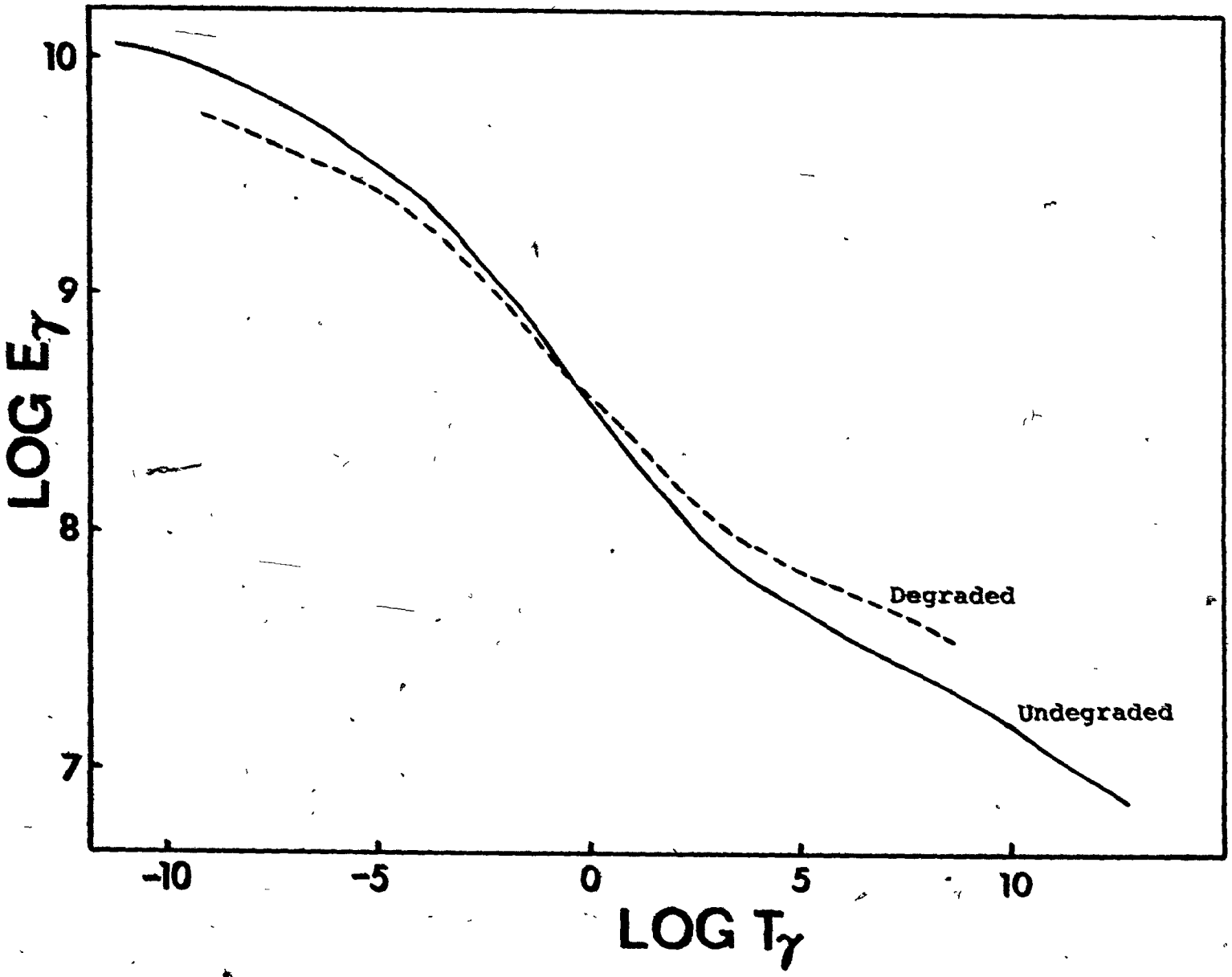
10
9
8
7
LOG E_γ
-10
-5
0
5
10
LOG T_γ
Degraded
Undegraded

FIGURE 11.

10-sec. modulus vs. temperature for "Nafion"-H, "Nafion"-K, PS, PS 3.8 (Na)h and PS 7.9 (Na)l.

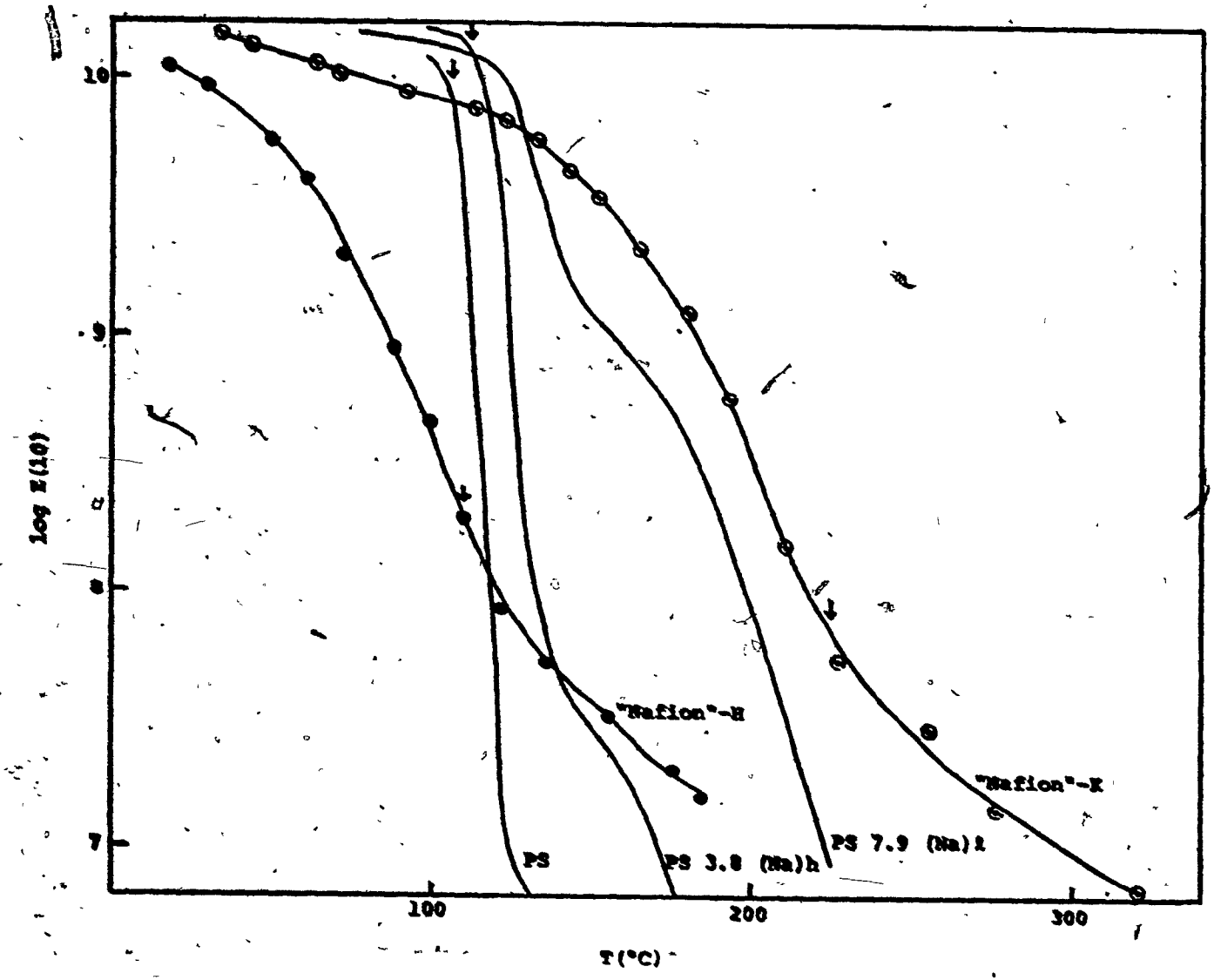
Log E(10)
10
9
8
7
100
200
300
T(°C)
"Nafion"-H
"Nafion"-K
PS
PS 3.8 (Na)h
PS 7.9 (Na)t

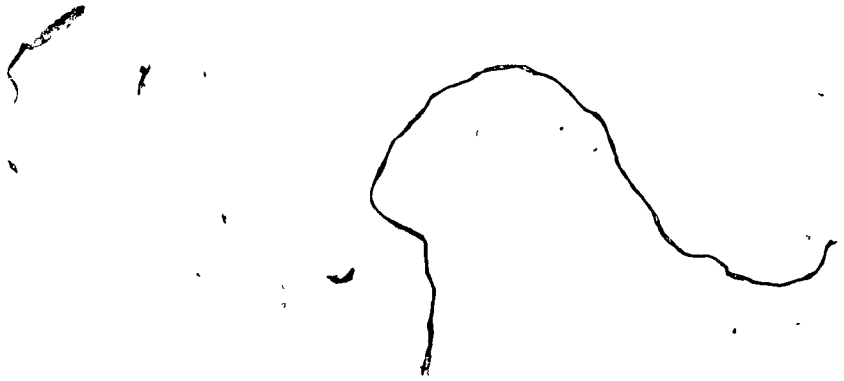

FIGURE 12.

Mechanical loss tangent vs. temperature for "Nafion"-H and "Nafion"-Cs at ca. 1 Hz. Dashed lines represent values for the β peak above background.

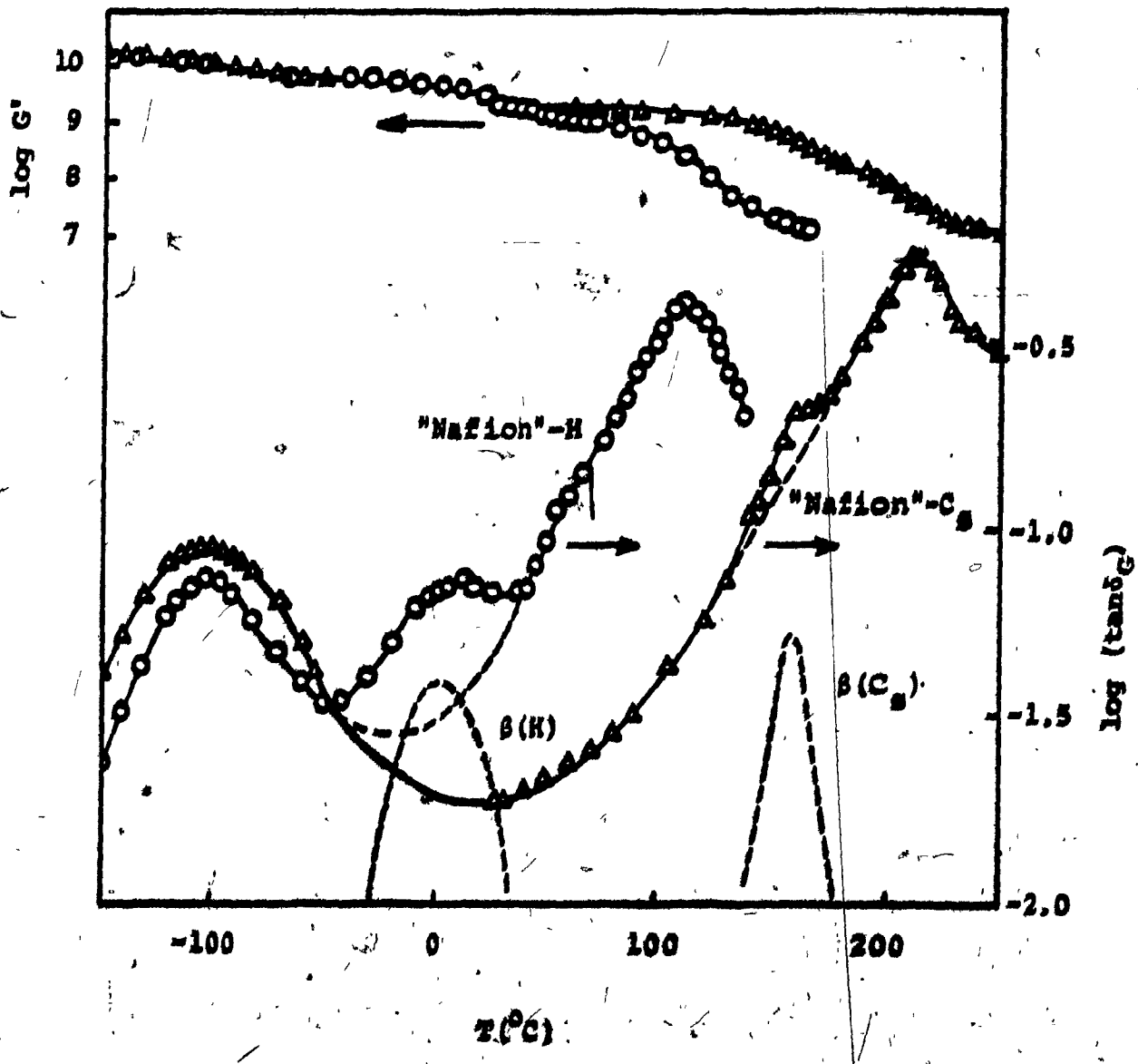
log G'
10
9
8
7
"Nafion"-H
"Nafion"-Cs
β(H)
β(Cs)
-0.5
-1.0
-1.5
-2.0
log (tanδ)
-100
0
100
200
T(°C)

FIGURE 13.

Mechanical loss tangent vs. temperature for "Nafion"-K at ca. 1 Hz. Dashed lines represent values for the β peak above background.

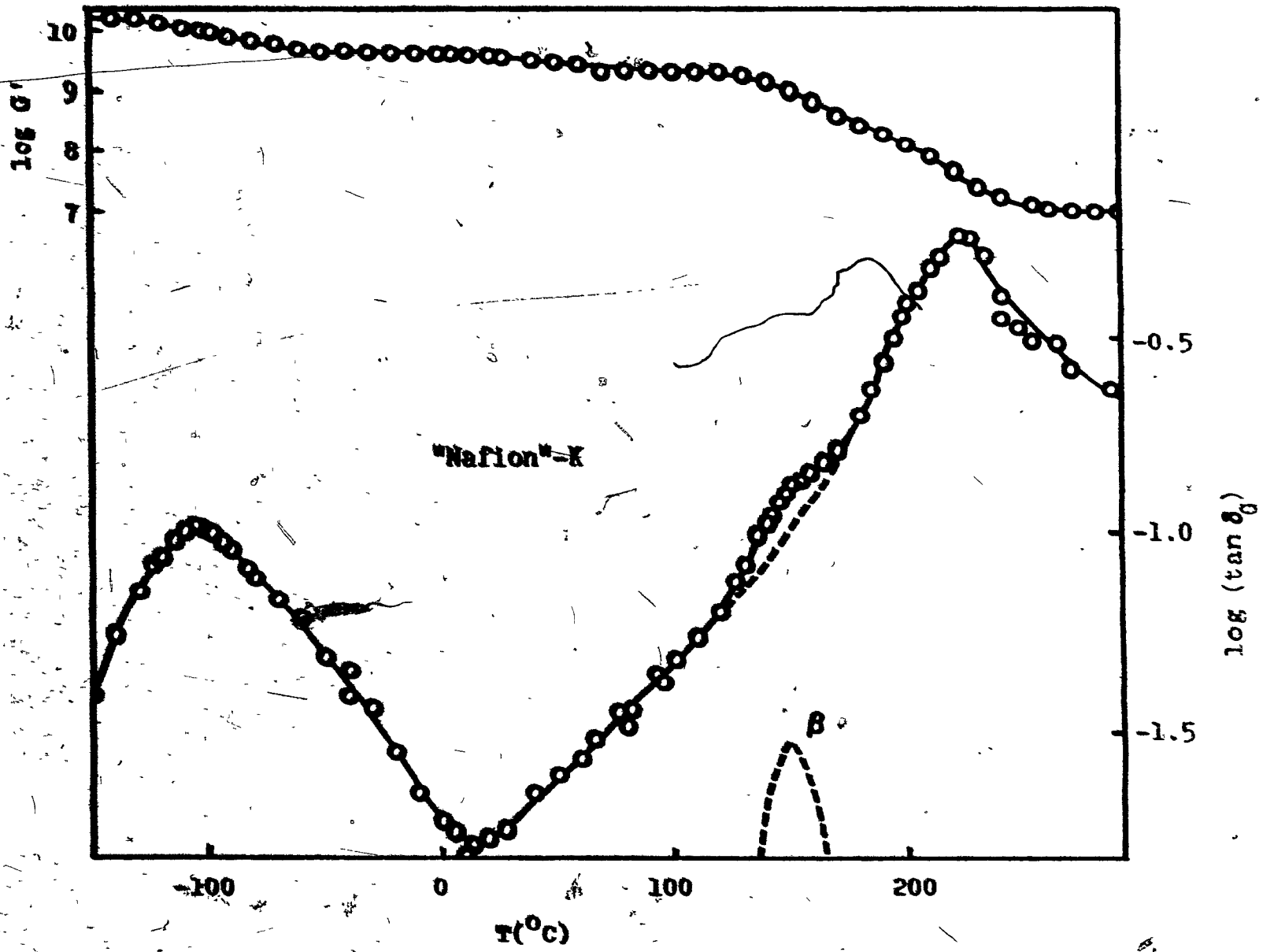
log σ'
10
9
8
7
"Nafion"-K
β
-0.5
-1.0
-1.5
log (tan δ)
-100
0
100
200
T(°C)

FIGURE 14.

Mechanical loss tangent vs. temperature for "Nafion"-Na at ca. 1 Hz.

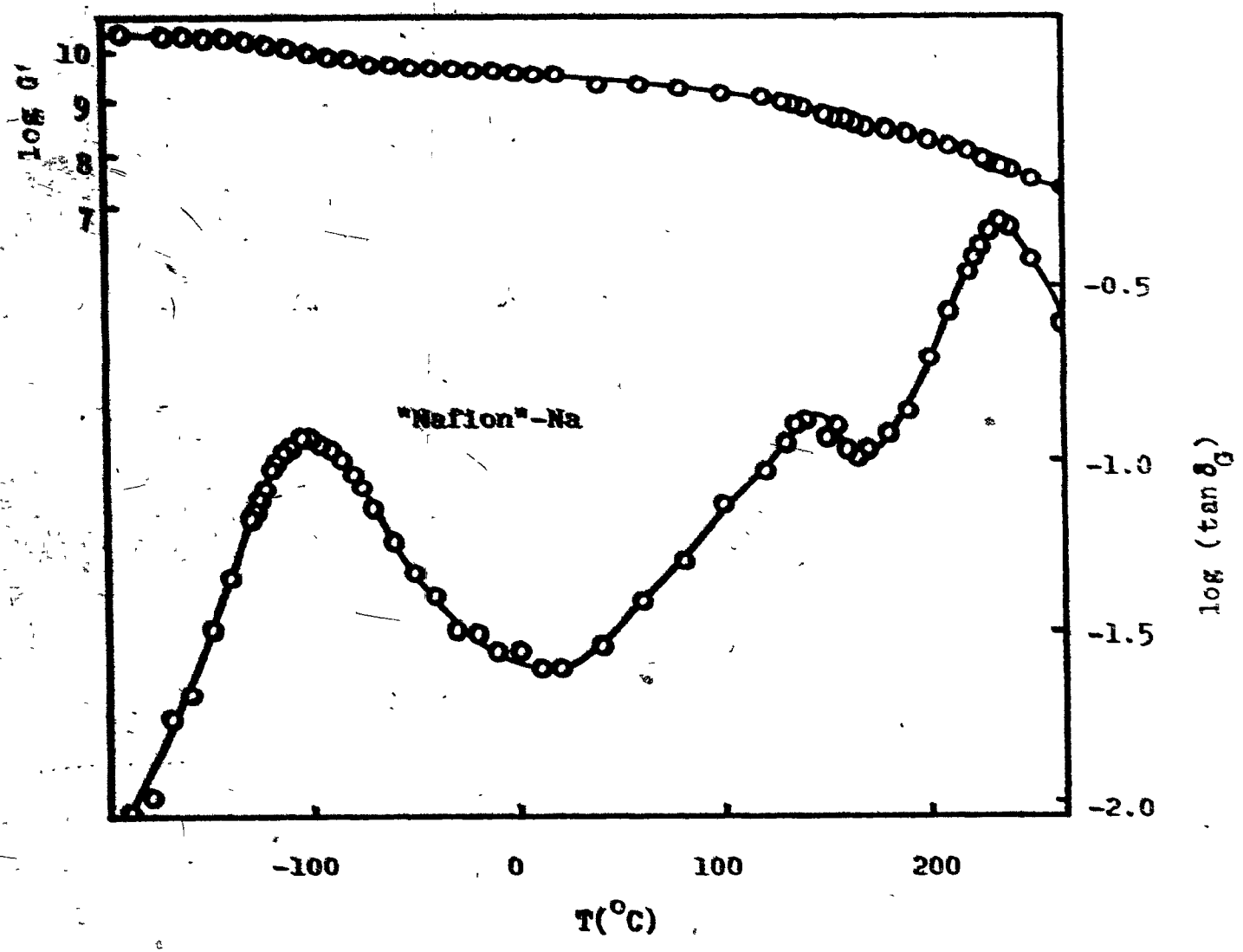
log σ'
10
9
8
7
"Nafion"-Na
-0.5
-1.0
-1.5
-2.0
log (tan δ_σ)
-100
0
100
200
T(°C)

FIGURE 15.

Mechanical loss tangent vs. temperature for "Nafion"-Li at ca. 1 Hz. Dashed lines represent values for the β peak above background.

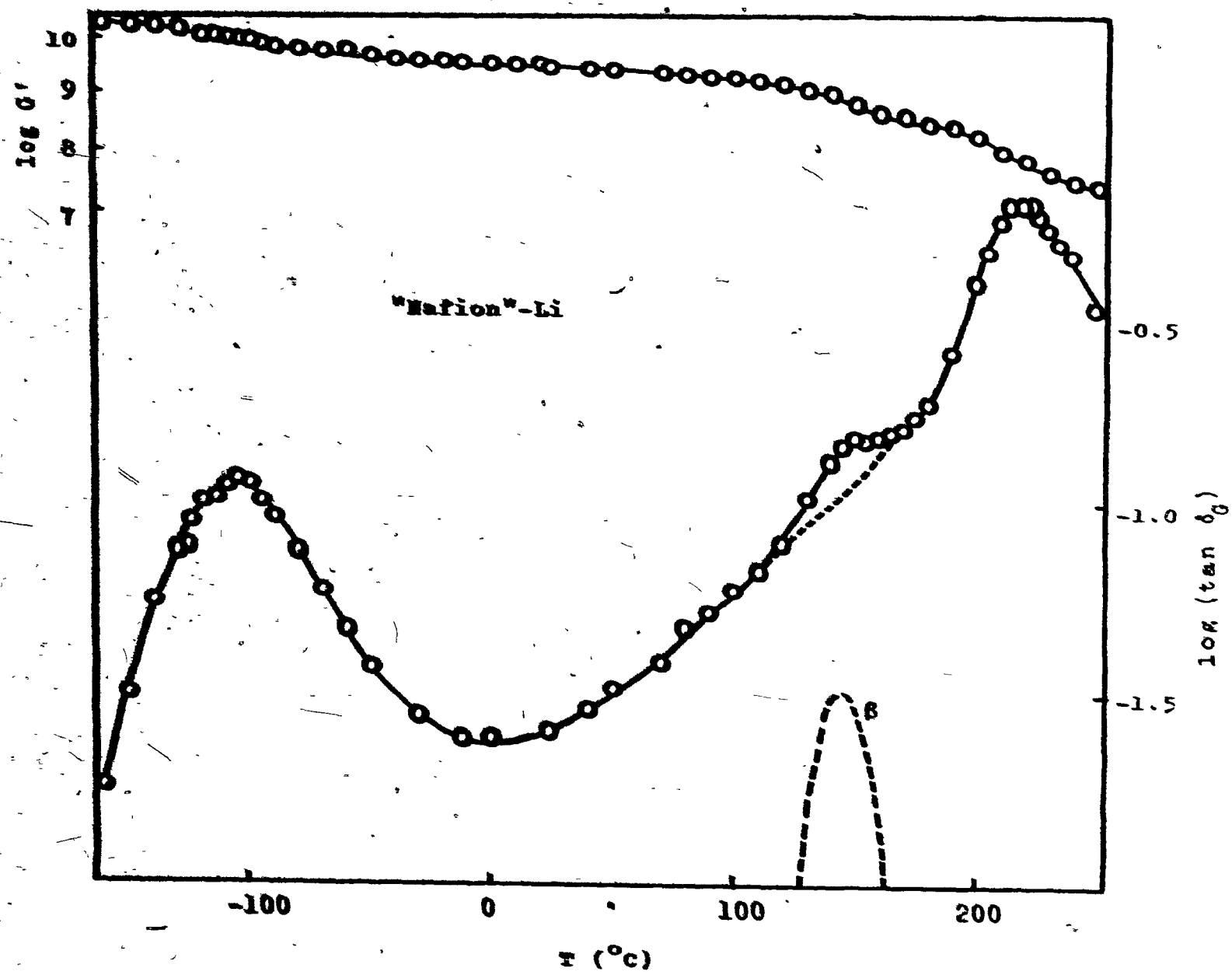
10
9
8
7
log G'
"Nafion"-Li
-0.5
-1.0
-1.5
log (tan δ)
β
-100
0
100
200
T (°C)

FIGURE 16.

Mechanical loss tangent vs. temperature for "Nafion"-H samples with varying water content at ca. 1 Hz.

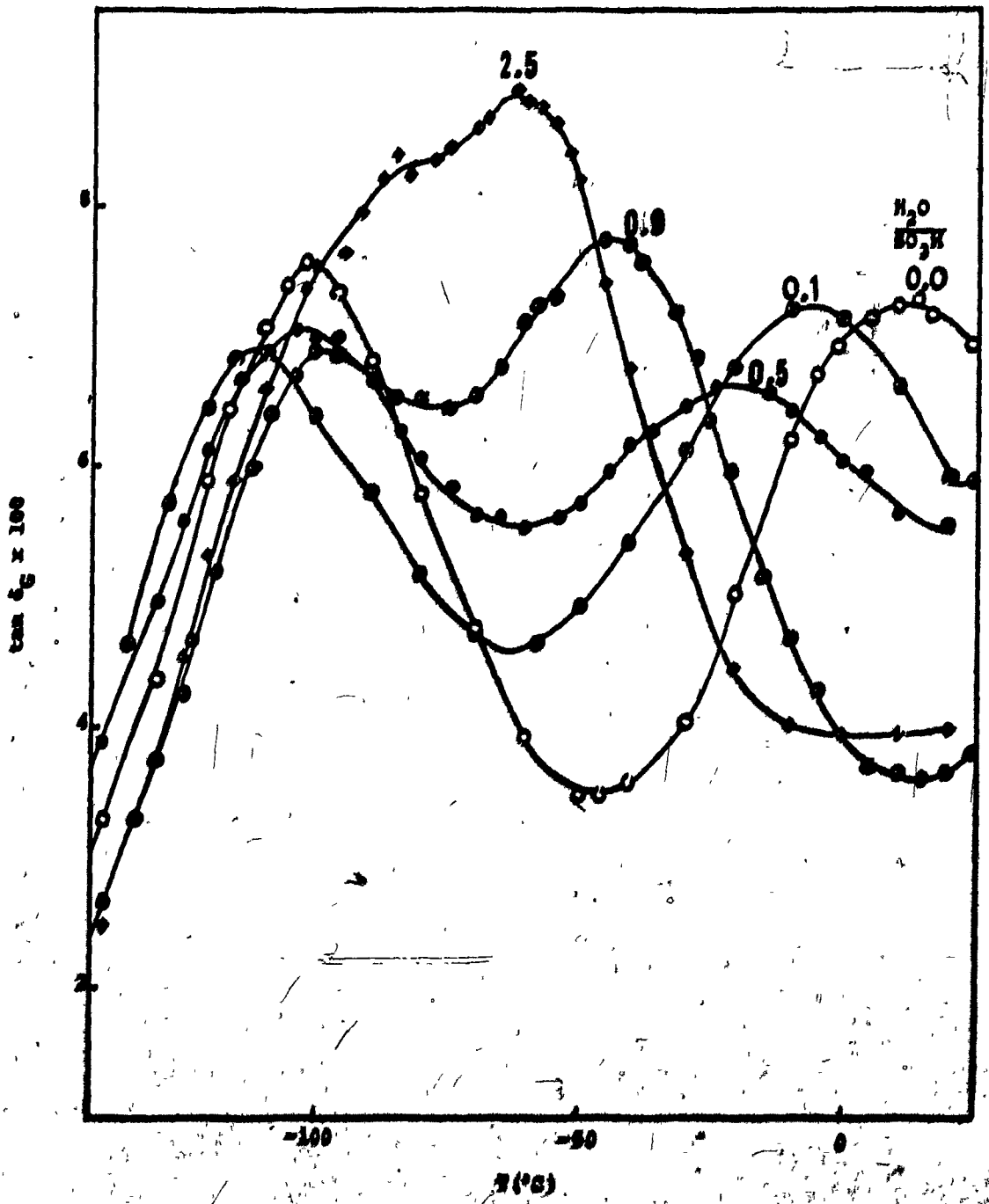
2.5
1.0
0.5
0.1
0.0
$\frac{H_2O}{SO_3K}$
8
6
4
2
-100
-50
0
T (°C)

FIGURE 17.

Shear storage and loss modulus (G' and G'') vs. temperature for "Nafion"-H samples with varying water content at ca. 1 Hz.

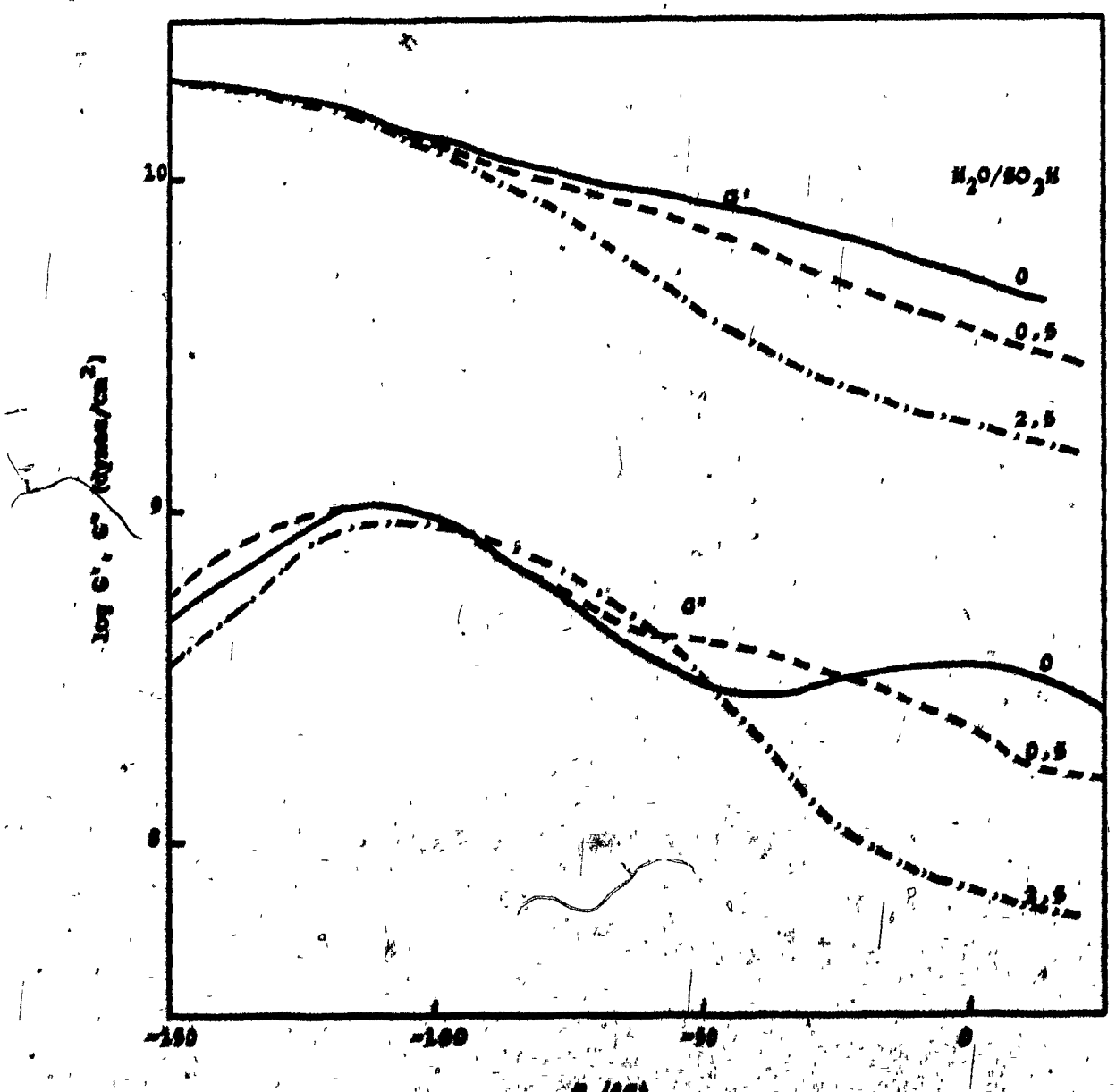
10
0
-150
-100
-50
0
T (°C)
log σ', σ'' (dynes/cm²)
σ'
σ''
H₂O/SO₃H
0
0.5
2.5
0
0.5
2.5

FIGURE 18.

Mechanical loss tangent vs. temperature for "Nafion"-H samples with varying degree degradation (% weight loss) at ca. 1 Hz.

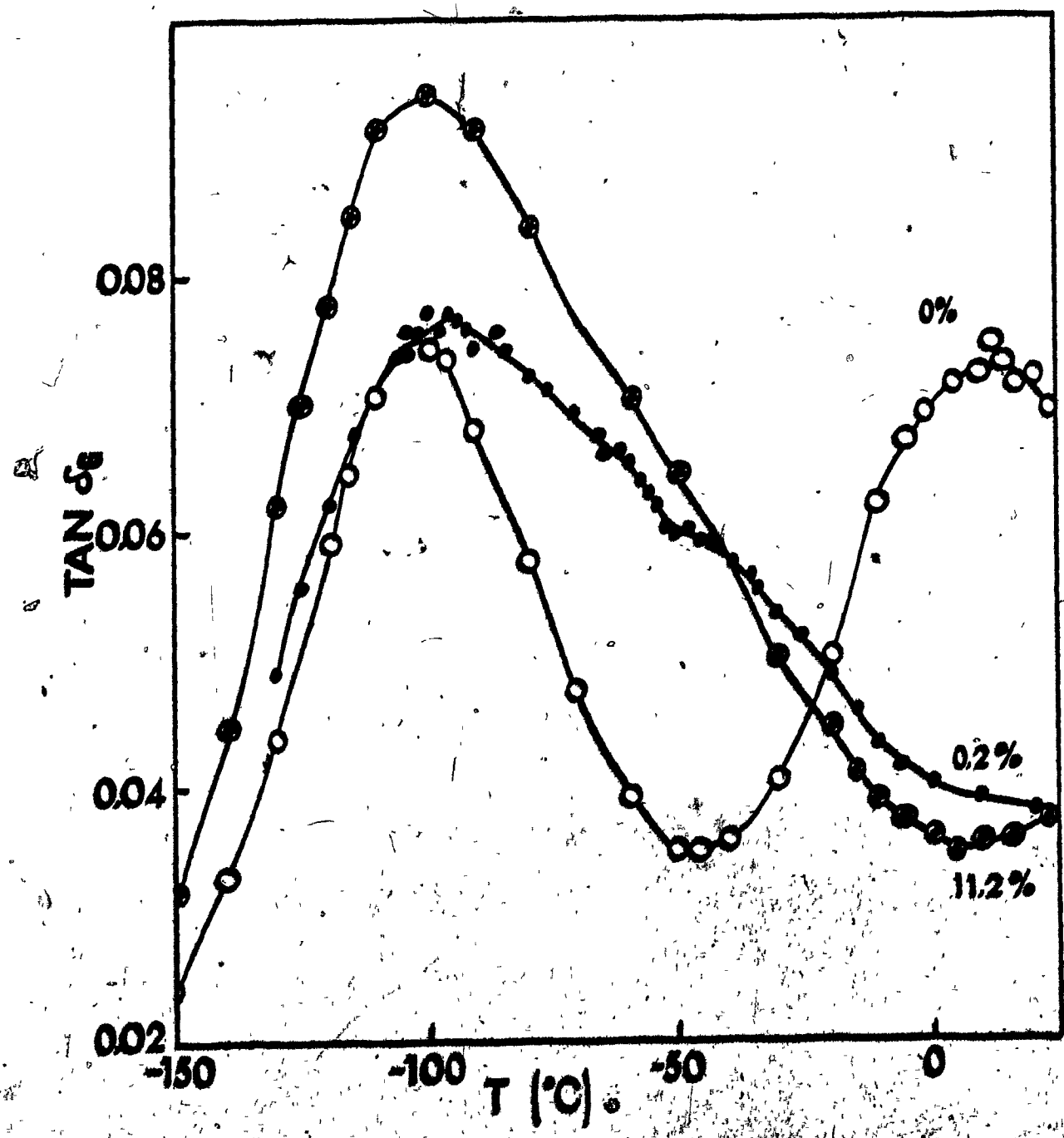
0.08
0.06
0.04
0.02
TAN δ
-150
-100
-50
0
T (°C)
0%
0.2%
11.2%

FIGURE 19.

Shear storage and loss modulus (G' and G") vs. temperature for "Nafion"-H samples with varying degree degradation at ca. 1 Hz.

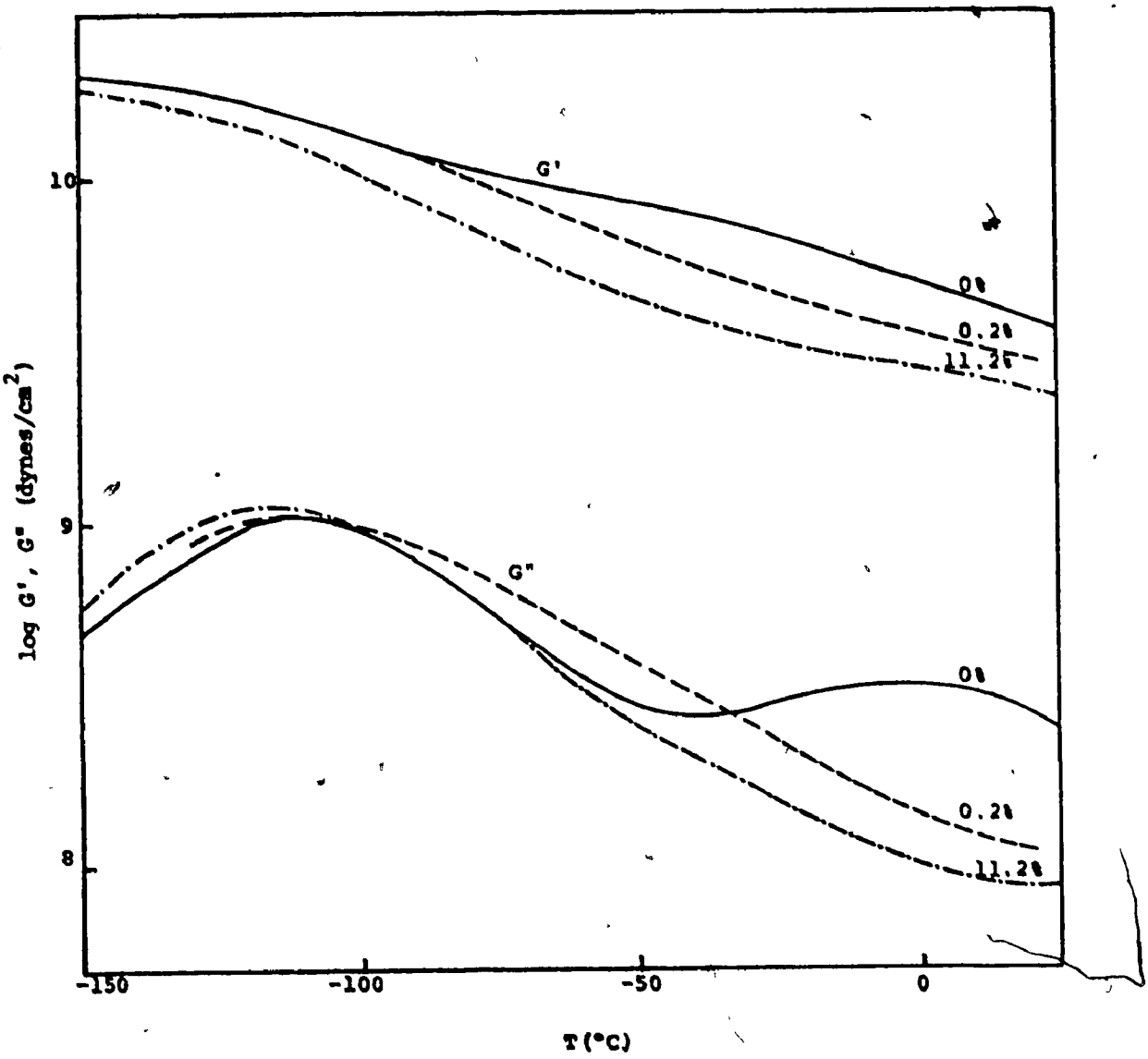
G'
G"
0%
0.2%
11.2%
0%
0.2%
11.2%
10
9
8
-150
-100
-50
0
log G', G" (dynes/cm²)
T (°C)

FIGURE 20.

Shear storage modulus ($0^{\circ}C$, ca. 1 Hz) vs. weight loss for "Nafion"-H.

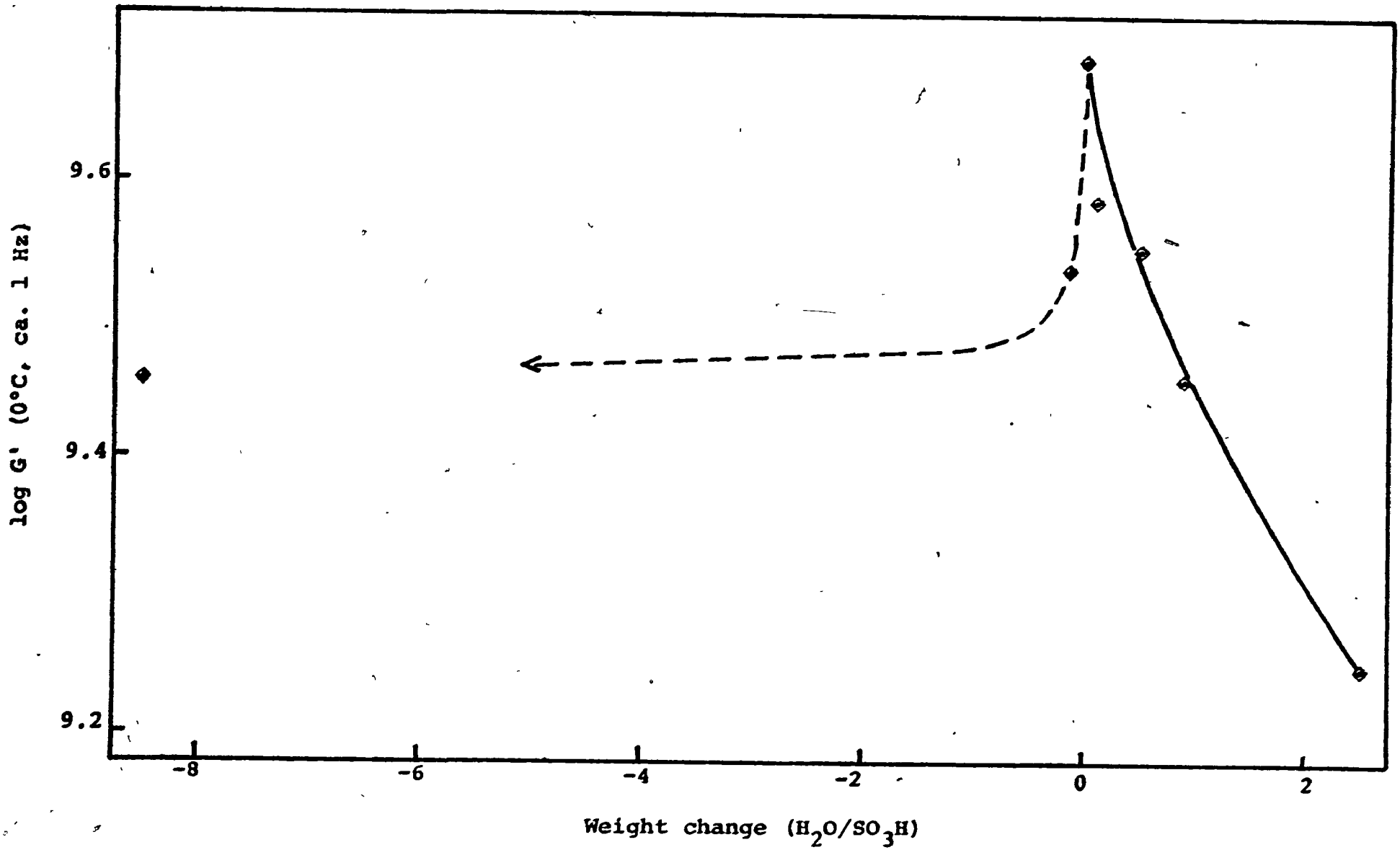
9.6
9.4
9.2
log G' (0°C, ca. 1 Hz)
-8
-6
-4
-2
0
2
Weight change (H_2O/SO_3H)

FIGURE 21.

Mechanical loss tangent vs. temperature for "Nafion"-Li with varying water content at ca. 1 Hz.

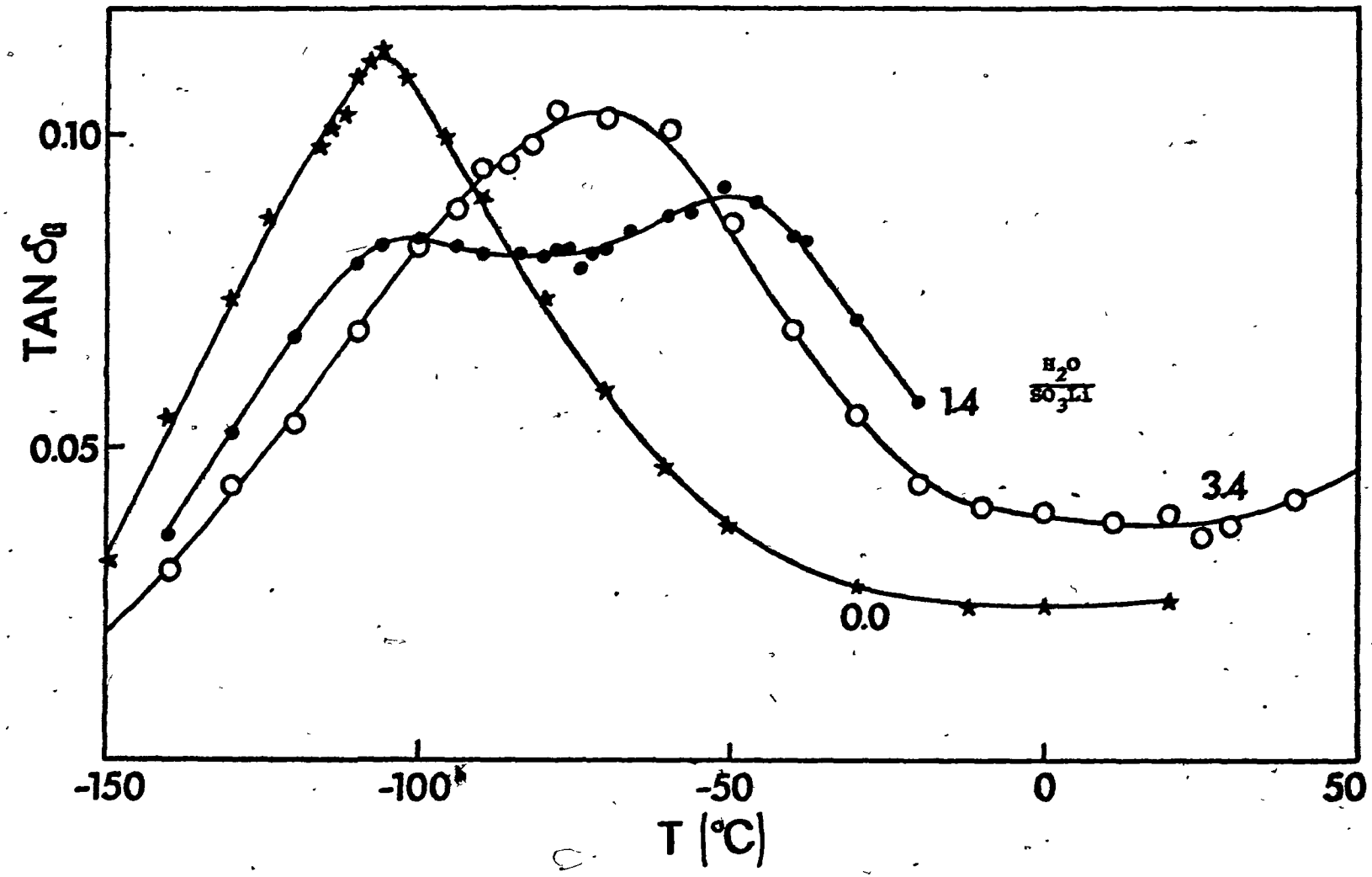
0.10
0.05
TAN δ
-150
-100
-50
0
50
T (°C)
1.4
3.4
0.0
H2O / SO3Li

FIGURE 22.

Mechanical loss tangent vs. temperature for "Nafion"-Na with varying water content at ca. 1 Hz.

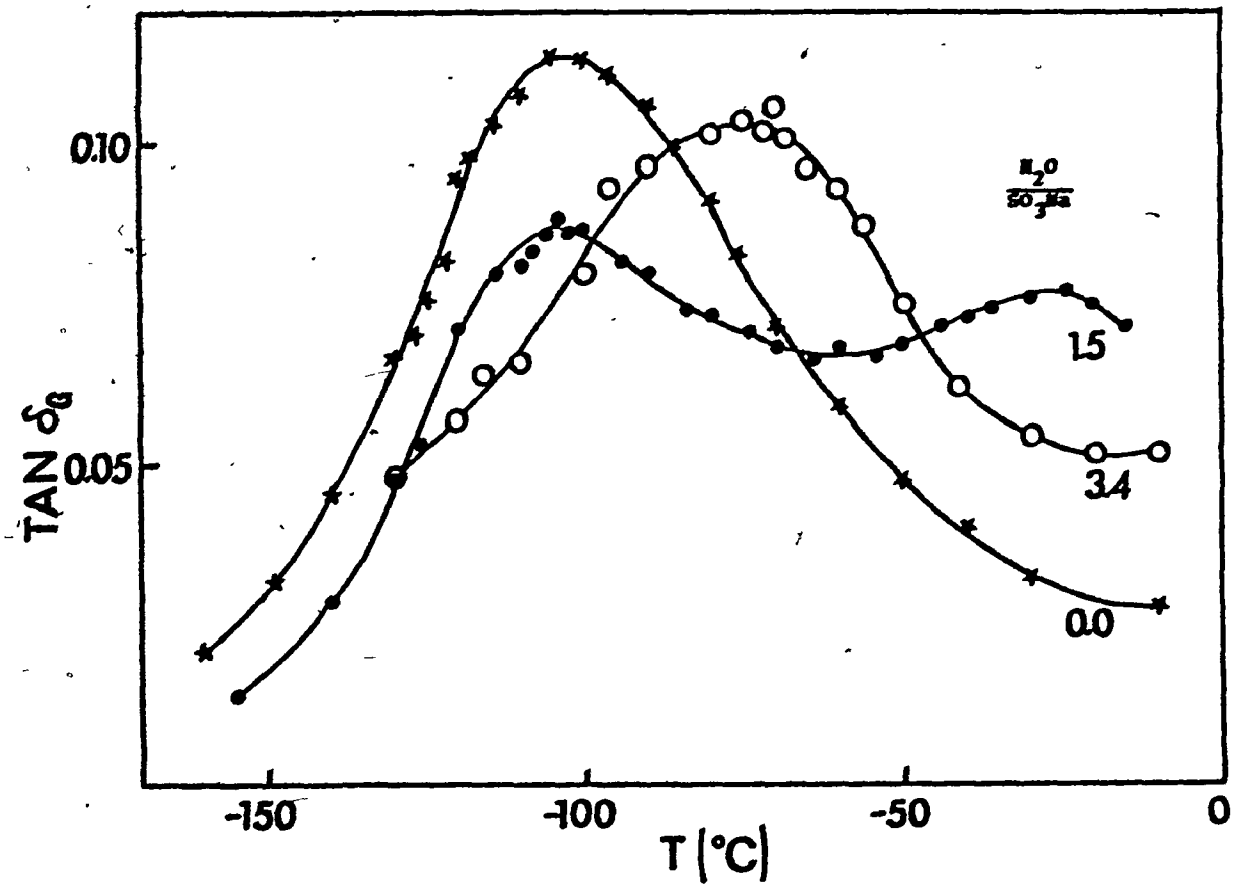
0.10
0.05
TAN δ_G
$\frac{H_2O}{SO_3Na}$
1.5
3.4
0.0
-150
-100
-50
0
T [°C]

FIGURE 23.

Mechanical loss tangent vs. temperature for "Nafion" with various counterion in the γ-relaxation region at ca. 1 Hz.

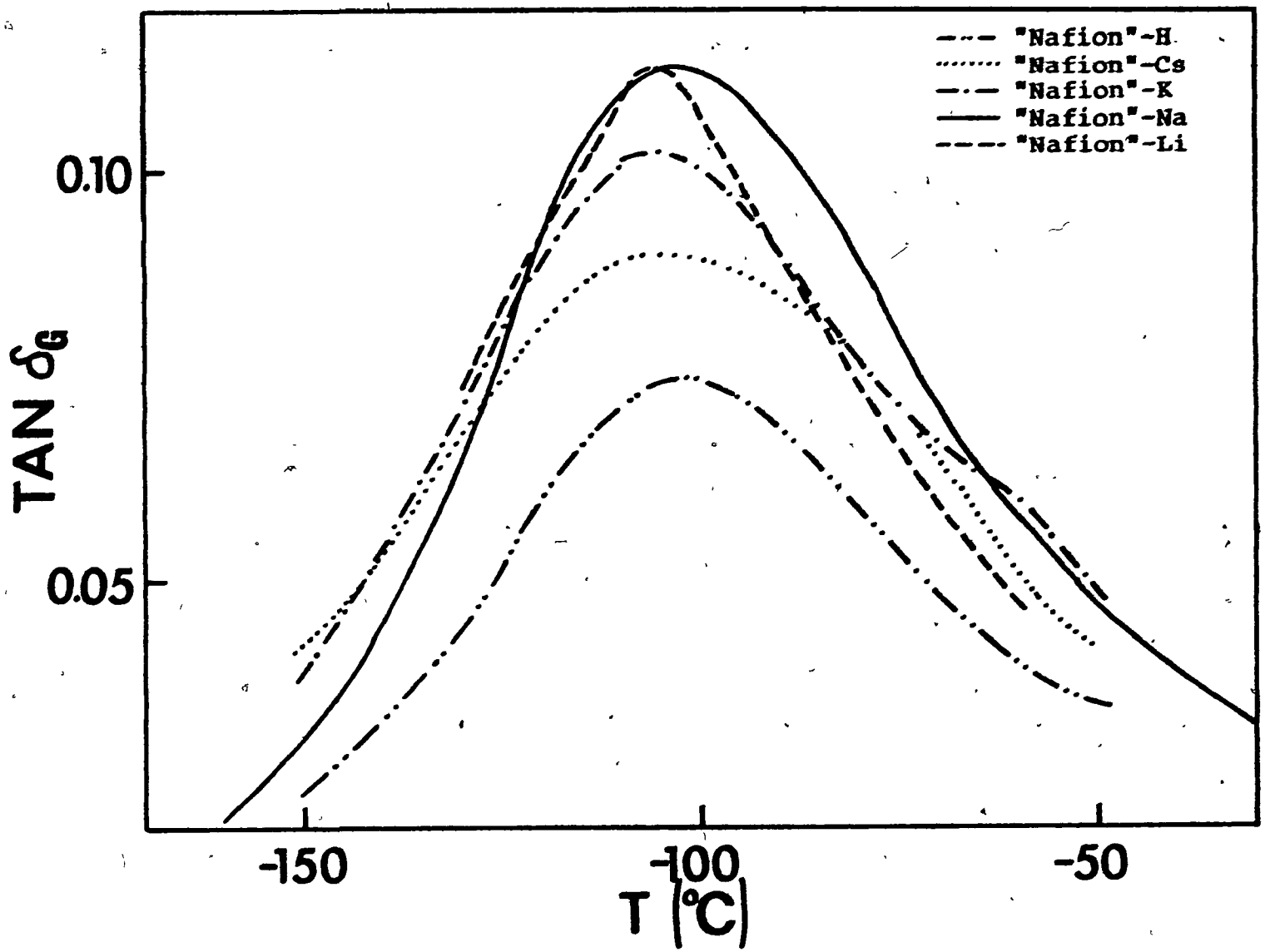
"Nafion"-H
"Nafion"-Cs
"Nafion"-K
"Nafion"-Na
"Nafion"-Li
0.10
0.05
TAN δG
-150
-100
-50
T (°C)

FIGURE 24.

Log ν vs. 1/T plot for "Nafion" samples and literature values for PTFE at the γ-relaxation region.

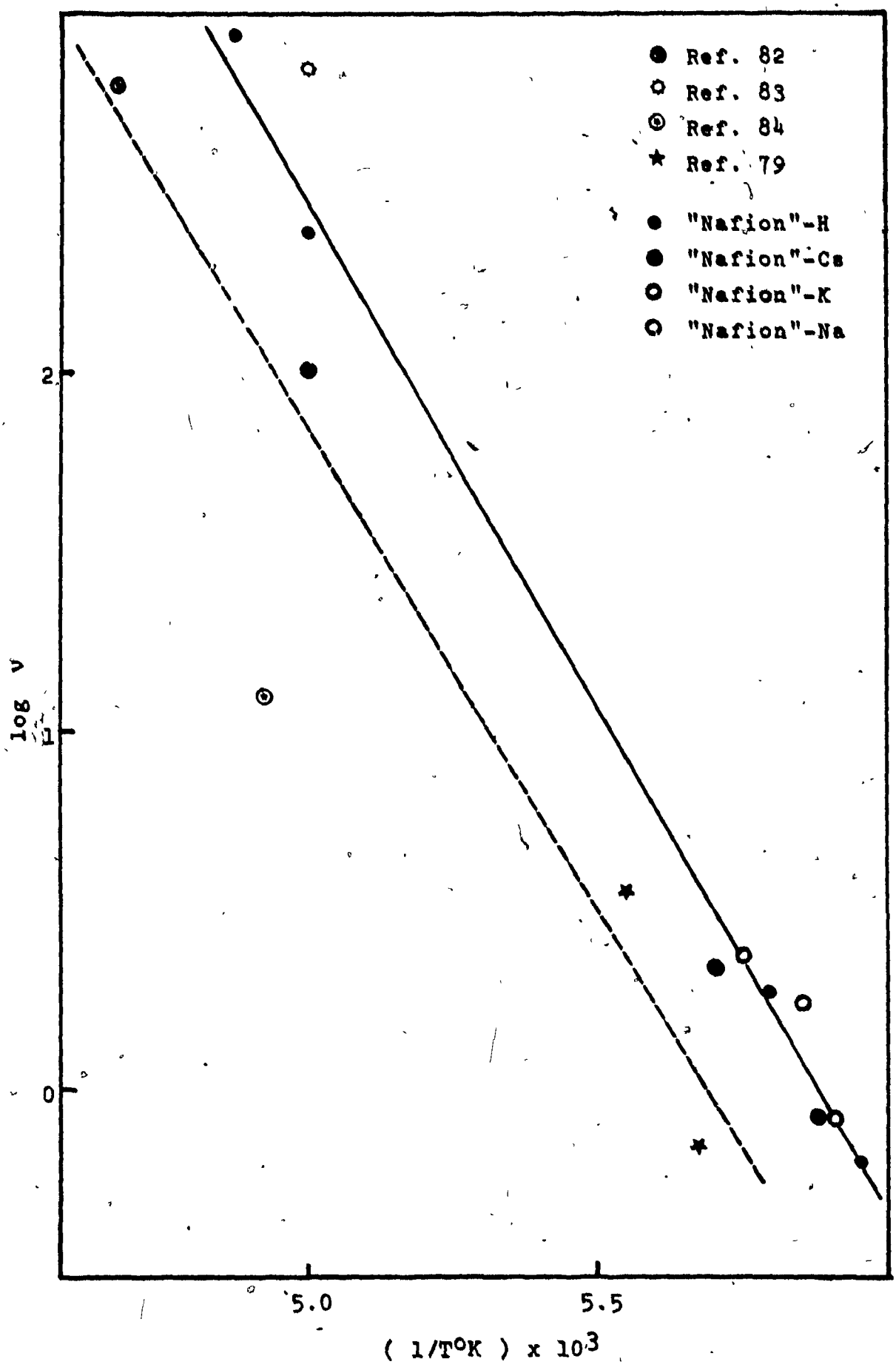
Ref. 82
Ref. 83
Ref. 84
Ref. 79
"Nafion"-H
"Nafion"-Cs
"Nafion"-K
"Nafion"-Na
2
1
0
log v
5.0
5.5
(1/T°K) x 10³

FIGURE 25.

Dielectric loss tangent vs. temperature for "Nafion"-H with 0.7 H_2O/SO_3H at 100 Hz, 1kHz and 10kHz.

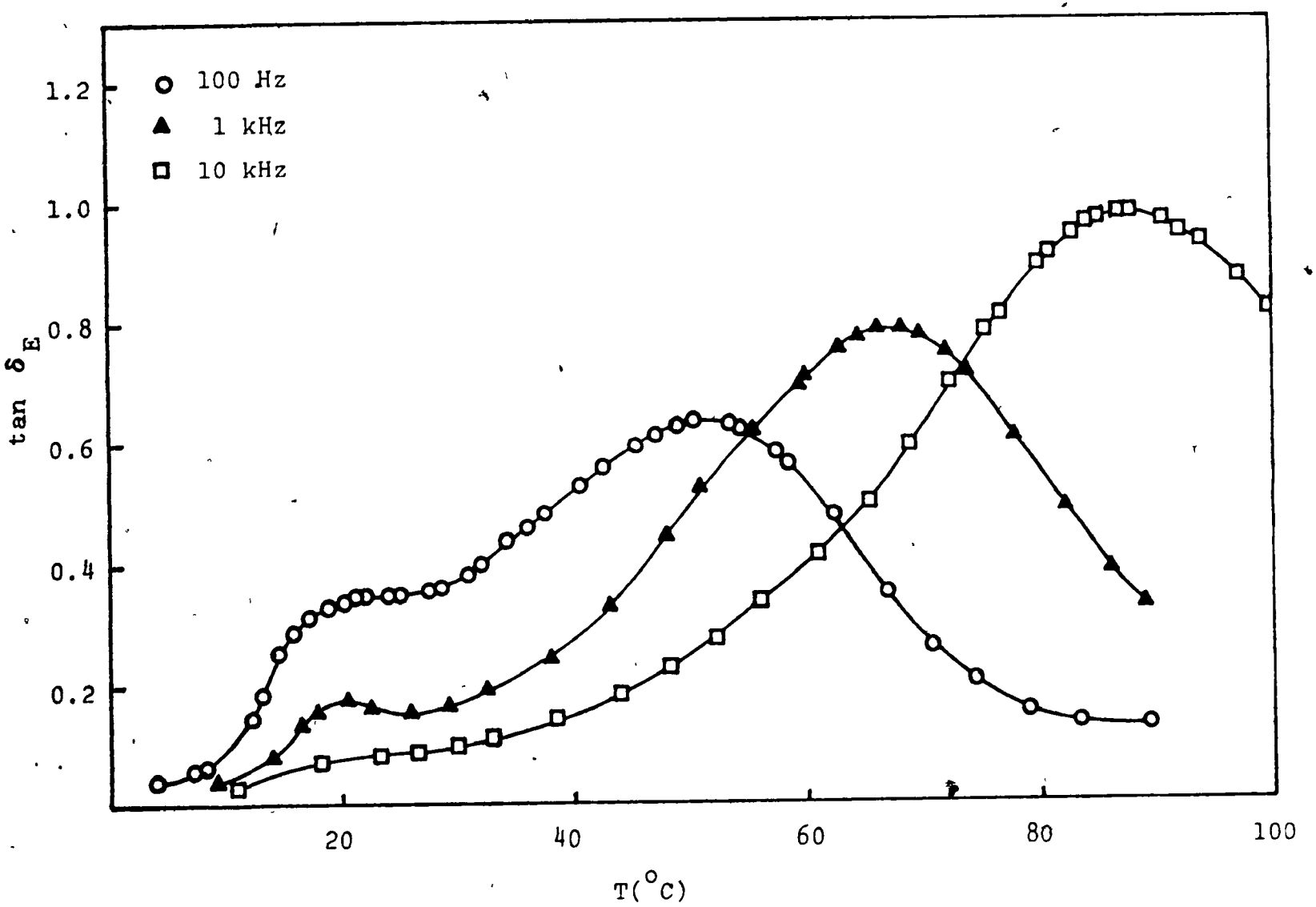
100 Hz
1 kHz
10 kHz
1.2
1.0
0.8
0.6
0.4
0.2
tan δE
20
40
60
80
100
T(°C)

FIGURE 26.

Dielectric loss tangent vs. temperature for "Nafion"-H with 1.4 H_2O/SO_3H at 100 Hz, 1kHz and 10kHz.

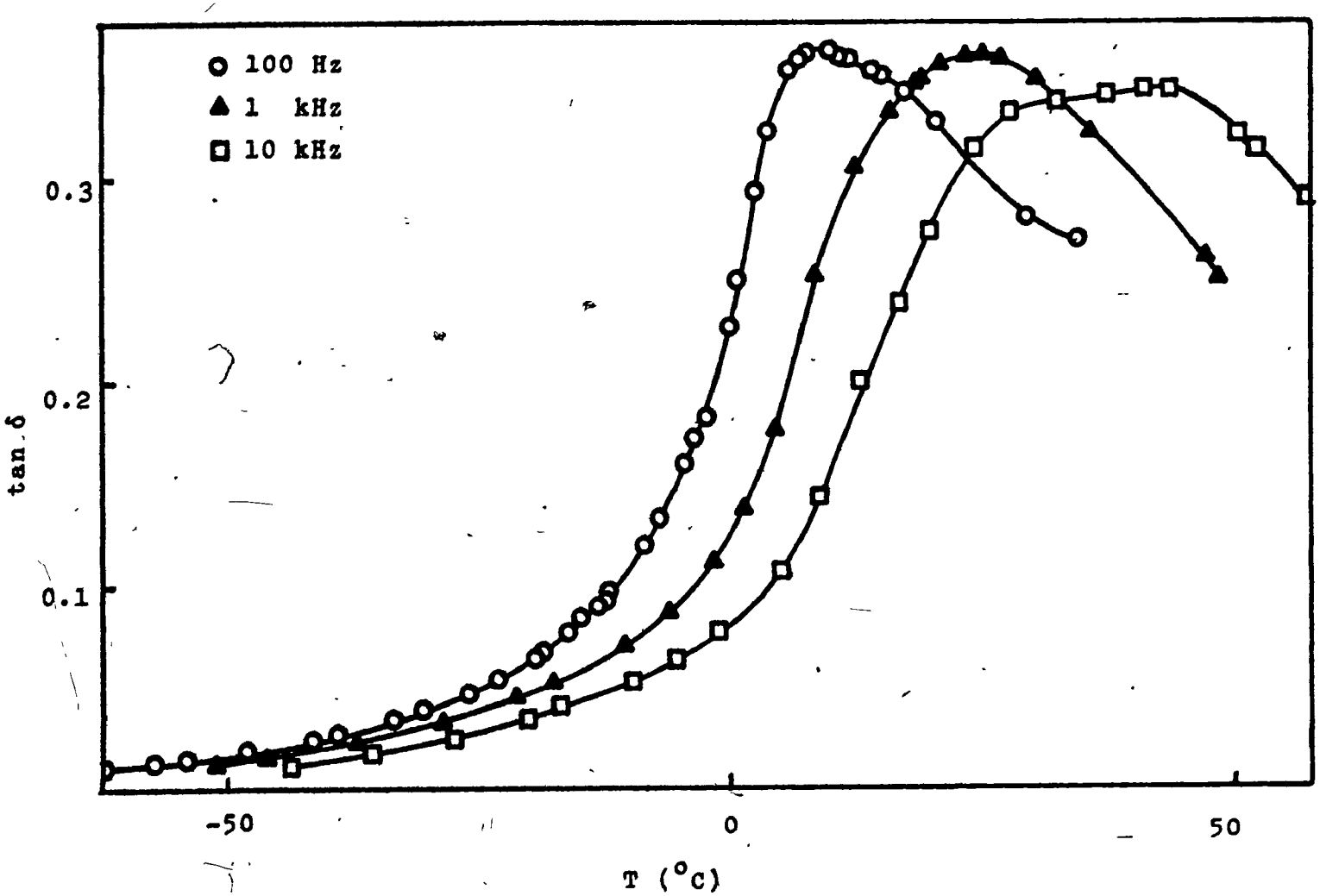
100 Hz
1 kHz
10 kHz
0.3
0.2
0.1
tan δ
-50
0
50
T (°C)

FIGURE 27.

Dielectric loss tangent vs. temperature for "Nafion"-H with 1.7 H_2O/SO_3H at 100 Hz, 1kHz and 10kHz.

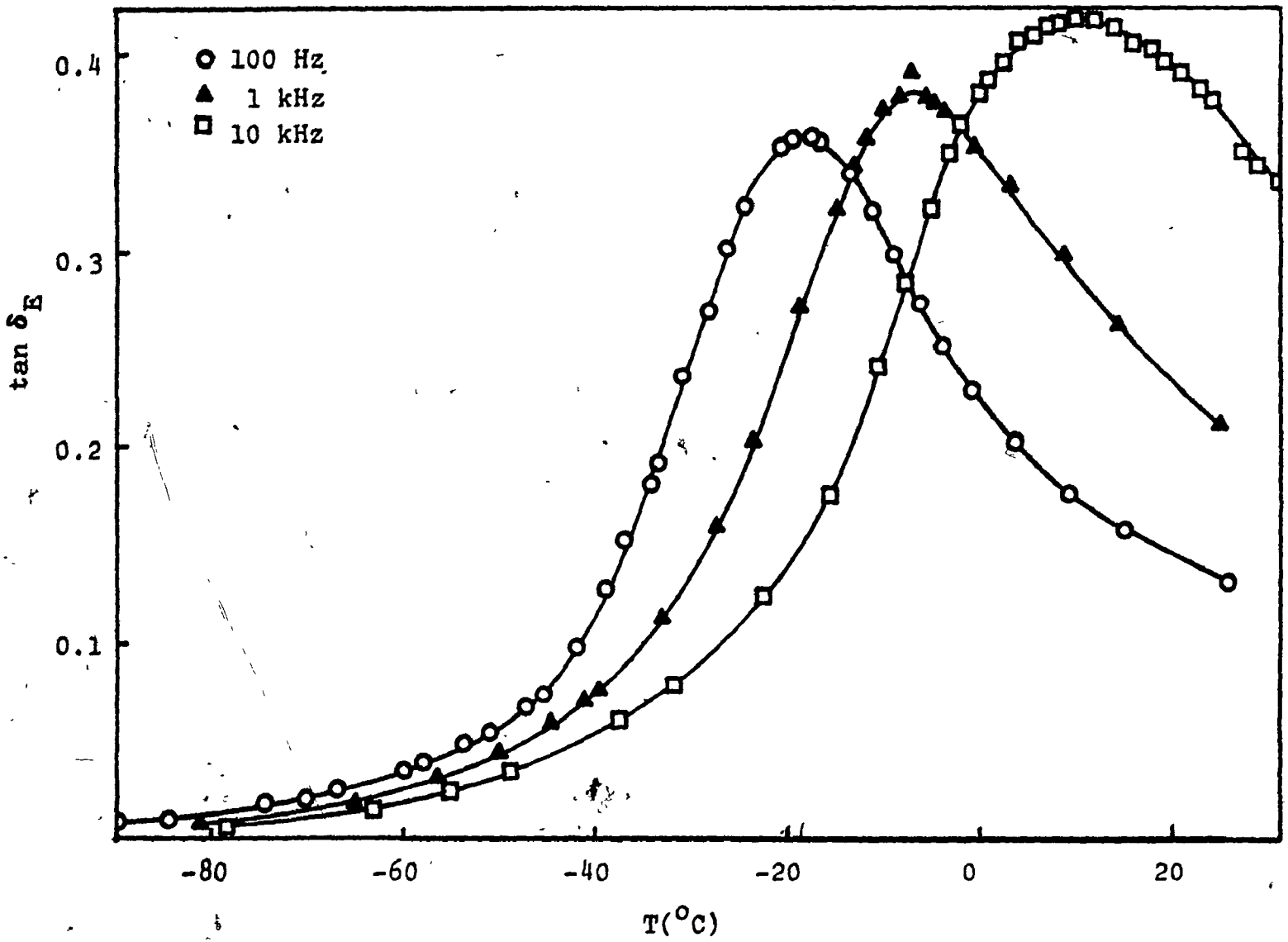
100 Hz
1 kHz
10 kHz
0.4
0.3
0.2
0.1
tan δE
-80
-60
-40
-20
0
20
T(°C)

FIGURE 28.

Dielectric loss tangent vs. temperature for "Nafion"-H with 2.1 H_2O/SO_3H at 100 Hz, 1kHz and 10kHz.

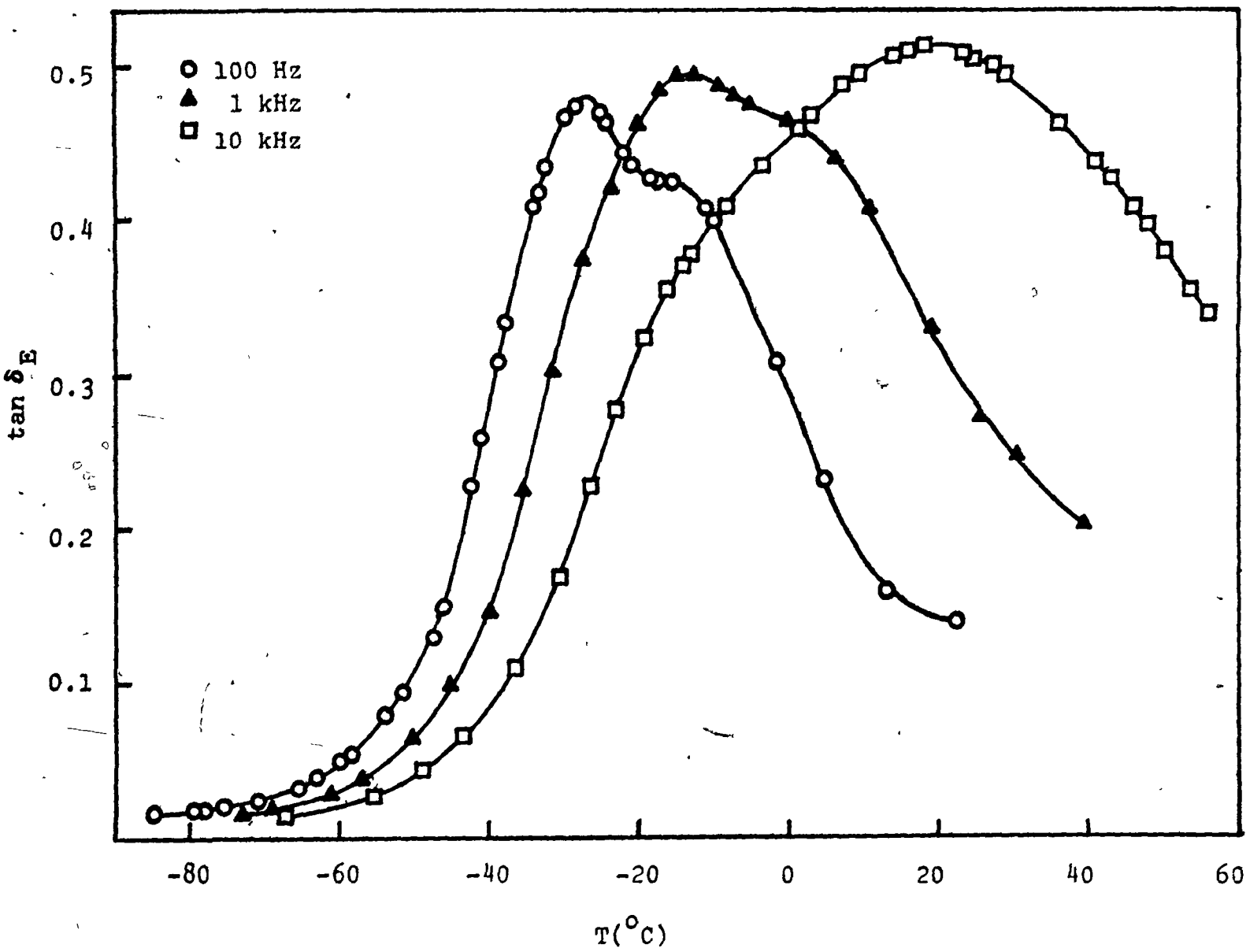
100 Hz
1 kHz
10 kHz
0.5
0.4
0.3
0.2
0.1
tan δE
-80
-60
-40
-20
0
20
40
60
T(°C)

FIGURE 29.

Dielectric loss tangent vs. temperature for "Nafion"-H with 3 H_2O/SO_3H at 100 Hz, 1kHz and 10kHz.

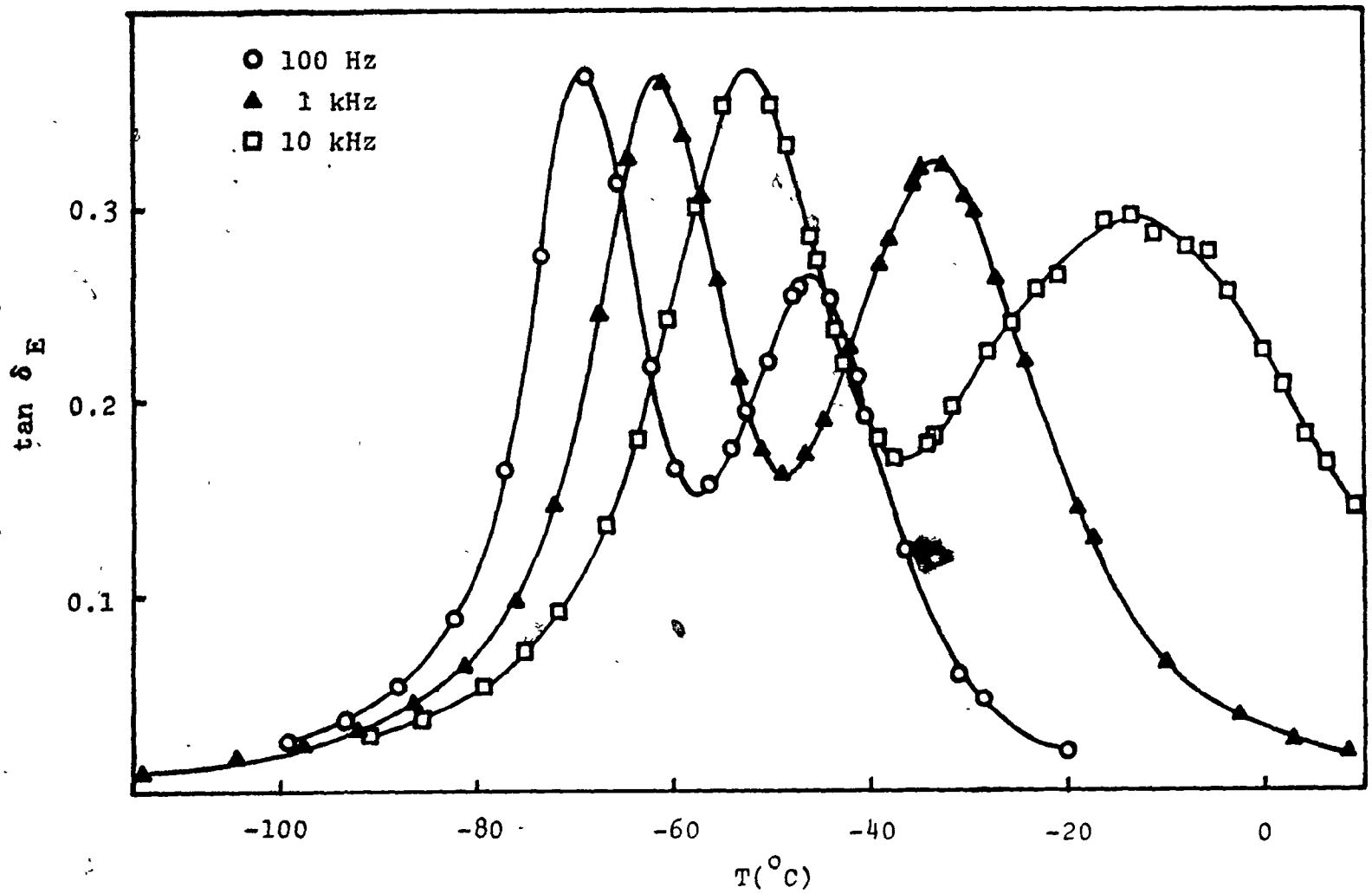
100 Hz
1 kHz
10 kHz
tan δE
0.3
0.2
0.1
-100
-80
-60
-40
-20
0
T(°C)

FIGURE 30.

Dielectric loss tangent vs. temperature for "Nafion"-H with 4 H_2O/SO_3H at 100 Hz, 1kHz and 10kHz.

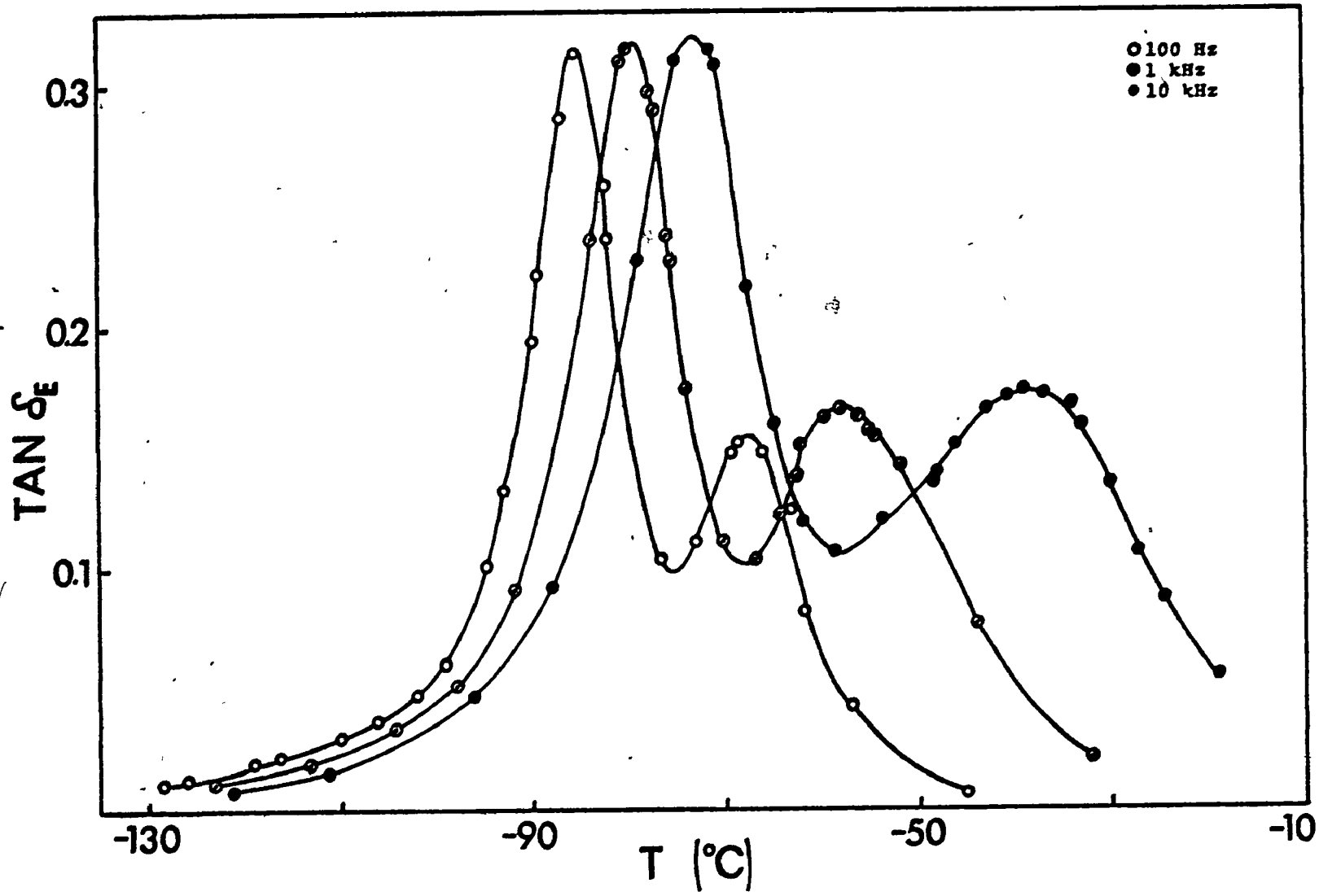
100 Hz
1 kHz
10 kHz
0.3
0.2
0.1
TAN δE
-130
-90
-50
-10
T (°C)

FIGURE 31.

Dielectric loss tangent vs. temperature for "Nafion"-H with varying water content at 100 Hz.

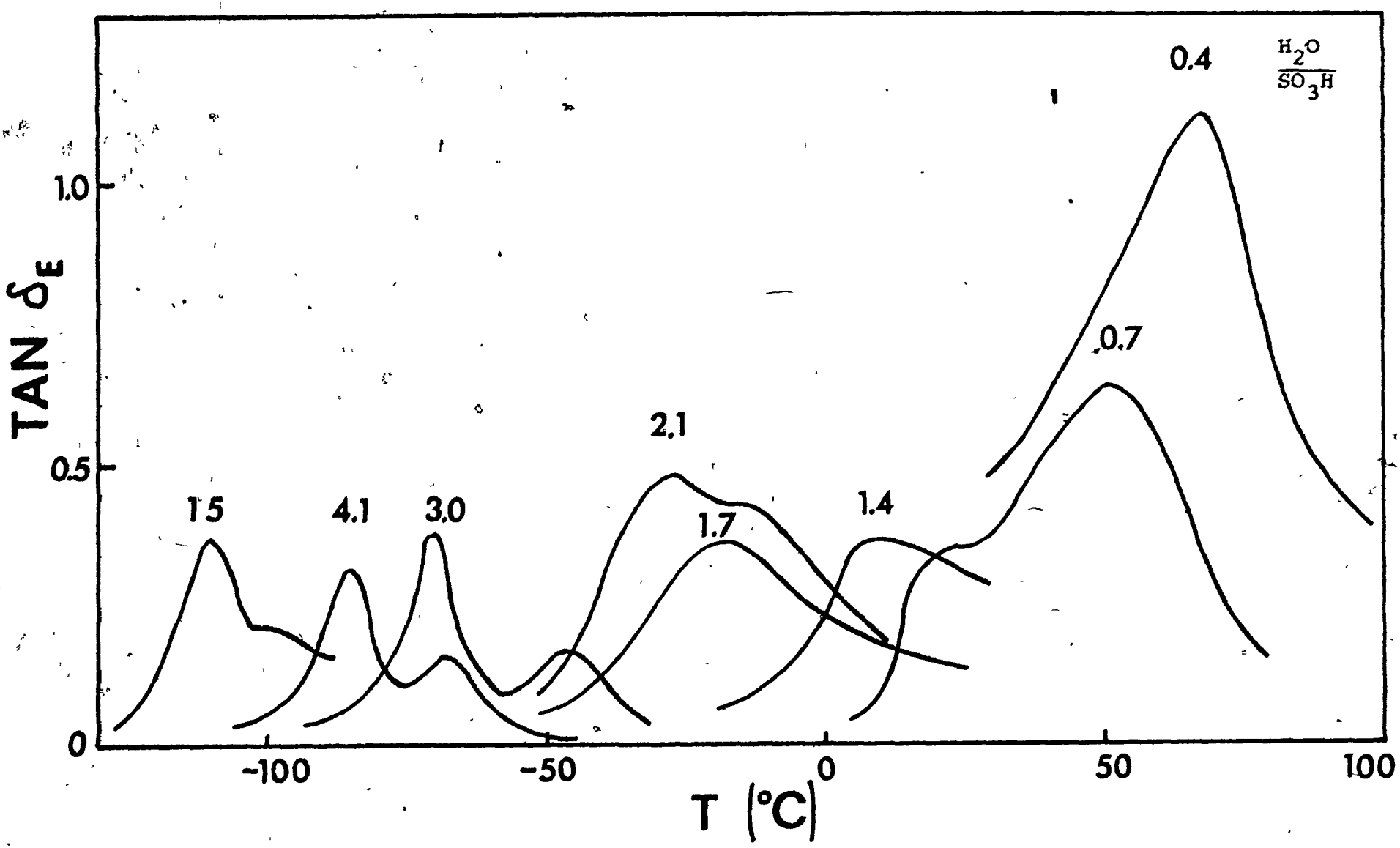
TAN δ_E
1.0
0.5
0
-100
-50
0
50
100
T (°C)
0.4
$\frac{H_2O}{SO_3H}$
0.7
2.1
1.5
4.1
3.0
1.7
1.4

FIGURE 32.

Mechanical β peak position and dielectric major peak position vs. water content for "Nafion"-H.

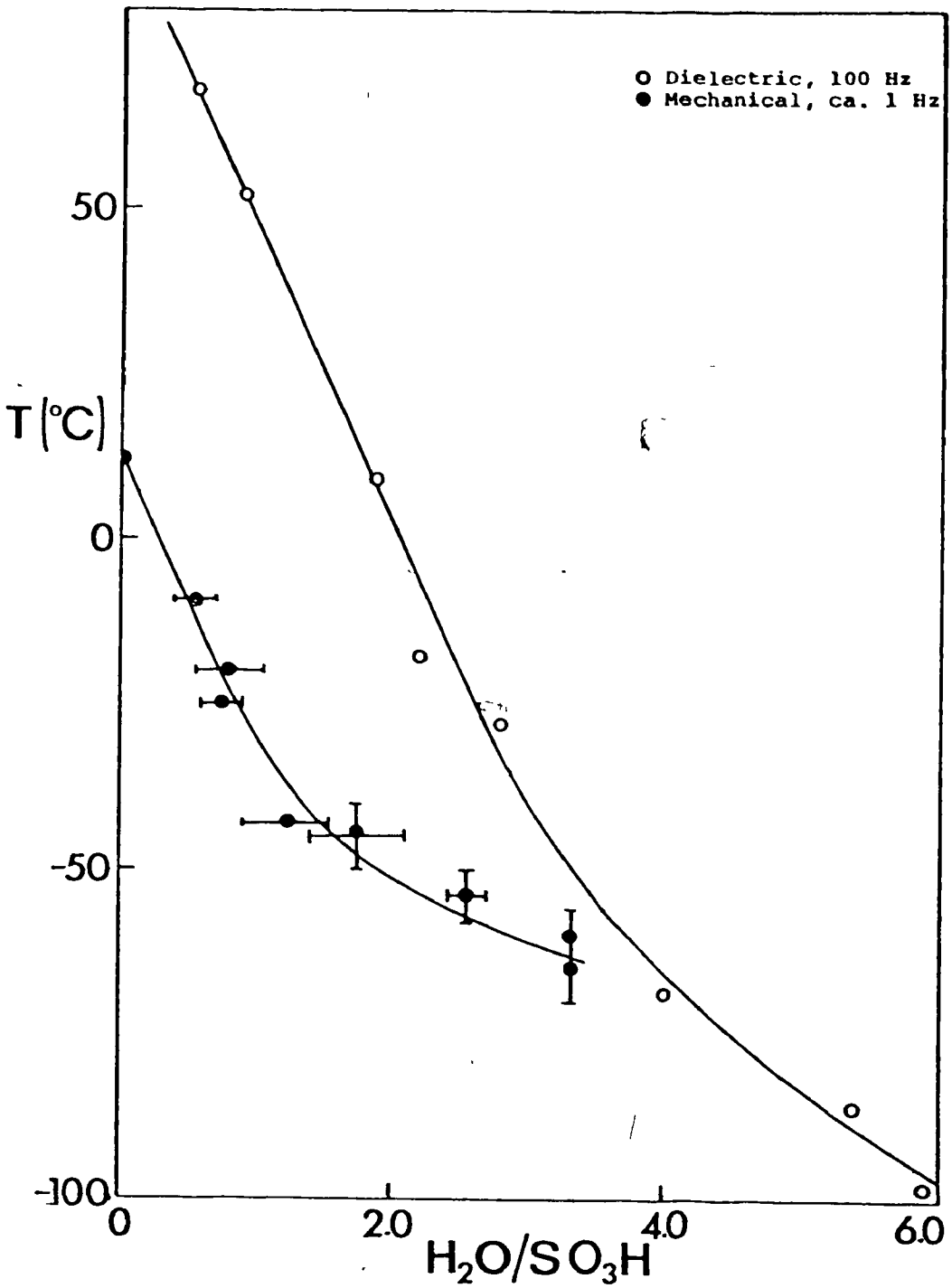
O Dielectric, 100 Hz
● Mechanical, ca. 1 Hz
50
0
-50
-100
T (°C)
0
2.0
4.0
6.0
H2O/SO3H

FIGURE 33.

Log ν vs. 1/T for dielectric major peak for "Nafion"-H.

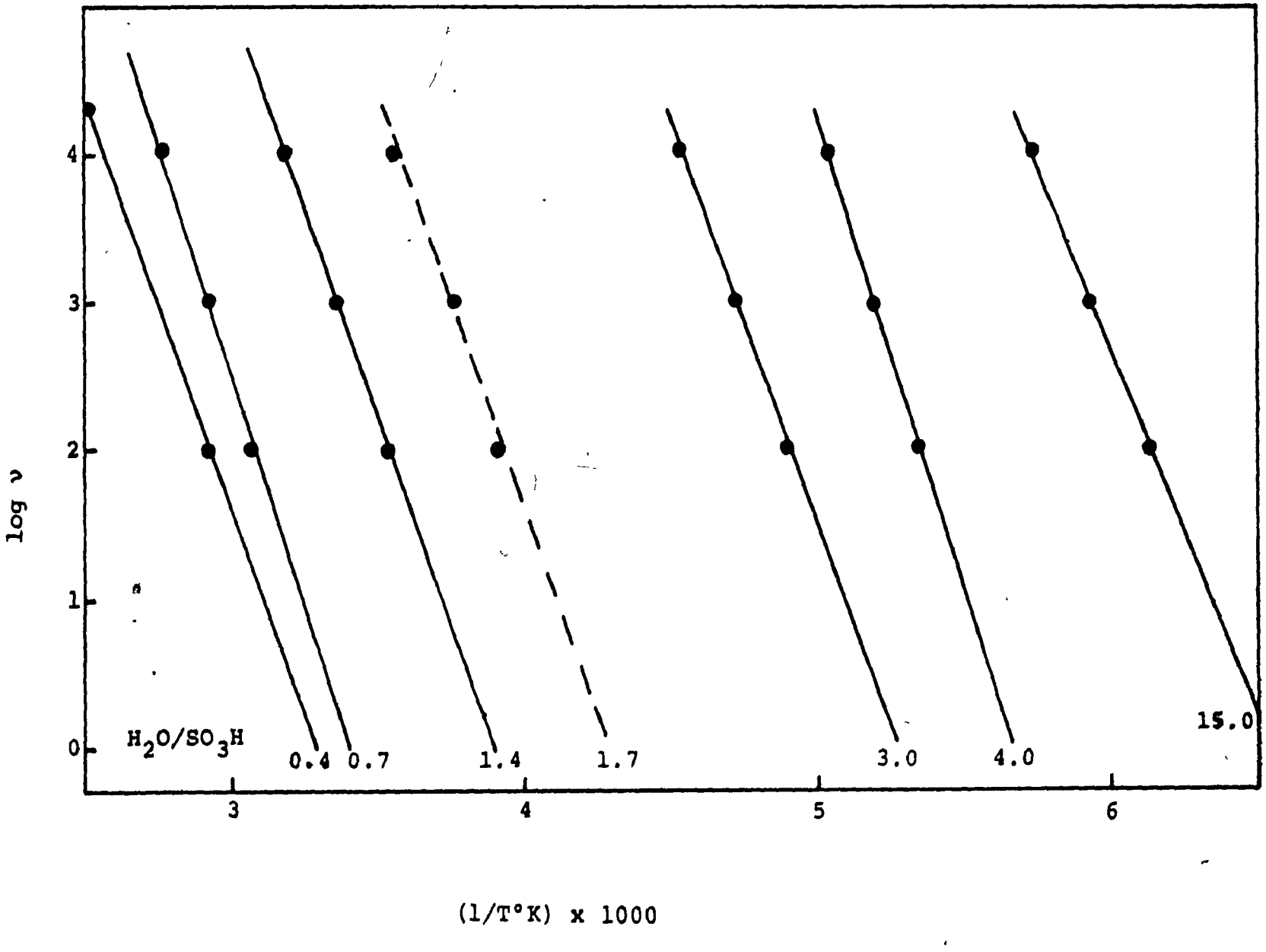
log ν
4
3
2
1
0
H_2O/SO_3H
0.4
0.7
1.4
1.7
3.0
4.0
15.0
3
4
5
6
(1/T°K) x 1000

FIGURE 34.

Dielectric loss tangent vs. temperature for "Nafion"-K with 1.9 H_2O/SO_3H at 100 Hz, 1kHz and 10kHz.

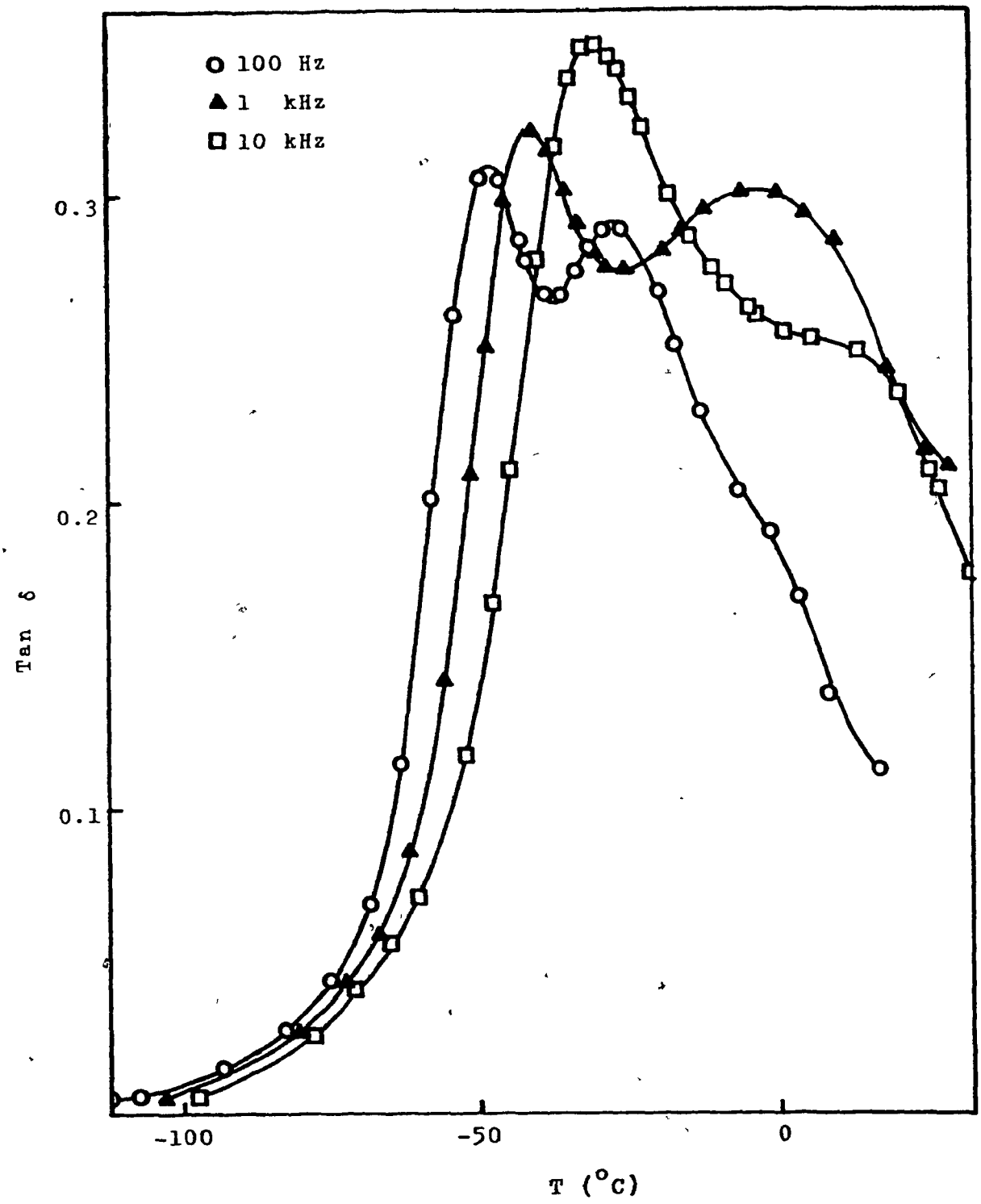
100 Hz
1 kHz
10 kHz
0.3
0.2
0.1
Tan δ
-100
-50
0
T (°C)

FIGURE 35.

Dielectric loss tangent vs. temperature for "Nafion"-K with 3.6 H_2O/SO_3H at 100 Hz, 1kHz and 10kHz.

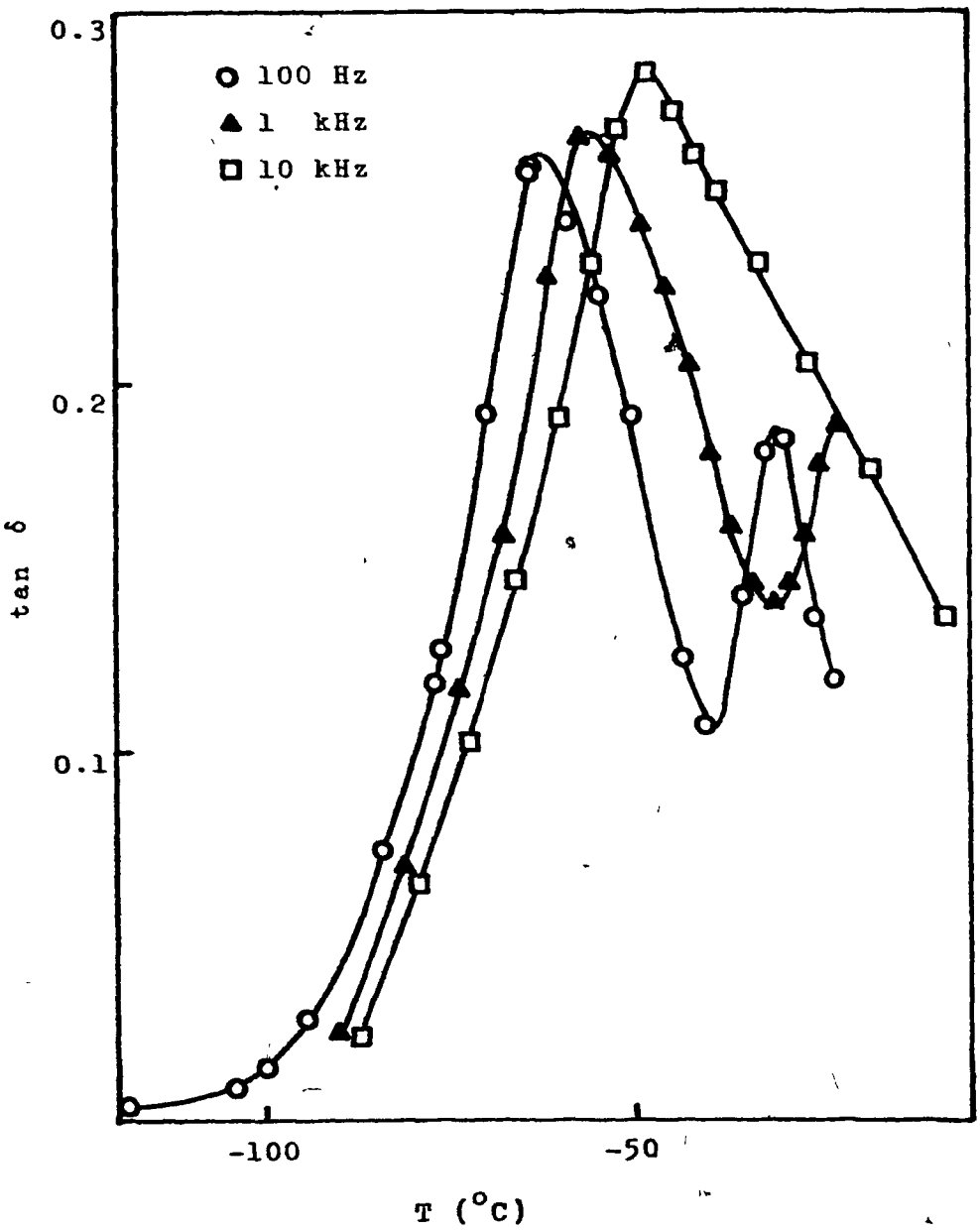
0.3
0.2
0.1
tan δ
100 Hz
1 kHz
10 kHz
-100
-50
T (°C)

FIGURE 36.

Dielectric loss tangent vs. temperature for "Nafion"-K with varying water content at 100 Hz.

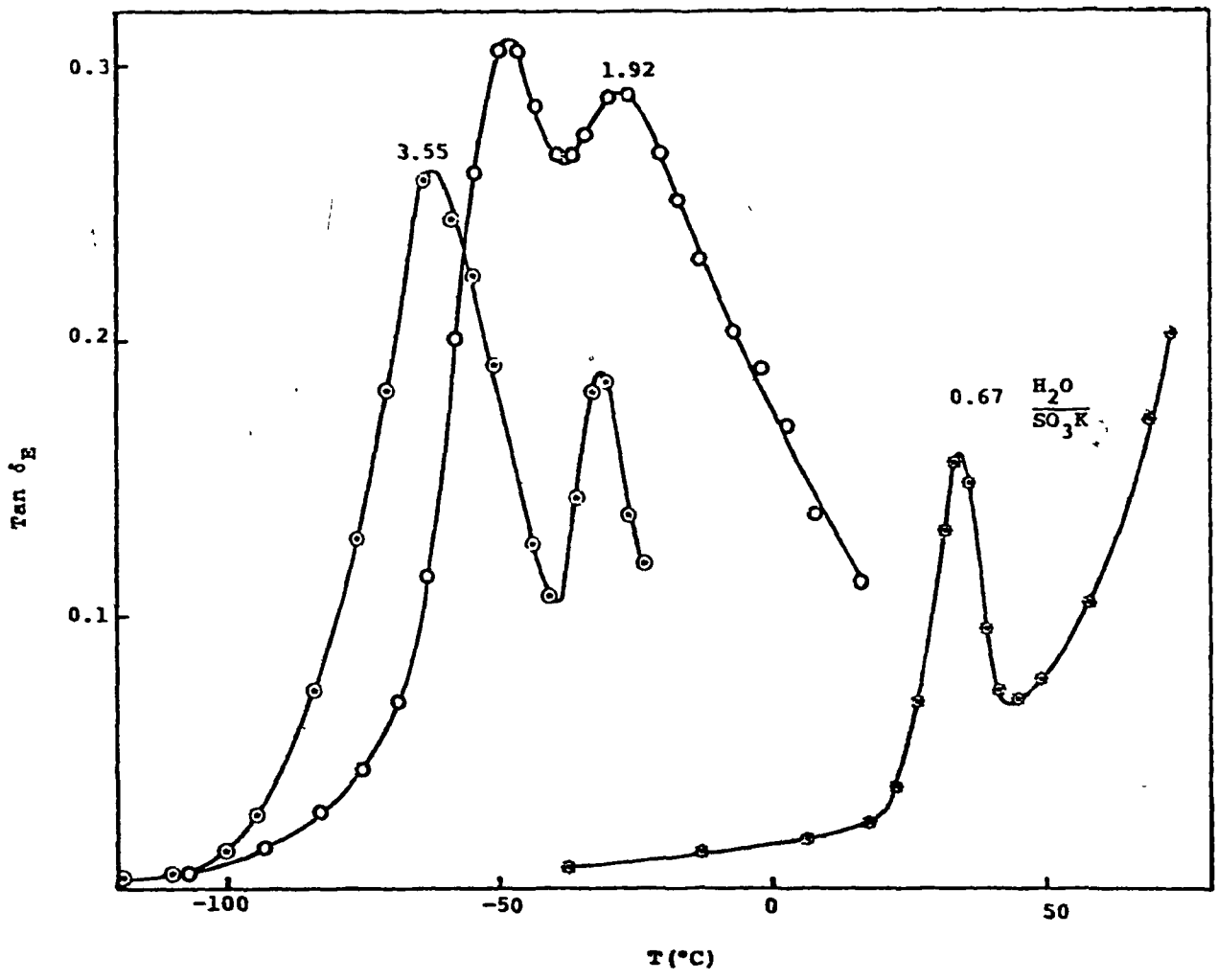
0.3
0.2
0.1
Tan δ_E
3.55
1.92
0.67
$\frac{H_2O}{SO_3K}$
-100
-50
0
50
T(°C)

FIGURE 37.

Mossbauer spectrum of "Nafion"-Fe (EW = 1155).

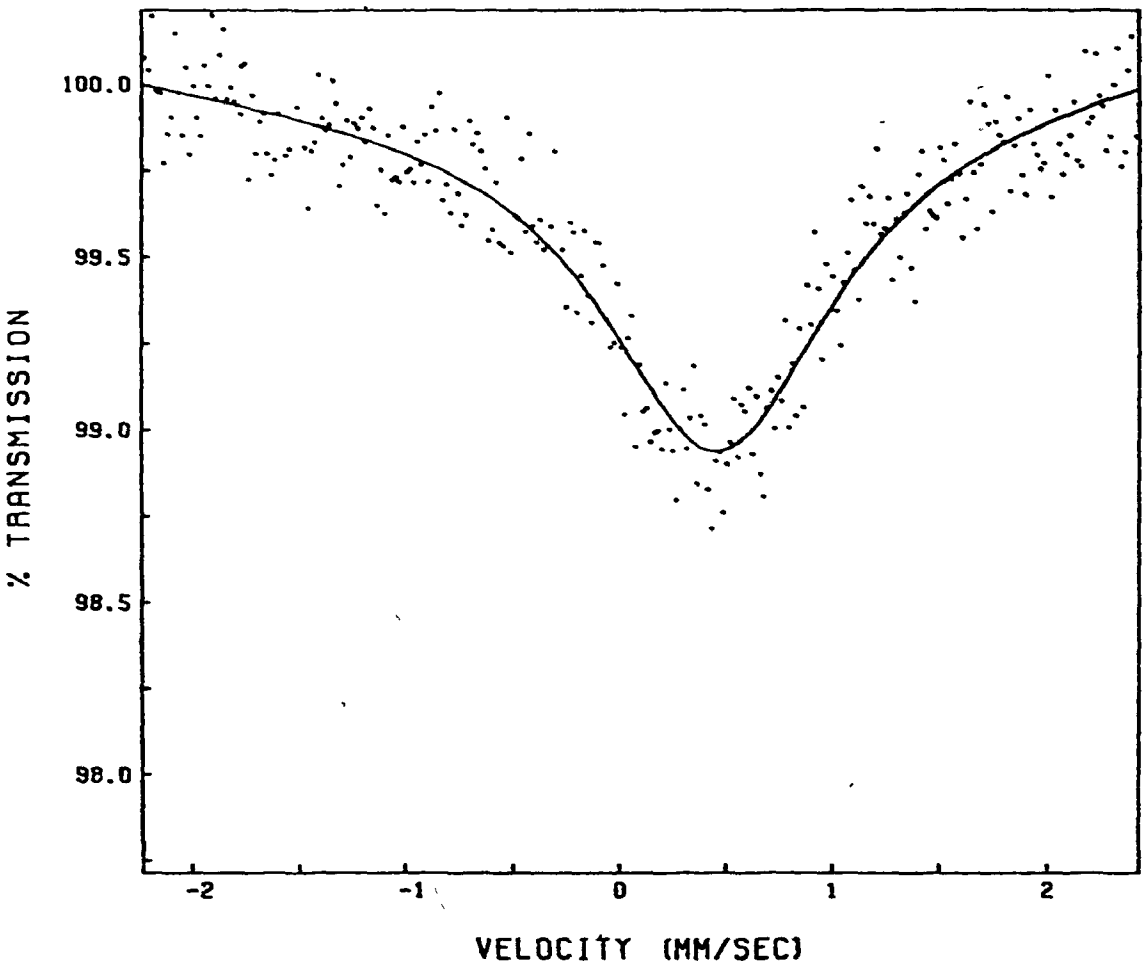
100.0
99.5
99.0
98.5
98.0
% TRANSMISSION
-2
-1
0
1
2
VELOCITY (MM/SEC)

FIGURE 38.

Mossbauer spectrum of "Nafion"-Fe (EW = 1365)
Singlet fitting.

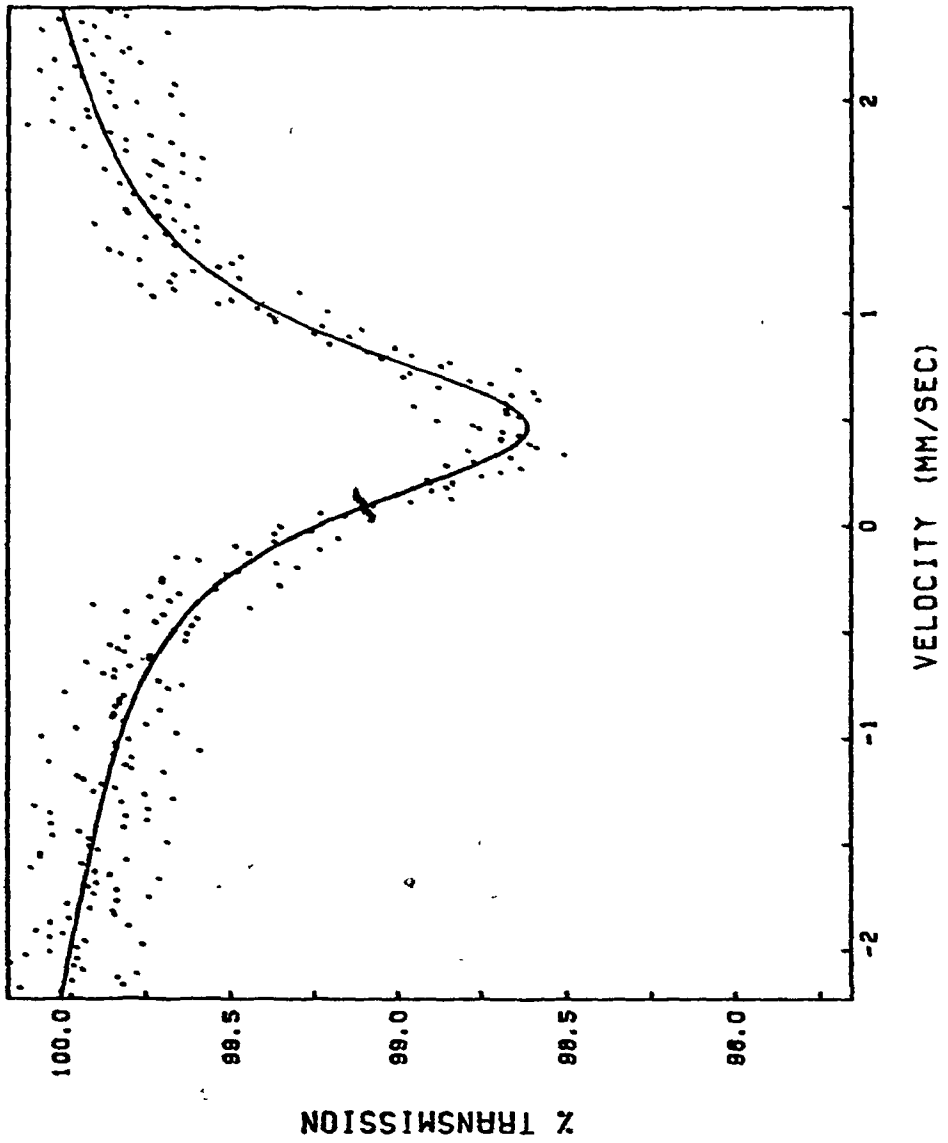
% TRANSMISSION
100.0
99.5
99.0
98.5
98.0
VELOCITY (MM/SEC)
-2
-1
0
1
2

FIGURE 39.

Mossbauer spectrum of "Nafion"-Fe (EW = 1365)
Doublet fitting.

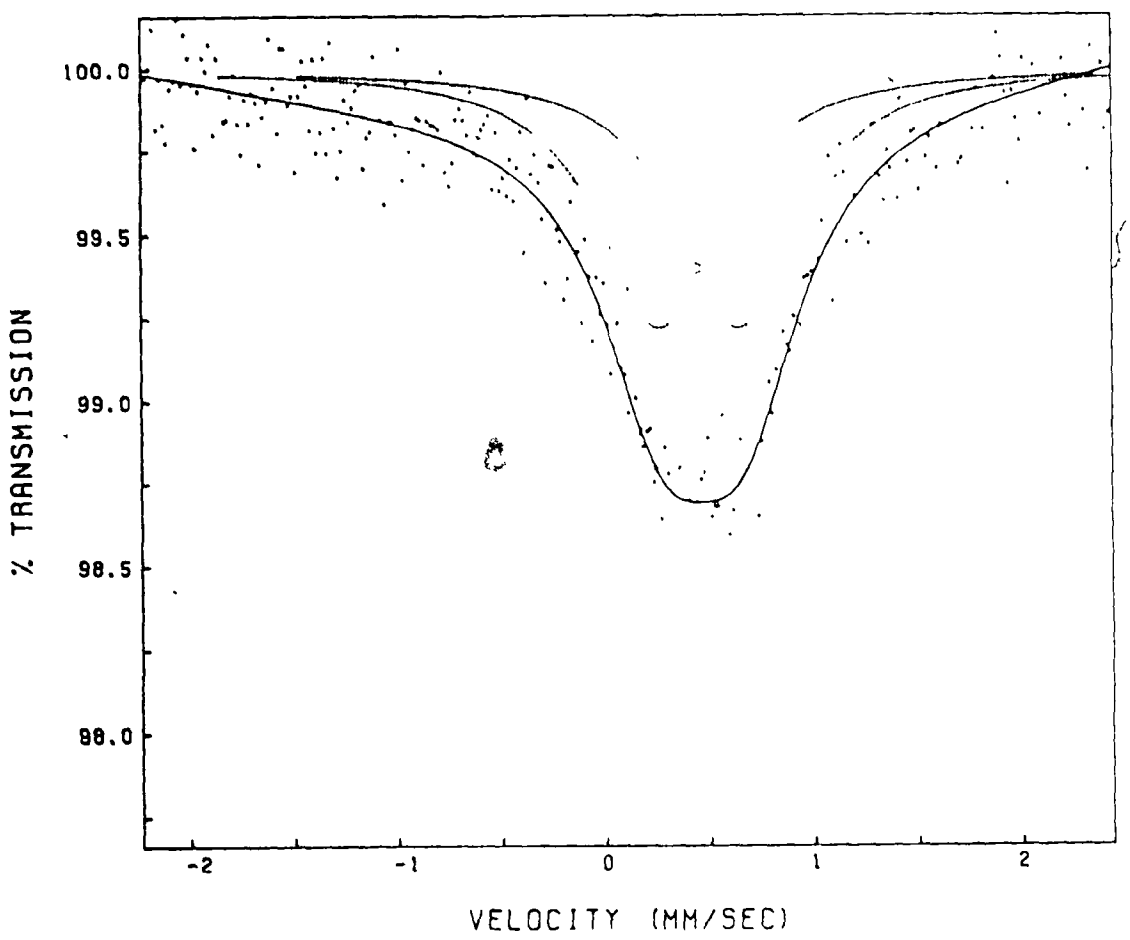
100.0
99.5
99.0
98.5
98.0
% TRANSMISSION
-2
-1
0
1
2
VELOCITY (MM/SEC)

4. DISCUSSION

4.1 Glass Transition and Linear Expansion

While the agreement between DSC and tan δ results for the glass transition of the "Nafions" is gratifying, the values obtained by the above technique are seemingly inconsistent with the low value of the 10-second modulus, $E_r(10)$, for the same materials at the glass transition temperature. As can be seen in Fig. 11, for the styrene ionomers the $E_r(10)$ value at the glass transition temperature is of the order of 10^{10} dynes/cm^2, while for the "Nafions" the value is two orders of magnitude lower, both for the acid and the salt. Also, an inspection of Fig. 5 reveals that in the glassy region the stress relaxation master curve for "Nafion"-H is placed ca. 10 orders of magnitude of time below that for the styrenes, reflecting the same problem as was found in the isochronal modulus curve. On the basis of the stress relaxation or modulus temperature curves, it might be tempting to think of the glass transition as being closer to 30°C for the acid and to 100°C for the potassium salt. The acid does show a tan δ peak (ca. 1 Hz) at 23°C, but this peak is extremely small (tan δ = 0.07) in comparison with the glass transition peak (tan δ = 0.4). Furthermore, the salt shows no peak or shoulder at 100°C, the β region appearing only 40 to 60° higher; however, here again the peak value of tan δ above the background is only 0.04 to 0.06, which suggests that it is, most probably, not the glass transition. Thus, in spite of the low value of the modulus, it seems preferable to take the high temperature tan δ peaks (i.e. ca. 110°C for the acid and ca. 220°C for

the salts) as the glass transition temperature. Also, the results of studies on wet samples, to be discussed later, support this interpretation.

If this low value of the modulus at the glass transition is correct, then some type of unusual packing in these materials is to be inferred. This unusual packing, incidentally, might also correlate with the high water transport and high dimensional expansion that is observed. The densities of the materials are most revealing in this context. The density of the "Nafion" precursor (the material in which the $-SO_3H$ group is replaced by SO_2F) is ca. 2.1 for an equivalent weight of 2100[85] and that of PTFE is 2.0[86]. By contrast, the densities of the acid and salts are appreciably lower, suggesting the presence of voids (or pores) and channels.

4.2 Transient Studies

Despite the absence of crystallinity, as revealed by x-ray studies, the stress relaxation master curves for the "Nafions" (Figs. 5 - 7) are quite broad, resembling those of the styrene ionomers much more so than those of polystyrene or other non-ionic and non-crystalline polymers. Furthermore, time-temperature superposition breaks down for both the dry potassium salt below 180°C and the acid in the presence of 0.5 H_2O/SO_3H. These data, together with the presence of halo at a low angle in SAXS, suggest that in the "Nafions" the ions are clustered in the same way as in the other ionomers. It should be recalled, in this context, that, clustering is taken to mean not just simply small

scale ion aggregation of the type leading to crosslinking, but large scale clustering incorporating a large number of ions and also some non-ionic material.

The failure of time-temperature superposition is a very strong indication that the ionic regions contribute to the relaxation process. Most probably this involves a reorganization of the cluster, possibly a hopping of sulfonate terminated side chains. This would represent a secondary relaxation mechanism and contribute to the total relaxation. The breadth of the distribution of relaxation times (Fig. 8) as well as the breadth of the modulus-temperature curves (Fig. 11) also support the idea that this polymer is phase separated, since it parallels the behavior in the styrenes. The fact that superposition applies in the dry acid but fails in the presence of 0.5 H_2O/SO_3H is puzzling, but might indicate that the secondary process, while present, contributes very little to the total relaxation in the dry material. This is consistent with the finding in plasticized poly (sodium acrylate) that water, even in large amounts, decreases the lifetime of the clusters without destroying them[88].

The re-establishment of time-temperature superposition in the potassium salt is also consistent with the behavior of a low molecular weight clustered polystyrene ionomer containing 7.9 mol% sodium methacrylate. In contrast to the high molecular weight styrene ionomers, which remain thermorheologically complex even at the highest temperatures which were studied, in that particular low molecular weight sample time-temperature superposition is re-established above ca. 180°C. This suggests that

at those high temperatures the secondary mechanism does not contribute appreciably to the relaxation, possibly because of a breakdown, or shortening of the life-time, of the clusters. In many other polymers, it has been shown that molecular weight has a strong effect on phase separation, with high molecular weight samples showing the greatest tendency to phase separate. Furthermore, it is found that ion clusters can maintain their integrity up to 180°C in other ionomers as well[15,80].

A comparison of the master curves of degraded and undegraded "Nafion"-H (Fig. 10) reveals that the long-time modulus, which correlates with crosslinking, increases with degradation. This fact, coupled with the lower water absorption of the degraded sample, and the disappearance of the SAXS peak (Table 4) suggests that above 180°C the ion clusters decompose, and, that possibly smaller ionic aggregates or multiplets are formed. These multiplets behave as temporary cross-links, a phenomenon which is also found in many other ionomers.

It is worth noting that for "Nafion" linear viscoelasticity is valid only for small deformations (less than 2%) as is also the case for PTFE[89]. For the latter, it has been suggested[89] that the nonlinearity arises from the inherent crystallinity and deformation induced crystallization. However, no crystallinity is found in "Nafion", and the cause of the nonlinear behavior must therefore lie elsewhere.

The failure of time-temperature superposition could be caused either by nonlinear viscoelasticity or by the presence of a second relaxation mechanism. In the former case, superposition should be achieved by vertical shifting as well as the unusual horizontal shifting. This is not found, however, indicating that a second mechanism is the

probable cause of the non-superimpossibility. Moreover, the fact that for the "Nafion"-K superposition is re-established above 180°C, indicates that the nonsuperimpossibility is not due to nonlinearity. Also, the small angle x-ray scattering peak which was observed in "Nafions", suggests that well defined large ion aggregates exists, which may be the locus of the proposed secondary relaxation.

4.3 Dynamic Studies

A dynamic mechanical investigation of the α relaxation in the acid, which has been ascribed to the glass transition, reveals that water (ca. 3 H_2O/SO_3H) has only a minor effect on the magnitude or position of the peak. This tends to reinforce the identification of the peak as due to the glass transition of the non-ionic phase. Water would not be expected to interact with the hydrophobic fluorocarbon backbone, but would interact strongly with the ionic regions. Therefore, if this peak were due to the ionic regions, then a strong lowering of its position would be expected as the water content is increased, as is found in the case of nylon[90].

In the salts, the position of the α peaks for Na^+, K^+ and Cs^+ salts is in qualitative agreement with the q/a effect which has been found operative in many ion-containing polymers[91]. This effect suggests that the glass transition should be proportional to the ratio of the cation charge, q, to the distance between centers of charge, a. The fact that the Li^+ salt does not fit this relation suggests possibly that some of the SO_3H groups have not been converted into SO_3Li form because of the selective rule (Li<H<Na<K<Cs). The effect

of water on the position of the α peak could not be studied because the desorption rate of water in these materials is high at the glass transition.

The mechanical β peak in the dry acid occurs at 23°C at ca. 1 Hz and moves to lower temperatures with increasing water content. Similar behavior is seen in the salt, a shoulder appearing at ca. 150°C in the dry materials, and again moving to lower temperatures with increasing water content, although now as a small peak. The downward motion of the peak with increasing moisture parallels the behavior found in many other polar polymers such as polyacrylamide[92], nylon[93] and polyvinyl alcohol[94]. This type of behavior is most probably due either to a change in the nature of the moving group which is responsible for the specific relaxation, or to a change in the barrier which hinders the motion of the group, or to both. In the "Nafions", however, a third possibility exists. Since the polar groups probably exist in clusters, it is quite possible that we are dealing with the glass transition of these highly polar regions. This interpretation is reinforced by the drastic decrease in peak temperature with water content (Figs. 16, 21 and 22). The drastic effect of water is, incidentally, further evidence against identifying the β peak with the glass transition of the bulk phase, since PTFE would not be expected to interact with H_2O. As can be seen, the α peak, at least in the acid, is insensitive to water, and is thus most likely the glass transition. With regard to the β region, on the other hand, the higher tan δ values observed in the dielectric experiments, compared to those observed in the mechanical tests, again indicate that we are dealing with the polar

regions. It is however, also possible that the β peak is due to a more specific motion within the ionic region or of a polar group, such as the ether oxygen or a water-ether complex.

Only very few experiments were performed on the mechanical β peak in the salts. In so far as it has been studied, its behavior as a function of water content parallels that of the acid, except that the peak is much smaller in the dry salt than in the acid, and it occurs at ca. 150°C. It is reasonable to infer that the ionic regions in the salts hold together much more tightly than those in the acid, and thus contribute much less to the relaxation. The absence of the β peak in the degraded sample again reinforces the suggestion that the β peak reflects a relaxation in the ionic region, since, as discussed previously, the ionic clusters are destroyed as degradation proceeds.

Since the position and the activation energy of the γ peak in both the acid and the salt are the same as those found in PTFE, there is little doubt that in all cases it is due to the same mechanism. The height of the peak is affected somewhat by the type of ion used, but this effect is not drastic. It is worth recalling that the height of this peak is also affected by the level of crystallinity in PTFE.

The dielectric results are most unusual. Clearly the major relaxation of the acid involves two peaks (Figs. 27 and 33), the mechanism of the higher peak being probably independent of water content throughout the region. While the position and the height of that peak varies with water content, its activation energy does not. It

is conceivable, although by no means certain, that this peak is due to the glass transition of the polar regions. This is supported by the rapid change of the peak position with water content, but would appear to be inconsistent with the observed invariance of the activation energy. The origin of the minor peak remains unknown.

4.4 X-ray Scattering and Mossbauer Effect Spectroscopy

The presence of a SAXS peak is clear evidence in support of the clustering suggestion. Many ion-containing polymers show this behavior, among them the ionomers based on ethylene and styrene. Single peak data are difficult to interpret, but the presence of such a peak, without a doubt, is related to the presence of distinct scattering centers in the polymer.

The Mossbauer effect is a technique well suited for the study of the influence of condensed phases on the binding and mobility of exchangeable cations in polyanionic frameworks.

The values of the isomer shift for both equivalent weights correspond to an effective 4s electron contribution[70] of ca. 5%. They indicate that the bonding between Fe^{3+} and the polymer sulfonate group is predominantly ionic[98]. This is in agreement with previous results[99-103] on other materials. Ferric ion has a d^5 electronic configuration and hence a spherically symmetric charge distribution. It should, therefore, be characterized by the absence of any electric field gradient at the nucleus unless an unsymmetric environment produces such a gradient. However, the small quadrupole splitting in the high equivalent weight sample suggests that the 4s electron distribution of Fe in the high equivalent weight "Nafion" is partially distorted in

contrast to the low equivalent weight sample. Furthermore, the wide linewidth indicates either that a distribution of environments exist, or that the ions diffuse. The former seems more likely, although both are possible.

4.5 Diffusion and Drying

The difference in the drying behavior between the acid and the salt is profound. Figure 1 shows clearly that the interaction of water with the acid is much stronger than with the salt; already at 100°C the salt can be obtained in a dry state, while a temperature of over 160°C is necessary for the acid. It is also clear that the salt is much more stable than the acid at high temperatures, the degradation curve for the salt being ca. 130°C higher than for the acid. These results parallel the findings of the Du Pont group[85].

The diffusion coefficient for water in the acid is extremely high, higher than that for any other partly ionic or non-ionic polymer for which data are available. It is comparable to that of the ion exchange resins and only one order of magnitude lower than the self-diffusion coefficient of water itself[104]. Furthermore, the activation energy for diffusion is only 4.8 Kcal/mole, close to that for the ion exchangers and for self-diffusion of water. Table 5 compares the diffusion coefficients and activation energies for diffusion for a wide range of representative polymers, showing that "Nafion" is, indeed very permeable and comparable to the completely ionic ion exchangers. This fact reinforces the suggestion of unusual packing of the polymer chains in the "Nafions". This low density packing is undoubtedly due to the presence of the ionic aggregates. It should be noted, however, that

the presence of ions does not always decrease the diffusion coefficient for water. In the case of polystyrene, for example, at 9.7 mol% of ions (i.e. in the clustering region), the diffusion coefficient *vis a vis* the non-ionic material is decreased by a factor of 500 (see Table 5).

TABLE 5

DIFFUSION COEFFICIENTS OF WATER IN COMMON POLYMERS AND SELF-DIFFUSION COEFFICIENT OF WATER

	Temperature (°C)	D(cm^2/sec)	E_D (Kcal/mole)	Reference
Self-diffusion of Water	25	3×10^{-5}	4.41	102
"Nafion"-H (EW = 1155)	28	2.3×10^{-6}	4.8	
(EW = 1365)	28	2.6×10^{-6}		This work
Polystyrene-sulfonate				
(4% DVB)	25	9.1×10^{-6}	4.6	103
(16% DVB)	25	2.2×10^{-6}	5.2	
Polystyrene	26	5.5×10^{-7}		Appendix II
Polyethylene(ρ = 0.922)	25	2.3×10^{-7}	14.2	104
Ethyl Cellulose	25	1.8×10^{-7}	6.3	105
Polymethyl methacrylate	50	1.3×10^{-7}	11.6	106
Polyvinyl chloride	30	1.6×10^{-8}	10	107
Nylon 6	25	9.7×10^{-10}	6.5	108
Styrene Ionomer	25	9.0×10^{-10}		Appendix II

5. CONCLUSIONS

Perhaps the most interesting conclusion of this study concerns the supermolecular structure of the "Nafions". It is suggested that the sulfonate groups are highly ionic, as revealed by Mossbauer effect results, and these ions in the materials are clustered, i.e. present in large aggregates containing also some fluorocarbon material. This suggestion is based on both the rheological properties of the material and the existence of a small angle x-ray scattering peak.

The glass transition is much higher than would be expected on the basis of rheological data alone. The discrepancy suggests an unusual packing effect, which is also supported by the high value of the diffusion coefficient for water and the low activation energy as well as by the decrease of density on neutralization.

The failure of time-temperature superposition in the materials suggests the presence of two relaxation mechanisms, one due to chain diffusion (as in normal organic polymers) and the other to the presence of ionic clusters (as are also found in the clustered styrene ionomers, among others). The secondary mechanism most probably involves a hopping of ion-terminated chains from one cluster to another. The clusters seem to become mobile above 180°C, as suggested by re-establishment of time-temperature superposition above that temperature in the salts.

The β peak in dynamic studies is probably also related to the ionic regions. Its position is strongly affected by the presence of water, and may reflect the glass transition in those regions. Dielectrically, a double peak is observed which is also highly sensitive to water. The

γ peak is of the same origin as in PTFE.

The diffusion coefficient for water is extremely high, higher than in any other non-ionic or partly ionic polymer for which data are available, and comparable to that of ion exchange resins although the polymer has a very different structure. The activation energy is comparable to that for self-diffusion in pure water.

It is evident that the "Nafions" resemble other organic ionomers in a wide range of properties, notably in the presence of ion clustering and the resultant effect on the rheology of the materials. By contrast, the dramatic decrease in the density upon ionization and the accompanying increase in the diffusion coefficient for water are novel features, not encountered in other ionomers. The reason for this difference needs to be elucidated. Finally, the dynamic mechanical studies suggest that, at least in the presence of water, the glass transition of the ionic regions may be lower than that of the matrix. This has also not been encountered in other ionics.

REFERENCES

1. G. F. Baumann, Advances in Chemistry Series, 96, 30 (1969).
2. R. H. Kinsey, Applied Polymer Symposia, 11, 77 (1969).
3. R. W. Rees and D. J. Vaughan, Polymer Preprint, 6, 296 (1965).
4. T. C. Ward and A. V. Tobolsky, J. Appl. Polym. Sci., 11, 2403 (1967).
5. E. P. Otocka and T. K. Kwei, Macromolecules, 1, 301 (1968).
6. E. F. Bonotto and E. F. Bonner, Macromolecules, 1, 510 (1968).
7. W. J. MacKnight, L. W. McKenna and B. E. Reed, J. Appl. Phys., 38, 4208 (1968).
8. P. J. Phillips and W. J. MacKnight, J. Polym. Sci., A2, 8, 727 (1970).
9. K. Sakamoto, W. J. MacKnight and R. S. Porter, J. Polym. Sci., A2, 8, 277 (1970).
10. S. R. Rafikov et al, Vysokomol. Soyed., A15, 1974 (1973).
11. C. L. Marx and S. L. Cooper, J. Macromol. Sci., B9, 19 (1974).
12. W. E. Fitzgerald and L. E. Nielsen, Proc. Roy. Soc., A282, 137 (1964).
13. N. Z. Erdi and H. Morawetz, J. Colloid Sci., 19, 708 (1964).
14. A. Eisenberg and M. Navratil, J. Polym. Sci., B10, 537 (1972).
15. A. Eisenberg and M. Navratil, Macromolecules, 6, 604 (1973).
16. M. Navratil and A. Eisenberg, Macromolecules, 7, 84 (1974).
17. A. Eisenberg and M. Navratil, Macromolecules, 7, 90 (1974).
18. B. F. Goodrich, British Patent 707, 425 (1954).
19. W. Cooper, J. Polym. Sci., 28, 195 (1958).
20. E. P. Otocka and F. R. Eirich, J. Polym. Sci., A2 6, 921 (1968).

21. E. P. Otocka and F. R. Eirich, J. Polym. Sci., A2, 6, 933 (1968).

22. M. Pineri, C. Meyer, A. M. Levelut, and M. Lambert, J. Polym. Sci., Polym. Phys., 12, 115 (1974).

23. J. Moacanin and E. F. Cuddihy, J. Polym. Sci., C14, 313 (1966).

24. A. Eisenberg, Adv. Polym. Sci., 5, 59 (1967).

25. A. Eisenberg, Macromolecules, 3, 147 (1970).

26. C. L. Marx, D. F. Caulfield and S. L. Cooper, Macromolecules, 6, 344 (1973).

27. W. J. MacKnight, W. P. Taggart and R. S. Stein, J. Polym. Sci., C45, 113 (1974).

28. G. M. Estes, S. L. Cooper and A. V. Tobolsky, in "Reviews in Macromolecular Chemistry" Vol. 5, Pt. 2, 167 (1970).

29. S. L. Aggarwal, ed., "Block Polymers", Plenum Press, (1970).

30. D. J. Meier, J. Polym. Sci. C26, 81 (1969).

31. J. D. Ferry, "Viscoelastic Properties of Polymers", Wiley, New York, (1970), Chp. 16.

32. W. J. MacKnight, T. Kajiyama, and L. McKenna, Polymer Eng. Sci., 8, 267 (1968).

33. H. Matsuura and A. Eisenberg, J. Polym. Sci., Phys., in press.

34. A. Eisenberg, H. Farb and L. G. Cool, J. Polym. Sci., A2, 4, 855 (1966).

35. A. Eisenberg, M. King and N. Navratil, Macromolecules, 6, 734 (1973).

36. D. J. Vaughan, Du Pont Innovation, 4, No.3, 10 (1973).

37. H. H. Gibbs and R. N. Griffin, "Fluorocarbon Sulfonyl Fluorides", U.S. Pat. 3,041,317 (June 26, 1962).

38. D. J. Connolly and W. F. Gresham, "Fluorocarbon Vinyl Ether Polymers", U.S. Pat. 3,282,875 (Nov. 1, 1966).

39. R. E. Putnam and W. D. Nicoll, "Fluorocarbon Ethers Containing Sulfonyl Groups", U.S. Pat. 3,301,893 (Jan. 31, 1967).

40. L. K. Blair and W. G. Grot, "Perfluorovinylacetyle Fluoride", U.S. Pat. 3,454,633 (July 8, 1969).

41. P. R. Resnick, "Preparation of Sulfonic Acid Containing Fluorocarbon Vinyl Ethers", U.S. Pat. 3,560,568 (Feb. 2, 1971).

42. W. F. G. Grot, "Surface-Activated Fluorocarbon Objects", U.S. Pat. 3,692,569 (Sept. 19, 1972).

43. W. G. F. Grot, G. E. Munn and P. N. Walmsley, "Perfluorinated Ion Exchange Membranes", presented at the 141st National Meeting, The Electrochemical Society, Houston, Texas, May 7-11, 1972.

44. W. G. F. Grot, Chem. Ing. Tech., 44, 167 (1972).

45. W. G. F. Grot, Chem. Ing. Tech., 47, 617 (1975).

46. W. G. Grot, "Method for Increasing the Liquid Absorptive Capacity of Linear Fluorocarbon Sulfonic Acid Polymer", U.S. Pat. 3,684,747 (Aug. 15, 1972).

47. F. B. Leitz, M. A. Accomazzo and S. A. Michalek, "Development of Electrochemical Hypochlorite Generator". Paper presented at the 141st Meeting of the Electrochemical Society, Houston, Texas, (1972).

48. Hooker Chemical Corporation (R. Falvo), DOS 2409193 (Feb. 26, 1974).

49. J. E. Currey, A. T. Emery, C. S. McLarty, "Future Trends in Chlorine Cells". Paper presented at the Chlorine Bicentennial Symposium, San Francisco, 1974.

50. L. J. Nuttall and W. A. Titterington, "General Electric's Solid Polymer Electrolyte Water Electrolysis". Paper presented at the Conference on the Electrolytic Production Hydrogen, London, Feb. 25, 1975.

51. K. Hass, Chem. Ing. Tech., 47, 124, No. 4 (1975).

52. L. P. Rigdon and J. E. Harrar, Anal. Chem., 46, 696 (1974).

53. J. E. Harrar and R. J. Sherry, Anal. Chem., 47, 601 (1975).

54. W. J. Blaedel and R. A. Niemann, Anal. Chem. 47, 1455 (1975).

55. A. Eisenberg, and T. Sasada, Proc. Second Internat. Conf. Physics of Non-crystalline Solids, Delft, July, 1964, p.99.

56. L. A. Teter, "The Viscoelastic Properties of Some Inorganic Polymers", Ph.D. Thesis, U.C.L.A. 1966.

57. R. L. Bergen, Jr., "Testing of Polymers", Vol. 2 (1966).

58. R. E. Kelchner and J. J. Aklonis, J. Polym. Sci., A2, 9, 609 (1971).

59. B. Cayrol, "Segmental Mobility in Poly-p-Phenylene Ethers", Ph.D. Thesis, McGill University, 1972.

60. L. E. Nielsen,"Mechanical Properties of Polymers", Reinhold, 1967.

61. J. D. Ferry, "Viscoelastic Properties of Polymers", Wiley, New York, (1970).

62. F. Schwarzl and A. V. Staverman, Appl. Sci. Research, A4, 127 (1953).

63. M. Navratil, "Structures and Viscoelastic Properties of Styrene-based Ionomers", Ph.D. Thesis, McGill University, 1972.

64. J. Williams, Ph.D. Thesis, McGill University, in preparation.

65. D. R. Bland and E. H. Lee, J. Appl. Phys., 26, 1497 (1955).

66. N. G. McCrum, B. E. Read and G. Williams, "Anelastic and Dielastic Effects in Polymeric Solids", Wiley, New York, (1967), Chp. 1, p. 10.

67. R. D. McCammon and R. N. Work, Rev. Sci. Instru., 36, 1169 (1965).

68. H. Shechter, M. Ron, S. Niedzwiedz and R. H. Herber, Nucl. Instrum. Meth. 44, 268 (1966).

69. D. W. Hafemeister, G. De Pasquali, H. Waard, Phys. Rev., 135, B 1089 (1964).

70. L. R. Walker, G. K. Wertheim and V. Jaccarino, Phys. Rev. Letters 6, 98 (1961).

71. H. Frauenfelder, "The Mossbauer Effect", W. A. Benjamin, New York, (1962).

72. V. I. Goldanskii, "The Mossbauer Effect and Its Application to Chemistry", Consultants Bureau, New York, (1964).

73. G. K. Wertheim, "Mossbauer Effect: Principles and Applications", Academic Press, (1964).

74. L. May, "An Introduction to Mossbauer Spectroscopy", Plenum Press, New York, (1971).

75. G. M. Bancroft, "Mossbauer Spectroscopy", McGraw Hill, England, (1973).

76. J. Crank, "The Mathematics of Diffusion", Oxford University Press, (1956).

77. J. Crank and G. S. Park, "Diffusion in Polymers", Academic Press, (1968), pp 16 and 141.

78. G. J. van Amerongen, Rubber Chem. & Tech., 37, 1065 (1964).

79. N. G. McCrum, J. Polym. Sci., 34, 355 (1959).

80. A. V. Tobolsky, P. F. Lyons and N. Hata, Macromolecules, 1, 515 (1968).

81. R. B. Taylor and A. V. Tobolsky, J. Applied Polyn. Sci., 8, 1563 (1964).

82. D. W. Robinson, quoted by J. A. S. Smith in Discussions Faraday Soc., 19, 207 (1955).

83. J. A. Sauer and D. E. Kline, J. Polym. Sci., 18, 491 (1955).

84. K. Schmieder and K. Wolf, Kolloid Z., 127, 65 (1952).

85. W. G. F. Grot, unpublished data.

86. R. C. Weast, ed., "Handbook of Chemistry and Physics", 50th Edition (1970) p. C-769.

87. H. Yasuda, C. E. Lamaze and A. Schindler, J. Polym. Sci., A2, 9, 1579 (1971).

88. A. Eisenberg, M. King and T. Yokoyama, in "Water-Soluble Polymers", N. Bikales, ed., Plenum Publ. Co.,(1973), p. 349.

89. K. Nagamatsu, T. Yoshitomi and T. Takemoto, J. Colloid Sci., 13, 257 (1958).

90. A. Eisenberg, H. Matsuura and T. Yokoyama, J. Polym. Sci., A2, 9, 2131 (1971).

91. A. Eisenberg, Macromolecules, 4, 125 (1971).

92. J. Kolarik and K. Dusek, J. Macromol. Sci., B10, 157 (1974).

93. Y. S. Papir, S. Kapur, C. E. Rogers and E. Baer, J. Polym. Sci., A2, 10, 1305 (1972).

94. M. Takayanagi, Mem. Fac. Eng. Kyushu Univ., 23 (No. 1), 1 (1963).

95. T. F. Schatzki, J. Polym. Sci., 57, 496 (1962).

96. N. E. Erickson, in "Advances in Chemistry Series", Vol. 68, (1967) p. 94.

97. S. Y. Wang, A. H. Lu and P. K. Tseng, Chin. J. Phys., 2, 50 (1964).

98. V. I. Baranovskii, G. M., Gorodinskii, L. M. Krizhanskii, B. I. Rogozev and S. B. Tomilov, Radiokhimiya, 8, 365 (1966).

99. J. L. Mackey and R. L. Collins, J. inorg. nucl. Chem. 29, 655 (1967).

100. I. P. Suzdalev, A. S. Plachinda, E. F. Makarov and V. A. Dolgopolov, Zh. fiz. Chim., 41, 2831 (1967).

101. A. Johansson, J. inorg. nucl. Chem., 31, 3273 (1969).

102. J. H. Wang, J. Am. Chem. Soc., 73, 4181 (1951).

103. G. E. Boyd and B. A. Soldano, J. Am. Chem. Soc., 75, 6091 (1954).

104. D. Jeschke and H. A. Stuart, Z. Naturf., 16a, 37 (1961).

105. J. D. Wellons and V. Stannett, J. Polym. Sci., A1, 4, 593 (1966).

106. J. A. Barrie and B. Platt, J. Polym. Sci., 4, 303 (1963).

107. P. M. Doty, W. H. Aiken and H. Mark, Ind. Engng. Chem. ind. (int.), 38, 788 (1946).

108. T. Asada and S. Onogi, J. Colloid Sci., 18, 784 (1963).

APPENDIX I

Program for the Calculation of Shift Factors

The following program is designed to compute the shift factors for a series of stress relaxation runs at successively increasing temperatures. It requires a discrete set of force versus time data at each temperature, plus a number of parameters including T_g (or any convenient reference temperature); α_g and α_l (these need only be estimates); σ, Δl and B, as defined in Section 2.5.

Program "MASCURVE"

```
C     SHIFT FACTORS FROM FORCE VS TIME
C
C  SECTION 1 ... ONE SET PER SAMPLE  (MAX. 40 CURVES)
C
C    1ST CARD    NAME :  ALPHAMERIC LABEL OF 80 CHARACTERS                  20A4
C
C    2ND CARD    ALPHAG :  EXPANSION COEF. ABOVE  TG        * 10**6        F10.3
C                ALPHAL :  EXPANSION COEF. BELOW  TG        * 10**6        F10.3
C     IF EXP. COEFFS. ARE NOT KNOWN, ASSUME THEM TO BE ZERO
C                TG     :  IN DEG. C                                       F10.3
C  IPRINT = 0 : ALL DATA & RESULTS PRINTED                                  I5
C  JPRINT = 0 : MODULI TABLE FOR THESIS PRINTED                             I5
C  IPUNCH = 0 : PUNCH OUT MODULI & SHIFT FACTORS FOR CALCOMP PLOT           I5
C  NN     : NO. OF CURVES TO BE PRINTED PER SHEET (FOR JPRINT)              I5
C
C          3RD CARD
C  IPLOT1 = 0 : PLOT LOG E VS LOG T                  1 = 1 DON'T PLOT       I5
C  IPLOT2 = 0 : PLOT MASTER CURVE                    1 = 1 DON'T PLOT       I5
C  IPLOT3 = 0 : PLOT LOG E VS 1                      1 = 1 DON'T PLOT       I5
C  IWLF   = 0 : CALCULATE WLF CONSTANTS & ENERGY     1 = 1 DON'T            I5
C  IMAT   = 0 : CALCULATE MAXIMUM RELAXATION TIMES   1 = 1 DON'            I5
C  IRED   = 0 : CALCULATE REDUCED MODULI             1 = 1 DON'T            I5
C
C  SECTION 2  ... ONE SET PER CURVE  (MAX. 50 POINTS)
C
C    1ST CARD    KRUN :   EXPERIMENT NUMBER                                 I10
C                TEMP :   EXPERIMENTAL TEMPERATURE IN DEG. C                F10.3
C                DEL  :   DELTA LENGTH IN CM.                               F10.4
C                TF   :   FINAL TIME                                        F10.0
C
C    2ND CARD    CUMM : TRANSDUCER COMPLIANCE IN CM/G * 10**6               F10.3
C                DL   : DIMENSION OF LENGTH OF SAMPLE IN CM                 F10.3
C                DT   : DIMENSION OF THICKNESS OF SAMPLE IN CM              F10.3
C                DW   : DIMENSION OF WIDTH OF SAMPLE IN CM                  F10.3
C                ASYMF: ASYMMETRY  FACTOR OF THE BENDING CLAMP.             F10.3
C                       IF SYMMETRIC.  = 0.5
C                MODE : DEFORMATION MODE                                    I10
C    MODE = 0 FOR BENDING ,     = 1 FOR STRETCHING
C
```

```
C     NEXT CARDS F(L) : FORCE MEASURED ( 8 DECADE PER CARD )              F8.1
C      UP TO 5/CARDS: FORCE READINGS: IF NO READING TAKEN. LEAVE BLANK
C
C     ********** A T T E N T I O N    **********
C     USE A MINUS VALUE (SAY. -100 ) FOR NEXT KNOW TO SEPARATE MASTER CURVES
C
C     TIME ARRAY .  IN SECONDS
C       2       2.5      3       4       5       6       8       10      13      16
C      20       25       30      40      50      60      80      100     130     160
C     200      250      300     400     500     600     800     1000    1300    1600
C    2000     2500     3000    4000    5000    6000    8000    10000   13000   16000
C   20000    25000    30000   40000   50000   60000   80000   100000  130000  160000
C
C      E(I.J) AND MT(I.J) ARE CONVERTED TO LOGARITHMS. MAXIMA OF I AND J ARE 50
C      AND 40 RESPECTIVELY.
C
C      IPUNCH  : PUNCH OUT WILL BE
C      NAME
C      TEMP.. M     (M = NO. OF POINTS )
C      E(I)      ( IN LOGARITHM )
C      K.NMAX.EMIN. EMAX
C      K = NO. OF CURVES. NMAX =MAXIMUM TIME FOR ALL CURVES.
C      EMIN = MINIMUM OF MODULUS. EMAX = MAXIMUM OF MODULUS
C      CUMA(I)              WITH RESPECT TO   TG
C
      COMMON NAME(20) .E(50.40).MT(50.40).T(50).NMAX.JSIGN
      DIMENSION F(50).WT(50).IIT(50).CUMA(40).DEG(40).U(40).V(40).M(40)
      REAL*8       BLANK/8H      /.LS/6HLOG E /.LD/6H--------/
      INTEGER VE(40)/'F6.2'.'A6'.'F7.1'.' 17 '/ . DASH/'-'/
      INTEGER VF(43) /'(1X.'.'17'.'.1X.'.'F6.2'.'.'.'F6.2'.'.'.'F6.2'.'.'.'
     1F6.2'.'.'.'F6.2'.'.'.'F6.2'.'.'.'F6.2'.'.'.'F6.2'.'.'.'F6.2'.'.'.'
     2F6.2'.'.'.'F6.2'.'.'.'F6.2'.'.'.'F6.2'.'.'.'F6.2'.'.'.'F6.2'.'.'.'
     3F6.2'.'.'.'F6.2'.'.'.'F6.2'.'.'.'F6.2'.'.'.'F6.2'.')'/
      DO   1   J = 1.5
      K = 10 * ( J - 1 )
      L = 10 ** ( J - 1 )
      T(K+1) = 2.0 * L
      T(K+2) = 2.5 * L
      T(K+3) = 3.0 * L
      T(K+4) = 4.0 * L
      T(K+5) = 5.0 * L
      T(K+6) = 6.0 * L
      T(K+7) = 8.0 * L
      T(K+8) = 10.0 * L
      T(K+9) = 13.0 * L
    1 T(K+10)= 16.0 * L
      DO 2 I = 1. 50
      WT (I) = 0.
      DO 2 J = 1.40
    2 MT(I.J) = 0
      DO 3 I = 1. 3
      WT(I) = 9.0
      WT(I+3) = 0.1
    3 WT(I+6) = 0.01
 1200 READ(5. 8 . END = 1400 )  NAME
      WRITE(6. 4) NAME
    4 FORMAT('1'.20A4)
    5 FORMAT(3F10.3.4I5)
      READ(5.5) ALPHAL.ALPHAL.TG.IPRINT. JPRINT.IPUNCH.NN
      READ (5.7) IPLOT1.IPLOT2.IPLOT3.IWLP.IMAT. IRED
    7 FORMAT(9I5)
      WRITE(6. 5) ALPHAL.ALPHAL.TG.IPRINT . JPRINT.IPUNCH.NN
      WRITE(6.7) IPLOT1.IPLOT2.IPLOT3.IWLP.IMAT.IRED
      IF(IPUNCH.EQ.0) WRITE(7. 8) NAME
    8 FORMAT(20A4)
      CUMA(1)=0.
      K=0
      KL = 0
      EMAX = 0.0
```

```
      EMIN = 14.0
      MMAX =  0
 1000 READ(5,11, END=1100)  KRUN, TEMP, DEL, TF
   11 FORMAT( I10, F10.3,F10.4,F10.0 )
      IF(KRUN.LT.0)                    GO TO 1100
      K=K+1
      KL = KL + 1
      IF(KL.GT.9) KL = KL - 9
      DO 14 J=1,50
   14 E(J,K) = 0.0
      DEG(K)=TEMP
      READ(5,16) CORR, DL, DT, DW, ASYMF, MODE
   16 FORMAT(5F10.3,I10)
      PER = 100.0 * DEL/ DL
C     DETERMINE THE TIME RANGE
      DO 18    I = 1,50
      IF( T(50-I).EQ.TF ) M = 50 - I
   18 CONTINUE
      READ(5,19)(F(L),L=1,M)
   19 FORMAT(10(3X, F5.1))
      IF(IPRINT .NE.0) GO TO 20
      WRITE(6,12) KRUN, TEMP, DEL, PER, TF, KL
   12 FORMAT(/,5X,31('- - '),/,'   RUN',I5,F10.1,' DEG.C   DEL =',F7.4,
     1' DR',F6.1,' % (SHOULD BE < 1%)       FINAL TIME =',F7.0,17X,'SYMBO
     2L =',I2)
      WRITE(6,16)CORR, DL, DT, DW, ASYMF, MODE
      WRITE(6,17) (F(L),L=1,M)
   17 FORMAT( 10F10.1)
C     CALCULATE THE SHAPE FACTOR
   20 ALPHA = ALPHAG
      IF(TEMP.GT.TG) ALPHA = ALPHAL
      ALPHA = ALPHA * 0.000001
      CORR = CORR * 0.000001
      DT = DT * ( 1 + ALPHA * (TEMP -  25.))
      DW = DW * ( 1 + ALPHA * (TEMP -  25.))
      IF(MODE.NE.0) GO TO 23
      C = ((DL*ASYMF/DT)**3)*981.*4.*(1-ASYMF)/DW
      GO TO 24
   23 C = (981. * DL) / ( DW * DT )
   24 S = C *(TG+273.16)/(TEMP+273.16)*(1.+3.*ALPHA*(TEMP-TG))
      DK = S
      IF(SHED.NE.0) DK = C
C     F(M) REPRESENTS MODULI INSTEAD OF FORCE UNTIL NEXT CURVE
      WSUM=0.
      ALG=0.
      DO 120 J=1,M
      F(J) = DK * F(J)/(DEL-CORR*F(J))
      IF(F(J).GT.1.0)      E(J,K) = ALOG10(F(J))
      IF(E(J,K).GT.EMAX) EMAX = E(J,K)
      IF(E(J,K).LT.EMIN.AND.E(J,K).NE.0.0) EMIN = E(J,K)
      IF(K.EQ.1.OR.WT(J).EQ.0.0) GO TO 130
      IF(J.GT.NPN.OR.E(J,K).LT.2(NPN,K-1)) GO TO 120
      DO 32  N = J,NPF
      IF(E(N,K-1).GT.0.0) GO TO 33
```

```
   32 CONTINUE
   33 IF (E(N,K-1).LT.E(J,K)) GO TO 130
      DO 131  L =  N, MPR
      I = L - 1
      IF(E(L,K-1).GT.E(J,K).OR.E(L,K-1).EQ.0.0) GO TO 131
   35 IF(E(I,K-1).GT.0.0) GO TO 37
      I = I - 1
      GO TO 35
C     L.GT.I .AND. L.GE.J
C     J.LT.I .OR. J.GT.I
   37 T1   = ALOG10(T(J))
      T2   = ALOG10(T(I))
      T3   = ALOG10(T(L))
      DET = T3 - T2
      DEE = E(I,K-1) - E(L,K-1)
      EE = E(I,K-1) - E(J,K)
      ALG = ALG +WT(J)*(T1-T2-EE*DET/DEE)
      WSUM = WSUM + WT(J)
      GO TO 130
  131 CONTINUE
  130 CONTINUE
C   CALCULATE MAXIMUM  RELAXATION TIME
      IF(IMRT.NE.0) GO TO 50
      SU = 0.0
      SV = 0.0
      SUU = 0.0
      SUV = 0.0
      N = 0
      MK = M - 10
      DO 40 J = MK, M
      IF(E(J,K).EQ.0.0) GO TO 40
      N = N + 1
      SU = SU + T(J)
      SV = SV + E(J,K)
      SUU = SUU + T(J)*T(J)
   40 SUV = SUV + E(J,K)*  T(J)
      SLOPE = (SU*SV-N*SUV)/(SU*SU-N*SUU)
      RMAX = -1/(2.303*SLOPE)
      IF(RMAX.GT.0) RLOG = ALOG10(RMAX)
      WRITE(6,42) RMAX,RLOG,N
   42 FORMAT(/,5X,'MAX. RELAX. TIME =',E10.3,' SEC.',F10.4,I10)
   50 IF(K.EQ.1) GO TO 51
      IF(WSUM.LE.0.0)  WSUM = 1.0
      ALG=ALG/WSUM
      CUMA(K)=ALG+CUMA(K-1)
   51 MPR=M
      IF(M.GT.MMAX) MMAX = M
      DO 52      I = 1,M
      WT(I,K) = (ALOG10(T(I)) - CUMA(K)) * 10.0
   52 CONTINUE
      IF(IPRINT .NE.0) GO TO 55
      WRITE(6, 54)  M, C, S, ALG, CUMA(K)
   54 FORMAT(1H0,'NO. OF POINTS =',I3,10X,'APPARENT SHAPE FACTOR =',E10.
     13,10X,'REDUCED SHAPE FACTOR =',E10.3,//,1X,'LOG SHIFT =',F8.4,10X,
```

```
     2*CUMULATIVE SHIFT =*,F9.3,/)
      WRITE(6,55) (MT(J,K),E(J,K),J=1,M)
   55 FORMAT(10(16,F7.3))
   56 IF(IPUNCH.NE.0) GO TO 1000
      WRITE(7,58) TEMP, M ,KHUN
   58 FORMAT( F10.1,2I10 )
      WRITE(7,59) (E(J,K), J=1,M)
   59 FORMAT ( 10 F 8.4 )
      GO       TO     1000
 1100 IF(DEG(K).GT.TG) GO TO 60
      AREF = CUMA(K) + 1.0
      GO TO 64
   60 DO 160 I=1,K
      IF(DEG(I)-TG) 160,61,62
   61 AREF = CUMA(I)
      IS = I + 1
      GO TO 64
   62 IS = 1
      IF(I.EQ.1) GO TO 63
      AREF=CUMA(I)+(CUMA(I-1)-CUMA(I))*(DEG(I)-TG)/(DEG(I)-DEG(I-1))
      GO TO 64
   63 AREF=CUMA(I)+(CUMA(I+1)-CUMA(I))*(DEG(I)-TG)/(DEG(I)-DEG(I+1))
   64 DO 65  J=1,K
   65 CUMA(J)=CUMA(J)-AREF
      GO TO 67
  160 CONTINUE
      IWLF = 1
      WRITE(6,66)
   66 FORMAT(1H0,5X,31(1H- ),//,40X,*TG OUT OF RANGE*)
   67 WRITE(6,68)(DEG(L),CUMA(L),L=1,K)
   68 FORMAT(1H0,5X,31(1H- ),/,30X,*TEMP, C LOG SHIFT REL, TO TG*,/,7(
     *F10.1,F8.3))
      IF(IPUNCH.EQ.0) WRITE(7,169) K,NMAX,EMIN,EMAX
  169 FORMAT( 2I5,2F10.4)
      IF(IPUNCH.EQ.0) WRITE(7,69)(CUMA(I),I=1,K)
   69 FORMAT(10F8.3)
C     PLOTTING
      IF(IPLOT1.EQ.0) CALL PLOTE(1, EMAX,EMIN,1,NMAX,1,K,2)
      IF(IPLOT3.EQ.0) CALL PLOTE(3,EMAX,EMIN,1, 50 ,1,K,10)
      IF(IPLOT2.NE.0) GO TO 90
      IKK = K/12 + 1
      IKK = K/IKK + 1
      NJ = 1
      DO 81   I = 1,4
      NA = NJ + IKK
      IF(NA.GT.K) NA = K
      N1  = MT(1,NJ)
      N2 = MT(1,NA) + 35
      JJJ = (NJ-1)/9
      JSIGN = NJ - JJJ * 9
      YMAX = 0.0
      YMIN = 14.0
      DO 82 J= NJ,NA
      DO 82 N = 1,NMAX
```

```
      IF(F(N,J).EQ.0.0) GO TO 82
      IF(E(N,J).LT.YMIN) YMIN = E(N,J)
      IF(E(N,J).GT.YMAX) YMAX = E(N,J)
   82 CONTINUE
      CALL PLOTL(2.,YMAX,YMIN,N1,N2,N3,N4,-3)
      IF(N4.GE.K) GO TO 90
      N3 = N4 - 1
   81 CONTINUE
C     CALCULATE W. L. F. CONSTANTS
   90 IF(IALF.NE.0) GO TO 800
      SU = 0.0
      SV = 0.0
      SUU = 0.0
      SUV = 0.0
      DO 91 I = IS,K
      U(I) = DEG(I) - TG
      V(I) = U(I)/CUMA(I)
      SU = SU + U(I)
      SV = SV + V(I)
      SUU = U(I)*U(I) + SUU
   91 SUV = SUV + U(I)*V(I)
      N = K - IS + 1
      SLOPE =(SU*SV -N*SUV)/(SU*SU-N*SUU)
      C1 = -1/SLOPE
      INTER = (SV-SLOPE*SU)/N
      C2 = - INTER*C1
      DELTAH = 2.303 * 1.987*C1*C2/1000.0
      DO 93 I = IS, K
      DIV = (DEG(I)+273.16)/(C2+U(I))
   93 H(I) = DELTAH*DIV*DIV
      WRITE(6, 4) NAME
      WRITE(6,92)
   92 FORMAT(/,5X,'TEMP.',5X,'T-TG',5X,'LOG A',5X,'(T-TG)/LOG A',6X,'ENE
     1RGY',/)
      WRITE(6,94) (DEG(I),U(I),CUMA(I),V(I),H(I),I=IS,K)
   94 FORMAT(F10.1,F10.1,F9.2,F14.2,F15.2)
      WRITE(6,95) TG,C1,C2,DELTAH
   95 FORMAT(1HU,' TG =',F7.1,10X,'C1 =',F8.1,10X,'C2 =',F8.1,10X,'ACTIV
     1ATION ENERGY =',F15.3,' KCAL/MOLE')
      CH1 = 0.0
      DO 96 I = IS,K
      Y2 = V(I) - INTLH-SLOPE*U(I)
   96 CH1 = CH1 + Y2*Y2/V(I)
      WRITE(6,97) CH1,SLOPE,INTER
   97 FORMAT(///,3X,'CHI SQ. =' , F10.3, 10X,'SLOPE =',E10.3,10X,'INTERCE
     1PT =',E10.3)
      WRITE(6,98)
   98 FORMAT(///,3X,'UNIVERSAL W.L.F. CONSTANTS ARE C1 = 17.44  C2 = 51.
     16',///,10X,'ACTIVATION ENERGY = ~.1 KCAL/MOLE')
  800 IF(JPRINT .NE.0) GO TO 1200
      DO 70  I = 1, NMAX
      TT(I) = T(I)
   70 CONTINUE
      DO 700 L = 1,10
```

```
      IF( MM.GT. 20) MM = 20
      M1 = 1 + (L-1)*MM
      M2 = L*MM
      IF(M1.GT. K) GO TO 1200
      IF(M2.GT.K) M2 = K
      WRITE(6, 71) (CC(I), I = M1,M2)
   71 FORMAT(1H1,' TEMP', F20.6,1)
      WRITE(6, 72) (CUMA(I), I=M1,M2)
   72 FORMAT(' LOG A ',20F6.1)
      WRITE(6,73) (LS , I = M1, M2)
   73 FORMAT(1H0,2X,'TIME  ',20A6)
      WRITE(6,77) (LO,I=M1,M2)
   77 FORMAT(1H , 9('-'),20A6)
      DO 76 J = 1, NPAX
      VF(2) = VE(4)
      MM = 2
      IG = 1
      DO 75 I = M1,M2
      MM = MM + 2
      IF(E(J,I).EQ.0) GO TO 74
      VF(MM) = VE(I)
      IG = 0
      GO TO 75
   74 E(J,I) = BLANK
      VF(MM) = VE(2)
   75 CONTINUE
      IF(IG.NE.0) GO TO 76
      IF(J.EQ.2) GO TO 78
      WRITE(6,VF)IT(J),(E(J,I), I = M1, M2)
      GO TO 76
   78 VF(2) = VE(3)
      WRITE(6,VF) T(J), (E(J,I), I = M1, M2)
   76 CONTINUE
  700 WRITE(6,77) (LO,I=M1,M2)
      GO TO 1200
 1400 STOP
      END
```

```
      SUBROUTINE PLOTE (INDEX,YMAX,YMIN,M1,M2,N3,N4,MBI)
      COMMON NAME(20) ,E(50,40),MT(50,40),T(50),NMAX,JSIGN
      DIMENSION NA(125)
      INTEGER DIGIT(10)/'1','2','3','4','5','6','7','8','9','0'/
      INTEGER BLANK/' '/,DASH/'-'/
      WRITE(6, 4) NAME
    4 FORMAT('1',20A4)
      YSCALE = 120.0/(YMAX-YMIN)
      WRITE(6,6) YMAX,YMIN,YSCALE
    6 FORMAT(/,2F20.2,F20.4)
      IF(INDEX.EQ.3) MBI = 10
      LK = 0
```

```
1000 DO 84   I = 1,125
  84 NA(I) = BLANK
     LK = LK + 1
     DO 100  I=1,12
     IF(I.LT.YMIN.OR.I.GT.YMAX) GO TO 100
     J = ( I - YMIN) * YSCALE
     IF ( I.GT. 10) GO TO  87
     NA(J+2) =     DIGIT(I)
     IF(I.EQ.10) GO TO 88
     GO TO 100
  87 NA(J+2) = DIGIT(I-10)
  88 NA(J+1) = DIGIT(1)
 100 CONTINUE
     WRITE(6,89)  (NA(I),  I = 1,125 )
  89 FORMAT ( '0',   125A1,///)
     IF(LK.GT.1) RETURN
     DO 190 N = N1,N2
     DO 92 I =1,125
  92 NA(I) = BLANK
     IF(INDEX.EQ.3) GO TO 30
     NN = N
     N1 = N + NBI
     J = NB/ 10
     IF(NB - 10 * J ) 91,93,95
  93 NA(1)   = DASH
     NA(120) = DASH
     WRITE(6,94) J
  94 FORMAT(1H+,120X,I3)
     GO TO 96
  31 NBI = NBI + 1
  30 J = I(NBI) * 99.0/I(NMAX)
     NN = NBI
     IF(J-N) 31,32,96
  32 NA(1) = DASH
     NA(125) = DASH
     WRITE(6,34) I(NBI)
  34 FORMAT(1H+,120X,F6.0)
  96 J = 0
     IF(INDEX.EQ.2) GO TO 99
     DO 97  I = N3,N4
     J = J + 1
     IF(J.GT.9) J = J - 9

     IF ( F(NN,I).LE.0.0) GO TO 97
     L = (  F(NN,I) - YMIN) *YSCALE + 2
     NA(L) = DIGIT(J)
  97 CONTINUE
     GO TO 96
  99 J = JSIGN - 1
     DO 200 I =N3,N4
     J = J + 1
     IF(J.GT.9) J = J - 9
     DO 200  MN = 1 , NMAX
     IF(N.NE.INT(MN,1).OR.F(MN,I).EQ.0.0) GO TO 200
     L = (F(MN,I) - YMIN)* YSCALE + 2
     NA(L) = DIGIT(J)
 200 CONTINUE
  98 WRITE(6,98) (NA(I), I = 1,120)
  98 FORMAT(1H+,120A1,/)
 190 CONTINUE
     GO TO 1000
     END
```

Program for the Calculation of Distribution of Relaxation Times

```
C    CALCULATION OF RELAXATION SPECTRA FROM DYNAMIC MODULI BY USING CURVE FIT
C    METHOD. WRITTEN BY S. C. YEU        FEB. 1974
C
C      N   = NO. OF POINTS TO BE FITTED (MAX. 300)
C      WT  = ARRAY CONTAINING WEIGHTS TO BE APPLIED TO EACH CO-ORDINATE PAIR.
C      IF NO WEIGHTING IS DESIRED. WT SHOULD BE SET TO 1.0 FOR EACH PAIR.
C      COF = ARRAY LENGTH MXDG +1 WHICH CONTAINS THE COEFFICENTS
C            OF POWER ON RETURN FROM CURVFT.
C      NCOF = OUTPUT VARIABLE CONTAINING THE NUMBER OF COEF-
C             FICIENTS CALCULATED. NCOF-1 IS THE ORDER OF THE
C             POLYNOMIAL OF BEST FIT.
C      IPRINT = -1 SUPPRESSES ALL PRINTING.
C                0 LISTS COEFFICIENTS OF BEST FIT AND OTHER
C                  RELEVANT INFORMATION.
C      NF   =  NUMBER OF CONSTRAINTS (FIXED POINTS).
C      XF   =  ARRAY CONTAINING ABSCISSAE OF THE CONSTRAINTS.
C      YF   = ARRAY CONTAINING ORDINATES OF THE CONSTRAINTS.
C     XF AND YF CAN NOT HAVE VALUES THAT ARE PART OF X AND Y.
C      H(I) ARE THE RELAXATION SPECTRA ( IN LOG EXPRESSION) TIME SHOULD BE
C      TWICE OF ORIGINAL SCALE
C
       DIMENSION    X(300), Y(300), WT(300),XF( 25), YF( 25),NAME(20)
       DIMENSION YO(300), FO(300),SO(300), H(300), COF(26),S(300)
 1000  READ(5,2,END=1500) (NAME(I), I=1,20)
     2 FORMAT(20A4)
       WRITE(6,5) (NAME(I), I=1,20)
     5 FORMAT(1H1,///,5X,20A4)
       READ(5,1)          N,NF
     1 FORMAT (            2I10)
       READ(5,3) (X(J), J=1,N)
       READ (5,3) (Y(J), J = 1,N)
     3 FORMAT (8F10.3)
       DO 4 I = 1, N
     4 WT(I) = 1.0
       ISCAL = 1
       MXDG = 25
       IF(MXDG.GT.(N-2))  MXDG = N-2
       IF(NF.EQ.0) GO TO 19
       IF(NF.GT.MXDG) NF = MXDG
       DO 6    L = 1, NF
     6 READ(5,7)  XF(L), YF(L)
     7 FORMAT (2F10.3)
       WRITE(6,18)  (XF(L), YF(L), L =1,NF)
    18 FORMAT ( 2F10.3)
    19 IPRINT = 0
       CALL CURVFT(X,Y,WT,N,ISCAL,MXDG,COF,NCOF,IPRINT,NF,XF,YF)
C
       WRITE(6,5) (NAME(I), I=1,20)
       WRITE(6,20)
    20 FORMAT(///,10X,'X',12X,'Y',12X,'YO',12X,'1ST DERV.',11X,'2ND DERV.'
      1,15X,'S',19X,'H')
       DO 110   I = 1, N
       YO(I) = COF(1) + COF(2) * X(I)
       FO(I) = COF(2)
```

```
      SD(I) = 0.0
      IF (NCOF.LE. 2) GO TO 12
      DO 10  J = 3, NCOF
      YD(I) = YD(I) + COF(J)*X(I)**(J-1)
      FD(I) = FD(I) + (J-1)*COF(J)*X(I)**(J-2)
   10 SD(I) = SD(I) + (J-1)*(J-2)*COF(J)*X(I)**(J-3)
   12 S(I) = FD(I)*FD(I) + SD(I)/2.303 - FD(I)
C
C     LOGARITHMS LOGICAL CONTROLS
      IF(S(I).LE.0.0) GO TO 14
      H(I) =  Y (I) + ALOG10(S(I))
      GO TO 110
   14 H(I) = 0.0
  110 WRITE(6,13) X(I),Y(I),YD(I),FD(I),SD(I),S(I),H(I)
   13 FORMAT(3F14.3,3E20.8,F18.8)
      GO TO 1000
 1500 STOP
      END
```

APPENDIX II

Water Diffusion in Conventional polystyrene

Temperature : 26°C h : 0.91 mm

Time, t	$\sqrt{t}/h$	M_t/M_∞
3 min.	147.4	.1071
6 min.	208.5	.2143
9 min.	255.4	.2857
20 min.	380.7	.4286
25 min.	425.6	.5357
30 min.	466.2	.6786
40 min.	538.4	.7500
60 min.	659.3	.8571
120 min.	932.5	.9286
12 hr.		1.0000

D was calculated as 5.5×10^{-7} $cm^2/sec.$

Water Diffusion in Styrene Ionomers

The diffusion coefficients were calculated from the water uptake data obtained by Dr. M. Navratil (see Refs. 15 and 63).

Samples	D (cm^2/sec)
5.5(Na)*l*	6×10^{-9}
7.9(Na)*l*	9×10^{-10}
9.1(Na)*m*	7×10^{-10}
9.7(Na)*h*	9×10^{-10}

APPENDIX III

TABLES OF SUPPORTING DATA FOR FIGURES

PART ONE, FIGURE 1, PAGE 12

"Nafion"-H

Temp.(°C)	wt%
25.0	1.78
42.0	1.63
80.0	1.15
106.0	0.83
130.0	0.26
154.0	0.12
168.0	0.00
175.0	-0.01
181.0	-0.14
195.0	-0.58
207.0	-1.71
214.0	-3.87

"Nafion"-K

Temp.(°C)	wt%
25.0	0.36
77.0	0.16
85.0	0.09
89.0	0.00
95.0	0.00
101.0	0.00
105.0	0.00
119.0	0.00
164.0	0.00
195.0	0.00
212.0	0.00
265.0	-0.11
299.0	-0.20
329.0	-0.53
338.0	-9.73

PART ONE, FIGURE 2, PAGE 36

Temperature : 0°C
h : 0.12 cm

Time (sec.)	$\sqrt{t}/h$	M_t/M_∞
40.5	53.0	0.092
80.3	74.7	0.148
120.2	91.4	0.201
240.2	129.2	0.271
480.0	182.6	0.369
900.0	250.0	0.504
1800.8	353.6	0.707
3600.5	500.0	0.878
7200.9	707.2	0.938
10800.0	866.0	0.959

Temperature : 56°C
h : 0.12 cm

Time (sec.)	$\sqrt{t}/h$	M_t/M_∞
25.4	42.0	0.123
60.6	64.9	0.225
120.6	91.5	0.344
241.3	129.5	0.533
480.6	182.7	0.716
899.7	249.9	0.811
1800.5	353.6	0.875
3600.0	500.0	0.892

Temperature : 28°C
h : 0.13 cm

Time (sec.)	$\sqrt{t}/h$	M_t/M_∞
30.0	45.6	0.116
60.0	64.6	0.194
121.6	91.9	0.291
240.0	129.1	0.403
480.0	182.6	0.594
900.0	250.0	0.772
1800.0	353.6	0.867
3600.0	500.0	0.906
7200.0	707.1	0.941
14400.0	1000.0	0.965

Temperature : 99°C
h : 0.13 cm

Time (sec.)	$\sqrt{t}/h$	M_t/M_∞
10.4	26.9	0.124
25.3	41.9	0.221
60.7	64.9	0.389
122.2	92.1	0.591
239.3	128.9	0.739
358.6	157.8	0.816
480.7	182.7	0.861
905.7	250.8	0.952
1300.4	300.5	0.973

PART ONE, FIGURE 3, PAGE 37

Temperature (°C)	log D
0.0	-6.038
28.0	-5.636
56.0	-5.447
99.0	-5.000

PART ONE, FIGURE 5, PAGE 39

TEMP.	19.0	30.5	50.0	61.3	73.0	87.8	99.8	110.6	122.8	135.6	155.0	176.2	185.0
LOG A_T	11.5	10.1	7.7	6.4	4.4	2.6	1.5	-0.1	-1.9	-3.4	-5.6	-7.6	-8.8
TIME	LOG E	LOG E	LOG E	LOG E	LOG E	LOG E	LOG E	LOG E	LOG E	LOG E	LOG E	LOG E	LOG E
2	10.05					9.09	8.85	8.44	8.05	7.81			
3	10.05		9.80			9.06	8.80	8.40	8.01	7.78	7.56		
5	10.04	9.97	9.77	9.63	9.37	9.02	8.74	8.34	7.97	7.75	7.53	7.35	
10	10.03	9.95	9.74	9.59	9.31	8.94	8.66	8.27	7.92	7.72	7.50	7.31	7.19
30	10.00	9.92	9.68	9.54	9.22	8.83	8.54	8.17	7.85	7.67	7.46	7.26	7.14
100	9.98	9.88	9.63	9.47	9.12	8.68	8.41	8.06	7.79	7.62	7.41	7.21	7.08
200			9.60										
300	9.95	9.84	9.58	9.41	9.02	8.55	8.31	7.98	7.74	7.58	7.37	7.16	7.04
500			9.55										
800			9.52										
1000	9.91	9.78	9.50	9.32	8.89	8.43	8.21	7.89	7.68	7.52	7.32	7.11	6.98
2000	9.89			9.27		8.38							
3000	9.87	9.72	9.44		8.76		8.11	7.80	7.63	7.48	7.27	7.06	6.93
5000				9.17									
10000	9.82	9.66	9.36	9.10	8.62		8.01		7.57	7.41	7.22		6.85
20000		9.63		9.04									

PART ONE, FIGURE 6, PAGE 40

TEMP.	30.0	40.6	60.3	70.4	80.0	88.4	97.5
LOG A_T	10.4	8.1	6.4	4.7	2.9	1.6	-0.6
TIME	LOG E	LOG E	LOG E	LOG E	LOG E	LOG E	LOG E
2	9.82	9.74	9.66	9.53	9.26	8.97	
3	9.81	9.73	9.64	9.51	9.22	8.91	8.31
5	9.81						8.25
10	9.80	9.71	9.61	9.44	9.11	8.76	8.16
20	9.79						
30	9.78	9.69	9.57	9.38	9.00	8.64	8.05
50	9.77						
100	9.76	9.66	9.52	9.29	8.85	8.49	7.87
200	9.75						
300	9.74	9.63	9.46	9.20	8.71	8.35	7.72
500	9.73						
1000	9.72	9.59	9.38	9.06	8.51	8.18	7.48
2000	9.70						
3000	9.69	9.54	9.26	8.91	8.27	8.01	
5000	9.68						
10000	9.65	9.49	9.09	8.69			
16000	9.64						

TEMP.	34.0	43.6	64.0	71.0	92.6	113.4	123.2	133.0	143.0
LOG A_T	27.8	25.9	23.2	21.2	17.7	15.3	13.7	11.7	9.6
TIME	LOG E	LOG E	LOG E	LOG E	LOG E	LOG E	LOG E	LOG E	LOG E
2	10.16	10.13		10.02	9.94	9.89	9.84	9.77	
3	10.16	10.12	10.07	10.02	9.94	9.88	9.84	9.77	9.67
5	10.15	10.12	10.06	10.02	9.93	9.87	9.83	9.75	9.65
10	10.15	10.12	10.05	10.01	9.93	9.87	9.82	9.74	9.63
20	10.14	10.11	10.04	10.01	9.92	9.86	9.81	9.73	9.62
30	10.14	10.11	10.04	10.00	9.92	9.85	9.81	9.72	9.61
50	10.14	10.10	10.04	10.00	9.91	9.85	9.80	9.71	9.60
100	10.13	10.10	10.03	9.99	9.91	9.84	9.79	9.70	9.57
200	10.13	10.09	10.02	9.99	9.90	9.83	9.78	9.68	9.55
300	10.12	10.09	10.02	9.98	9.89	9.82	9.77	9.67	9.54
500	10.12	10.08	10.01	9.98	9.89	9.82	9.76	9.65	9.51
1000	10.11	10.07	10.01	9.97	9.88	9.80	9.74	9.63	9.48
2000	10.10	10.06	10.00	9.96	9.87	9.79	9.72	9.60	9.43
3000	10.09	10.05	9.99	9.95	9.86	9.78	9.71	9.58	9.40
5000	10.09	10.04	9.99	9.95	9.85	9.77	9.69	9.55	9.36
10000	10.07	10.03	9.97	9.94	9.83	9.75	9.66	9.50	9.29
25000									

TEMP.	159.0	172.0	180.0	193.2	210.2	227.0	256.0	276.0	320.4
LOG A_T	7.4	5.5	4.7	3.2	1.3	-0.2	-1.8	-3.9	-5.3
TIME	LOG E	LOG E	LOG E	LOG E	LOG E	LOG E	LOG E	LOG E	LOG E
2					8.42				
3	9.51		9.18	8.90	8.35	7.87	7.53	7.24	
5	9.49	9.27	9.15	8.84	8.27	7.79	7.50	7.20	
10	9.46	9.23	9.09	8.76	8.17	7.72	7.46	7.15	6.83
20	9.43	9.18	9.03	8.69	8.07	7.65	7.42	7.10	6.73
30	9.41	9.16	9.00	8.64	8.01	7.62	7.40	7.07	6.63
50	9.39	9.12	8.96	8.58	7.95	7.58	7.37	7.02	6.51
100	9.35	9.06	8.89	8.48	7.86	7.54	7.33	6.96	6.34
200	9.31	9.00	8.83	8.38	7.78	7.50	7.28	6.87	6.07
300	9.29	8.96	8.79	8.33	7.74	7.48	7.25		5.89
500	9.25	8.90	8.72	8.25	7.69	7.46	7.21	6.72	5.37
1000	9.19	8.82	8.64	8.12	7.64	7.42	7.15	6.57	
2000	9.12	8.73	8.55	8.02	7.59	7.38		6.39	
3000	9.07	8.66	8.49	7.96	7.57	7.36	7.06	6.25	
5000	9.01	8.58		7.90	7.53	7.33	7.02	5.97	
10000	8.91				7.50	7.29			
25000					7.45				

PART ONE, FIGURE 9, PAGE 43

TEMP.	25.0	50.2	58.6	62.4	74.6	87.6	96.2
LOG A_T	9.6	7.6	5.3	3.7	1.3	-1.8	-4.5
TIME	LOG E	LOG E	LOG E	LOG E	LOG E	LOG E	LOG E
2	9.75	9.61	9.43	9.22		8.18	7.84
3	9.74	9.59		9.18	8.69	8.14	7.82
5			9.38		8.66	8.10	7.80
10	9.70	9.55	9.34	9.09	8.61	8.05	7.77
20		9.54			8.56	8.01	7.75
30	9.67	9.52	9.27	9.00	8.53	7.99	7.74
50					8.49	7.97	7.72
100	9.63	9.48	9.20	8.88	8.44	7.93	7.70
200					8.38	7.91	7.68
300	9.59	9.44		8.79	8.35	7.89	7.67
500					8.31	7.87	7.65
1000	9.55	9.38	9.01	8.67	8.26	7.84	7.63
2000					8.20	7.82	7.61
3000		9.31	8.91	8.60	8.16	7.80	7.59
5000					8.12	7.78	7.57
10000			8.80		8.07	7.76	7.54
13000					8.06		

PART ONE, FIGURE 12, PAGE 46

"Nafion"-H

Temp. (°C)	G' (dyn/cm^2)	tanδ x100	Temp. (°C)	G' (dyn/cm^2)	tanδ x100
-150	1.98×10^{10}	2.4	100	4.50×10^{8}	31.5
-140	1.89	3.3	103	3.58	34.4
-130	1.77	4.37	107	2.86	38.4
-120	1.70	5.9	112	2.32	40.7
-116	1.60	6.46	117	1.52	37.8
-110	1.47	7.05	121	9.56×10^{7}	35.7
-108	1.42	7.3	125	8.83	32.3
-106	1.40	7.39	127	9.36	29.5
-104	1.31	7.54	131	5.10	26.2
-102	1.31	7.53	135	3.78	23.8
-100	1.30	7.4	137	3.78	21.97
-96	1.25	7.33	140	3.55	
-90	1.14	6.8	150	2.20	
-80	1.04	5.77	155	1.76	
-70	9.57×10^{9}	4.76	160	1.49	
-60	9.00	3.92	164	1.31	
-50	8.33	3.48			
-46	8.10	3.47			
-40	7.63	3.57			
-30	7.10	4.03			
-20	6.23	5.02			
-10	5.33	6.2			
-5	4.97	6.7			
0	4.87	6.91			
5	4.65	7.12			
10	4.36	7.22			
12	4.19	7.44			
14	4.13	7.27			
17	4.08	7.14			
20	3.80	7.17			
24	3.60	6.92			
35	1.75	6.91			
40	1.71	7.01			
45	1.52	8.11			
50	1.44	9.38			
55	1.26	11.3			
60	1.16	12.35			
65	1.08	14.19			
75	9.54×10^{8}	17.51			
80	8.60	20.0			
85	8.39	22.4			
90	6.30	26.33			
95	5.56	28.72			

PART ONE, FIGURE 12, PAGE 46 (Cont.)

"Nafion"-Cs

Temp. (°C)	G' (dyn/cm^2)	tanδ x100	Temp. (°C)	G' (dyn/cm^2)	tanδ x100
-150	1.97×10^{10}	4.17	208	5.1×10^{7}	49.3
-140	1.84	5.26	210	4.0	53.7
-130	1.68	6.72	214	3.49	52.0
-120	1.51	8.15	220	2.5	48.2
-115	1.36	8.6	224	1.95	45.0
-110	1.27	8.77	230	1.82	38.4
-105	1.17	8.96	236	1.56	35.1
-103	1.16	8.91	240	1.54	33.2
-100	1.10	8.94	250	1.18	29.7
-95	1.00	8.77			
-90	9.56×10^{9}	8.5			
-86	8.80	8.22			
-80	8.23	7.7			
-70	7.25	6.45			
-60	6.63	5.05			
-52	6.00	4.18			
25	2.02	1.9			
30	2.01	1.91			
40	1.94	2.03			
50	1.88	2.19			
60	1.87	2.4			
70	1.79	2.59			
80	1.73	2.89			
90	1.65	3.24			
105	1.54	4.33			
130	1.26	7.3			
140	9.9×10^{8}	10.9			
145	9.16	12.0			
150	7.91	13.8			
155	6.38	17.4			
160	4.81	20.2			
165	3.46	20.8			
170	2.72	21.6			
175	2.33	22.7			
180	1.73	25.4			
190	1.36	31.5			
195	1.06	35.7			
200	8.5×10^{7}	40.4			
206	5.4	48.9			

PART ONE, FIGURE 13, PAGE [redacted]

Temp. (°C)	G' (dyn/cm^2)	tanδ x100
-150	2.01×10^{10}	3.88
-140	1.83	5.42
-130	1.72	7.04
-124	1.54	8.30
-120	1.52	8.77
-115	1.36	9.50
-110	1.21	10.07
-106	1.17	10.2
-104	1.14	10.22
-102	1.07	10.08
-100	1.02	9.72
-98	9.99×10^9	9.84
-96	9.85	9.65
-94	9.25	9.39
-90	8.65	9.02
-84	7.62	8.16
-80	7.4	7.77
-70	6.41	6.7
-60	5.34	5.99
-50	4.85	4.83
-40	4.67	3.84
-30	4.65	3.55
-20	4.52	2.8
-10	4.31	2.17
0	4.12	1.84
6	4.17	1.75
10	3.95	1.53
13	4.05	1.66
21	3.93	1.7
27	3.42	1.78
40	3.16	2.19
50	2.97	2.42
60	2.67	2.67
62	2.50	2.65
64	2.45	3.16
66	2.24	3.02
68	2.11	3.39
70	2.01	4.19
72	2.09	3.59
74	2.07	3.57
76	1.94	3.5
78	2.12	2.97
80	2.03	3.23
82	1.99×10^9	3.53
84	2.01	3.62
86	2.06	5.37
88	2.04	5.43
90	2.15	5.63
92	2.13	4.44
98	2.15	5.33
100	2.01	4.82
104	2.13	5.55
110	2.13	5.38
120	2.01	6.22
126	1.82	7.55
130	1.69	8.39
136	1.54	9.85
140	1.45	10.43
142	1.33	11.06
144	1.26	12.98
146	1.19	12.08
148	1.07	12.63
150	9.99×10^8	13.45
152	9.57	13.54
154	8.79	13.78
156	7.83	14.35
158	7.16	14.5
160	6.55	13.64
164	5.36	15.19
170	4.07	16.34
180	3.02	19.97
190	2.06	27.7
192	1.88	29.7
194	1.72	31.7
196	1.66	32.7
198	1.46	36.6
200	1.29	39.3
202	1.19	40.9
204	1.1	42.8
210	8.25×10^7	48.1
214	6.8	51.2
222	4.02	58.5
225	3.3	59.5
227	2.96	56.9
230	2.51	56.8
233	2.33	50.8
240	1.67	40.9
248	1.38	33.7
253	1.33	30.9
264	9.96×10^6	31.0
270	9.96	26.6

PART ONE, FIGURE 14, PAGE 48

Temp. (°C)	G' (dyn/cm^2)	tanδ x100
-160	2.00×10^{10}	2.06
-149	1.80	3.17
-140	1.78	4.51
-130	1.65	6.63
-127		6.98
-125		7.55
-122		8.15
-120	1.41	9.42
-118		9.73
-114		10.28
-110	1.17	10.75
-105		11.29
-100	9.98×10^{9}	11.25
-96		11.00
-90	8.30	10.53
-86		9.89
-80	6.82	9.04
-76		8.24
-70	5.90	7.07
-60	5.30	5.79
-50	4.86	4.67
-40	4.66	3.98
-30	4.51	3.17
-10	4.11	2.74
0	3.84	2.79
9	3.69	2.51
20	3.59	2.49
24	2.33	2.31
40	2.14	2.88
60	1.97	3.86
80	1.67	5.12
100	1.44	7.32
120	1.14	9.3
130	9.48×10^{8}	11.16
135	8.47	12.2
140	7.46	12.8
150	5.48	11.57
155	5.03	12.28
160	4.47	10.41
165	3.99	10.14
170	3.46	10.72
180	3.04×10^{8}	11.88
190	2.62	13.8
200	2.03	19.7
210	1.59	26.9
219	1.24	35.4
222	1.01	38.7
226	9.0×10^{7}	42.5
230	8.07	46.7
235	6.2	49.5
240	5.62	47.4
250	3.81	38.3
265	2.41	24.9

Temp. (°C)	G' (dyn/cm^2)	tanδ x100
-166	2.17×10^{10}	1.32
-160	2.06	1.8
-150	1.87	3.13
-140	1.74	5.42
-130	1.62	7.34
-128		7.35
-126		7.47
-124		8.63
-122		9.77
-120	1.28	9.83
-116	1.27	9.8
-114	1.27	10.12
-112		10.31
-110	1.16	10.97
-108		11.14
-106		11.32
-104	1.04	10.85
-102		10.9
-100	9.58×10^9	11.06
-96	8.91	9.92
-90	7.79	8.93
-80	7.13	7.33
-70	6.53	5.86
-60	7.36	4.61
-50	5.31	3.73
-40	4.91	3.23
-30	4.66	2.76
-20	4.72	2.52
-12	4.26	2.43
0	4.20	2.44
10	3.98	2.52
20	3.83	2.53
24	2.75	2.5
40	2.53	2.84
50	2.38	3.23
70	2.09	3.88
80	2.00	4.62
90	1.91	5.06
100	1.75	5.97
110	1.61	6.69
120	1.42	7.72
130	1.21	10.2

Temp. (°C)	G' (dyn/cm^2)	tanδ x100
140	9.31×10^8	12.64
145	8.0	13.98
150	6.63	14.65
155	5.92	14.41
160	4.73	14.56
165	4.2	15.1
170	3.87	15.59
175	3.53	16.85
180	3.19	18.36
190	2.93	24.57
200	1.98	37.68
205	1.62	44.62
210	1.0	55.08
214	8.95×10^7	59.7
220	6.89	59.3
224	5.29	59.8
226	4.77	56.3
230	4.39	52.6
234	3.69	47.91
240	2.91	43.8
250	2.56	32.58

PART ONE, FIGURE 16, PAGE 50

0.1 H_2O/SO_3H		0.5 H_2O/SO_3H		0.9 H_2O/SO_3H		2.5 H_2O/SO_3H	
Temp. (°C)	tan δ x100	Temp. (°C)	tan δ x100	Temp. (°C)	tan δ x100	Temp. (°C)	tan δ x100
40	7.2	27	5.77	28	4.0	20	3.98
30	6.14	20	5.54	24	3.8	10	3.96
24	5.89	10	5.63	20	3.66	0	3.96
20	5.92	4	5.95	15	3.6	-10	4.0
10	6.61	0	6.02	10	3.64	-20	4.43
0	7.13	-4	6.22	5	3.74	-30	5.32
-10	7.19	-8	6.45	0	3.94	-40	6.75
-20	6.74	-10	6.41	-5	4.28	-45	7.39
-30	6.12	-14	6.56	-10	4.67	-50	8.16
-40	5.41	-16	6.54	-21	5.95	-52	8.39
-50	4.93	-20	6.51	-30	7.01	-55	8.63
-58	4.64	-22	6.56	-40	7.69	-58	8.75
-70	4.71	-24	6.61	-42	7.59	-60	8.79
-80	5.18	-26	6.62	-45	7.73	-62	8.88
-90	5.8	-30	6.45	-48	7.69	-65	8.79
-100	6.39	-32	6.38	-50	7.57	-68	8.65
-106	6.66	-36	6.26	-52	7.54	-70	8.59
-110	6.88	-40	6.18	-55	7.3	-72	8.51
-115	6.82	-44	5.94	-58	7.22	-75	8.44
-120	6.45	-50	5.7	-60	7.09	-78	8.33
-128	5.72	-60	5.52	-65	6.76	-80	8.35
-135	4.65	-66	5.62	-70	6.53	-83	8.22
		-70	5.62	-75	6.45	-85	8.39
		-74	5.83	-80	6.52	-88	8.2
		-80	6.04	-85	6.52	-90	8.09
		-84	6.26	-90	6.66	-92	7.93
		-90	6.73	-92	6.75	-95	7.63
		-94	6.86	-94	6.83	-98	7.47
		-96	6.98	-96	6.84	-100	7.53
		-100	6.98	-98	6.91	-102	7.36
		-104	7.05	-100	6.89	-105	7.07
		-106	7.06	-102	6.73	-110	6.58
		-110	6.87	-104	6.7	-115	5.89
		-114	6.67	-106	6.7	-120	5.31
		-120	6.13	-110	6.28	-125	4.52
		-125	5.57	-114	5.74	-130	3.75
		-130	4.98	-120	4.93	-140	2.48
		-140	3.87	-125	4.24	-150	1.8
		-150	2.8	-130	3.76		
				-140	2.67		
				-150	2.25		

* For 0.0 H_2O/SO_3H (see Figure 12)

0.5 H_2O/SO_3H

Temp. (°C)	G' (dyn/cm^2)	G" (dyn/cm^2)
27	2.59×10^{9}	1.50×10^{8}
20	2.73	1.51
10	2.99	1.69
4	3.28	1.95
0	3.57	2.15
-4	3.78	2.35
-8	3.83	2.47
-10	3.96	2.54
-14	4.20	2.76
-16	4.37	2.86
-20	4.56	2.97
-22	4.78	3.13
-24	4.82	3.19
-26	4.97	3.29
-30	5.28	3.40
-32	5.46	3.48
-36	5.79	3.63
-40	5.95	3.68
-44	6.41	3.80
-50	7.06	4.03
-54	7.31	4.1
-60	7.90	4.36
-66	8.36	4.70
-70	8.84	4.97
-74	9.55	5.57
-80	9.76	5.90
-84	1.02×10^{10}	6.38
-90	1.10	7.36
-94	1.15	7.9
-96	1.18	8.23
-100	1.26	8.79
-104	1.31	9.24
-106	1.33	9.42
-110	1.40	9.59
-114	1.47	9.81
-120	1.57	9.61
-125	1.69	9.41
-130	1.73	8.63
-140	1.98	7.65
-150	1.98	5.53

2.5 H_2O/SO_3H

Temp. (°C)	G' (dyn/cm^2)	G" (dyn/cm^2)
20	1.45×10^{9}	5.75×10^{7}
10	1.60	6.35
0	1.77	6.99
-10	1.99	8.01
-20	2.18	9.64
-30	2.54	1.35×10^{8}
-40	3.10	2.09
-45	3.42	2.53
-50	3.88	3.16
-52	4.17	3.50
-55	4.40	3.80
-58	4.77	4.17
-60	4.97	4.37
-62	5.39	4.79
-65	5.64	4.96
-68	6.27	5.43
-70	6.53	5.6
-72	6.74	5.74
-75	7.19	6.07
-78	7.96	6.63
-80	8.27	6.9
-82	8.61	7.08
-85	8.84	7.42
-88	9.67	7.94
-90	1.01×10^{10}	8.16
-92	1.04	8.29
-95	1.08	8.24
-98	1.18	8.81
-100	1.19	8.91
-102	1.24	9.09
-105	1.25	8.86
-110	1.40	9.21
-115	1.49	8.76
-120	1.60	8.52
-125	1.65	7.47
-130	1.75	6.58
-140	1.82	4.52
-150	1.96	3.53

* For 0.0 H_2O/SO_3H (see Figure 12)

0.2 wt% Degraded		11.2 wt% Degraded	
Temp.(°C)	tanδ x100	Temp.(°C)	tanδ x100
20	3.8	24	3.78
10	3.9	23	3.71
0	4.06	16	3.59
-6	4.16	10	3.56
-10	4.33	5	3.47
-16	4.64	0	3.6
-20	4.84	-5	3.73
-26	5.15	-10	3.9
-30	5.35	-15	4.11
-36	5.64	-20	4.42
-40	5.74	-25	4.58
-42	5.73	-30	4.87
-44	5.9	-35	5.12
-46	5.92	-40	5.4
-48	6.0	-45	5.34
-50	5.98	-50	5.61
-52	6.02	-60	6.4
-54	6.19	-65	6.71
-56	6.28	-70	7.58
-58	6.39	-75	8.05
-60	6.53	-80	8.93
-62	6.60	-85	9.22
-64	6.60	-88	9.78
-66	6.74	-90	9.6
-68	6.94	-92	9.72
-70	6.92	-95	9.83
-76	7.10	-98	9.85
-80	7.20	-100	9.80
-84	7.41	-102	9.72
-88	7.55	-105	9.69
-90	7.43	-108	9.38
-92	7.57	-110	9.15
-94	7.60	-115	8.47
-96	7.69	-120	7.79
-98	7.55	-125	6.99
-100	7.70	-130	6.2
-102	7.54	-140	4.48
-104	7.38	-150	3.12
-106	7.35		
-110	7.06		
-114	6.75		
-120	6.21		
-125	5.56		
-130	4.9		

* For 0 wt% Degraded (see Figure 12)

PART ONE, FIGURE 19, PAGE 53

0.2 wt% Degraded

T (°C)	G'	G"
20	2.90×10^9	1.10×10^8
10	3.21	1.25
0	3.44	1.40
-6	3.78	1.57
-10	3.91	1.69
-16	4.15	1.93
-20	4.32	2.09
-26	4.74	2.44
-30	4.84	2.59
-36	5.14	2.90
-40	5.39	3.10
-42	5.83	3.34
-44	5.92	3.50
-46	6.11	3.62
-48	6.16	3.70
-50	6.54	3.91
-52	6.58	3.96
-54	6.86	4.24
-56	7.04	4.42
-58	7.28	4.65
-60	7.50	4.90
-62	7.60	5.01
-64	7.97	5.26
-66	7.97	5.37
-68	8.16	5.67
-70	8.47	5.86
-76	9.46	6.71
-80	9.98	7.19
-84	1.04×10^{10}	7.70
-88	1.05	7.95
-90	1.16	8.69
-92	1.15	8.70
-94	1.20	9.15
-96	1.20	9.20
-98	1.30	9.80
-100	1.25	9.65
-102	1.32	9.93
-104	1.38	1.02×10^9
-106	1.39	1.02
-110	1.49	1.05
-114	1.50	1.01
-120	1.66	1.03
-125	1.74	9.67×10^8
-130	1.78	8.74

11.2 wt% Degraded

T (°C)	G'	G"
24	2.43×10^9	9.18×10^7
23	2.34	8.69
16	2.51	9.03
10	2.41	8.59
5	2.72	9.43
0	2.86	1.03×10^8
-5	2.87	1.07
-10	2.98	1.16
-15	3.13	1.29
-20	3.15	1.39
-25	3.36	1.54
-30	3.63	1.76
-35	3.77	1.93
-40	3.82	2.06
-45	4.30	2.30
-50	4.41	2.48
-60	4.97	3.18
-65	5.59	3.75
-70	5.88	4.46
-75	6.27	5.05
-80	7.32	6.54
-85	7.7	6.92
-88	7.5	7.34
-90	8.4	7.93
-92	8.5	8.26
-95	9.19	9.03
-98	9.38	9.24
-100	9.94	9.60
-102	1.02×10^{10}	9.92
-105	1.08	1.05×10^9
-108	1.16	1.08
-110	1.22	1.12
-115	1.32	1.12
-120	1.39	1.08
-125	1.54	1.08
-130	1.59	9.71×10^8
-140	1.79	8.01
-150	1.81	5.65

* For 0 wt% Degraded (see Figure 12)

PART ONE, FIGURE 20, PAGE 54

Weight Change (wt%)	Log G' (0°C, ca. 1 Hz)
2.5	9.247
0.9	9.458
0.5	9.552
0.1	9.586
0.0	9.687
-0.2	9.536
-11.2	9.457

PART ONE, FIGURE 21, PAGE 55

1.4 H_2O/SO_3Li		3.4 H_2O/SO_3Li	
Temp. (°C)	tanδ x100	Temp. (°C)	tanδ x100
-20	5.68	25	3.57
-30	7.02	20	3.89
-38	8.29	11	3.79
-40	8.37	0	3.98
-46	8.9	-10	4.02
-50	8.1	-20	4.4
-52	9.13	-30	5.47
-56	8.74	-40	6.84
-60	8.69	-50	8.56
-66	8.44	-60	10.06
-70	8.16	-70	10.28
-72	8.05	-78	10.35
-74	7.85	-82	9.86
-76	8.15	-86	9.55
-78	8.12	-90	9.44
-80	8.0	-94	8.83
-84	8.05	-100	8.21
-90	8.07	-110	6.82
-94	8.2	-120	5.36
-100	8.33	-130	4.35
-106	8.23	-140	3.03
-110	7.91	-158	1.27
-120	6.72		
-130	5.21		
-140	3.59		

* For 0.0 H_2O/SO_3Li (see Figure 15)

PART ONE, FIGURE 22, PAGE 56

1.5 H_2O/BO_3Na		3.4 H_2O/BO_3Na	
Temp. (°C)	tanδ x100	Temp. (°C)	tanδ x100
-15	7.07	20	6.18
-20	7.44	10	5.8
-24	7.68	-1	5.37
-30	7.56	-10	5.17
-36	7.41	-20	5.12
-40	7.26	-30	5.37
-44	7.09	-41	6.14
-50	6.82	-50	7.47
-54	6.67	-56	8.68
-60	6.76	-60	9.27
-64	6.59	-65	9.58
-70	6.8	-68	10.07
-74	7.01	-70	10.5
-80	7.27	-72	10.17
-84	7.37	-75	10.3
-90	7.94	-78	10.42
-94	8.13	-80	10.16
-100	8.66	-82	9.96
-102	8.62	-84	9.78
-104	8.82	-85	9.62
-106	8.6	-88	9.56
-108	8.35	-90	9.63
-110	8.11	-91	9.29
-114	8.0	-93	9.0
-120	7.08	-94	9.0
-126	5.3	-95	9.37
-130	4.75	-96	9.3
-140	2.87	-98	9.27
-155	1.4	-100	8.0
		-102	6.75
		-104	6.54
		-110	6.6
		-116	6.4
		-120	5.7
		-130	4.8

* For 0.0 H_2O/BO_3Na (see Figure 14)

PART ONE, FIGURE 23, PAGE 57

"Nafion"-H (see Figure 12)

"Nafion"-Cs (see Figure 12)

"Nafion"-K (see Figure 13)

"Nafion"-Na (see Figure 14)

"Nafion"-Li (see Figure 15)

PART ONE, FIGURE 25, PAGE 59

100 Hz	
Temp. (°C)	tanδ x 100
4.0	4.3
7.2	6.0
8.2	6.6
12.2	14.9
13.1	18.6
14.5	25.5
15.8	29.2
17.2	31.4
18.8	33.0
20.3	33.8
21.2	34.6
22.1	34.9
24,0	35.1
25.0	35.1
27.4	35.6
28.4	36.1
30.8	38.3
32.0	39.9
34.3	43.9
36.0	45.8
37.5	48.2
40.4	53.0
42.5	55.7
45.4	59.4
47.2	61.3
49.0	63.0
50.4	63.4
53.4	63.4
54.6	62.4
57.5	58.5
58.5	56.8
62.4	47.9
67.0	35.1
70.7	26.1
74.5	20.3
79.0	15.6
83.5	13.6
89.6	13.0

1 kHz	
Temp. (°C)	tanδ x 100
9.2	4.5
14.0	8.4
16.5	13.4
18.0	15.7
20.6	17.9
22.5	16.5
26.0	15.8
29.3	16.8
32.5	19.3
38.0	24.9
43.0	33.0
48.0	44.2
51.0	52.6
55.5	62.0
59.5	69.4
60.0	71.0
62.8	75.8
64.5	77.3
66.2	78.7
68.3	78.9
69.8	77.8
72.0	75.0
73.8	71.9
78.0	61.0
82.2	48.9
86.1	38.8
89.0	32.9

PART ONE, FIGURE 25, PAGE 59 (Cont.)

10 kHz

Temp. (°C)	tanδ x 100
11.0	3.3
18.3	7.6
23.3	8.6
26.5	9.1
30.0	10.0
33.0	11.4
38.5	14.4
44.0	18.4
48.2	22.8
52.2	27.6
56.1	33.5
61.0	41.2
65.4	50.0
69.0	59.6
72.5	69.9
75.6	78.5
76.8	81.0
80.1	89.4
81.0	91.4
82.9	94.3
84.3	96.2
85.2	97.1
87.0	98.0
88.0	97.9
90.7	96.5
92.2	95.0
94.0	93.2
97.2	86.9
99.7	81.8

PART ONE, FIGURE 26, PAGE 60

100 Hz		1 kHz		10 kHz	
Temp. (°C)	tanδ x100	Temp. (°C)	tanδ x100	Temp. (°C)	tanδ x100
-62.0	1.1	-51.0	1.2	-43.6	1.2
-57.3	1.3	-46.0	1.5	-35.4	1.8
-54.0	1.5	-37.0	2.3	-27.3	2.6
-48	2.0	-28.4	3.4	-20.1	3.5
-41.5	2.5	-21.2	4.5	-16.7	4.1
-39.0	2.8	-17.5	5.3	-9.4	5.3
-33.6	3.5	-10.5	7.1	-5.2	6.4
-30.6	4.0	-6.0	8.8	-1.0	7.8
-26.0	4.8	-1.6	11.2	5.2	10.7
-23.0	5.5	1.5	13.8	9.0	14.4
-19.3	6.5	4.5	17.6	13.0	20.0
-18.5	6.8	8.5	25.2	17.0	23.9
-16.0	7.8	12.5	30.5	20.0	27.4
-14.8	8.5	16.0	33.2	24.5	31.4
-13.0	9.0	18.5	34.6	28.0	33.2
-12.2	9.4	19.0	34.8	32.5	33.7
-12.0	9.8	21.0	35.5	37.5	34.0
-8.6	12.0	23.4	35.9	41.2	34.3
-7.0	13.4	25.1	36.0	43.8	34.2
-4.4	16.0	27.0	35.8	50.5	32.1
-3.6	17.3	30.6	34.7	52.3	31.4
-2.2	18.3	35.7	32.2	57.2	29.0
0.0	22.7	47.2	26.1		
0.7	25.0	48.5	25.0		
2.5	29.4				
3.8	32.2				
6.0	35.3				
7.0	35.8				
7.8	36.1				
10.0	36.2				
11.0	35.9				
11.9	35.8				
14.3	35.2				
15.2	35.0				
17.5	34.2				
20.5	32.7				
29.6	28.1				
34.5	27.0				

PART ONE, FIGURE 27, PAGE 61

100 Hz		1 kHz		10 kHz	
Temp. (°C)	tanδ x100	Temp. (°C)	tanδ x100	Temp. (°C)	tanδ x100
-90.0	1.0	-81.1	1.0	-78.2	0.8
-84.6	1.2	-65.0	2,1	-63.0	1.6
-74.5	1.9	-56.4	3.2	-55.0	2.5
-70.2	2.2	-50.0	4.6	-48.7	3.5
-66.9	2.6	-44.5	6.0	-37.6	6.2
-60.0	3.7	-41.0	7.1	-31.8	8.0
-58.0	4.1	-39.6	7.7	-22.5	12.5
-53.8	5.0	-33.0	11.4	-15.6	17.7
-51.0	5.6	-27.3	16.0	-10.5	24.2
-47.3	6.9	-23.4	20.4	-7.8	28.5
-45.6	7.6	-18.4	27.3	-5.0	32.3
-42.0	9.9	-14.8	32.2	-3.0	35.1
-39.0	12.9	-13.0	34.6	-2.0	36.6
-37.0	15.4	-11.8	35.9	0.0	38.2
-34.2	18.3	-10.0	37.3	1.0	38.8
-33.4	19.4	-8.2	38.1	2.4	39.7
-31.0	23.8	-7.0	39.2	4.0	40.7
-28.3	27.1	-5.5	38.0	5.7	41.1
-26.5	30.4	-4.6	37.7	6.7	41.4
-24.6	32.5	-3.5	37.3	7.0	41.5
-20.8	35.5	-0.5	35.6	7.5	41.7
-19.6	35.9	3.2	33.5	8.2	41.7
-17.6	36.0	8.7	29.9	10.0	41.9
-16.2	35.7	14.5	26.4	12.0	41.9
-13.5	34.2	25.0	21.2	14.0	41.6
-11.2	32.2			16.0	40.8
-9.0	30.1			18.0	40.4
-6.3	27.5			19.3	39.8
-4.0	25.3			21.0	39.3
-1.0	23.1			23.0	38.5
3.5	20.4			24.2	37.9
9.3	17.8			27.4	35.3
15.0	16.0			29.0	34.6
25.8	13.2			31.0	33.8

PART ONE, FIGURE 28, PAGE 62

100 Hz		1 kHz		10 kHz	
Temp. (°C)	tanδ x100	Temp. (°C)	tanδ x100	Temp. (°C)	tanδ x100
-84.8	1.7	-73.0	1.7	-67.2	1.6
-79.6	1.8	-69.0	1.9	-55.5	2.9
-78.0	1.9	-61.2	2.9	-49.0	4.5
-75.8	2.1	-57.0	3.9	-43.5	6.7
-71.0	2.5	-50.2	6.5	-36.4	11.1
-65.6	3.4	-45.0	10.0	-30.5	16.9
-63.0	4.1	-40.0	14.7	-26.5	22.7
-60.0	5.1	-35.5	22.4	-23.0	27.8
-58.4	5.6	-31.5	30.2	-19.2	32.5
-54.0	8.0	-27.3	37.6	-16.2	35.4
-51.6	9.4	-23.8	42.1	-14.0	37.1
-47.4	13.1	-20.0	46.3	-13.0	37.9
-46.0	15.1	-17.0	48.5	-8.2	40.9
-42.3	22.9	-14.7	49.4	-3.4	43.6
-41.0	26.1	-12.2	49.4	1.4	46.1
-38.8	30.8	-9.2	48.7	3.0	47.0
-37.7	33.6	-7.2	48.1	7.3	48.8
-34.0	40.9	-5.0	47.6	9.6	49.5
-33.4	41.7	0.0	46.4	14.1	50.7
-32.6	43.4	6.2	44.0	15.8	51.0
-29.8	46.7	10.7	40.8	18.2	51.3
-28.5	47.4	19.3	33.1	23.2	51.0
-25.2	47.0	25.6	27.3	24.6	50.7
-24.4	46.4	30.5	24.8	27.2	50.0
-22.0	44.5	39.6	20.2	29.0	49.5
-20.7	43.7			36.2	46.3
-18.5	42.8			41.0	43.8
-17.5	42.6			43.0	42.8
-15.4	42.4			46.0	40.9
-11.0	40.8			48.0	39.7
-10.0	40.0			50.1	38.1
-1.6	30.9			53.6	35.5
4.7	23.2			56.0	34.1
13.0	16.0				
22.3	14.2				

PART ONE, FIGURE 29, PAGE 63

100 Hz		1 kHz		10 kHz	
Temp. (°C)	tanδ x100	Temp. (°C)	tanδ x100	Temp. (°C)	tanδ x100
-99.0	2.7	-114.0	1.1	-91.0	3.0
-93.2	3.7	-104.5	1.8	-85.6	3.9
-88.0	5.5	-97.5	2.5	-79.2	5.6
-82.2	8.9	-92.0	3.2	-75.0	7.3
-77.0	16.5	-86.5	4.4	-71.5	9.3
-73.3	27.6	-81.2	6.5	-66.7	13.7
-68.7	36.7	-76.0	9.8	-63.6	18.1
-65.5	31.2	-72.2	14.6	-60.5	24.2
-62.2	21.7	-67.6	24.5	-57.6	30.1
-59.7	16.6	-64.4	32.5	-54.7	35.2
-56.2	15.7	-61.0	36.4	-50.0	35.2
-54.0	17.6	-58.9	33.7	-48.2	33.2
-52.4	19.6	-57.0	30.6	-46.0	28.5
-50.2	22.1	-55.5	26.3	-45.2	27.3
-47.8	25.5	-53.3	21.2	-43.6	23.8
-47.0	26.0	-51.0	17.6	-42.6	21.9
-44.0	25.4	-49.0	16.3	-39.2	18.2
-41.2	21.2	-46.6	17.3	-37.5	17.1
-40.5	19.2	-44.7	19.0	-34.0	17.9
-36.6	12.4	-42.0	22.7	-33.4	18.2
-31.0	6.1	-39.0	26.9	-31.5	19.7
-28.4	4.8	-38.0	28.3	-28.0	22.5
-20.0	2.1	-35.5	31.2		
		-34.7	31.9		
		-32.6	32.1		
		-30.3	30.6		
		-29.2	29.8		
		-27.2	26.3		
		-24.2	22.0		
		-18.9	14.6		
		-17.3	13.0		
		-10.0	6.6		
		-2.6	3.9		
		3.0	2.7		
		8.5	2.0		

PART ONE, FIGURE 30, PAGE 64

100 Hz		1 kHz		10 kHz	
Temp. (°C)	tanδ x100	Temp. (°C)	tanδ x100	Temp. (°C)	tanδ x100
-128.6	1.1	-123.0	1.0	-121.0	0.8
-126.0	1.3	-113.2	1.9	-111.2	1.5
-119.0	1.8	-104 2	3.3	-96.0	4.7
-116.2	2.1	-97.7	5.2	-88.0	9.1
-110.0	3.0	-91.7	9.0	-78.9	22,7
-106.2	3.6	-83.7	23.6	-75.0	31.0
-102.0	4.7	-80.4	30.9	71.5	31.4
-99.2	6.0	-80.0	31.5	-71.0	30.8
-94.7	10.0	-77.8	29.7	-67.8	22.6
-93.0	13.2	-77.2	28.9	-65.0	15.9
-90.0	19.4	-76.0	23.7	-62.0	11.9
-89.2	22.1	-75.6	22.7	-58.7	10.6
-87.0	28.6	-74.0	17.4	-53.7	11.9
-85.2	31.1	-70.2	11.0	-48.4	13.5
-82.4	25.8	-67.0	10.3	-48.0	13.9
-82.2	23.6	-64.2	12.2	-46.2	15.0
-76.8	10.3	-62.7	13.8	-43.0	16.5
-73.2	11.1	-62.2	15.0	-41.0	17.0
-69.5	14.7	-59.7	16.1	-39.3	17.3
-68.7	15.2	-58.1	16.5	-37.1	17.1
-66.2	14.8	-56.3	16.2	-34.3	16.7
-63.3	12.4	-55.0	15.7	-32.2	15.8
-62.9	8.1	-54.5	15.4	-30.2	13.4
-57.0	4.2	-52.0	14.2	-27.2	10.6
-45.0	0.6	-49.2	13.5	-24.5	8.5
		-44.0	7.6	-19.0	5.4
		-32.0	2.0		

PART ONE, FIGURE 31, PAGE 65

"Nafion"-H with 0.4 H_2O/SO_3H

Temp. (°C)	tanδ x100
29.0	47.9
33.3	51.1
38.5	59.3
41.5	64.1
50.0	80.1
52.7	85.0
54.7	89.6
58.0	96.5
60.3	101.6
61.3	103.8
64.0	108.5
67.5	112.0
69.2	111.2
72.5	101.9
74.4	94.7
75.7	86.8
78.0	77.6
83.6	58.6
85.0	54.9
86.0	53.1
87.5	50.8
92.0	44.7
97.5	38.1

"Nafion"-H with 15 H_2O/SO_3H

Temp. (°C)	tanδ x100
-127.5	3.3
-123.0	6.7
-122.3	7.6
-118.6	15.1
-117.0	19.4
-115.6	23.9
-113.2	30.9
-110.0	36.5
-108.0	33.6
-105.3	26.1
-101.0	20.9
-98.7	20.8
-95.0	19.1
-91.0	16.8
-89.9	16.3
-87.8	15.9

0.7 H_2O/SO_3H (Figure 25)

1.4 H_2O/SO_3H (Figure 26)

1.7 H_2O/SO_3H (Figure 27)

2.1 H_2O/SO_3H (Figure 28)

3.0 H_2O/SO_3H (Figure 29)

4.1 H_2O/SO_3H (Figure 30)

PART ONE, FIGURE 34, PAGE 68

100 Hz		1 kHz		10 kHz	
Temp. (°C)	tanδ x100	Temp. (°C)	tanδ x100	Temp. (°C)	tanδ x100
-112.0	0.5	-103.0	0.6	-97.2	0.6
-107.0	0.6	-80.5	2.7	-78.0	2.6
-93.2	1.5	-72.7	4.3	-71.0	4.1
-85.2	2.5	-66.8	5.9	-65.0	5.6
-83.0	2.8	-61.5	8.6	-60.0	7.1
-75.0	4.4	-55.4	14.2	-52.0	11.8
-68.5	6.9	-51.0	20.9	-47.6	16.7
-63.0	11.5	-48.6	25.1	-44.3	21.1
-57.7	20.1	-45.4	29.8	-40.0	27.9
-57.0	21.5	-40.8	32.1	-37.0	31.6
-54.0	26.2	-38.0	31.6	-34.5	33.8
-53.3	27.3	-37.8	31.5	-32.2	34.8
-49.6	30.7	-35.2	30.2	-30.0	34.9
-46.2	30.5	-33.0	29.1	-28.0	34.5
-43.0	28.5	-30.6	28.2	-26.5	34.1
-42.3	28.2	-28.6	27.7	-24.5	33.2
-41.9	27.9	-25.5	27.6	-22.3	32.2
-38.8	26.8	-19.0	28.2	-18.0	30.0
-36.0	26.8	-15.8	28.8	-14.5	28.6
-33.7	27.5	-12.0	29.5	-10.8	27.6
-31.5	28.3	-5.8	30.1	-8.5	27.1
-29.5	28.9	0.0	30.0	-4.5	26.3
-26.0	29.0	4.4	29.4	-3.2	26.1
-20.0	26.9	9.5	28.5	1.2	25.5
-17.0	25.1	18.6	24.3	5.8	25.3
-13.0	23.0	24.5	21.6	11.4	25.2
-7.0	20.4	28.5	21.1	13.5	24.9
-1.5	19.0			20.2	23.5
3.0	16.9			25.5	21.0
7.5	14.0			27.0	20.4
8.0	13.7			32.0	17.7
16.5	11.2				

PART ONE, FIGURE 35, PAGE 69

100 Hz		1 kHz		10 kHz	
Temp. (°C)	tanδ x100	Temp. (°C)	tanδ x100	Temp. (°C)	tanδ x100
-119.0	0.3	-90.0	2.5	-87.0	2.3
-110.0	0.6	-81.0	6.9	-79.0	6.5
-104.0	0.9	-73.5	11.7	-72.0	10.3
-100.0	1.4	-67.6	15.9	-65.7	14.7
-95.0	2.2	-61.5	22.9	-59.7	19.1
-93.4	2.7	-57.0	26.7	-55.5	23.2
-84.0	7.3	-53.0	26.2	-52.0	26.9
-77.0	11.9	-49.0	24.3	-48.0	28.4
-75.8	12.7	-45.2	22.6	-44.3	27.4
-70.5	18.2	-42.2	20.5	-41.5	26.2
-69.5	19.2	-39.4	18.1	-38.6	25.2
-64.0	25.7	-36.8	16.1	-35.6	24.3
-63.5	25.9	-34.0	14.5	-33.0	23.2
-58.6	24.4	-31.0	14.1	-30.5	22.2
-54.6	22.4	-29.0	14.6	-28.3	21.3
-50.5	19.1	-27.0	15.9	-26.6	20.5
-46.5	15.7	-25.0	17.8	-24.0	20.0
-43.6	12.6	-22.6	18.9	-22.0	19.4
-40.6	10.7			-19.3	18.0
-37.5	11.1			-18.0	17.7
-35.2	14.2			-16.5	17.4
-32.6	18.2			-13.6	15.5
-30.0	18.5			-10.7	14.4
-27.8	16.3			-8.0	13.6
-26.0	13.7			-6.3	13.5
-23.2	11.9				

PART ONE, FIGURE 36, PAGE 70

"Nafion"-K with
0.67 H_2O/SO_3H

Temp. (°C)	tanδ x100
-37.2	0.7
-13.0	1.3
2.5	1.7
6.5	1.8
11.5	2.0
17.8	2.5
23.0	3.7
26.0	5.9
26.8	6.9
27.8	8.0
29.8	10.5
31.8	13.1
33.5	15.6
36.2	14.9
39.3	9.5
40.0	8.5
41.5	7.2
43.4	6.9
45.0	7.0
49.3	7.7
58.2	10.4
63.6	13.5
69.0	17.1
73.0	20.4

* For 1.92 H_2O/SO_3H (Figure 34)

For 3.55 H_2O/SO_3H (Figure 35)

PART TWO

STRUCTURE-PROPERTY STUDIES OF PLASTICIZED POLYELECTROLYTES

1. INTRODUCTION

During the past twenty years, interest in the chemistry of polyelectrolytes (water-soluble polymers) has been continually increasing. The tremendous potential for polyelectrolytes has led to a vigorous drive to develop these materials, whose study has become a dynamic field of industrial research. The polyelectrolytes are used in four main areas -- water treatment, paper, textiles and oil recovery, although many other applications in smaller volume are known.

Aqueous solution studies of polyelectrolytes, have, of course, been going on for many years. There are several reasons for this, the most obvious being the importance of polyelectrolytes in biological systems. Chemical research in synthetic polymers is largely influenced by the commercial importance of the material; solid polyelectrolytes, at least up to the present, have found relatively few successful applications, and therefore have not been studied in great detail.

Thus, it seems that the study of polyelectrolytes in highly concentrated solution is important. It can not only serve to bridge the gap between the solid state and the very dilute solution state, but also it might suggest some applications for solid polyelectrolytes. One such study involved poly(sodium acrylate), PNaA[1], the viscoelastic properties of which have been studied as a function of degree of ionization and plasticizer content using water, formamide, ethylene glycol and glycerine as plasticizers. Furthermore, a number of glass transition temperature investigations involving the use of plasticizers have been

performed in several laboratories[2-6].

The previous study of concentrated solutions of polyelectrolytes reveals several noteworthy features. The dependence of the glass transition temperature of PNaA on the plasticizer content has been studied extensively[3]. It was found that the glass transition decreases markedly with the addition of plasticizer as is the case with other polymers. In a more recent study[1] on the viscoelastic properties of plasticized PNaA, it was found that ionization produces a drastic change in mechanical behavior. In the stress relaxation study[1], it was found that time-temperature superposition failed for every ionic material studied, although the magnitude of the deviations of the long-time moduli varied with the amount of type of plasticizer and with the degree of neutralization. This deviation was ascribed to the presence of a second relaxation mechanism[7] which has also been found in many ion-containing polymers, especially in the cluster region[8]. Several features of the modulus-temperature curves of these materials are noteworthy: As the ion content increases, the breadth of the transition increases, and the glassy modulus increases by about a factor of 3. It has been suggested that the increase in the glassy modulus is due to additional intermolecular bonding which results from the presence of ions. On the other hand, as the plasticizer content increases, the breadth of the transition and the glassy modulus decreases. Finally, from the comparison of the effect of different plasticizers at the same concentration, it was found that the glassy moduli and the glass transition temperatures

of the polymers are practically independent of the type of plasticizer. A great variation in the effect of these plasticizers is found only above T_g, in terms of the decrease in the modulus with temperature. It was suggested that the ions in plasticized PNaA are clustered, as evidenced by the x-ray diffraction data and the thermorheological complexity of the stress relaxation data.

Some of the properties of PNaA in concentrated solutions are obviously very different from those of the "Nafions" which have been described in Part One of this thesis. It is, therefore, reasonable to inquire whether different polyelectrolytes in concentrated solutions will yield very different properties or whether these materials will show strong family resemblances, independent of the detailed structure and ion type, with only the "Nafions" showing an appreciable difference due to the unique composition and structure of that material.

In an attempt to answer this question, three polymers differing appreciably in structure and type of ions were selected for investigation. These materials were dimethyl diallyl ammonium chloride (DMDAAC), 3-acrylamido-3-methylbutyl trimethylammonium chloride (AMBTAC) and sodium 2-acrylamido-2-methylpropanesulfonate (AMPS), the structures of which are shown below:

DMDAAC

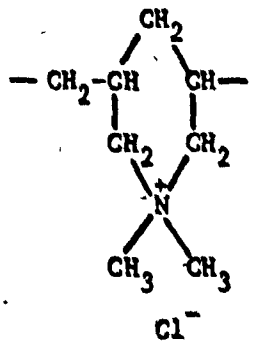

AMBTAC

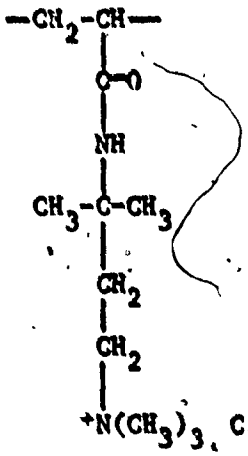

AMPS

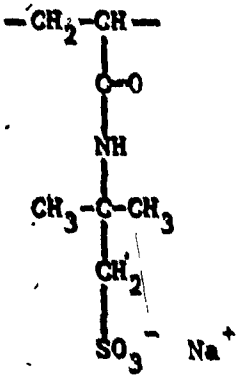

It should be noted that DMDAAC and AMBTAC differ drastically in structure but share a common ionic species, whereas AMBTAC and AMPS are structurally similar but possess very different ionic groups. All of these, in turn, differ from PNaA which is much simpler structurally and which contains sodium the carboxylate species.

The areas chosen for this exploratory study include the glass transition, dynamic mechanical properties and dielectric properties. These were selected because of the experimental ease and because of the great differences which have been found using these techniques in previous studies of PNaA and "Nafion". Since water is one of the plasticizers used extensively in these investigations and since the effect of water on various polar polymers has been investigated[9-26], it seems reasonable, before the conclusion of this introduction, to review briefly some relevant results of these investigations for illustration. A complete review is beyond the scope of this study.

It is well known that most of the low molecular weight compounds, such as water, will influence the mechanical behaviors of some polar polymers drastically. It has been reported that the α peak position moves to lower temperatures with increasing water content for polar polymers, such as collagen[9] and nylon[10-12] and ionic polymers, such as ionenes[2,5,6], poly(sodium acrylate)[1,3], and the ehtylene ionomers[13]. For those which were studied by dynamic methods, including collagen, nylon and ethylene ionomers, the tan δ peak height increases with increasing water content.

The effect of water on the sub-T_g relaxations differ from material to material. In some polymers, including ethylene ionomer[13],

polymethyl methacrylate[14,15], poly-2-hydroxylpropyl methacrylate[16], polyhexamethylene adipamide[17], poly(2,6-dimethyl-phenylene oxide[18] and polymethacrylamide[19], a new "water peak" appears, while the β peak remains unaffected upon addition of water. For a large number of other polymers, no new peak appears but the β peak is changed in some way by the presence of water. For materials, such as collagen[9], polyoxymethylene[20], polysulphone[21], polycarbonate[21], water does not influence the β peak position, but, does increase the peak height. For other polar polymers, such as nylon[11], poly-2-hydroxyl ethyl methacrylate[16], polyacrylamide[19], and polyethylene terephthalate[22-25], and also some ionomers, such as "Nafions", the β relaxation shifts to lower temperatures and in addition the peak height increasing. In contrast to this, the β peak for polyglycine[9] shifts to lower temperatures, but the peak height decreases with increasing water content.

The influence of water on the β relaxation has been ascribed by several authors to the motion of units of polymer segments complexed with water in the amorphous regions. (This occurs in the case of collagen[9], nylon[11,12], polysulphone[21], polycarbonate[21], etc.) It has also been proposed that water causes the weakening or even rupture of interchain bonding, leading to a shifting of the β relaxation to lower temperatures. (This occurs in the case of polyacrylamide[19], polymethacrylic acid[26], etc.)

It has been suggested that water can behave as an "antiplasticizer" in certain polymers, such as polycarbonate[21], and nylon[10]. In the studies of the plasticizing effect of water on nylon by Prevorsek et al[10], it was found that water changes into an antiplasticizer at temperatures

below the α' transition (which was ascribed by the same authors to the glass transition of the polymer). Allen et al[21] suggested that water acts as an antiplasticizer for polycarbonates due to the fact that the activation energy for the β relaxation in the wet sample is higher than that for the dry sample.

2. EXPERIMENTAL PROCEDURE

The un-plasticized samples, in powder form, were prepared by another laboratory. DMDAAC was synthesized by the method of Boothe[27] followed by dialysis to lower the NaCl content from 1-2% NaCl to < 0.02%. AMPS was synthesised by the method described by Murfin & Miller[28] while AMBTAC was prepared by the synthesis utilized by Hoke et al[29].

2.1 Drying and Thermal Stability

A sample (ca. 100 mg) was placed under vacuum at 25°C for several days until there was no further weight loss (<0.1 mg), and its weight was determined. Subsequently, the same sample was placed in the vacuum system, at a higher temperature, for another few days until another constant weight had been attained. The procedure was repeated for temperatures up to 205°C. The results are shown in Fig. 1, and will be described more fully below. It is obvious that a plateau is present in the drying curves of AMPS and DMDAAC, while an inflection point is evident at ca. 75°C for the AMBTAC; this point was taken as the drying temperature for all the samples.

2.2 Preparation of Plasticized Samples

Distilled water, formamide (Fischer Scientific), ethylene glycol (Matheson Coleman & Bell) and glycerine (Allied Chemical) were used without further purification.

2.2.1 Water-plasticized Samples

Since the polymers were quite hydrophilic, water contents of less

FIGURE 1.

Drying and thermal stability curves for DMDAAC, AMPS and AMBTAC.

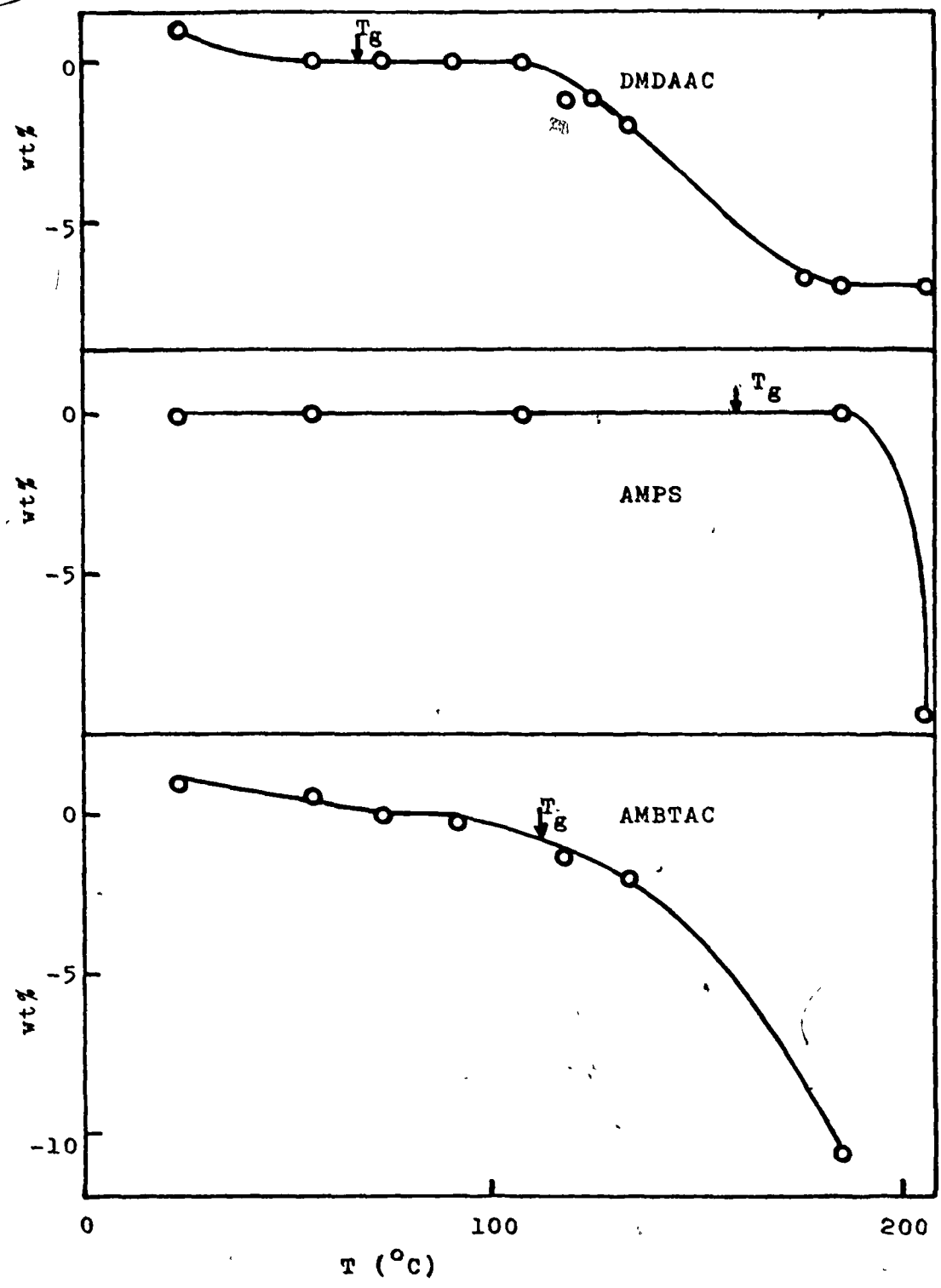
Tg
0
-5
wt%
DMDAAC
Tg
0
-5
wt%
AMPS
Tg
0
-5
-10
wt%
AMBTAC
0
100
200
T (°C)

than 35% could be obtained simply either by evaporating the water solution of the appropriate polymer or by allowing the dry polymer to absorb moisture until the desired degree of plasticization was reached. Both methods were employed, depending on convenience. A pressure of 70,000 psi was necessary for molding samples of less than 15% water content, at ca. 80°C. Samples containing more than 50% water were quite sticky and, as a result, were not suitable for testing.

2.2.2 Formamide and Ethylene Glycol Plasticized Samples

The polymer was dissolved in the plasticizer in a PTFE tray. The solution was then placed under vacuum at 80-90°C until the desired plasticizer content was obtained. Complete solution was essential, since inhomogeneous plasticization occurred if the polymer was not well dissolved. Water was avoided since traces of water would remain in the sample after drying, and these traces were found to influence the mechanical properties of the polymers.

AMPS and AMBTAC containing more than 15% plasticizer could be molded simply by heating the samples above their T_g, while, for plasticized DMDAAC samples, a pressure of 18,000 psi and an elevated temperature (60-80°C) were required.

2.2.3 Glycerine Plasticized Samples

Due to the high viscosity and high boiling point of glycerine, the method described above in section 2.2.2 could not be employed conveniently. In this case, only a slight excess weight of glycerine was added to the water solution of the polymer (too much glycerine caused foaming problems). The solution was then dried under vacuum at 90-100°C until the desired

glycerine content was obtained. Judging from the water-glycerine phase diagram[30]; the amount of water remaining in the samples was negligible. The samples were molded in the same way as described in section 2.2.2.

2.3 Calorimetric Studies

The glass transition temperatures were obtained using a Perkin Elmer Differential Scanning Calorimeter (Model DSC-1B) at a heating rate of 10°C/min. Samples containing ca. 12% water were molded first to the dimensions of the DSC sample pan, and then enclosed in the sample pan. Samples of high water content were prepared using the molded 12% samples, adding water and equilibrating and/or partially drying till the desired water content was achieved. The sample was weighed before and after each run. At the end of the experiment, on samples of high water content the samples were dried further to a lower water content, and the T_g redetermined. This procedure was repeated at progressively lower moisture contents. The T_g values for materials containing plasticizers other than water were not obtained by DSC.

2.4 Dynamic Mechanical Tests

Dynamic mechanical measurements were made under nitrogen atmosphere using a torsional pendulum, described previously at frequencies of ca. 1 Hz. Unless otherwise specified, all measurements were carried out with slow cooling rates (< 0.5°C/min). The T_g was identified by the maximum observed value of tan δ. Low tan δ values (< 0.5) were calculated by conventional methods, while for higher tan δ

values the ratio of amplitude was obtained by a trial and error method in moving the base line until the ratio of the first to the second half cycle amplitudes was equal to that of the second to the third half cycle amplitudes. This was done because the base line was found to drift at high values of tan δ.

Due to the brittleness of dry AMPS and AMBTAC samples and the difficulty in preparing dry DMDAAC samples, only plasticized samples were suitable for dynamic mechanical studies. Furthermore, since the plasticized AMPS and AMBTAC samples also became brittle at low temperatures, only cooling runs were made and in these cases, the experiments were terminated when the sample broke. Water desorption was observed also during the experiments. Thus, the range of water contents that could be studied for these materials was limited, on the one hand, by the brittleness of the samples of low water content, and on the other hand, by the rapid evaporation from those containing large amount of water.

2.5 Dielectric Experiments

Dielectric measurements were carried out on the instrument described in Section 2.7 of Part One of this thesis. Measurements were made over the temperature range -190°C to ca. 90°C and at frequencies of 100 Hz, 1kHz and 10kHz. Heating rates of less than 1°C per min. were employed. Three frequencies were measured in one single experiment to ensure the same experimental conditions at each frequency. It was observed that for low water content samples, water content increased during experiments.

3. EXPERIMENTAL RESULTS

In the first part of this section the results studied will be presented individually, for one material at a time. Subsequently, comparisons between different materials will be made.

3.1 D M D A A C

Unless specified, all measurements were performed on samples containing 0.02% NaCl.

3.1.1 Glass Transition

Fig. 3 shows a plot of T_g vs wt% water for DMDAAC together with the corresponding plots for AMPS and AMBTAC for comparison. For DMDAAC and AMBTAC, the T_g vs water content plot is similar, but quite different than the one for AMPS. The error bars reflect the desorption of water during the experiments.

3.1.2 Dielectric Studies

Fig. 4 presents the dielectric loss tangent at 1kHz as a function of temperature for DMDAAC with various water contents. Figs. 5-8 display the corresponding dielectric results for DMDAAC with various water contents. Two peaks are seen in most cases. The shape of the minor peak was obtained from the difference between the experimental curve and the estimated shape of the major peak for samples containing 1.2, 2.2 and 13.4 wt% water.

A plot of log ν vs 1/T is presented in Fig. 9. The major peak for the 1.2 wt% H_2O sample and the minor peak for all the others have an activation energy of 18 kcal/mole, while the minor peak for the 1.2 wt% H_2O sample and the major peak for all the others have an

activation energy of 21-22 kcal/mole. These two peaks are labeled as the β and γ relaxations respectively, and will be discussed later.

Fig. 10 shows the dielectric β and γ peak positions as a function of the water content, together with the corresponding plot for the α relaxation (obtained both by calorimetric and mechanical methods) and the mechanical γ relaxation.

3.1.3 Mechanical Studies

Fig. 11 shows G' and tan δ at ca. 2 Hz as functions of temperature for DMDAAC containing 10 wt% water (0.9 H_2O per ion pair) and 25 wt% water (2.2 H_2O per ion pair). It is obvious that both the α and γ peaks shift to lower temperatures with increasing water content. Also, G' decreases as the water content increases.

During the mechanical measurements, water was lost during the heating runs, presumably at the higher temperatures. Therefore, no further studies of this type were carried out. However, since the γ relaxation occurred at a very low temperature, the (measured) initial water contents are probably appropriate for those runs, i.e. 12 wt% and 27 wt%. Therefore, it is not surprising that the γ peak positions fall on the dielectric lines in Fig. 9, whereas the α peak positions do not.

Figs. 12 to 14 illustrate the plasticization effect of formamide, ethylene glycol and glycerine on the mechanical properties of DMDAAC containing 1-2% NaCl. Both G' and tan δ at ca. 1 Hz are given as functions of temperature. It is apparent that the largest peaks originate from the glass transition. The peaks shift to lower temperatures and also the heights of the peaks increase linearly with increasing plasticizer content. This will be shown in a subsequent figure for several materials

and plasticizers. Also, G' decreases as plasticizer content increases. A rubbery plateau is evident in all samples and the rubbery modulus decreases with increasing plasticization. For both formamide and ethylene glycol plasticized samples, the peak positions are a linear function of the plasticizer content, as can be seen in Fig. 15. The rates of T_g depression for formamide and ethylene glycol plasticized samples are 3.0°C/wt% and 2.6°C/wt% respectively. The rates for samples plasticized with water or glycerine were not determined, since the data for the glycerine plasticized samples show considerable scatter so that no meaningful line could be drawn, and only a single point for the water sample was measured. However, it is considered unlikely that the water plot would be linear (as can be seen in Fig. 3).

Table 1 summarizes the results for the different plasticizers used with DMDAAC. Figs. 16 and 17 show the effect of different plasticizers on DMDAAC, at concentrations of 24± 1 wt% and 43± 2wt% respectively. It is interesting to note that DMDAAC plasticized by 25 wt% water shows no rubbery plateau, but does show a well separated β peak, which is not seen when the other plasticizers are used.

3.2 A M P S

3.2.1 Glass Transition

The lowering of the glass transition temperature with increasing water content was shown in Fig. 3. It is not surprising that the T_g of the dry material is rather high by comparison to other non-ionic organic polymers.

TABLE 1 Glass Transition Depression by Different Plasticizers in DNDAAC

Plasticizer	Wt%	ΔT_g (°C)	ΔT_g/Wt%	Average
Water	10	31 *	3.10	2.43
-	25	44	1.76	
FA	10	31	3.10	3.03
	24	70	2.91	
	41	126	3.07	
EG	14	36	2.57	2.58
	23	59	2.56	
	46	120	2.61	
GL	9	10	1.11	2.41
	24	88	3.66	
	42	103	2.45	

* Estimated value

3.2.2 Mechanical Studies

Fig. 18 shows the temperature dependence of G' and tan δ as a function of water content. No dry sample was studied due to the difficulty of sample preparation. A large uncertainty in peak position is anticipated due to the loss of water content at elevated temperatures. However, it is clear that the peak height is proportional to the water content. No sub-T_g relaxation is found (as discussed later). As the water content increases, G' is lowered and the tendency to flow, is increased as indicated by the storage modulus plot.

In Fig. 19 the effects of different plasticizers (at 24 wt%) on the mechanical properties of AMPS are compared. The glycerine-plasticized sample twisted at elevated temperatures, so that only a part of the curve is shown for that run.

3.3 A M B T A C

3.3.1 Glass Transition

The glass transition temperature vs water content was shown in Fig. 3. It is clear that the effect of water on the glass transition of AMBTAC is similar to that of DMDAAC, which also contains quaternary ammonium groups.

3.3.2 Mechanical Studies

Fig. 20 displays G' and tan δ as functions of temperature for various plasticizers (24 wt%) for the AMBTAC system. For the formamide and ethylene glycol plasticized samples, a shoulder is found on the low temperature side of T_g. The glycerine plasticized sample shows only one relatively symmetric T_g peak, but a β peak becomes significant as the glycerine content increases to 43 wt% (as shown in Fig. 21).

3.4 Water Absorption

Although this phenomenon was not studied quantitatively, it was observed that under ambient humidity, the equilibrium water uptake is inversely in related to the glass transition temperature. AMPS (T_g = 170°C) absorbs ca. 8 wt%, AMBTAC (T_g = 112°C) absorbs ca. 11 wt%, and DMDAAC (T_g = 68°C) absorbs ca. 20 wt% water.

3.5 Summary of Plasticization Results

3.5.1 Mechanical Studies

Figs. 22 to 25 illustrate the plasticizing effects of water, formamide, ethylene glycol and glycerine, respectively, on all the polymers studied. Fig. 25 also includes the result of glycerine-plasticized PNaA[1] for comparison. It is apparent from these figures that the response of DMDAAC to the different plasticizers is different from those of AMPS and AMBTAC in that the former usually shows a well developed rubbery plateau. The results are summarized below:

(1) Of all the samples studied, DMDAAC with non-aqueous plasticizers shows the most clearly developed rubbery plateau.

(2) In water plasticized DMDAAC samples, a clear sub-T_g relaxation (γ peak) is seen. Such a peak is not observed in water plasticized samples of AMPS or AMBTAC.

(3) In the samples of DMDAAC plasticized for formamide, a rather broad peak is observed in the vicinity of T_g. For the other polymers, the peak is somewhat sharper and higher.

(4) At a constant weight concentration, ethylene glycol tends to make the α peak of DMDAAC smaller than those of AMPS and AMBTAC.

3.5.2 Dielectric

Only DMDAAC was studied with only water as a plasticizer. Therefore, no separate summary of results is presented.

Figure 2.

Phase diagram of water-glycerine.

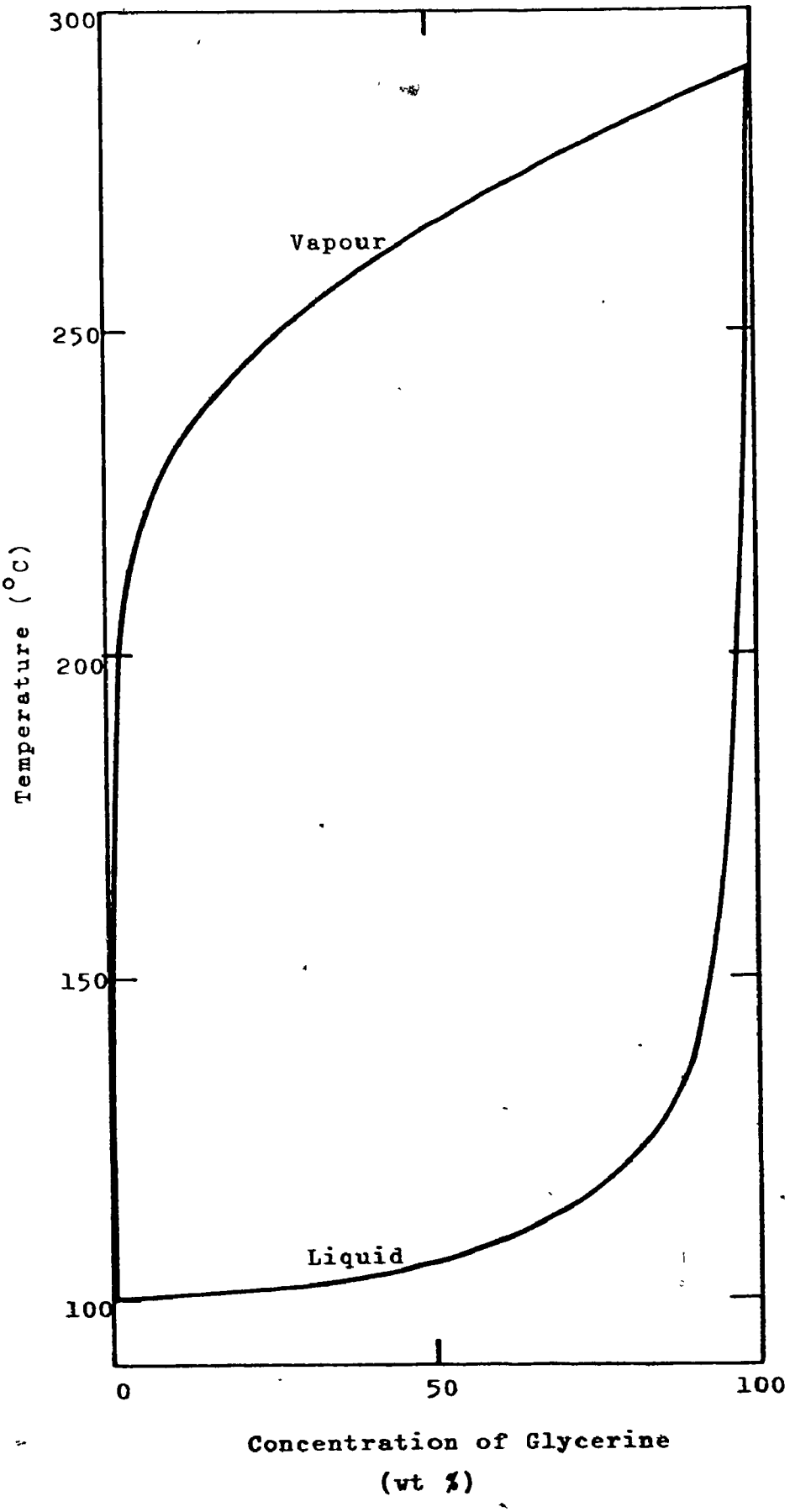
300
250
200
150
100
Vapour
Liquid
Temperature (°C)
0
50
100
Concentration of Glycerine
(wt %)

Figure 3.

Glass transition temperatures vs. water content for DMDAAC, AMPS and AMBTAC.

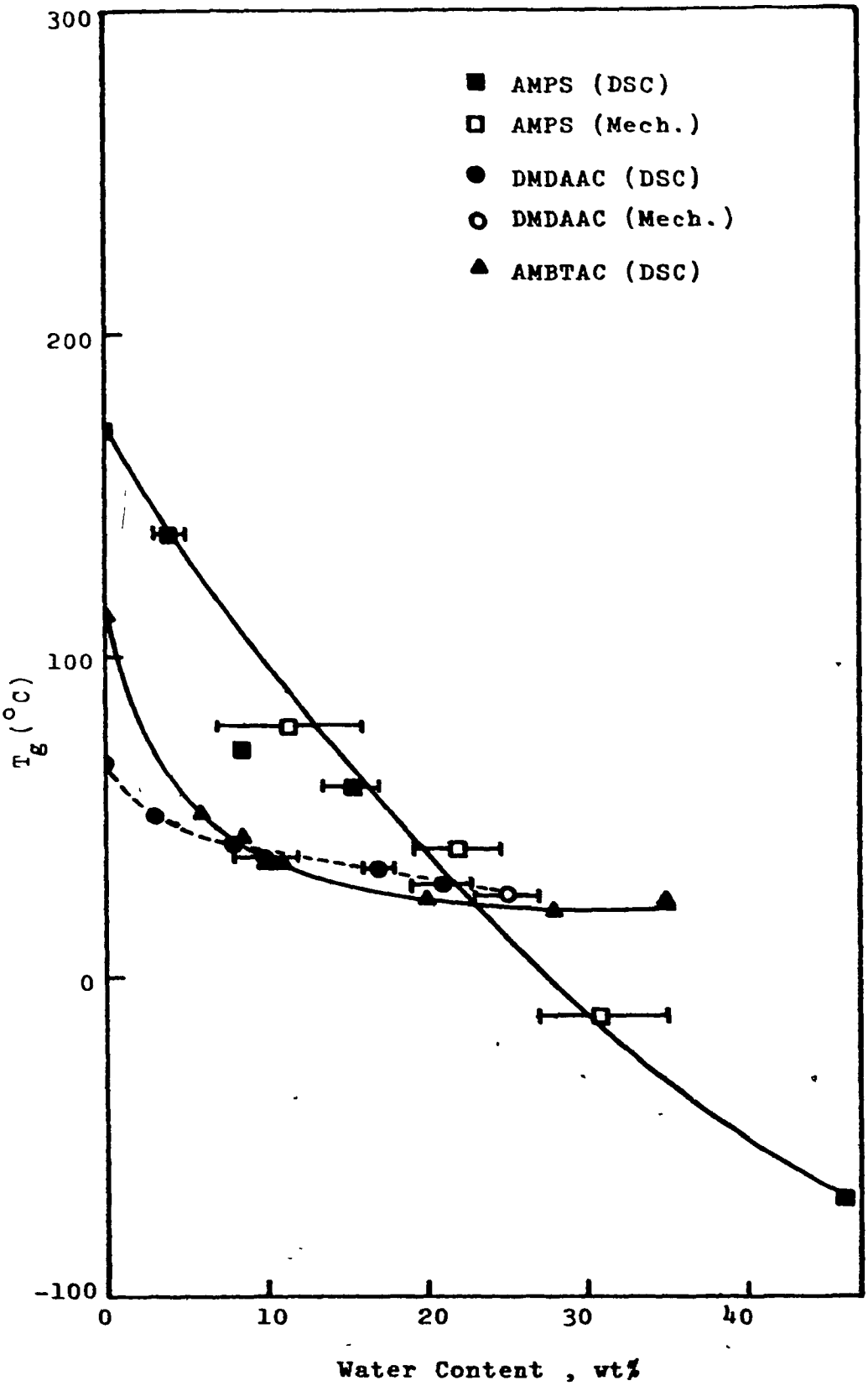
300
200
100
0
-100
T_g (°C)
0
10
20
30
40
Water Content , wt%
AMPS (DSC)
AMPS (Mech.)
DMDAAC (DSC)
DMDAAC (Mech.)
AMBTAC (DSC)

Figure 4.

Dielectric loss tangent vs. temperature for DMDAAC with varying water content at 1 kHz.

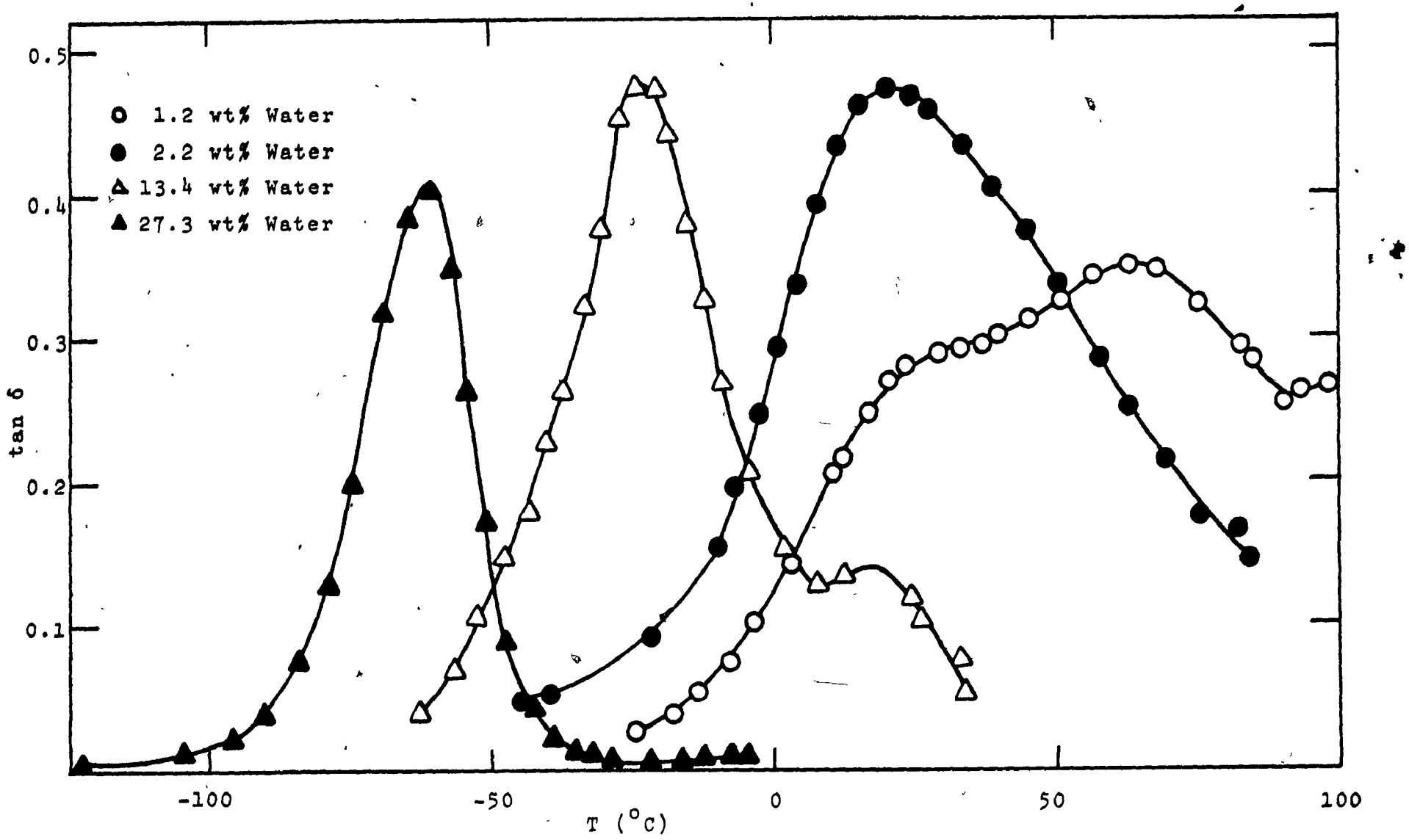
1.2 wt% Water
2.2 wt% Water
13.4 wt% Water
27.3 wt% Water
0.5
0.4
0.3
0.2
0.1
tan δ
-100
-50
0
50
100
T (°C)

Figure 5.

Dielectric loss tangent vs. temperature for DMDAAC with 1.2 wt% water at 100 Hz, 1 kHz and 10 kHz.

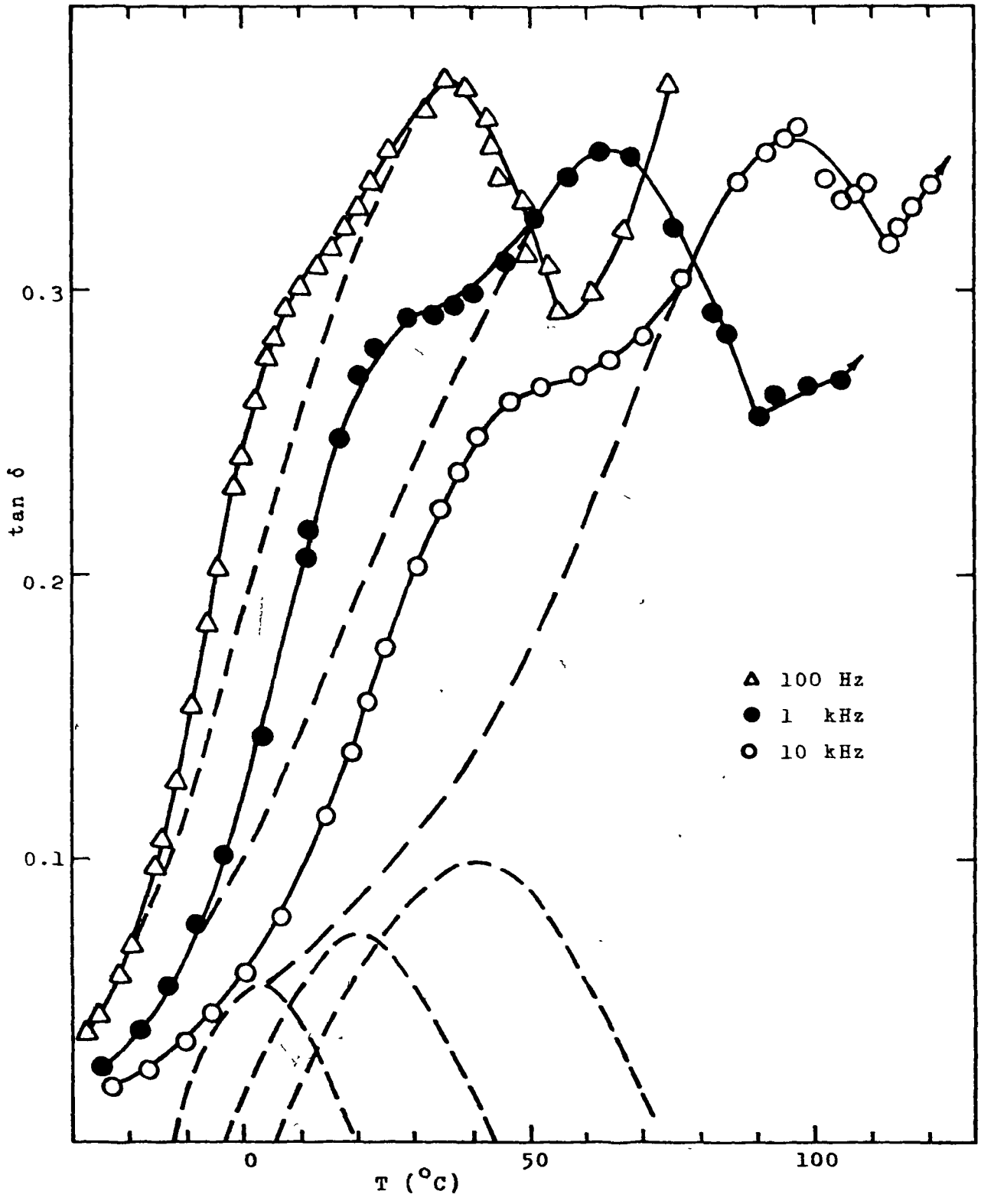
0.3
0.2
0.1
tan δ
0
50
100
T (°C)
100 Hz
1 kHz
10 kHz

Figure 6.

Dielectric loss tangent vs. temperature for DMDAAC with 2.2 wt% water at 100 Hz, 1 kHz and 10 kHz.

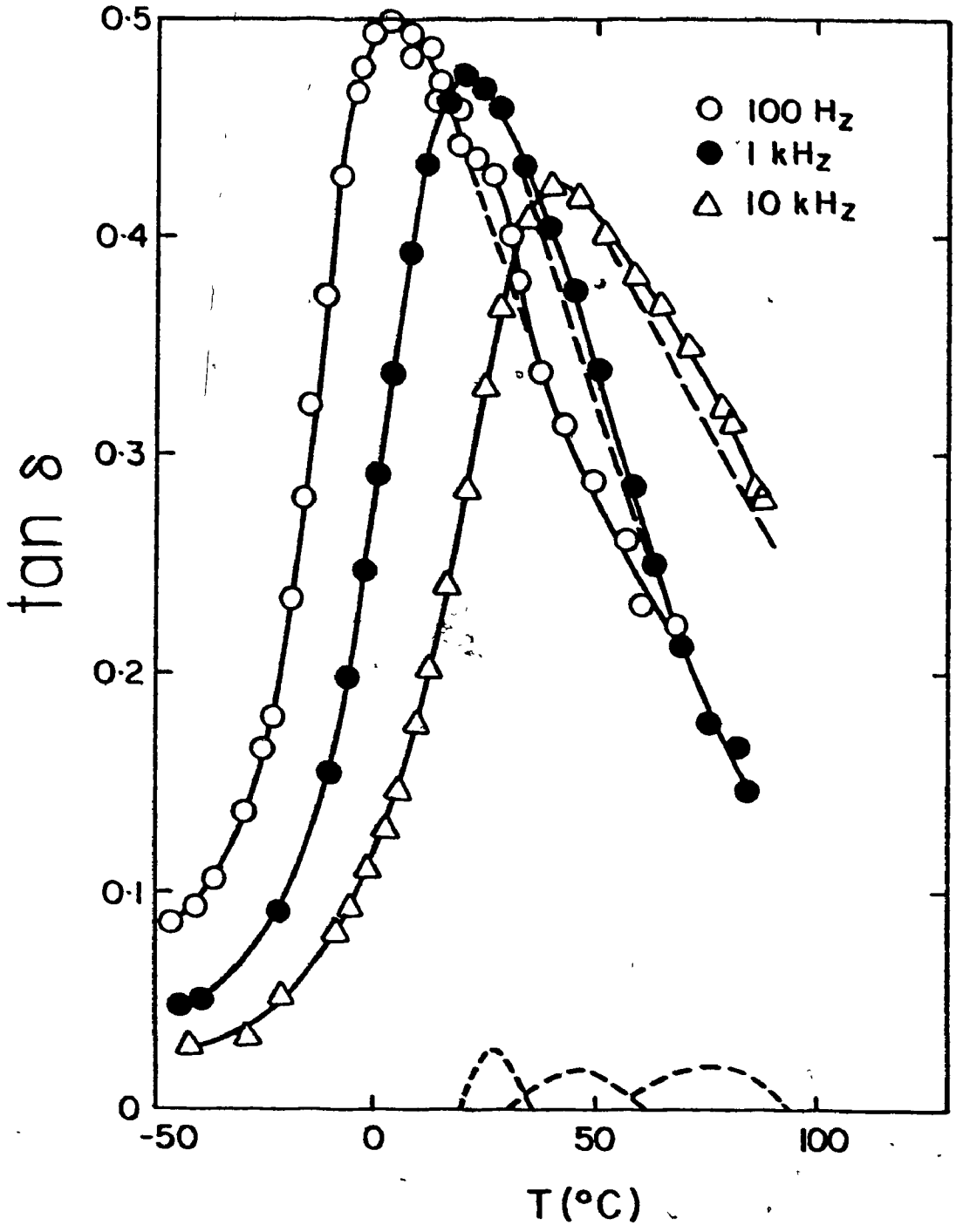
0·5
0·4
0·3
0·2
0·1
0
tan δ
-50
0
50
100
T (°C)
100 Hz
1 kHz
10 kHz

Figure 7.

Dielectric loss tangent vs. temperature for DMDAAC with 13.4 wt% water at 100 Hz, 1 kHz and 10 kHz.

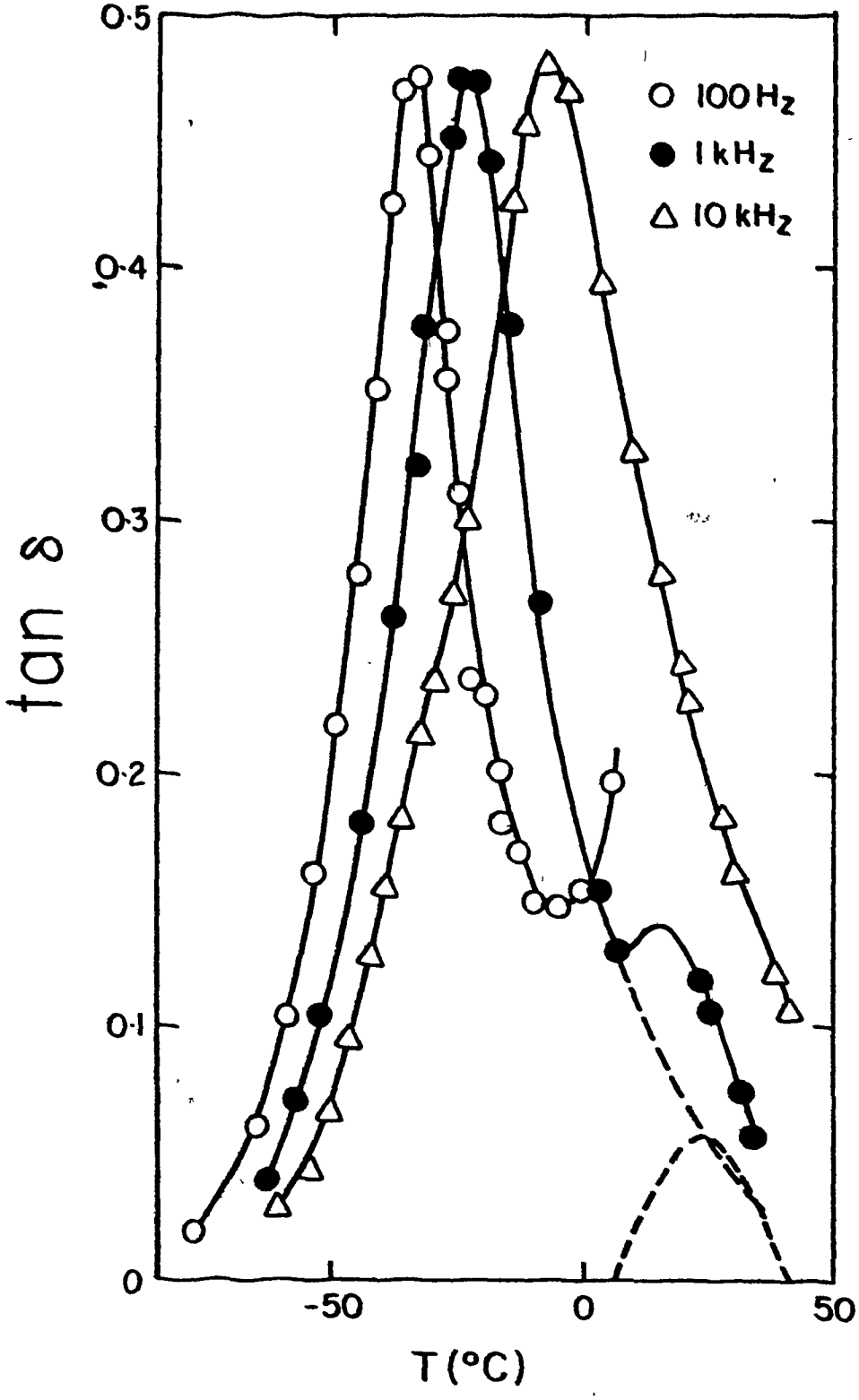
0·5
0·4
0·3
0·2
0·1
0
tan δ
100 Hz
1 kHz
10 kHz
-50
0
50
T (°C)

Figure 8.

Dielectric loss tangent vs. temperature for DMDAAC with 27.3 wt% water at 100 Hz, 1 kHz and 10 kHz.

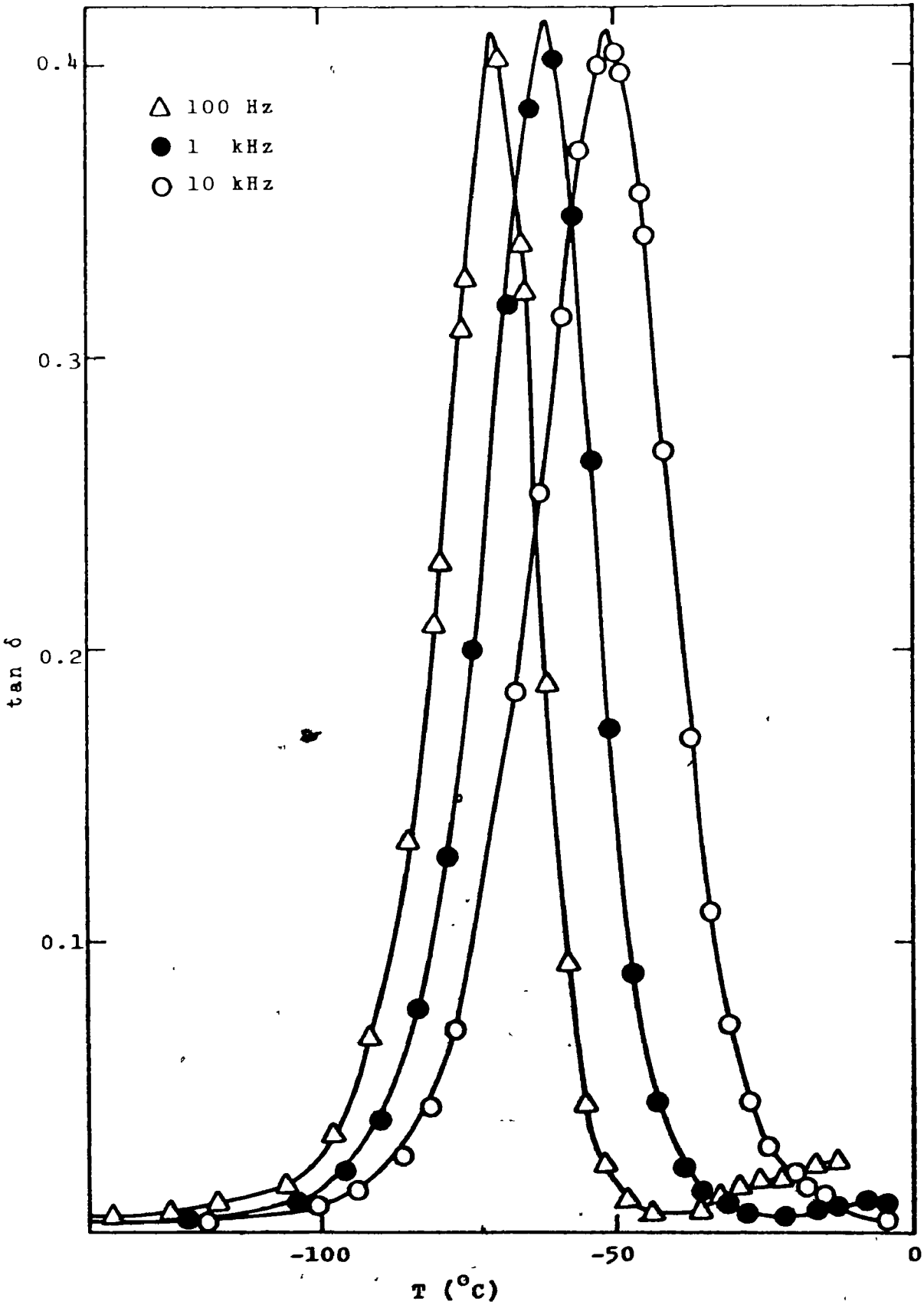
0.4
0.3
0.2
0.1
tan δ
△ 100 Hz
● 1 kHz
○ 10 kHz
-100
-50
0
T (°C)

Figure 9

Log ν vs. 1/T for dielectric β and γ peaks and mechanical γ peak for DMDAAC.

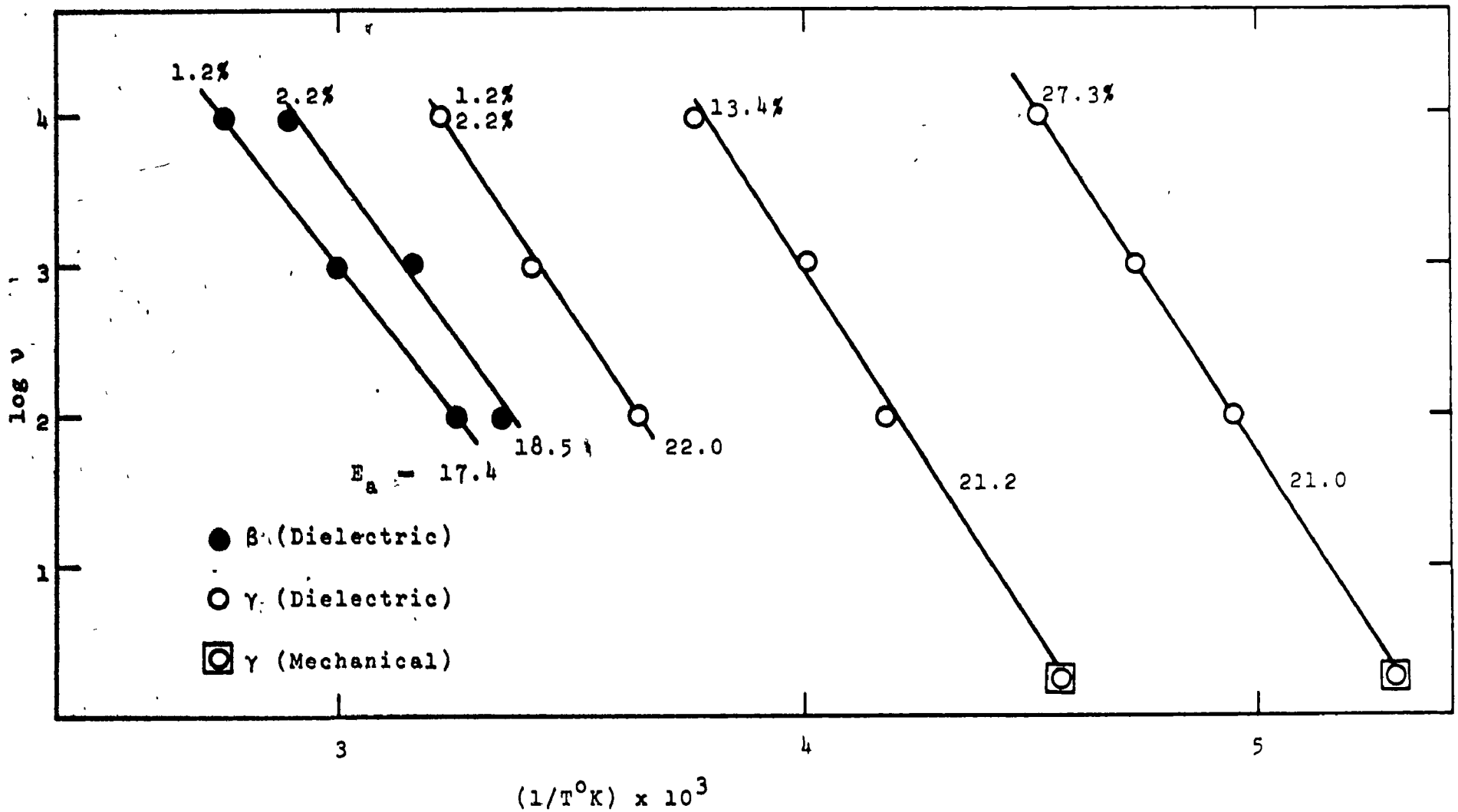
1.2%
2.2%
1.2%
2.2%
13.4%
27.3%
18.5
22.0
21.2
21.0
E_a = 17.4
β (Dielectric)
γ (Dielectric)
γ (Mechanical)
log ν
4
3
2
1
3
4
5
(1/T°K) x 10^3

Figure 10.

Dielectric β and γ peak position along with α relaxation and mechanical γ peak position as a function of water content for DMDAAC.

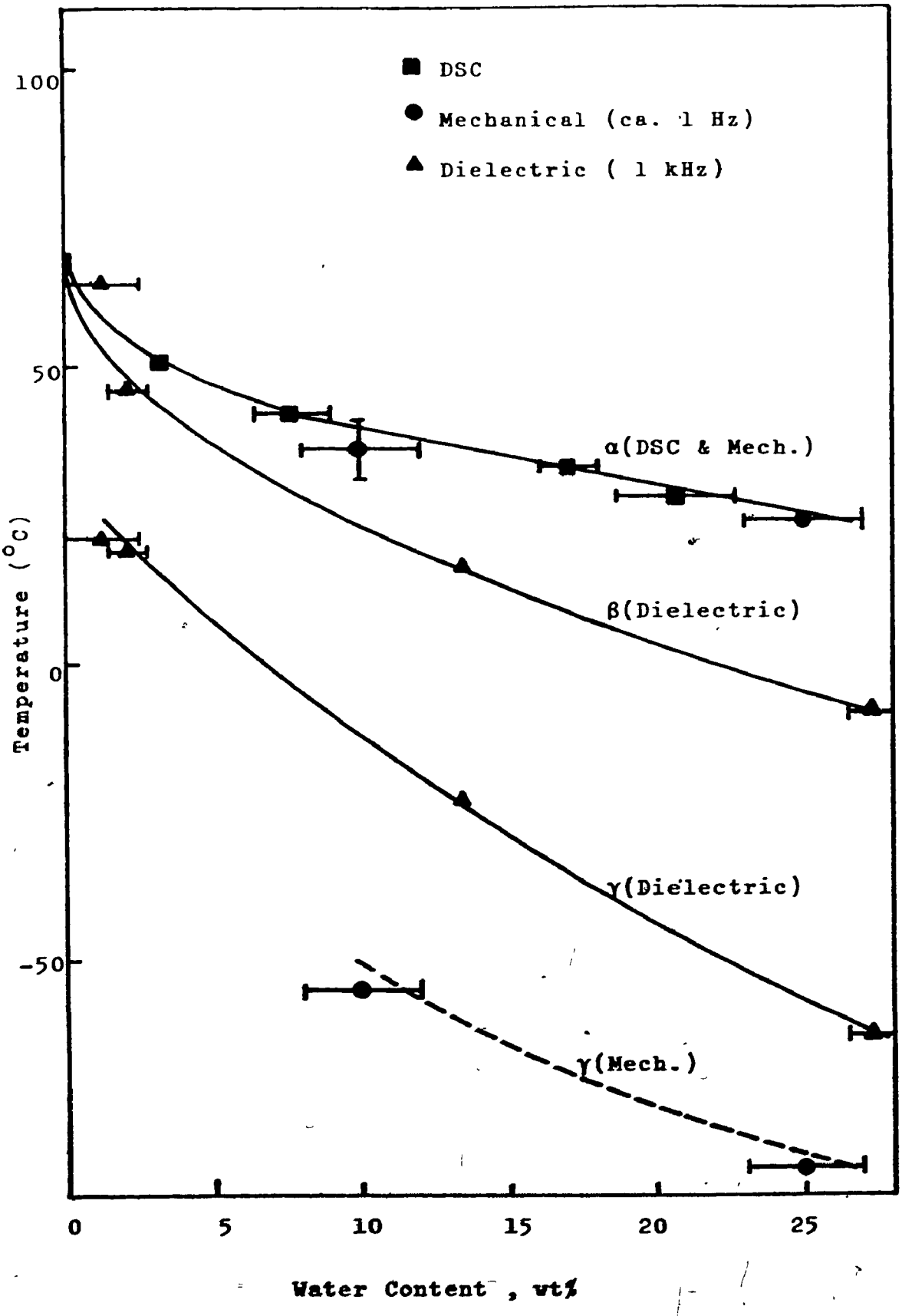
DSC
Mechanical (ca. 1 Hz)
Dielectric (1 kHz)
100
50
0
-50
Temperature (°C)
α(DSC & Mech.)
β(Dielectric)
γ(Dielectric)
γ(Mech.)
0
5
10
15
20
25
Water Content , wt%

Figure 11.

G' and tanδ vs. temperature for DMDAAC containing 10 wt% water and 25 wt% water at ca. 2 Hz.

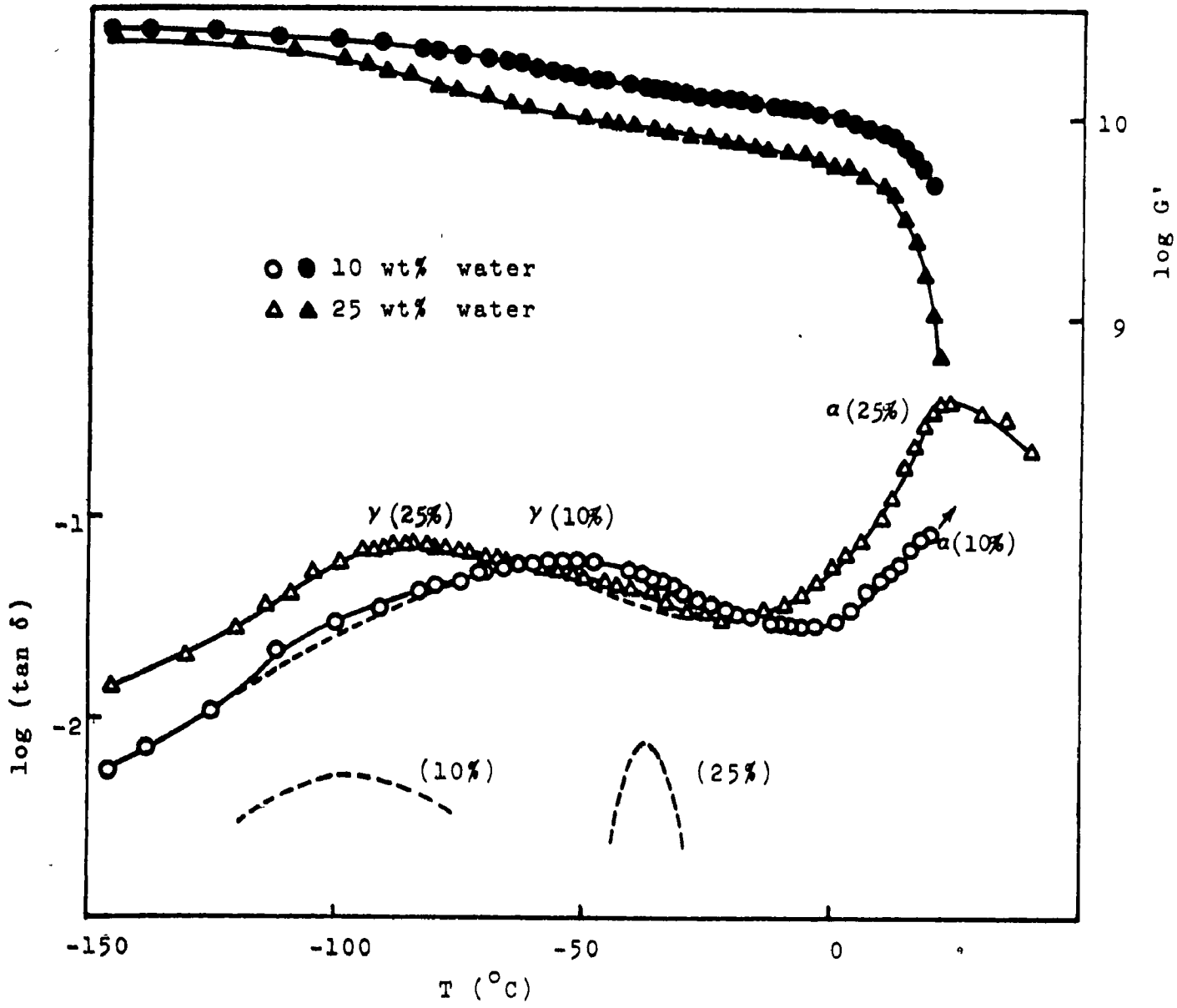
10 wt% water
25 wt% water
α(25%)
γ(25%)
γ(10%)
α(10%)
(10%)
(25%)
log (tan δ)
log G'
-1
-2
10
9
-150
-100
-50
0
T (°C)

Figure 12.

G' and tanδ vs. temperature for DMDAAC containing varying formamide content at ca. 1 Hz.

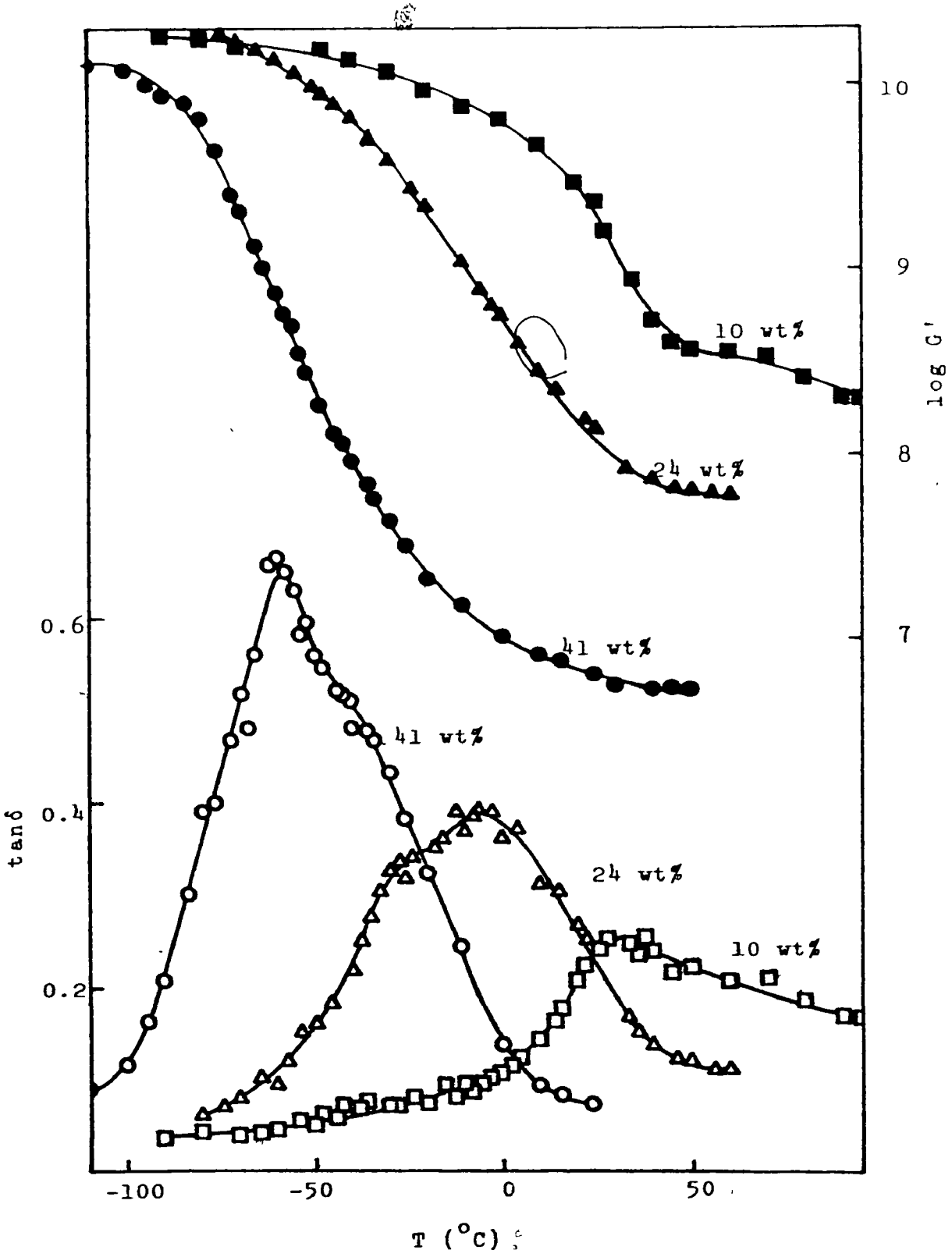
10
9
8
7
log G'
10 wt%
24 wt%
41 wt%
0.6
0.4
0.2
tanδ
41 wt%
24 wt%
10 wt%
-100
-50
0
50
T (°C)

Figure 13.

G' and tanδ vs. temperature for DMDAAC containing varying ethylene glycol content at ca. 1 Hz.

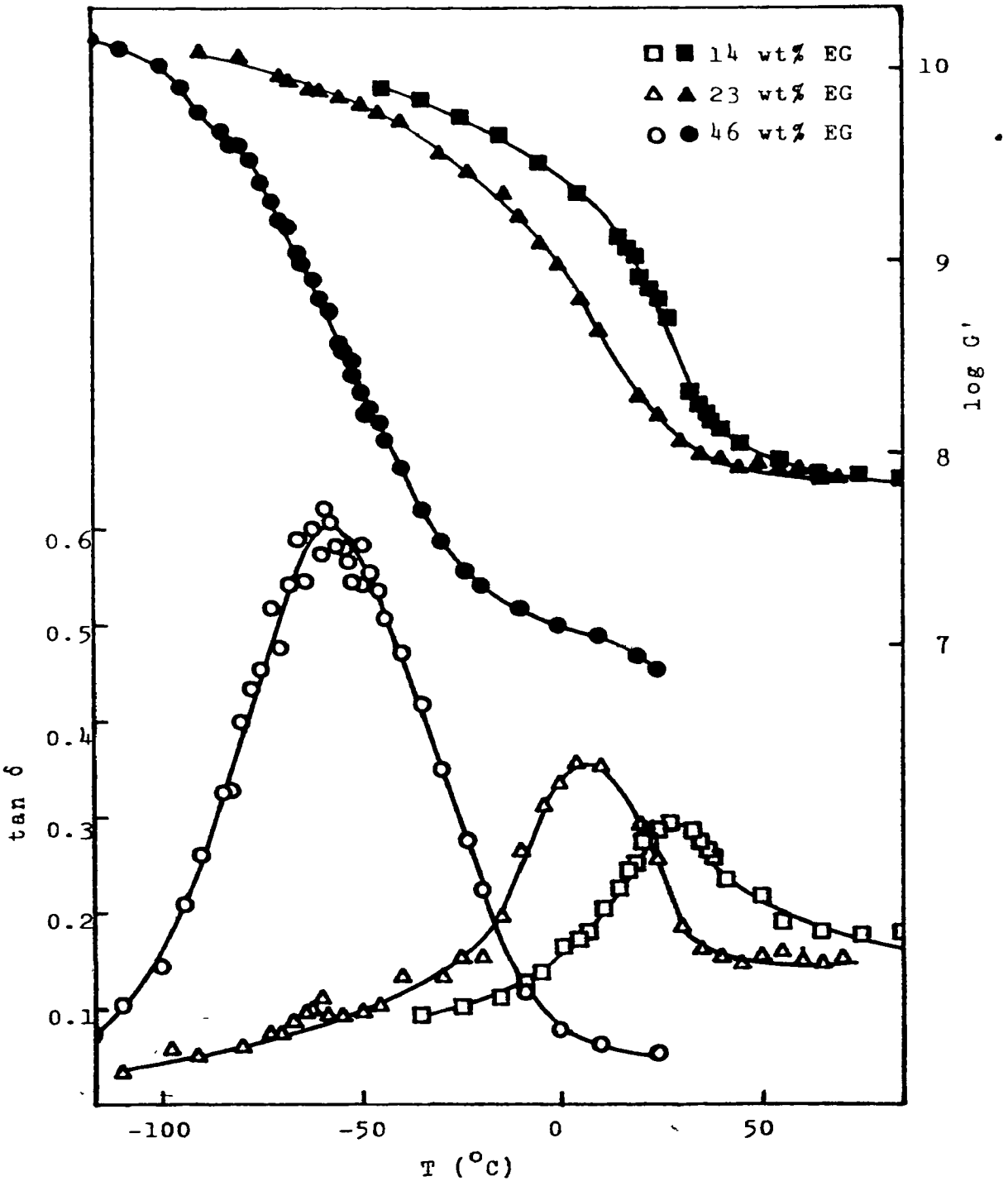
14 wt% EG
23 wt% EG
46 wt% EG
log G'
10
9
8
7
tan δ
0.6
0.5
0.4
0.3
0.2
0.1
-100
-50
0
50
T (°C)

Figure 14.

G' and tanδ vs. temperature for DMDAAC containing varying glycerine content at ca. 1 Hz.*

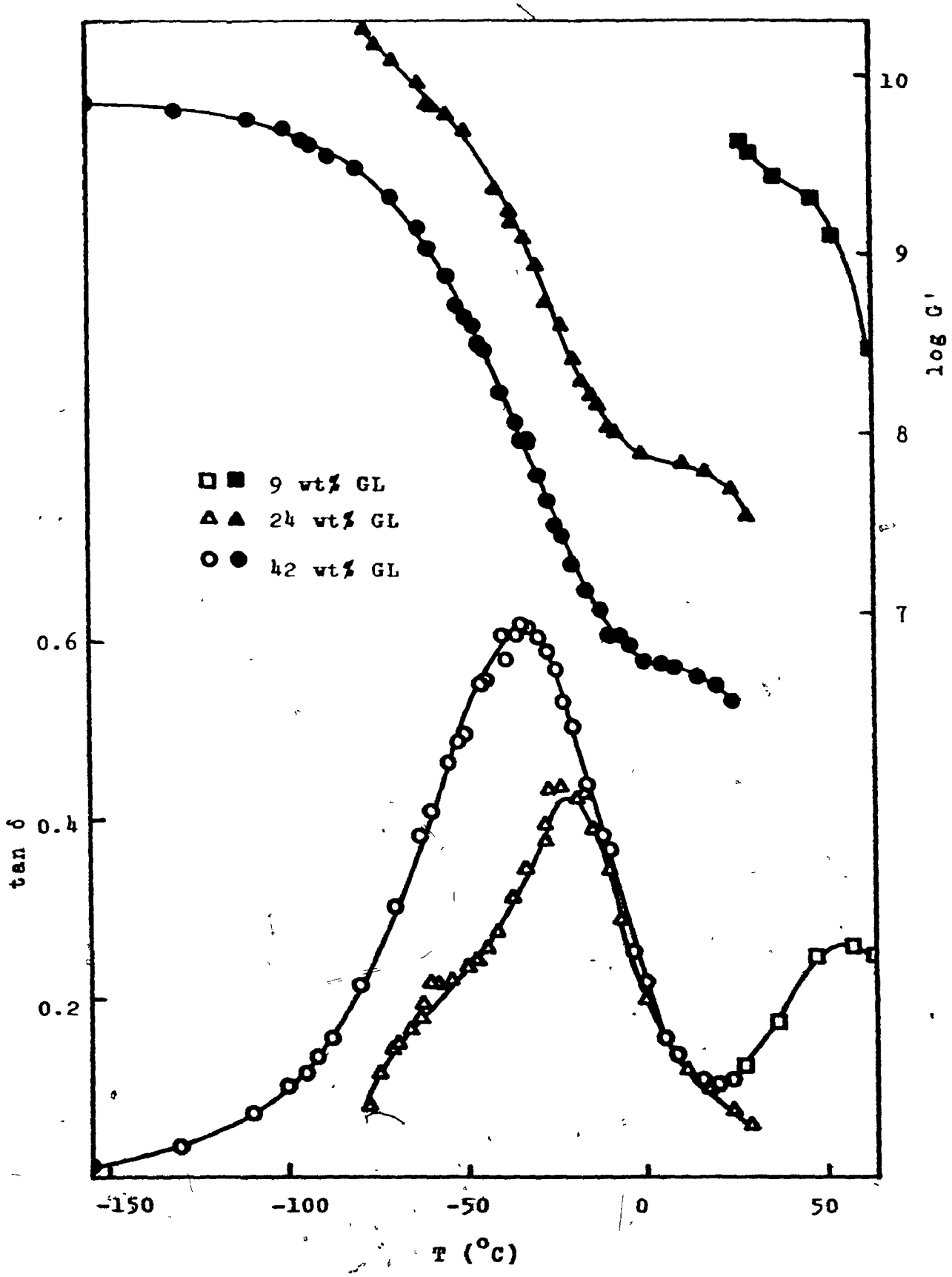
9 wt% GL
24 wt% GL
42 wt% GL
tan δ
0.6
0.4
0.2
log G'
10
9
8
7
-150
-100
-50
0
50
T (°C)

Figure 15.

Glass transition temperature vs. water, formamide and ethylene glycol content for DMDAAC.

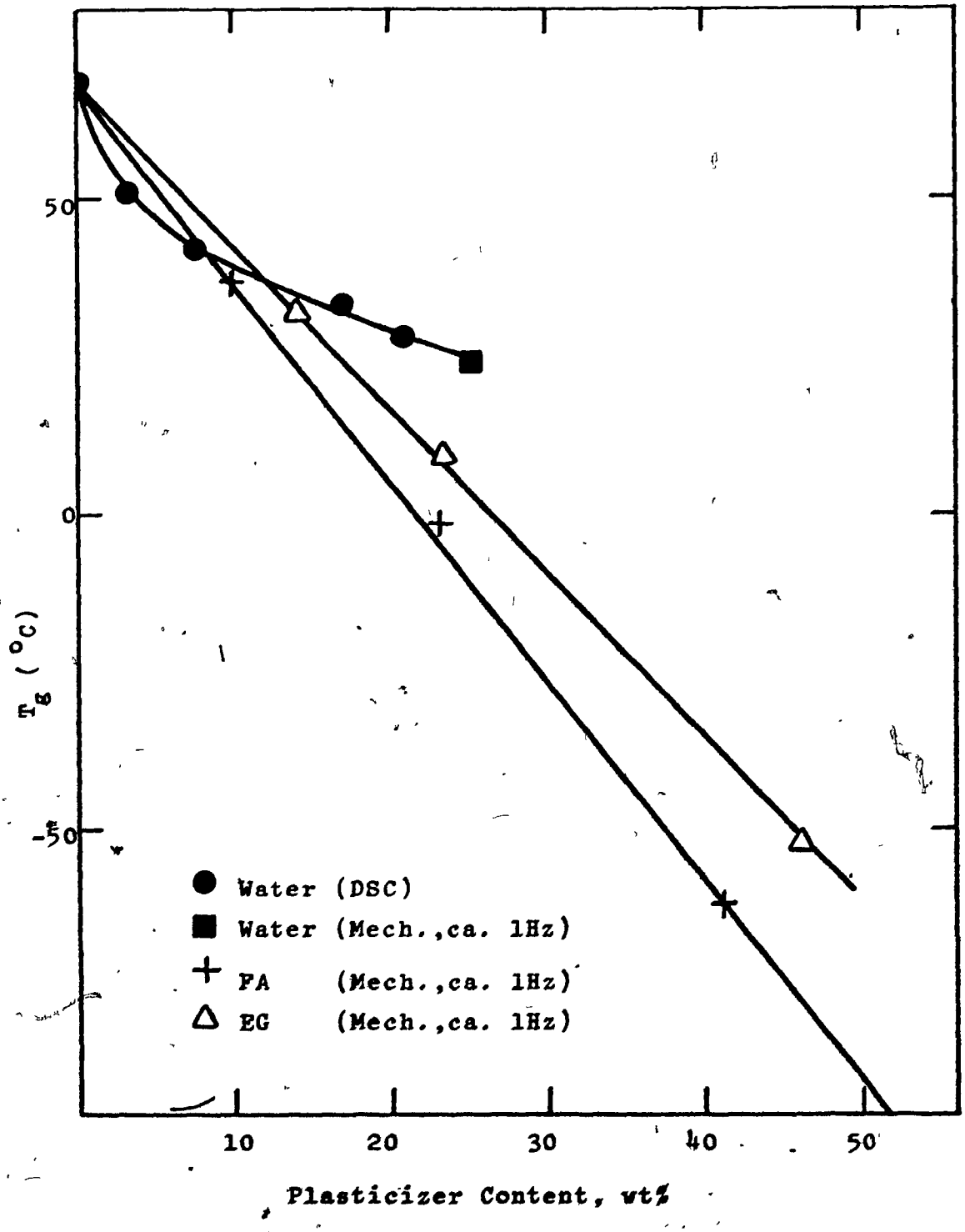
50
0
-50
T_g (°C)
Water (DSC)
Water (Mech.,ca. 1Hz)
PA (Mech.,ca. 1Hz)
EG (Mech.,ca. 1Hz)
10
20
30
40
50
Plasticizer Content, wt%

Figure 16.

G' and tanδ vs. temperature for DMDAAC containing ca. 24 wt% of various plasticizers.

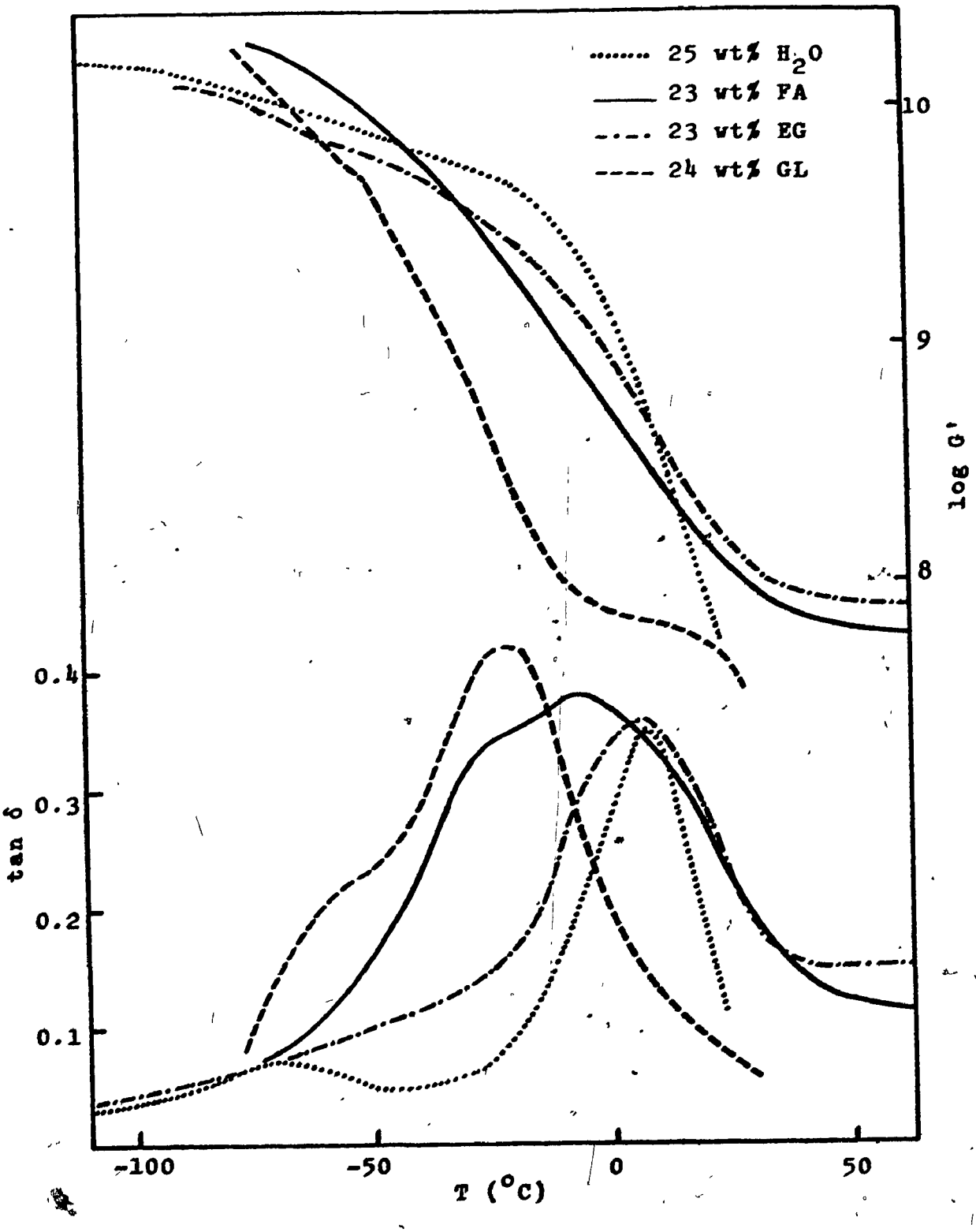
25 wt% H_2O
23 wt% FA
23 wt% EG
24 wt% GL
log G'
10
9
8
tan δ
0.4
0.3
0.2
0.1
-100
-50
0
50
T (°C)

Figure 17.

G' and tanδ vs. temperature for DMDAAC containing ca. 43 wt% of various plasticizers.

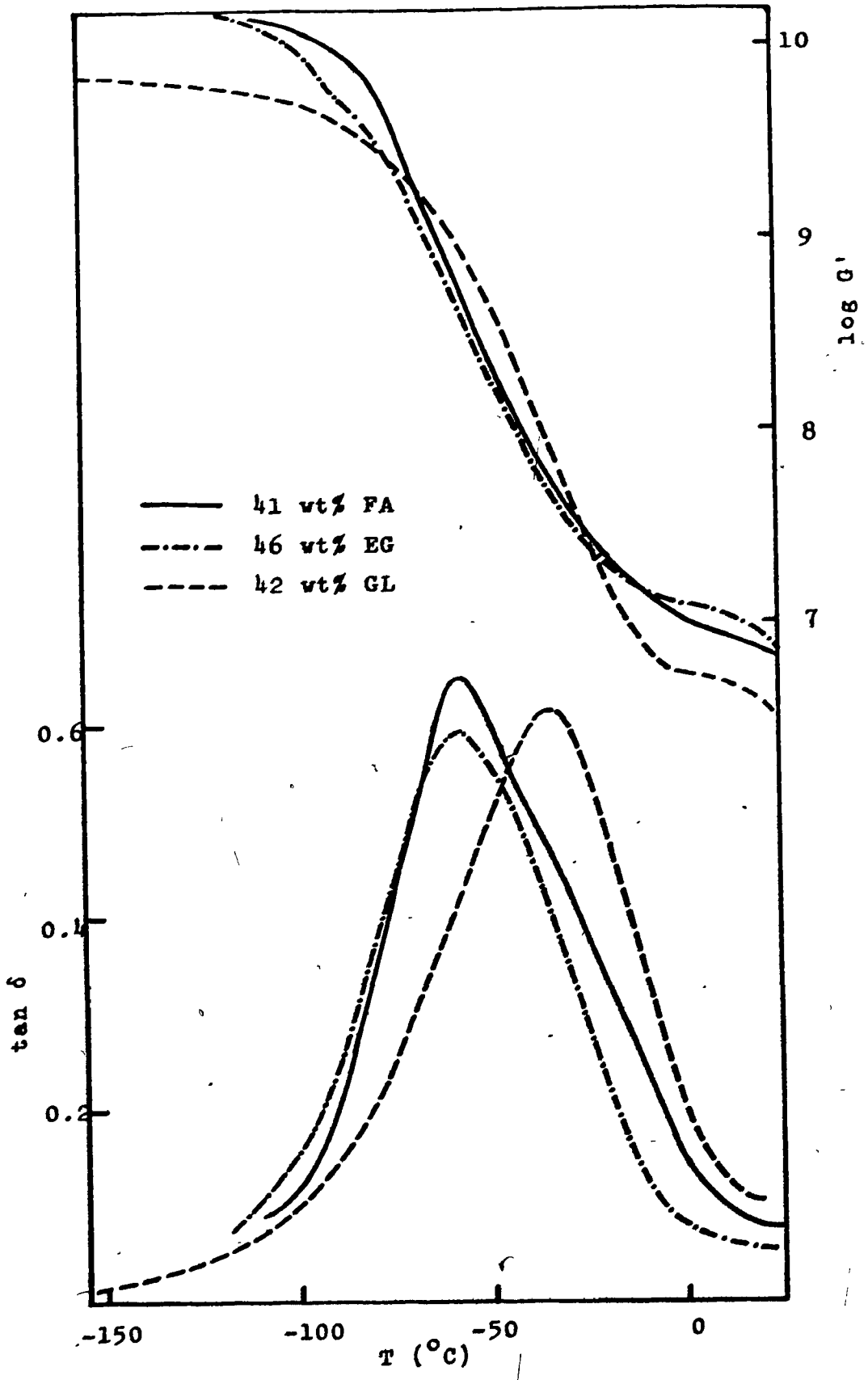
10
9
8
7
log G'
41 wt% FA
46 wt% EG
42 wt% GL
0.6
0.4
0.2
tan δ
-150
-100
-50
0
T (°C)

Figure 18

G' and tanδ vs. temperature for AMPS containing varying water content at ca. 1 Hz.

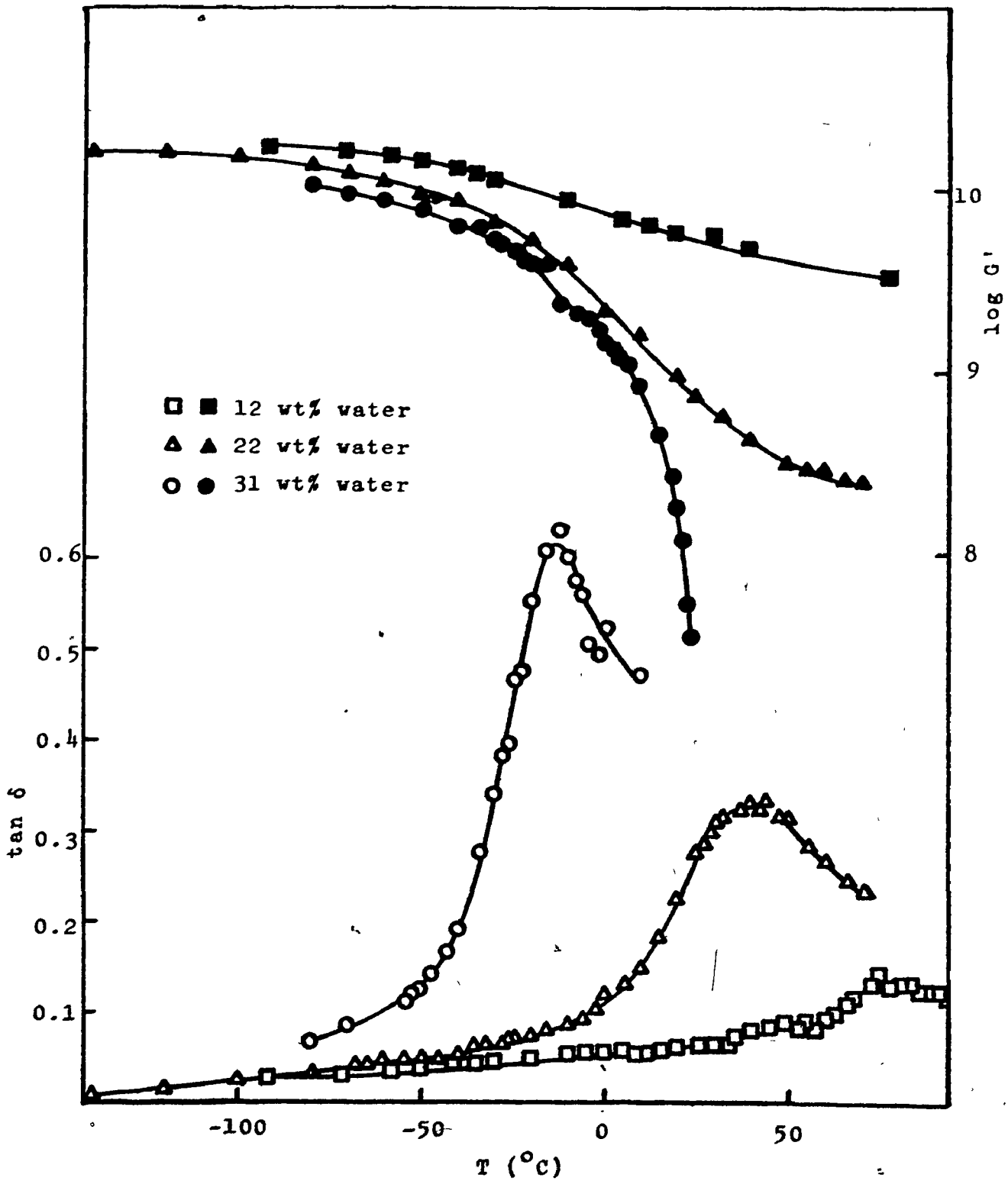
12 wt% water
22 wt% water
31 wt% water
log G'
10
9
8
tan δ
0.6
0.5
0.4
0.3
0.2
0.1
-100
-50
0
50
T (°C)

Figure 19.

G' and tanδ vs. temperature for AMPS containing ca. 24 wt% of various plasticizers.

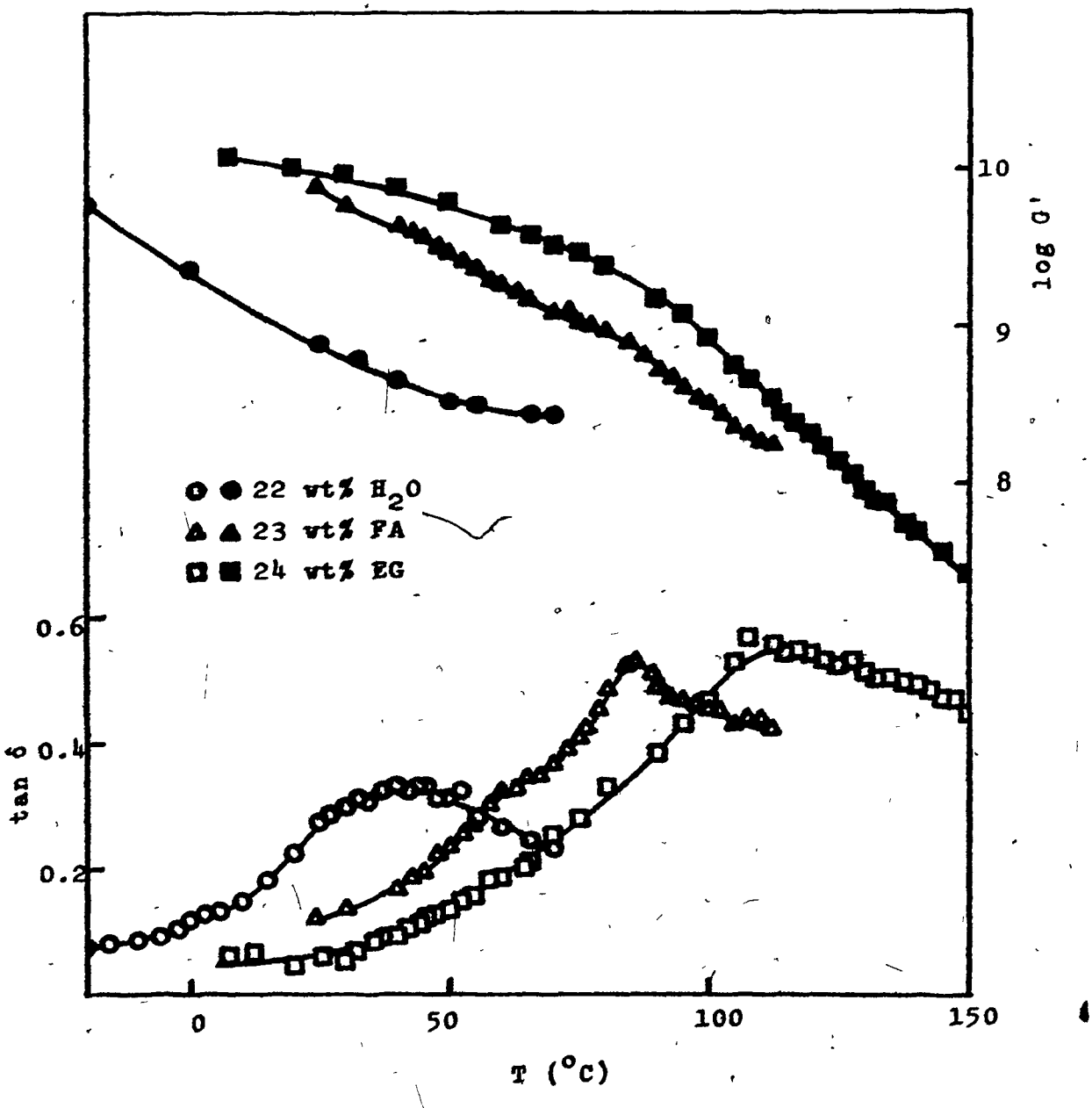
10
9
8
log G'
22 wt% H_2O
23 wt% FA
24 wt% EG
0.6
0.4
0.2
tan δ
0
50
100
150
T (°C)

Figure 20.

G' and tanδ vs. temperature for AMBTAC containing ca. 24 wt% of various plasticizers.

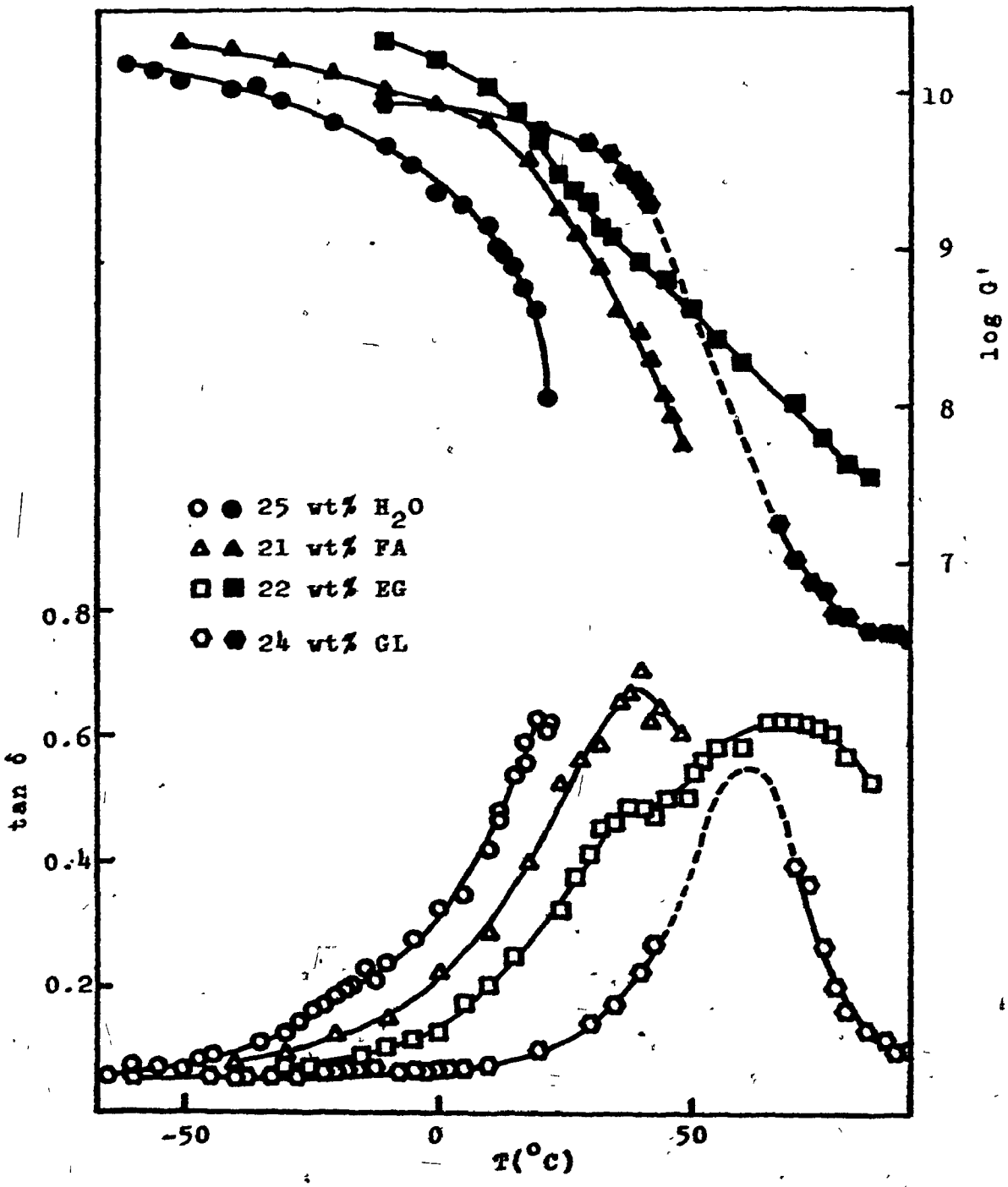
10
9
8
7
log G'
0.8
0.6
0.4
0.2
tan δ
25 wt% H_2O
21 wt% FA
22 wt% EG
24 wt% GL
-50
0
50
T(°C)

Figure 21.

G' and tanδ vs. temperature for AMBTAC containing 24 wt% and 43 wt% glycerine.

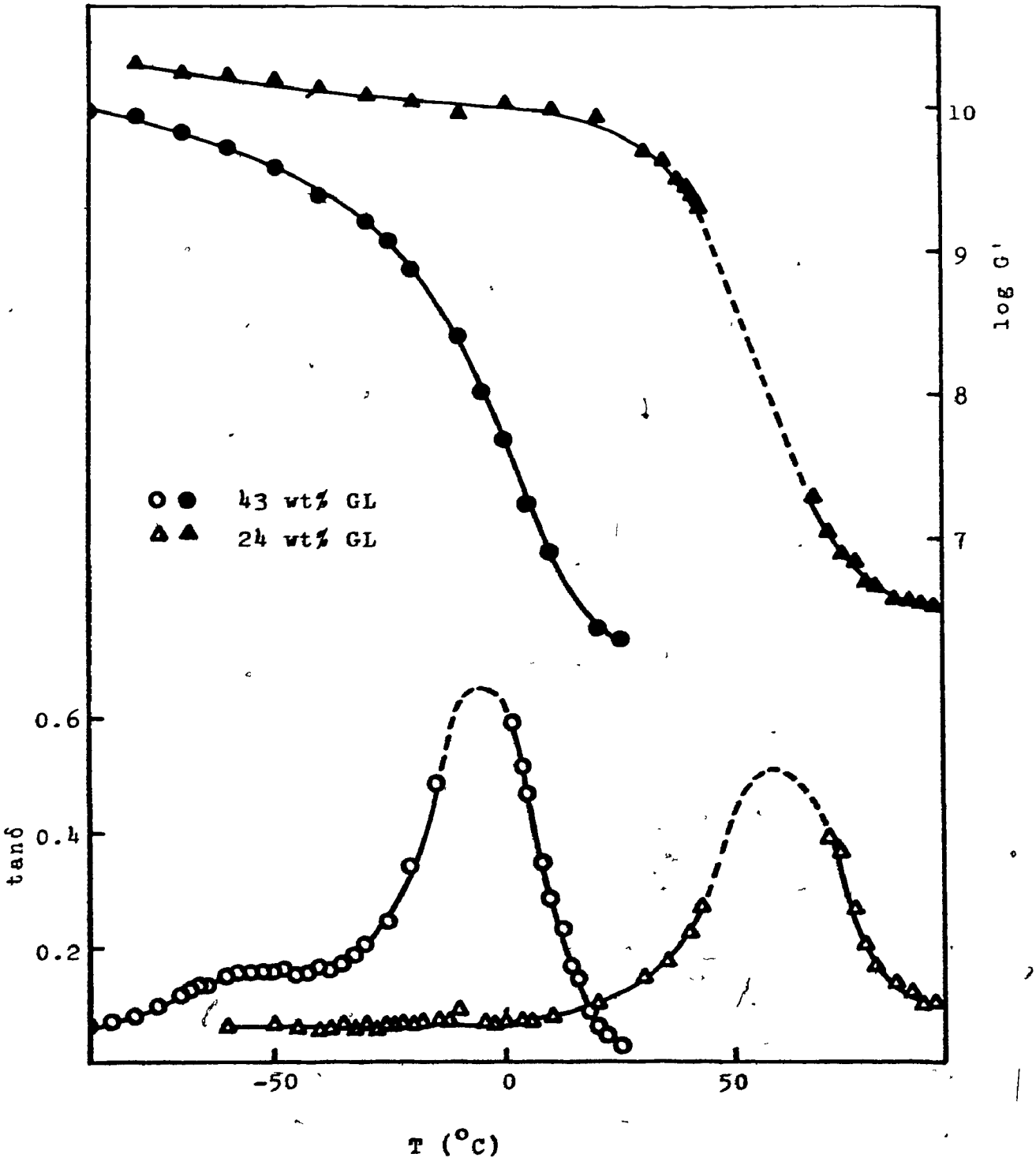
43 wt% GL
24 wt% GL
log G'
10
9
8
7
tanδ
0.6
0.4
0.2
-50
0
50
T (°C)

Figure 22.

G' and tanδ vs. temperature for various polyelectrolytes with ca. 24 wt% water.

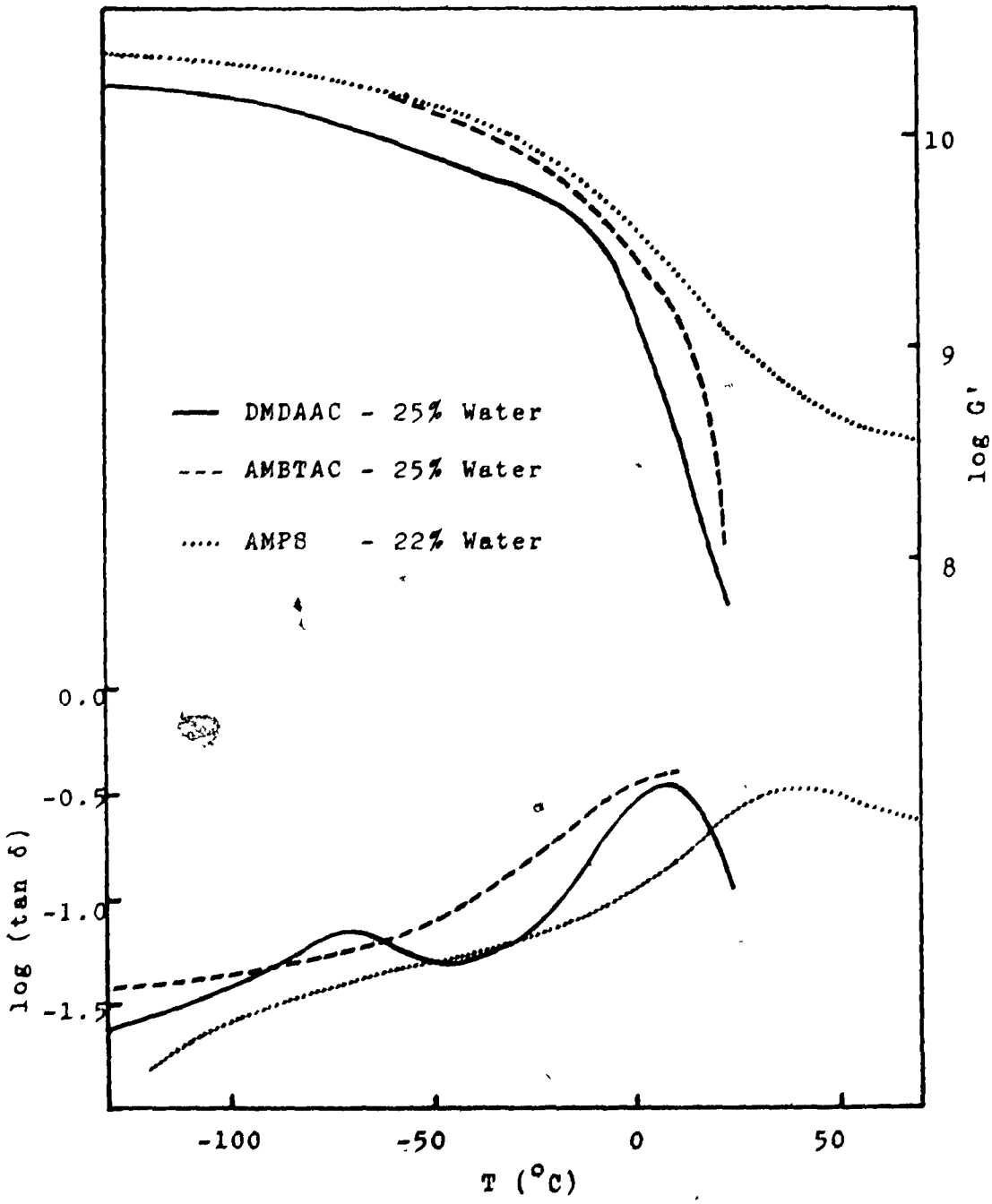
DMDAAC - 25% Water
AMBTAC - 25% Water
AMPS - 22% Water
10
9
8
log G'
0.0
-0.5
-1.0
-1.5
log (tan δ)
-100
-50
0
50
T (°C)

Figure 23.

G' and tanδ vs. temperature for various polyelectrolytes with ca. 24 wt% formamide.

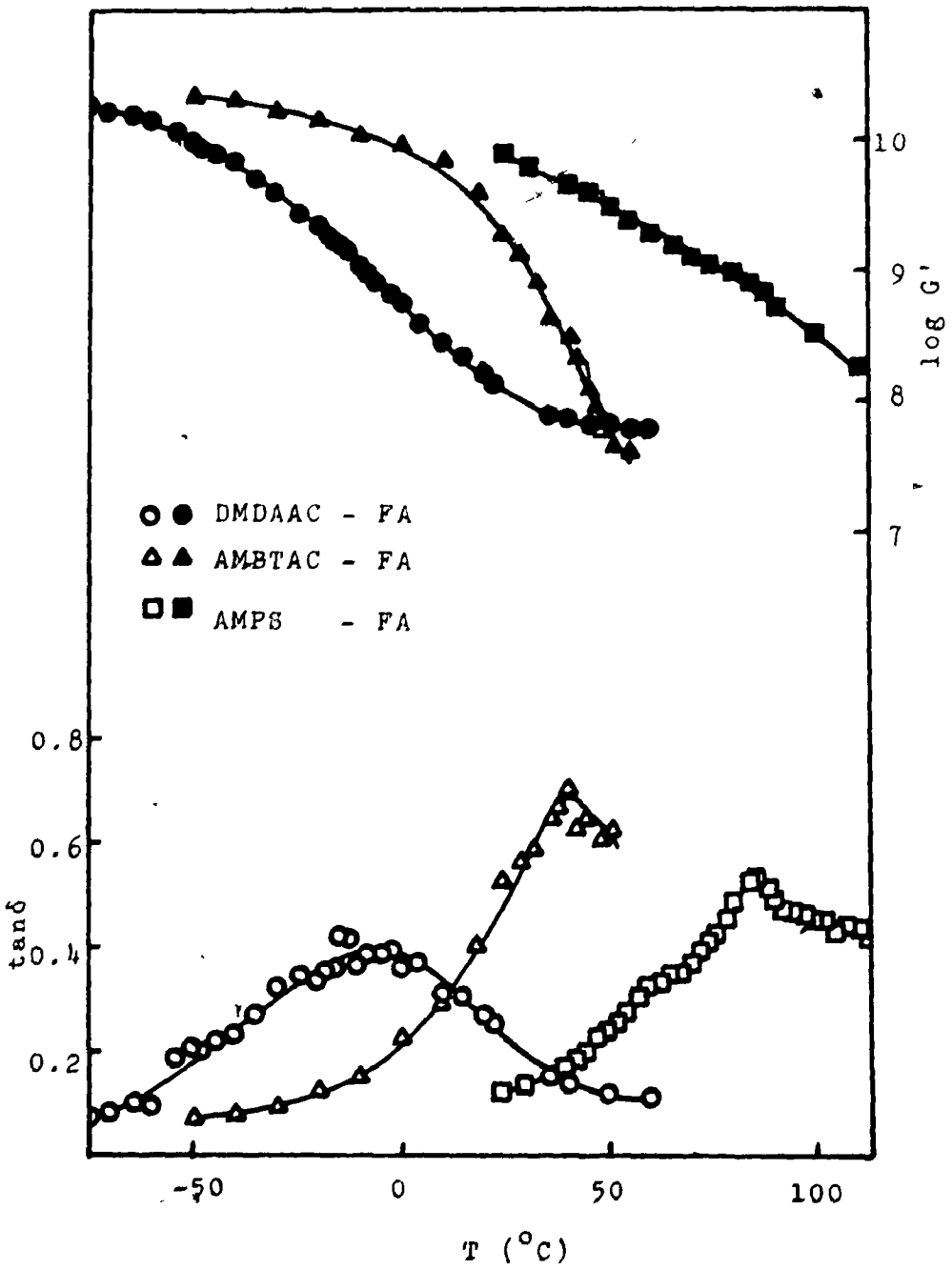
10
9
8
7
log G'
DMDAAC - FA
AMBTAC - FA
AMPS - FA
0.8
0.6
0.4
0.2
tanδ
-50
0
50
100
T (°C)

Figure 24.

G' and tanδ vs. temperature for various polyelectrolytes with ca. 24 wt% ethylene glycol.

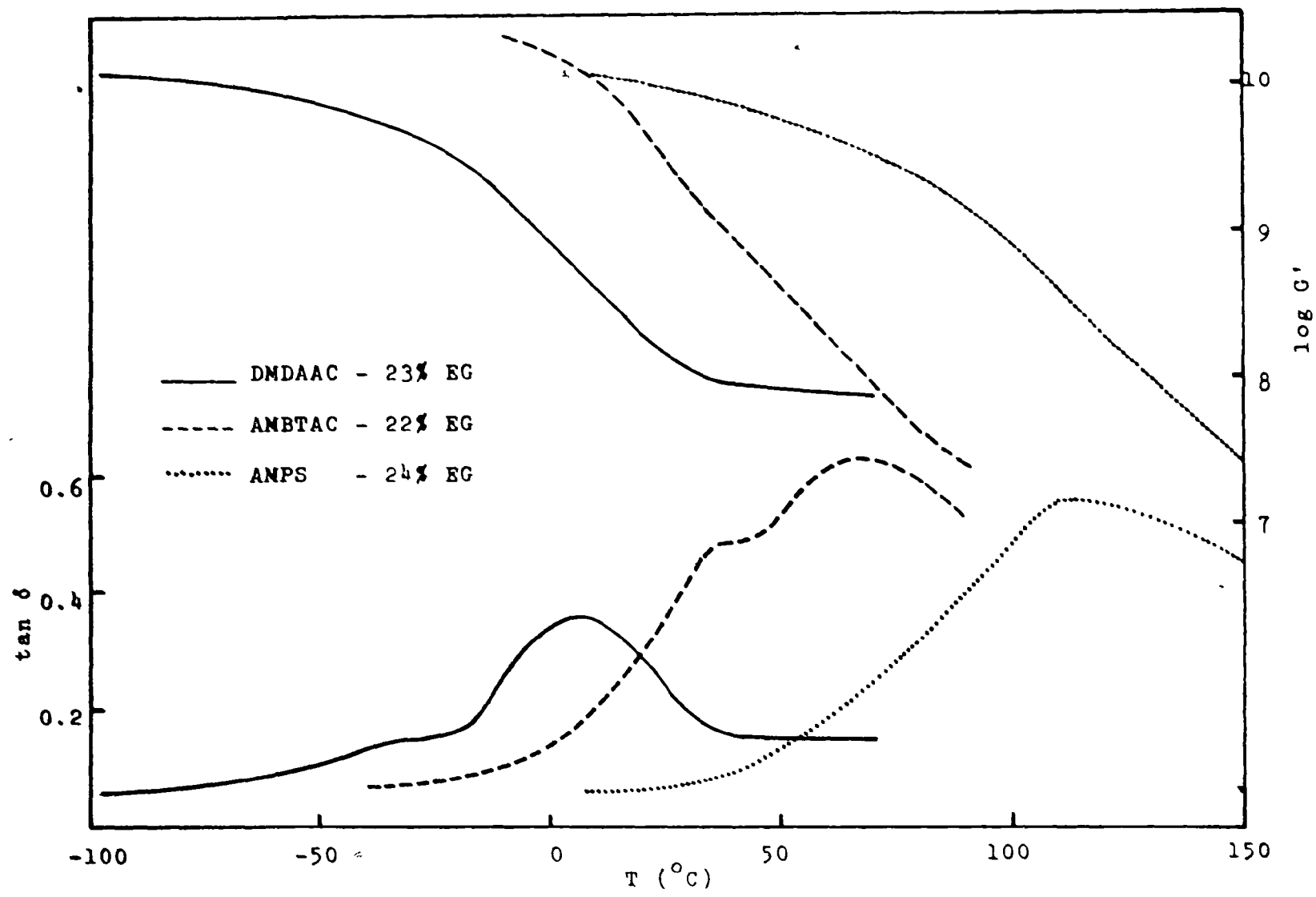
DMDAAC - 23% EG
AMBTAC - 22% EG
AMPS - 24% EG
tan δ
0.6
0.4
0.2
log G'
10
9
8
7
-100
-50
0
50
100
150
T (°C)

Figure 25.

G'and tanδ vs. temperature for various poly-electrolytes with ca. 43 wt% glycerine.

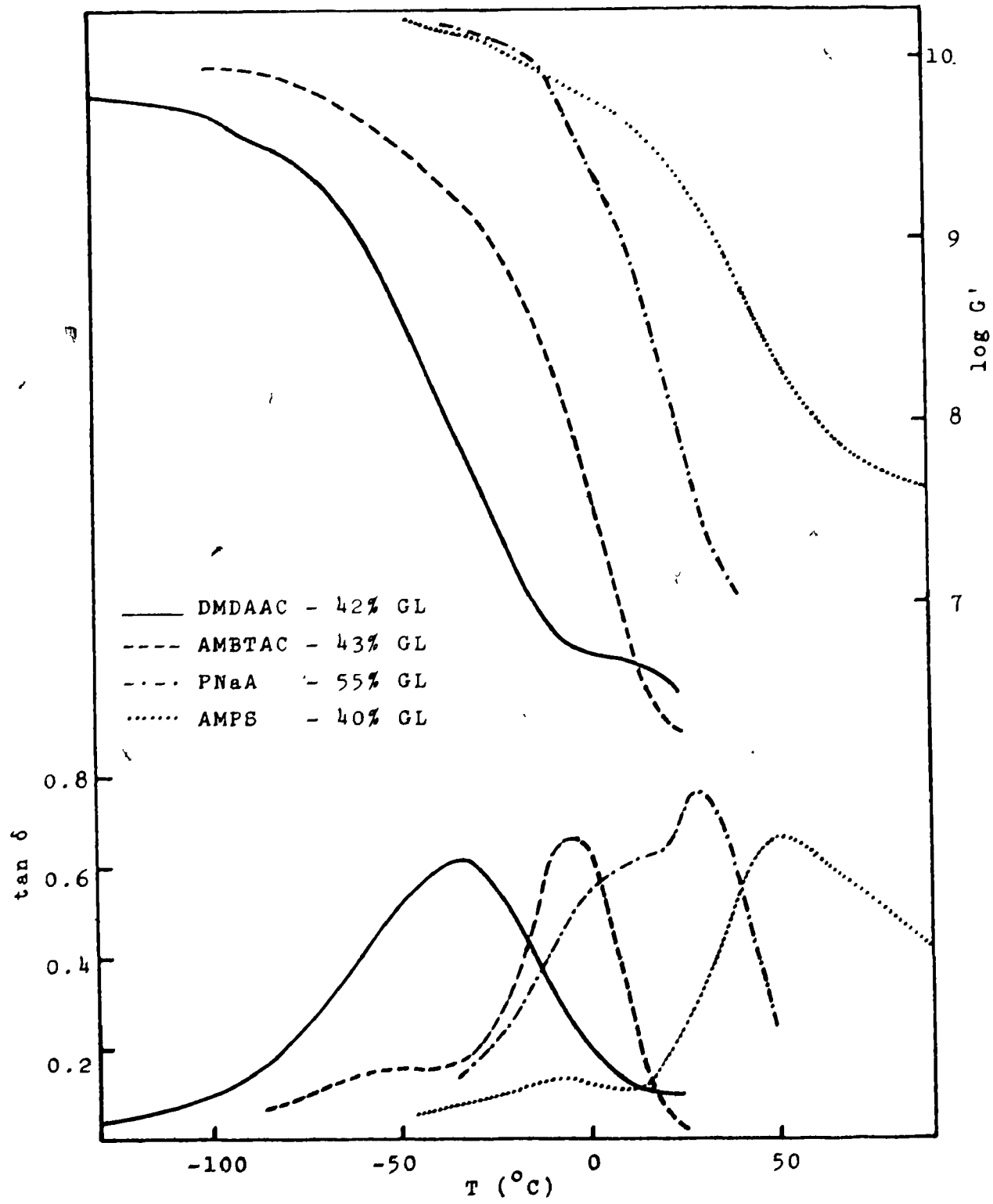
10
9
8
7
log G'
DMDAAC - 42% GL
AMBTAC - 43% GL
PNaA - 55% GL
AMPS - 40% GL
0.8
0.6
0.4
0.2
tan δ
-100
-50
0
50
T (°C)

4. DISCUSSION

4.1 Drying and Thermal Stability

The thermogravimetric results presented in Fig. 1, suggest very clearly that the polymers containing quaternary ammonium ions decompose at much lower temperatures than the material containing sodium sulfonate groups. It seems reasonable to expect that AMPS in the acid form would be also less stable by analogy with the results for "Nafions" and sulfonated polysulfone[33].

4.2 Glass Transition

One of the significant results of this study is the effect of the type of ion on the glass transition and its change with water content, as shown in Fig. 3. Fig. 26 compares these results with those for several other ion-containing polymers which have been studied previously in various laboratories, i.e. PNaA, "Nafions", 6,8-ionene, 2,3-oxyethylene ionene and 4,4-oxyethylene ionene. Two noteworthy features emerge: first, the glass transitions of the polyanionic materials (i.e. "Nafion"-Na, AMPS and PNaA) tend to be higher than those of the polycationic materials (i.e. DMDAAC, AMBTAC and ionenes). The glass transition temperatures of all these materials most probably is related to the ratio of the ionic charge (q) to the internuclear distance between cation and anion at closest approach (a)[34], the quaternary ammonium chloride group is very bulky in comparison to the sodium sulfonate or carboxyl groups, i.e. the distance between the chloride ion and the positively charged center is larger than that between the sodium ion and the negatively charged center. The dependence of glass transition temperature on q/a is consistent

Figure 26.

Glass transition temperature vs. water content for various ion-containing polymers.

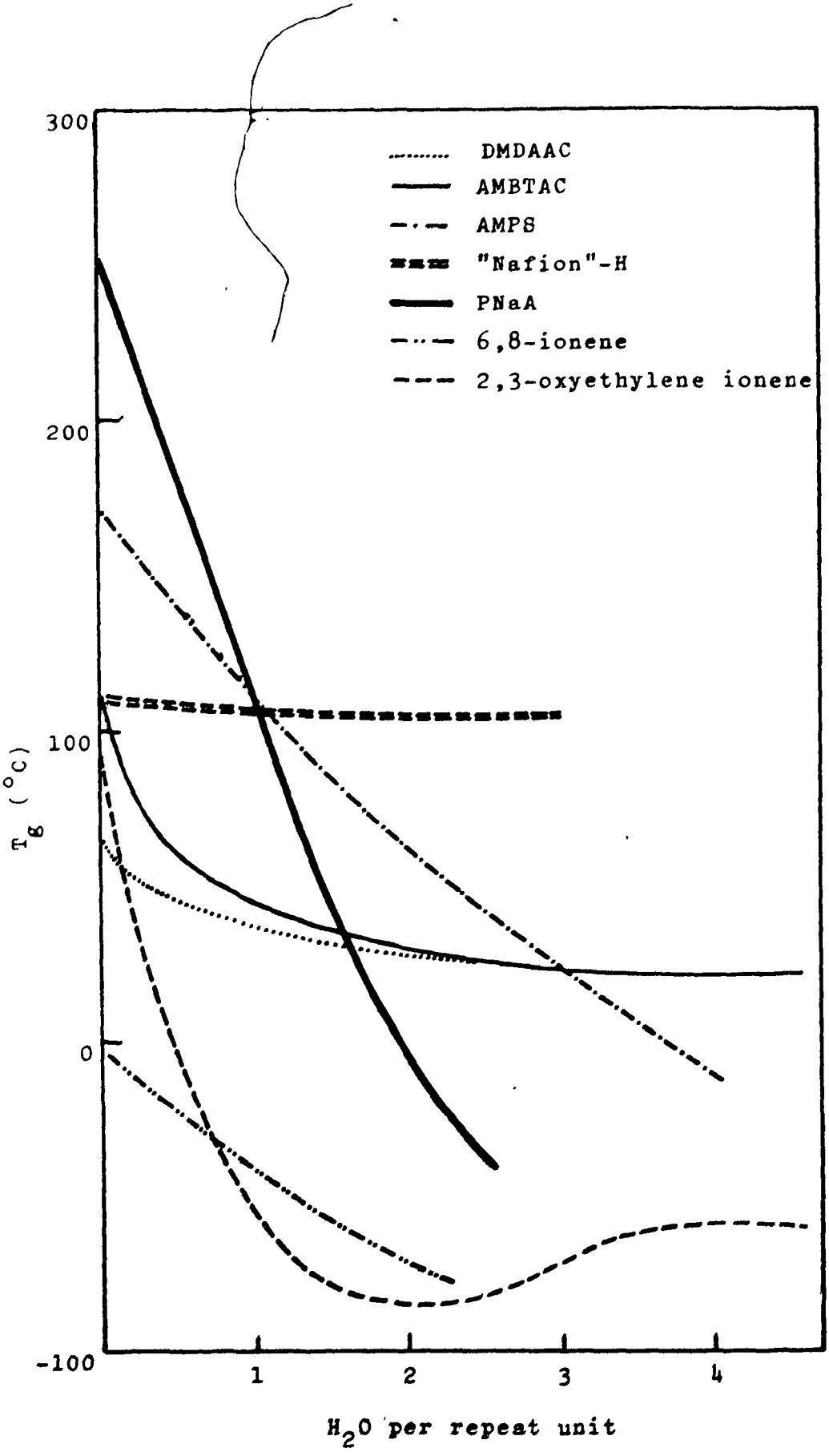
DMDAAC
AMBTAC
AMPS
"Nafion"-H
PNaA
6,8-ionene
2,3-oxyethylene ionene
300
200
100
0
-100
T_g (°C)
1
2
3
4
H_2O per repeat unit

with the findings for other ionics, e.g. the polyphosphates[35], the silicates[36], the aliphatic ionenes[2] and the "Nafions".

It has been known that polymers containing aromatic rings in the backbone chain have, in general, higher glass transitions than those containing only CH_2 sequences. In contrast to this, the glass transition temperature of AMBTAC is higher than that of DMDAAC which has a ring structure albeit an aliphatic one. Several explanations for this phenomena come to mind: the first possibility is that the ions in AMBTAC might be clustered while those in DMDAAC are not (or less so). The ions in DMDAAC are located on the rings and since only one methylene unit connects the rings, clustering might necessitate appreciable distortions of the backbone. By contrast, in AMBTAC the ions are located at the ends of side chains, and this fact might lead to much easier ion aggregation and the larger cluster or multiplet sizes. The known effects of clustering on the glass transition[4] suggest that the glass transition should rise more rapidly with ion content for AMBTAC than for DMDAAC. In addition, AMBTAC may be subject to hydrogen bonding, which would also tend to raise the glass transition and thus contribute to the observed effect.

It would be undoubtly more precise to compare the ionic polymers and non-ionic polymers of the same structure. The *q/a* effect suggests that the polyanionics would show a greater increase in the glass transition temperature than the polycationics. However, non-ionic polymers of identical structure as those of the ionics were not available for all the materials studied here.

Fig. 26 also reveals that the change in glass transition temperature with water content is very different for the polycationics and for the

polyanionics. In PNaA and AMPS, the glass transition temperature decreases with increasing water content at an appreciable rate over the entire range studied. By contrast, in DMDAAC, AMBTAC and the ionenes, initially the glass transition temperature decreases rapidly but the rate of decrease falls appreciably above ca. 20 wt% water, and in some cases even increases beyond that point. Considering the range of structures studied here, it seems reasonable to suggest this trend is general for quaternary ammonium polymers and independent of the structure of the materials. "Nafion"-H remains unusual in that the glass transition temperature is practically independent of water content.

Only for DMDAAC was the glass transition temperature investigated as a function of plasticizer content for materials other than water. In the range studied, dT_g/dc is seen to be linear for both FA and EG, in marked contrast to the behavior of water, as was shown in Fig. 15.

4.3 Mechanical and Dielectric Studies

4.3.1 α Relaxation

4.3.1.1 Effect of Water: In so far as water influences the position of the α relaxation, it has been discussed in Section 4.2 above. It is of interest now to correlate the amount of plasticizer with the tan δ peak height. This could be done only for AMPS (Fig. 18). It is seen clearly that the peak height increases with increasing water content, though not in a linear fashion; this is seen in Fig. 27 along with other results which will be discussed later.

Table 2 lists the change of peak height and peak position for the α relaxation determined in this work along with those obtained on other materials by a number of other workers for the sake of comparison.

Figure 27.

α peak height vs. plasticizer content for DMDAAC and AMPS.

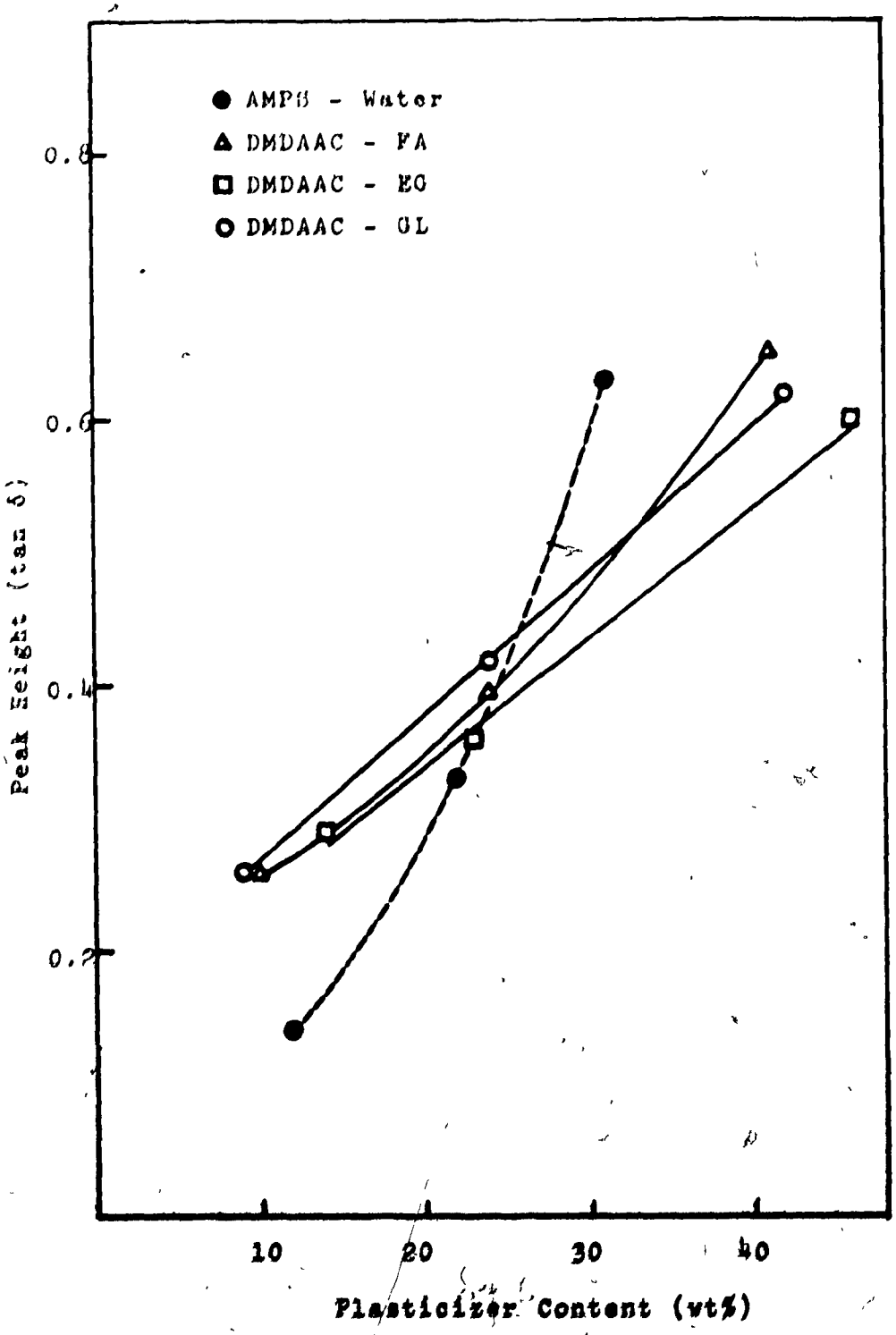
AMPS - Water
DMDAAC - FA
DMDAAC - EG
DMDAAC - GL
0.8
0.6
0.4
0.2
Peak Height (tan δ)
10
20
30
40
Plasticizer Content (wt%)

Table 2 Effect of Plasticizers on Glass Transition of Polymers

Polymer (T_g in ^oC)	Plasticizer	Change of Intensity (tan δ /%)	Change of position (^oC /%)	Range (%)	Method (Freq. in Hz)	Reference
DNDAAC (68)	Water	*	-1	0-28	DSC	This work
		*	0	28-50	DSC	"
	FA	0.01(L)	-3	10-41	M(≈ 1)	"
	EG	0.01(L)	-2.6(L)	14-46	M(≈ 1)	"
	GL	0.01(L)	**	9-42	M(≈ 1)	"
AMPS (168)	Water	0.03	-7	12-31	M(≈ 1)	"
ANBTAC (112)	Water	*	-15	0-10	DSC	"
			0	10-50	DSC	"
"Nafion"-H (110)	Water	0.02	-0.5	0-4	M(≈ 1)	"
PMaA (250)	Water	*	-7	0-46	DSC	3
	FA	*	-4	20-60	DSC	38
Ethylene ionomer(50)	Water	0.0003	-7	0-2	D(10^4)	13
6,8-ionene (0)	Water	*	-3	2-29	DSC	2
2,3-oxyethylene ionene (89)	Water	#	-10	0-15		
			0	15-60	M(≈ 1)	6
4,4-oxyethylene ionene (22)	Water	#	-6	0-15	M(≈ 1)	
			0	15-68		6
Collagen(147)	Water	0.002	-3.7(L)	10-35	M(≈ 1)	9
Nylon (95)	Water	0.03	-37	1-2	M(110)	10,11

M : mechanical D: dielectric L:linear ** data scattered # relative intensity

The rate at which the peak increases for AMPS is seen to be large and comparable to that of nylon, although the effect in AMPS persists to much higher water content than in nylon. By contrast, the rate of change of the peak position is moderate, and well within the range for non-ionic polar materials.

The very low peak height for the 12 wt% sample in Fig. 18 is noteworthy. This low value of tan δ might suggest that we are dealing with a water peak here, but the agreement of the peak positions with the DSC results argues in favour of this peak being the T_g. It is impossible to study the dry sample by mechanical means, so more thorough discussion of this problem is not warranted. In general, however, the tan δ peak height at T_g for ionic polymers are lower than those for the non-ionics[39].

4.3.1.2 Effect of Other Plasticizers: The effect of plasticizer content on the α peak height for materials other than water has been investigated most extensively in the case of DMDAAC. These results are also shown in Fig. 27. It is seen that a linear relationship exists between these two parameters, the rate of increase in tan δ being 0.01 per wt% of plasticizer for FA, EG and GL. Thus, it is not surprising that at constant weight percent of plasticizer the α peaks occur at approximately the same height; this was seen in Figs. 16 and 17 for ca. 24 wt% and ca. 43 wt% of plasticizers. This general type of behavior is also observed in AMBTAC, and, to a lesser extent, in AMPS. These phenomena are similar to those found in water plasticized nylon[11] and collagen[9] in which the solvation effect cause the rupture of interchain bonding and thus influences the glass transition.

When we look at the same plasticizer in different polymers, we again find that a constant weight fraction of plasticizer gives a relatively constant peak height. This is seen particularly in Fig. 25 for GL in various polymers and to a lesser extent also in Figs. 23 and 24 for FA and EG.

Another noteworthy feature is the behavior of the pseudo rubbery modulus with increasing plasticizer content. As has been observed before for PNaA, that modulus decreases with increasing plasticizer content. Two distinct possibilities exist which might explain this change in the modulus. One is based on the assumption that the ions are solvated and that the entanglement spacings is inversely related to the volume fraction of the polymer[37]. Thus, the modulus should be proportional to the volume fraction of the polymer. This is evidently not the case, as can be seen, for example, in Fig. 12. The rubbery modulus varies from ca. 6×10^6 to ca. 4×10^8 dyne/cm^2 for a change of polymer content from 59 wt% to 90 wt%. A far more likely possibility is that only some of the ions are hydrated and that extensive residual ionic cross-linking is presented even at high plasticizer contents.

4.3.2 β and γ relaxations

The sub-T_g relaxations were investigated only for DMDAAC, primarily by the dielectric technique. Fig. 4 shows clearly that two relaxations are seen in the region investigated; the one occurring at the higher temperature is labeled β and the peak position of both the β and the γ relaxations are shown in Fig. 10. It is seen clearly that the tan δ peak height of the β relaxation decreases with increasing water content from ca. 0.35 at 1.2 ± 1.2 wt% water down to 0.01 at 27 wt% water. This

fact, coupled with the constancy of the activation energy of the β relaxation (shown in Fig. 9 for the 1.2 and 2.2 wt% samples) i.e. 17.4 kcal/mole and 18.5 kcal/mole), suggests that the mechanism responsible for these peaks may originate from an unhydrated part of the repeat units.

The γ peak height changes only slightly with water content in the range of 2.2 to 27.3 wt% water, but is very small below that value. This fact, coupled with the constancy of the activation energy (22.0, 21.2 and 21.0 kcal/mole for the 1.2, 13.4 and 27.3 wt% samples) suggests that we may be dealing with a particular hydrated species or possibly with a water peak. It is noteworthy that the γ peak for the 13.4 wt% and 27.4 wt% samples is also active mechanically. The β peak could not be studied mechanically in the dry sample, and was not found in samples containing 13.4 wt% and 27.4 wt% water (Fig. 11). The positions of both γ peaks which were found change with water content, and they are seen to fall on the same line as the dielectric peaks when plotted as log ν vs 1/T in Fig. 9

Data for AMPS and AMBTAC have not been obtained over a wide enough range of experimental variables to permit a discussion of the β and γ relaxations. From the data that have been obtained on these systems, as well as from DMDAAC with plasticizers other than water, it seems clearly that no important sub-T_g relaxation are present (although one has been found by mechanical means for DMDAAC). The absence of mechanical sub-T_g peaks can be related to the brittleness of the materials.

The effect of water on sub-T_g relaxations, especially the β relaxation is summarized for a few representative polymers in Tables 3

and 4. Three different types of behavior can be distinguished. For nylon, poly-2-hydroxyethyl-methacrylate, polyacrylamide, polyglycine, polyethylene terephthalate, "Nafions", DMDAAC, the position of the β peak decreases appreciably with increasing water content while the peak height increases, more or less, rapidly. The second group, which consists of polyoxymethylene, collagen, polysulphone, polycarbonate, and poly(2,6-dimethyl phenylene oxide), the β peak position remains unchanged although the peak height increases with increasing water content. Finally, in the third group of materials which include ethylene ionomer, poly-2-hydroxypropyl methacrylate, polymethyl methacrylate, polymethacrylamide and poly(2,6-dimethyl-phenylene oxide), a complete new water peak appears, which may or may not, move with water content, but the intensity always increases as the water content increases. DMDAAC falls clearly in the first catalogue. It resembles "Nafions" in this aspect, but differs to ethylene ionomer. The reason remains unknown at this stage.

Table 3 Effect of Water on δ relaxation of polymers

Polymer	tan δ at 0% water	approximate change of tanδ per %	position at 0% water(^{o}K)	approximate change in position (^{o}C / %)	Range (%)	Method (Freq. in Hz)	Ref.
DMDAAC				-2	1-27	D(10^3)	This work
"Nafion"-H	0.07	0.8	296	-40	0-3	N(= 1)	This work
Nylon	0.01	0.02	230	-20	0-2	N(= 1)	11
poly-2-hydroxy-ethyl methacrylate	0.006	0.002	260	-9	0-5(v)	N(900)	16
Polyacrylamide	0.02	0.0002	248	-10	0-6(v)	N(= 1)	19
Polyethylene terephthalate	0.005	0.01	233	-7	0-1	N(100)	23
Polyoxymethylene	0.01	0.03	260	0	0-0.5	N(= 1)	20
Collagen	0.01	0.003	260	0	0-35	N(= 1)	9
Polysulphone	0.002	0.01	220	0	0-1	D(10^3)	21
Polycarbonate	0.005	0.01	201	0	0-0.3	D(10^3)	21

D : dielectric N : mechanical v : volume %

Table 4 Polymers which possessed water peak

Polymer	tan δ at 0% water	change in tan δ per %	position at 0 % water(°K)	change in position (°C / %)	Range (%)	Method (Freq. in Hz)	Ref.
Ethylene ionomer		0.006	233	-0.2	1-2**	D(10^3)	13
Poly-2-hydroxypropyl methacrylate	0.005	0.001	248	-0.1	0-10(v)	N(10^4)	16
Polymethyl methacrylate	0.008	*	169	*	0-1	N(= 1)	15
Polymethacrylamide	0.008	0.001	153	0	5-40(v)	N(= 1)	19
Poly(2,6-dimethyl-phenylene oxide)	0.01	*	176	*		N(57)	31

D : dielectric N : mechanical v : volume %

* : one water content was determined

** : two water content was determined

5. CONCLUSION

The profound effect of ions on the mechanical behavior of ion-containing polymers has been recognised for a long time. The clearest example is the glass transition. The ionic forces, expressed as q/a, predominates over the other forces such as Van der Wasl and hydrogen bonding interactions. This is demonstrated clearly by the behavior of the glass transition temperature of these materials.

The type of ion plays a crucial role in determining the glass transition phenomena in ionic polymers, both plasticized and unplasticized, regardless of the environment in which the ion is placed.

With increasing plasticizer content, the α relaxation position shifts to lower temperature and the peak height increases. This phenomena is commonly encountered in most polar polymers, and is ascribed to the solvation of the polar groups, i.e. a polymer-solvent complex is formed. This hypothesis is supported by the fact that the pseudo rubbery modulus decreases with increasing plasticizer content, which, in turn, decreases the polymer volume fraction.

It is interesting to note that water has an effect on these polyelectrolytes which is quite different from other plasticizers used in this study.

REFERENCES

1. A. Eisenberg, M. King and T. Yokoyama, In "Water-Soluble Polymers", N. Bikales, ed., p. 349, Plenum Publ. Co., 1973.
2. A. Eisenberg, H. Matsuura and T. Yokoyama, Polymer J., 2, 117 (1971).
3. A. Eisenberg, H. Matsuura and T. Yokoyama, J. Polym. Sci., A2, 9, 2131 (1971).
4. H. Matsuura and A. Eisenberg, J. Polym. Sci., Phys. Ed., in press.
5. T. Tsutsui, T. Sato and T. Tanaka, Polymer J., 5, 332 (1973).
6. T. Tsutsui, R. Tanaka and T. Tanaka, J. Polym. Sci., Phys. Ed., 13, 2091 (1975).
7. A. Eisenberg, M. King and M. Navratil, Macromolecules, 6, 734 (1973).
8. A. Eisenberg and M. Navratil, Macromolecules, 6, 604 (1973).
9. E. Baer, R. Kohn and Y. S. Papir, J. Macromol. Sci., Phys. B6,761(1972).
10. D. C. Prevorsek, R. H. Butler and H. K. Reimschuessel, J. Polym. Sci., A2, 9, 867 (1971).
11. Y. S. Papir, S. Kapur, C. E. Rogers and E. Baer, J. Polym. Sci., A2, 10, 1305 (1972).
12. A. J. Curtis, J. Res. Nat. Bur. Stand., 65A, 185 (1961).
13. B. E. Read, E. A. Carter, T. M. Connor and W. J. MacKnight, Brit. Polym. J., 1, 123 (1969).
14. Y. Wada and K. Yamamoto, J. Phys. Soc. Japan, 11, 887 (1956); ibid 12, 374 (1957).
15. W. C. Call and N. G. McCrum, J. Polym. Sci., 50, 489 (1961).
16. M. C. Shen and J. D. Strong, J. Applied Phys., 38, 4197 (1967).
17. A. Woodward, J. M. Crissman and J. A. Sauer, J. Polym. Sci., 44, 23 (1960).

18. A. Eisenberg and B. Cayrol, J. Polym. Sci., C35, 129 (1971).

19. J. Kolarik and J. Janacek, J. Polym. Sci., C16, 441 (1967).

20. N. G. McCrum, J. Polym. Sci., 54, 561 (1961).

21. G. Allen, J. McAinsh and G. M. Jeffs, Polymer, 12, 85 (1971).

22. W. Reddish, Trans. Faraday Soc., 46, 459 (1950).

23. T. Kawaguchi, J. Polym. Sci., 32, 417 (1958).

24. D. E. Kline and J. A. Sauer, Polymer, 2, 401 (1963).

25. K. H. Illers and H. Breuer, J. Colloid Sci., 18, 1 (1963).

26. J. Kolarik and M. Stol, Polymer J., in press.

27. J. E. Boothe, U.S. Pattent 3,461,163 (Aug. 12, 1969); U.S. Patent 3,472,740 (Oct. 14, 1969).

28. D. L. Murfin and L. E. Miller, U.S. Patent 3,478,091 (Nov. 11, 1969); U.S. Patent 3,506,707 (April 14, 1970).

29. D. I. Hoke, D. L. Surbey and W. R. Oviatt, J. Polym. Sci. A1, 10, 595 (1972).

30. J. Timmerman,"The Physical - Chemical Constants of Binary Systems In Concentrated Solutions", Vol. 4, Interscience Publ. Inc., New York (1960).

31. B. Cayrol, "Segmental Mobility in Poly-p-Phenylene Ethers". Ph.D. Thesis, McGill University, 1972.

32. R. D. McCammon and R. N. Work, Rev. Sci. Instru., 36, 1169 (1965).

33. A. Noshay and L. M. Robeson, Polymer Preprints, 16, 81 (1975).

34. A. Eisenberg, Macromolecules, 4, 125 (1971).

35. A. Eisenberg, H. Farb and L. G. Cool, J. Polym. Sci. A2, 4, 855 (1966).

36. A. Eisenberg and K. Takahashi, J. Non. Cryst. Solids, 3, 279 (1970).

37. T. G. Fox and V. R. Allen, J. Chem. Phys., 41, 344 (1964).

38. M. King, Ph.D. Thesis, McGill University, 1972.

39. A. Eisenberg and M. Navratil, Macromolecules 7, 90, (1974).

APPENDIX

TABLES OF SUPPORTING DATA FOR FIGURES

PART TWO, FIGURE 1

Temp. (°C)	Weight Change (wt%)		
	DMDAAC	AMPS	AMETAC
24	1.0	0.0	1.0
57	0.0	0.0	0.6
74	0.0		0.0
91	0.0		-0.2
108	0.0	0.0	
118	-1.2		-1.3
125	-1.2		
134	-2.0		-2.0
177	-6.8		
186	-7.0	0.0	-10.6
206	-7.0	-9.3	

PART TWO, FIGURE 3

AMPS

Water content (wt%)	T_g (°C)
0.0	170 *
4.1 ± 0.8	138 *
8.6 ± 0.2	71 *
11.6 ± 4.4	77
15.4 ± 1.7	58 *
21.9 ± 2.7	40
31.0 ± 4.0	-13
46.0 ± 1.0	-70 *

DMDAAC

Water content (wt %)	T_g (°C)
0.0 ± 0.0	68 *
3.4 ± 0.1	51 *
7.8 ± 1.3	42 *
10.3 ± 2.1	36 ± 4
17.0 ± 1.0	33 *
21.0 ± 2.0	28 *
25,0 ± 2.0	24

AMBTAC

Water content (wt%)	T_g (°C)
0.0	112 *
6.0	51 *
8.6	43 *
10.0	36 *
11.0	36 *
20.0	24 *
28.0	20 *
35.0	23 *
50.0	20 *

* Determined by DSC

PART TWO, FIGURE 5

100 Hz		1 kHz		10 kHz	
Temp. (°C)	tanδ x100	Temp. (°C)	tanδ x100	Temp. (°C)	tanδ x100
-27.3	3.93	-24.5	2.69	-22.9	2.0
-26.0	4.28	118.0	3.97	-16.7	2.6
-21.7	5.95	-13.2	5.5	-10.2	3.6
-19.5	6.9	-7.8	7.66	-5.4	4.59
-15.4	9.7	-3.3	10.2	0.6	6.09
-14.2	10.66	2.9	14.4	6.4	8.0
-11.7	12.76	10.8	20.7	14.3	11.6
-9.0	15.4	11.8	21.6	18.7	13.8
-6.3	18.3	16.7	24.9	21.6	15.6
-4.4	20.3	20.5	27.0	24.7	17.5
-1.8	23.2	23.5	28.0	30.5	20.4
-0.5	24.2	29.2	29.0	34.5	22.4
1.8	26.2	33.0	29.3	37.5	23.7
4.0	27.8	36.5	29.6	40.8	24.9
4.9	28.3	39.8	30.0	46.5	26.2
7.2	29.4	45.5	31.2	51.7	26.7
9.4	30.1	50.7	32.7	58.4	27.1
13.1	30.9	56.4	34.1	64.0	27.6
15.4	31.5	62.4	35.0	70.0	28.5
17.5	32.2	67.9	34.8	76.9	30.5
19.6	32.8	75.6	32.3	86.5	33.9
22.4	33.8	82.4	29.3	91.5	34.9
25.8	35.0	84.6	28.6	94.9	35.4
31.7	36.4	90.3	25.7	95.9	35.6
35.5	37.47	93.2	26.3	102.0	34.1
38.5	37.2	99.0	26.7	105.7	33.4
42.3	36.1	104.0	27.0	106.6	33.5
43.3	35.1			107.7	33.7
44.5	34.1			113.0	31.8
48.2	33.1			114.3	32.3
49.5	31.4			117.0	33.0
53.1	30.9			120.0	33.8
55.0	29.3			122.5	34.7
60.9	29.9			127.7	37.6
66.5	32.2				
74.2	37.3				
80.5	45.3				
89.3	65.8				
100.6	96.9				

PART TWO, FIGURE 6

100 Hz		1 kHz		10 kHz	
Temp. (°C)	tanδ x100	Temp. (°C)	tanδ x100	Temp. (°C)	tanδ x100
-46.4	8.58	-43.8	4.8	-42.6	3.04
-40.8	9.34	-39.3	5.2	-38.2	3.28
-36.2	10.7	-21.8	9.2	-20.7	5.31
-30.0	13.7	-10.0	15.6	-8.7	8.26
-25.5	16.7	-6.6	19.8	-5.5	9.4
-23.2	18.1	-2.4	24.9	-1.2	11.2
-19.5	23.5	1.1	29.3	2.2	12.9
-16.5	28.1	4.1	33.8	5.2	14.8
-14.0	32.3	8.0	39.3	9.3	17.7
-11.0	37.4	11.5	43.3	12.3	20.3
-8.0	42.8	15.4	46.2	16.4	24.1
-4.5	46.8	20.1	47.4	21.0	29.1
-3.4	47.7	23.9	46.8	25.0	33.2
0.0	49.5	27.2	46.0	28.5	36.8
3.0	50.0	33.2	43.3	34.0	40.9
6.5	49.4	38.7	40.4	39.8	42.4
7.0	49.0	44.3	37.6	45.5	41.8
10.4	48.8	50.0	33.9	51.6	40.2
13.9	47.2	57.3	28.6	58.4	38.3
14.6	46.4	62.5	25.1	64.0	36.9
17.9	45.9	69.0	21.5	70.0	34.9
19.4	44.1	75.8	17.9	78.3	32.2
22.2	43.6	82.0	16.7	80.0	31.6
22.9	42.2	84.6	14.7	86.0	28.3
26.1	42.9			86.8	28.1
30.7	40.2				
31.9	37.9				
37.6	33.8				
42.8	31.4				
48.3	28.8				
55.6	26.0				
60.9	23.4				
67.5	22.2				

PART TWO, FIGURE 7

100 Hz		1 kHz		10 kHz	
Temp. (°C)	tanδ x100	Temp. (°C)	tanδ x100	Temp. (°C)	tanδ x100
-77.6	1.8	-62.8	3.97	-60.7	2.76
-65.0	6.1	-56.8	7.05	-55.5	4.51
-58.9	10.4	-52.5	10.5	-50.8	6.75
-54.0	16.1	-48.0	14.8	-46.7	9.58
-49.4	22.0	-43.7	18.1	-42.7	12.84
-45.1	27.8	-40.5	22.9	-39.4	15.67
-41.3	35.2	-37.5	26.3	-36.5	18.4
-38.5	42.6	-33.5	32.3	-32.7	21.67
-35.6	47.2	-30.8	37.73	-30.0	23.8
-34.5	47.4	-27.0	45.23	-26.0	27.3
-31.6	44.5	-24.3	47.55	-23.4	30.1
-28.3	37.6	-21.7	47.28	-20.8	33.4
-27.6	35.7	-18.9	44.3	-18.2	37.5
-25.0	31.0	-15.3	37.9	-14.5	42.7
-22.5	26.8	-12.5	32.8	-11.8	45.9
-20.0	23.3	-8.8	26.9	-7.8	48.2
-17.0	20.2	-4.6	20.95	-3.8	47.0
-16.1	18.2	1.4	15.3	3.3	39.4
-13.3	17.0	7.5	12.99	9.0	32.8
-9.7	15.1	11.7	13.64	14.8	28.0
-5.5	14.8	23.8	11.85	19.7	24.46
0.4	15.3	25.4	10.73	21.3	23.1
5.4	19.7	32.4	7.42	27.5	18.2
		33.8	5.6	30.5	16.2
				38.0	12.2
				41.0	10.6

PART TWO, FIGURE 8,

100 Hz		1 kHz		10 kHz	
Temp. (°C)	tanδ x100	Temp. (°C)	tanδ x100	Temp. (°C)	tanδ x100
-153.2	0.47	-123.0	0.52	-151.6	0.36
-142.3	0.55	-104.0	1.14	-120.4	0.51
-136.0	0.59	-96.0	2.14	-101.3	0.92
-126.0	0.70	-90.3	3.9	-94.3	1.50
-118.0	1.04	-84.0	7.7	-87.3	2.76
-106.3	1.66	-78.9	12.9	-82.2	4.44
-98.0	3.43	-74.4	20.0	-77.7	7.0
-92.0	6.76	-68.2	31.8	-71.8	8.8
-85.4	13.47	-64.5	38.5	-67.2	18.6
-81.0	20.9	-60.7	40.3	-63.0	25.4
-80.0	23.0	-57.0	34.9	-59.6	31.5
-76.3	31.0	-54.0	26.4	-56.0	37.1
-75.6	32.7	-51.0	17.3	-53.0	40.1
-70.0	40.3	-47.0	8.9	-50.1	40.4
-66.0	33.9	-43.0	4.5	-49.2	39.9
-65.5	32.3	-38.8	2.23	-46.0	35.7
-61.8	18.96	-35.2	1.38	-45.2	34.2
-58.2	9.3	-32.2	1.02	-42.0	26.8
-55.0	4.4	-28.9	0.76	-37.7	17.0
-51.9	2.3	-21.7	0.6	-34.3	11.0
-48.2	1.16	-16.1	0.8	-31.2	7.2
-44.1	0.7	-12.8	0.96	-27.7	4.5
-40.2	0.64	-7.2	1.05	-24.5	3.0
-36.3	0.8	-5.6	1.00	-20.2	1.97
-33.1	1.12			-18.5	1.72
-30.2	1.42			-15.3	1.33
-26.4	1.67			-11.[illegible]	1.36
-22.6	1.75			-4.6	0.53
-17.3	2.58				
-13.8	2.37				
-10.5	4.67				
-10.0	4.06				
-2.9	4.38				

PART TWO, FIGURE 9

Dielectric Data

Water Content (wt %)	β relaxation			γ relaxation		
	100Hz	1kHz	10kHz	100Hz	1kHz	10kHz
1.2 ± 1.2	36	64	96	2	21	40
2.2 ± 0.7	27	47	77	4	20	40
13.4 ± 0.3	-	16	-	-34	-23	-7
27.3 ± 0.7	-	-8	-	-71	-62	-52

Mechanical Data

Water Content (wt %)	γ relaxation	Frequency
10 ± 2	-54	1.8 Hz
25 ± 2	-85	2.6 Hz

PART TWO, FIGURE 11

10 wt% water			25 wt% water		
Temp. (°C)	G' (dyn/cm^2)	tanδ x100	Temp. (°C)	G' (dyn/cm^2)	tanδ x100
-146	2.83×10^{10}	0.56	-145	2.57×10^{10}	1.42
-138	2.81	0.71	-130	2.49	2.0
-125	2.73	1.05	-120	2.37	2.73
-112	2.60	2.15	-114		3.62
-100	2.50	3.00	-109	2.21	4.07
-91	2.38	3.52	-104		5.29
-83	2.24	4.30	-99	1.98	5.85
-80	2.17	4.60	-94	1.84	6.82
-75	2.09	4.80	-92		6.81
-71		5.36	-90	1.71	6.95
-70	1.97	5.37	-88		7.25
-66	1.93	5.67	-86	1.66	7.29
-63	1.90	5.96	-84		7.41
-60	1.77	5.98	-82		7.25
-57	1.76	6.15	-80	1.46	7.05
-54	1.69	6.08	-78		6.96
-51	1.65	6.06	-76	1.39	6.91
-48	1.57	6.05	-75		6.80
-46	1.57	5.87	-73		6.63
-41	1.50	5.51	-69	1.29	6.33
-38	1.45	5.32	-68		6.19
-36	1.42	5.02	-65	1.18	5.94
-34	1.42	4.97	-63		5.95
-32	1.37	4.55	-61	1.13	5.74
-30	1.34	4.17	-58		5.56
-27	1.30	3.93	-57		5.21
-24	1.29	3.75	-55	1.06	5.28
-21	1.25	3.55	-52		5.17
-19	1.23	3.35	-50	9.89×10^{9}	4.97
-16	1.20	3.23	-46	9.54	4.77
-12	1.16	3.02	-43	9.39	4.52
-10	1.14	3.03	-40	9.25	4.36
-8	1.12	2.93	-36	8.88	4.22
-6	1.10	2.89	-33	8.45	3.76
-3	1.05	2.90	-29	8.10	3.36
1	1.01	3.10	-25	8.02	3.30
4	9.62×10^{9}	3.51	-22	7.64	3.00
7	8.97	4.32	-19	7.53	3.02
10	8.33	4.88	-16	7.24	3.00
12	8.10	5.39	-13	6.87	3.43
14	7.22	5.95	-10	6.73	3.73
16	6.38	7.17	-6	6.63	4.04
18	5.65	7.93	-3	6.22	4.69
20	4.81	8.39	0	5.65	5.60

PART TWO, FIGURE 11 (Cont.)

25 wt% (Cont.)

Temp. (°C)	G' (dyn/cm^2)	tanδ x100
3	5.81×10^9	6.43
6	5.08	7.60
10	4.49	9.80
12	4.10	12.6
14	3.16	17.6
16	2.37	23.5
18	1.65	29.0
20	1.02	33.7
22	5.13×10^8	36.7
24	4.27	37.7
26	3.80	37.0
30		36.7
35		32.6
40		21.3
50		15.1
58		10.8

PART TWO, FIGURE 12,

10 wt%

Temp. (°C)	G' (dyn/cm^2)	tanδ x100
-90	1.87×10^{10}	3.74
-80	1.81	4.34
-70	1.63	4.02
-64		4.25
-60		4.61
-54		5.86
-52		6.83
-50		5.23
-48	1.59	6.52
-46		6.48
-44		6.08
-42		7.16
-40	1.38	7.43
-38		6.99
-36		7.69
-34		7.11
-30	1.21	7.29
-28		7.41
-24		8.26
-20	9.26×10^{9}	7.67
-17		9.74
-15		9.72
-13		8.30
-10	7.55	9.80
-8		8.90
-5		9.86
-3		10.1
0	6.38	10.7
3		11.5
5		12.5
10	4.64	14.5
14		16.6
16		17.9
20	2.92	21.0
22		22.6
26	2.27	24.2
28	1.60	25.3
34	8.73×10^{8}	24.9
36		23.6
38	5.97	25.7
40	5.29	24.0
45	4.04	21.7
50	3.64	22.4
60	3.55	20.9

10 wt% (Cont.)

Temp. (°C)	G' (dyn/cm^2)	tanδ x100
70	3.32×10^{8}	21.2
80	2.57	18.7
90	2.01	17.0
95	1.97	16.8

24 wt%

Temp. (°C)	G' (dyn/cm^2)	tanδ x100
-80		6.36
-74	1.89×10^{10}	7.23
-70	1.68	8.04
-64	1.51	10.3
-58	1.35	12.3
-54	1.15	15.2
-50	9.71×10^{9}	16.2
-46		18.6
-40	6.60	23.2
-38		25.0
-35	4.95	27.7
-33		30.0
-30	3.96	32.7
-28		33.0
-26		32.0
-24	2.70	34.4
-22		33.0
-20	2.21	34.9
-18	1.84	35.4
-16	1.65	36.4
-13	1.34	39.2
-10	1.10	37.1
-8	9.37×10^{8}	38.7
-6	7.71	39.5
-4	7.15	39.1
-3	6.33	38.9
0	5.52	36.6
4	3.89	37.3
10	2.79	31.3
15	2.19	30.7
20	1.53	26.9
22	1.33	25.4
33	8.17×10^{7}	17.0

PART TWO, FIGURE 12 (CONT.)

24 wt% (Cont.)

Temp. (°C)	G' (dyn/cm^2)	tan δ x100
36	7.52×10^7	15.2
40	7.24	13.8
46	6.52	12.6
50	6.32	12.0
56	6.07	11.1
60	6.02	11.1

41 wt%

Temp. (°C)	G' (dyn/cm^2)	tan δ x100
-110	1.35×10^{10}	9.14
-100	1.23	12.0
-94	1.03	16.5
-90	8.89×10^9	21.1
-84	8.02	30.5
-80	6.62	39.5
-76	4.59	40.5
-72	2.59	47.2
-70	2.10	52.1
-68	2.02	48.4
-66	1.38	56.7
-64	1.06	65.7
-62	1.02	66.0
-60	7.73×10^8	66.9
-58	5.96	65.3
-56	5.02	63.2
-54	3.62	5.86
-52	2.87	6.00
-50	2.61	5.73
-48	1.90	5.51
-46	1.48	5.26
-44	1.33	5.24
-42	1.15	5.21
-40	9.39×10^7	4.83
-36	7.07	4.81
-34	5.84	4.70
-30	4.51	4.35
-26	3.29	3.86
-20	2.13	32.6

41 wt% (Cont.)

Temp. (°C)	G' (dyn/cm^2)	tan δ x100
-11	1.55×10^8	24.7
0	1.07	14.0
10	8.56×10^7	9.54
16	7.8	8.43
24	6.84	7.58

PART TWO, FIGURE 13

14 wt%			23 wt%		
Temp. (°C)	G' (dyn/cm^2)	tan δ x100	Temp. (°C)	G' (dyn/cm^2)	tan δ x100
-45	7.97×10^9		-110	1.25×10^{10}	3.60
-35	6.90	9.49	-98	1.25	5.96
-25	5.62	10.2	-91	1.25	5.09
-15	4.49	11.2	-80	1.26	6.08
-9		12.8	-73	9.07×10^9	7.59
-5	3.22	13.8	-70	9.07	7.47
1		16.4	-67	8.64	8.84
5	2.22	17.1	-58	7.33	9.50
7		18.1	-55	7.01	9.23
11		20.6	-50	6.51	9.75
15	1.35	22.7	-46	5.93	10.5
17	1.15	24.7	-40	5.33	13.5
19	1.06	25.1	-30	3.67	13.5
21	8.23×10^8	27.5	-25	2.89	15.4
23	7.07	27.7	-20	2.7	15.6
25	6.37	28.8	-15	2.2	19.7
27	5.04	29.5	-10	1.70	26.5
33	2.08	28.4	-4	1.23	31.3
35	1.76	27.4	0	9.67×10^8	33.8
37	1.63	26.6	4	6.27	35.7
38	1.46	26.0	10	4.24	35.3
41	1.32	23.6	20	1.95	29.2
45	1.13	21.9	24	1.57	25.7
55	9.07×10^7	19.1	30	1.17	18.8
65	7.68	18.0	35	9.70×10^7	16.2
75	7.57	17.7	40	9.09	15.4
85	7.46	18.1	45	8.26	14.8
			50	8.95	15.6
			55	8.27	16.0
			60	8.26	15.2
			65	7.4	14.8
			70	7.4	15.3

PART TWO, FIGURE 13 (CONT.)

46 wt%

Temp. (°C)	G' (dyn/cm^2)	tanδ x100
-118	1.45×10^{10}	7.4
-110	1.29	10.5
-100	1.04	14.6
-94	8.0×10^{9}	20.7
-90	6.05	26.3
-84	4.75	32.8
-82	4.07	33.0
-80	4.13	40.1
-78	3.43	43.4
-75	2.61	45.6
-72	2.09	52.0
-70	1.66	47.8
-68	1.51	54.3
-66	1.12	59.1
-64	9.74×10^{8}	54.8
-62	8.05	60.2
-60	6.57	57.4
-59	6.49	62.2
-58	5.55	61.5
-56	3.69	58.2
-54	3.46	58.1
-53	3.02	56.8
-52	2.56	54.6
-50	2.09	58.3
-49	1.6	54.3
-48	1.73	55.4
-46	1.44	53.7
-44	1.18	50.8
-40	8.35×10^{7}	47.1
-35	5.14	41.9
-30	3.46	35.1
-24	2.46	27.4
-20	2.02	22.5
-9	1.54	11.8
0	1.27	7.98
10	1.12	6.21
19	8.9×10^{6}	
24	7.55	5.43

PART TWO, FIGURE 14

9 wt%

Temp. (°C)	G' (dyn/cm^2)	tan δ x100
27.8	4.26×10^9	12.5
30.0	3.73	13.6
36.8	2.71	17.4
47.0	2.15	24.8
55.0	1.29	25.8
63.5	2.88×10^8	24.9
68.0		23.8

24 wt%

Temp. (°C)	G' (dyn/cm^2)	tan δ x100
-77.0	1.81×10^{10}	8.09
-74.0	1.48	11.55
-71.0		14.35
-69.0	1.20	14.8
-66.0		17.22
-63.5		17.95
-62.6	9.11×10^9	19.4
-60.0	6.97	22.6
-58.4	6.89	21.8
-58.2	6.67	23.9
-55.7		20.36
-55.0	5.84	22.0
-52.0		23.2
-50.0	4.82	23.4
-47.2		24.16
-44.4		25.77
-41.7	2.34	27.4
-37.5	1.71	31.26
-37.2	1.48	31.8
-33.9	1.23	34.59
-30.9	8.73×10^8	39.4
-30.7	8.88	37.6
-27.3	5.3	43.32
-23.5	3.95	43.8
-23.3	3.85	43.7
-19.5	2.59	42.24
-17.0	1.97	42.9

24 wt% (Cont.)

Temp. (°C)	G' (dyn/cm^2)	tan δ x100
-15.0	1.61×10^8	38.96
-13.6	1.42	38.17
-10.6	1.10	34.4
-8.2	1.01	28.8
-0.5	7.7×10^7	19.8
11.0	6.83	12.04
17.2	6.07	10.1
24.0	4.94	7.52
28.2	3.52	5.96

PART TWO, FIGURE 14 (CONT.)

42 wt%

Temp. (°C)	G' (dyn/cm^2)	tan δ x100
-155	7.22×10^9	1.14
-130	6.56	3.45
-110	5.74	7.13
-100	5.15	10.18
-95	4.42	11.75
-92	4.20	13.6
-88	3.63	15.7
-80	3.12	21.7
-70	2.12	30.2
-63	1.44	38.1
-60	1.12	41.0
-55	7.84×10^8	46.5
-52	5.27	48.9
-50	4.53	49.8
-48	3.99	55.3
-46	3.3	55.2
-44	3.01	55.7
-40	1.72	60.7
-39	1.64	58.0
-36	1.19	60.8
-34	9.4×10^7	62.0
-32	9.38	61.4
-30	5.97	60.3
-27	4.28	58.7
-25	3.2	56.9
-23	2.77	53.2
-20	1.83	50.6
-17	1.38	44.0
-13	1.05	38.2
-10	7.7×10^6	36.8
-7	7.55	28.8
-4	6.73	25.3
0	5.42	21.9
5	5.38	15.4
8	5.05	13.7
16	4.5	10.9
20	4.0	10.6
24	3.27	11.0

PART TWO, FIGURE 15

Plasticiser	Concentration (wt%)	T_g (°C)
Water	0	68 *
	3.4	51 *
	7.8	42 *
	17.0	33 *
	21.0	28 *
	25.0	24
FA	10.0	37
	23.0	-2
	41.0	-62
EG	14.0	32
	23.0	9
	46.0	-52

* Determined by DSC

PART TWO, FIGURE 16

For 25 wt% Water, see Figure 11

23 wt% FA , see Figure 12

23 wt% EG , see Figure 13

24 wt% GL , see Figure 14

PART TWO, FIGURE 17

For 41 wt% FA , see Figure 12

46 wt% EG , see Figure 13

42 wt% GL , see Figure 14

PART TWO, FIGURE 18

12 wt%			22 wt%		
Temp. (°C)	G' (dyn/cm^2)	tan δ x100	Temp. (°C)	G' (dyn/cm^2)	tan δ x100
-91.5	1.74×10^{10}	2.95	-140	1.69×10^{10}	0.89
-71.0	1.63	3.27	-120	1.62	1.52
-58.0	1.56	3.70	-100	1.53	2.66
-50.0	1.44	4.02	-79	1.40	3.47
-41.0	1.3	4.42	-70	1.23	3.95
-35.0	1.22	4.46	-68		4.23
-30.0	1.16	4.79	-64		4.42
-20.0	1.03	5.01	-60	1.12	4.94
-10.0	8.78×10^9	5.54	-58		4.84
-6.0		5.75	-54		4.97
0.0		5.74	-51	9.79×10^9	4.53
2.5		5.83	-50		5.02
5.0	6.77	5.96	-47		5.04
8.5		5.66	-46		4.78
12.0	6.27	5.74	-44		4.71
16.0		5.85	-42		5.21
20.0	5.69	6.17	-40	8.79	5.31
26.0		6.55	-36		6.38
30.0	5.54	6.63	-34		6.33
34.0		6.67	-32		6.41
36.0		7.47	-30	6.61	6.38
40.0	4.69	8.04	-28		6.56
45.0		8.56	-26		7.10
49.0		9.01	-24		7.34
51.0		9.09	-20	5.35	7.56
53.0		8.28	-16		8.07
55.0		9.02	-10	3.91	8.83
57.0		8.26	-6		9.30
60.0		9.42	-2		10.5
63.0		9.92	0	2.15	12.0
66.0		11.2	3		12.7
68.0		11.8	6		13.3
72.0		13.3	10	1.61	14.9
74.0		14.5	15	1.33	18.3
77.0	3.55	13.0	20	9.54×10^8	22.6
80.0		13.3	25	7.21	27.7
83.0		13.3	27	6.47	28.7
85.0		12.5	29	6.12	30.0
87.0		12.4	31	6.03	31.1
90.0		12.6	33	5.60	31.4
93.0		12.0	37	4.83	32.2
			40	4.19	33.3
			42	3.93	32.4

PART TWO, FIGURE 18 (CONT.)

22 wt% (Cont.)

Temp. (°C)	G' (dyn/cm^2)	tan δ x100
44	3.67×10^8	33.6
46	3.31	33.4
48	3.33	31.6
50	3.05	31.4
56	2.90	28.4
60	2.85	26.8
66	2.58	24.6
70	2.50	23.3

31 wt%

Temp. (°C)	G' (dyn/cm^2)	tan δ x100
-80	6.07×10^9	6.81
-70	5.47	8.85
-60	5.03	10.6
-54		11.3
-52		12.3
-50	4.40	12.6
-47		14.4
-43		16.9
-40	3,56	19.2
-34	3.60	27.9
-30	3.02	34.1
-28	2.88	38.4
-26	2.70	39.7
-24	2.61	46.7
-22	2.31	47.8
-20	2.23	55.5
-16	2.22	60.9
-12	1.35	63.3
-10	1.10	60.3
-8	1.15	57.6
-6	1.13	56.2
-5	1.09	50.8
-2	1.11	49.7
0	1.42	49.1
1	9.14×10^8	52.6
2	1.03×10^9	
3	7.33×10^8	
4	6.71	
5	7.44	
6	6.65	
7	6.13	
10	4.72	47.2
15	2.55	
19	1.48	
20	9.99×10^7	
21	6.62	
23	2.99	
25	1.93	

PART TWO, FIGURE 19

23 wt% FA			24 wt% EG		
Temp. (°C)	G' (dyn/cm^2)	tan δ x100	Temp. (°C)	G' (dyn/cm^2)	tan δ x100
24	7.76×10^9	12.5	8	1.23×10^{10}	6.16
30	5.94	13.7	12		6.42
40	4.40	17.1	20	1.07	4.98
43	4.05	18.9	26		5.99
45	3.75	19.8	30	9.42×10^9	5.53
48	3.22	22.4	32		7.17
50	2.98	23.9	36		8.44
53	2.58	25.5	38		9.21
54	2.41	27.3	40	7.78	9.39
55	2.38	28.6	42		10.7
58	1.91	30.2	44		11.6
61	1.75	32.3	46		12.2
63	1.62	32.9	48		12.9
65	1.50	34.7	50	6.03	13.3
67	1.47	35.0	52		15.1
70	1.27	36.8	54	5.35	15.9
73	1.24	39.1	58	4.85	18.3
75	1.07	41.0	60	4.48	19.3
76	1.11	42.4	64	4.01	20.2
77	1.00	44.3	66	3.76	20.7
79	9.21×10^8	45.6	70	2.97	25.7
81	8.70	48.8	75	2.89	28.1
84	7.60	52.8	80	2.43	33.0
85	7.11	49.1	90	1.46	38.5
86	7.10	53.5	95	1.15	43.3
89	5.65	51.3	100	8.4×10^8	46.9
90	5.53	49.0	105	5.45	53.3
93	4.54	47.3	108	4.53	57.2
95	4.04	46.8	112	3.44	55.6
98	3.44	46.5	114	2.75	54.6
100	3.17	46.0	117	2.38	54.8
102	2.69	45.3	120	2.01	54.3
105	2.23	43.0	122	1.66	53.3
108	2.01	44.4	125	1.32	53.8
110	1.90	44.0	128	1.09	53.3
112	1.74	42.2	130	8.83×10^7	51.9
			132	7.65	50.8
			134	7.5	
			138	5.31	
			140	4.83	
			142	4.41	
			145	3.58	
			148	2.74	
			150	2.52	

* For 25 wt% Water, see Figure 18

PART TWO, FIGURE 20

25 wt% Water			21 wt% FA		
Temp. (°C)	G' (dyn/cm^2)	tan δ x100	Temp. (°C)	G' (dyn/cm^2)	tan δ x100
-70	1.75×10^{10}	5.79	-50	2.21×10^{10}	7.11
-65		6.05	-40	1.97	8.04
-61	1.61	7.39	-30	1.59	9.55
-55	1.43	7.37	-20	1.37	12.41
-50	1.26	7.21	-10	1.06	15.19
-47		8.56	0	8.65×10^{9}	22.56
-44		9.36	10	6.63	28.8
-42		10.17	18	3.72	40.09
-40	1.09	11.77	24	1.85	52.4
-35	1.14	11.68	28	1.28	56.45
-30	9.02×10^{9}	12.63	32	7.66×10^{8}	59.4
-27		14.64	36	4.25	65.4
-24		16.74	38	3.08	66.7
-22		17.41	40	2.94	70.6
-20	6.54	19.17	42	2.02	62.6
-18		20.04	44	1.21	64.2
-16		20.25	48	5.55×10^{7}	60.2
-12		21.4			
-10	4.70	24.1			
-5	3.46	27.9			
0	2.32	32.7			
55	1.95	34.9			
10	1.42	42.0			
12	1.04	47.0			
15	8.07×10^{8}	54.1			
17	5.68	59.4			
19	4.24	62.9			
22	1.17	61.1			

PART TWO, FIGURE 20 (CONT.)

22 wt% EG			24 wt% GL		
Temp. (°C)	G' (dyn/cm^2)	tan δ x100	Temp. (°C)	G' (dyn/cm^2)	tan δ x100
-35		7.25	-60	1.62×10^{10}	6.05
-25		7.15	-50	1.50	6.16
-15		9.49	-45		5.87
-10	2.2×10^{10}	10.3	-40	1.33	5.59
-5		11.86	-38		5.78
0	1.62	12.78	-35		6.59
5		17.67	-33		5.89
10	1.11	20.28	-30	1.17	6.17
15	7.58×10^{9}	25.49	-28		5.91
20	5.01	32.47	-26		6.22
24	3.10	32.62	-24		6.19
27	2.46	37.86	-22		6.72
30	2.07	41.84	-20	1.05	6.67
32	1.72	45.37	-18		7.1
35	1.24	48.56	-16		6.96
38	1.01	48.94	-14		7.22
40	8.60×10^{8}	47.83	-12		7.12
41	8.0	48.83	-10	8.69×10^{9}	8.97
43	6.24	47.4	-8		6.23
45	6.42	50.19	-6		6.42
49	4.66	50.02	-4		6.57
51	4.25	54.59	-2		6.64
53	3.69	56.39	0	1.03×10^{10}	6.74
55	2.75	58.15	2		7.04
60	1.98	58.2	4		7.29
64	1.51	62.92	6		7.15
67	1.38	62.77	10	9.29×10^{9}	7.95
70	1.05	62.56	20	8.30	10.06
72	8.40×10^{7}	62.29	30	6.43	14.54
75	7.66	61.95	35	5.47	17.63
77	6.70	60.93	40	4.79	22.51
80	4.27	57.02	42	3.91	26.99
84	3.60	53.13	70	1.03×10^{7}	39.3
			73	7.51×10^{6}	36.3
			76	6.46	26.6
			78	4.72	20.2
			80	4.53	16.5
			84	3.68	13.5
			88	3.55	11.9
			90	3.43	10.3
			93	3.33	10.3

PART TWO, FIGURE 21

43 wt%

For 24 wt%, see Figure 20

Temp. (°C)	G' (dyn/cm^2)	tan δ x100
-85		7.18
-80	8.32×10^9	8.09
-75		9.90
-70	6.38	11.9
-68		12.6
-66		13.5
-64		13.7
-60	5.09	14.8
-58		15.7
-55		15.5
-53		16.0
-50	3.75	15.9
-48		16.2
-45		15.6
-42		15.8
-40	2.40	16.8
-38		16.3
-35		17.4
-32		18.8
-30	1.56	20.7
-26	1.15	24.9
-21	7.26×10^8	34.2
-15	4.54	48.9
-10	2.52	
-8	1.82	
-5	1.02	
-3	4.91×10^7	
0	4.8	
2	3.2	59.7
4	2.01	51.7
5	1.75	47.1
8	7.46×10^6	34.6
10	7.76	28.5
12	5.82	23.0
14	4.69	16.9
16	3.38	14.6
18	3.12	8.86
20	2.34	6.22
22	2.38	4.87
25	1.92	2.89

PART TWO, FIGURE 22

DMDAAC - 25 wt% Water

Temp. (°C)	G' (dyn/cm^2)	tan δ x100
-150		1.55
-145		1.72
-140		1.98
-135		2.24
-133		2.25
-130	1.77x10^{10}	2.41
-128		2.48
-126		2.48
-123		2.93
-120		3.03
-118		2.77
-115	1.77	3.11
-112		3.22
-108		3.59
-106		3.91
-103		4.02
-100	1.55	4.7
-98		4.75
-96		5.03
-95		4.49
-92		4.94
-90	1.46	4.81
-88		5.48
-86		5.71
-84		6.04
-82		7.00
-80	1.29	6.27
-78		6.55
-76	1.24	6.95
-74		7.7
-72		7.0
-70	1.18	7.21
-68		6.54
-66	1.02	6.87
-64		6.87
-62		5.73
-60	9.76x10^9	6.12
-58		5.6
-56		5.39
-54		4.81
-52		4.77
-50	7.98	4.95

DMDAAC - 25 wt% Water

Temp. (°C)	G' (dyn/cm^2)	tan δ x100
-48		4.73
-46		4.58
-44		4.50
-42		4.67
-40	6.91x10^9	5.29
-38		5.73
-36		6.19
-34		5.78
-32		6.04
-30		6.81
-28	5.62	6.57
-26		6.56
-24		7.1
-22		7.81
-20	4.82	9.22
-18		10.5
-16		11.85
-14		13.72
-12		15.44
-10	3.28	16.86
-6	2.58	21.8
-2	1.75	25.5
0	1.51	28.1
2	1.15	30.7
4	9.19x10^8	32.7
6	8.02	34.6
8	5.25	34.7
10	3.9	34.0
14	2.11	28.3
18	1.25	20.6
24	5.67x10^7	11.4

For AMBTAC - 25Wt% Water, see Figure 20

For AMPS - 22 wt% Water, see Figure 18

PART TWO, FIGURE 23

For DMDAAC - 24 wt% FA, see Figure 12

AMBTAC - 21 wt% FA, see Figure 20

AMPS - 23 wt% FA, see Figure 19

PART TWO, FIGURE 24

For DMDAAC - 23 wt% EG, see Figure 13

AMBTAC - 22 wt% EG, see Figure 20

AMPS - 24 wt% EG, see Figure 19

PART TWO, FIGURE 25

For DMDAAC - 42 wt% GL, see Figure 14

AMBTAC - 43 wt% GL, see Figure 21

AMPS - 40 wt% GL, see NEXT PAGE

PNaA - 55 wt% GL, see M. King's Thesis

PART TWO, FIGURE 25 (CONT.)

AMPS - 40 wt% GL

Temp, (°C)	G' (dyn/cm^2)	tan δ x100
-46	1.66×10^{10}	5.7
-40	1.51	6.7
-30	1.27	9.0
-20	1.06	10.8
-12	8.61×10^{9}	12.86
0	6.4	12.6
10	4.76	11.6
23	2.34	24.2
30	1.58	32.7
36	9.79×10^{8}	44.0
40	6.72	56.6
43	5.17	68.4
44	4.41	60.5
50	2.29	65.0
52	1.77	
56	1.54	
60	1.09	61.8
64	9.38×10^{7}	
70	6.38	53.1
80	5.23	49.6
86	4.68	41.6
90	4.28	42.0

CONTRIBUTIONS TO ORIGINAL KNOWLEDGE

The important findings of the present investigation are summarized at the conclusion of each part of this thesis, and are briefly listed below.

This is the first extensive investigation of the viscoelastic properties and supermolecular structure of "Nafions". It is found that:

(a) The material behaves only in some respects like other ionomers, such as the ethylene or styrene analogues. The ions in "Nafion" are clustered, and the clustering is affected by degradation.

(b) The glass transition of the ionic regions may be lower than that of the matrix at least in the presence of water. This appears to be unique to "Nafion", since it has not been encountered in other ionomers.

(c) The diffusion coefficient for water, and the thermal expansion coefficient, are much higher than those for any other polymers. This may be due to an unusual packing effect.

(d) The glass transition temperature of the polyelectrolytes studied depends on the type of ion, but not on the ionic environment. It is again found that, as in many other ion-containing polymers, the coulomb forces largely determine the glass transition temperature.

(e) Plasticization greatly improves the mechanical properties of these polyelectrolytes in the solid state by making them much tougher. Water has a plasticization effect on these polyelectrolytes which differs greatly from other plasticizers. Also, the loss of water from the polymer is easier than that of other plasticizers.

SUGGESTIONS FOR FURTHER WORK

The understanding of the ion clustering in ion-containing polymers is the main goal of the research dealing with this new class of materials. Any investigation which can contribute to an unambiguous understanding of the formation, structure and stability of ion clusters is therefore of great importance.

"Nafion" is a novel material which is being used increasingly in many chemical processes relating to the reduction of both pollution and energy costs. Because of the increasing importance of these two aspects, i.e. pollution and energy cost, it is expected that the number of uses of "Nafion" will increase rapidly in the next few years, and that its properties will need to be exhaustively documented. In particular, new uses must be anticipated, so that properties which are of secondary importance now but which may be of importance in future uses, will also be known.

The considerations above indicate that a very large amount of work has yet to be done on these materials and a complete proposal is beyond the scope of this thesis. Thus only the most important aspects will be considered.

(a) It is clear that stress relaxation studies on "Nafion"-H with water content less than 0.5 H_2O/SO_3H are required, so that the critical water content at which time-temperature superposition begins to fail can be established.

(b) Also, further detailed work is required for an unambiguous

identification of the glass transition phenomena. The α relaxation of "Nafion"-H observed in the present study has been ascribed to the glass transition of the matrix, and is observed to shift to much higher temperatures upon complete neutralization. There is undoubtedly a need to investigate this relaxation as a function of ion concentration.

(c) Stress relaxation studies on samples containing various ion concentration are also desirable, since the critical ion concentration for ion clustering can be determined from these studies. The dependence of stress relaxation on ion concentration also requires further study. Since it is difficult to prepare partially neutralised samples of "Nafion" which are homogenous, the ion concentration is best varied by changing the equivalent weight. The molecular weight dependence of stress relaxation therefore needs to be established. Establishing the dependence of the flow properties on molecular weight is particularly important, since this should increase the understanding of the disappearance of the second mechanism at temperatures above 180°C, i.e. in the flow region.

(d) The x-ray diffraction method is a powerful tool for investigating ion aggregation. The equivalent weight dependence of ion clustering could be examined by this technique, but the crystallinity of the PTFE portion may interfere for extremely high equivalent weight samples.

(e) It is found that ion clustering in "Nafion" is affected during degradation. For a better understanding of ion clustering, it may be worthwhile to investigate the degraded samples. Since the dynamic mechanical study of degraded samples was only performed below room temperature, it is reasonable to study the behavior from room temperature up to the glass transition temperatures.

(f) It is seen from Fig. 10 of Part One that "Nafion"-H shows rubberlike behavior on degradation. Stress relaxation studies on samples with varying degrees of degradation could furnish considerable information on the thermal stability of the matrix and the ion clusters.

(g) Again, some dielectric relaxation studies of the degraded samples should be done to help in understanding the unusual dielectric results obtained for the un-degraded samples.

(h) The "Nafion" precusor (a non-ionic material) is an important material for further study. The distinct effect of ions may be revealed by comparing the properties of "Nafion" (which contains ions) to that of its precusor. Certainly, dynamic mechanical, stress relaxation, dielectric, and x-ray studies would be of value.

(i) In the previous study of plasticized poly(sodium acrylate) it was shown that the ions in this material are clustered. An x-ray study of the supermolecular structures of the three polyelectrolytes, DMDAAC, AMPS and AMBTAC is essential for the understanding of the ion clustering in these ionic polymers.

(j) Some preliminary stress relaxation studies of plasticized DMDAAC have been tried and these show no evidence of any second mechanism in this material. Nevertheless, stress relaxation studies of plasticized AMPS and AMBTAC remain interesting because these two polyelectrolytes differ greatly in structure from DMDAAC.

(k) The dielectric relaxation method is a superior technique for studying brittle samples. It is easy to obtain the activation energy for molecular motion. It would be interesting to study the dielectric behaviour of these polyelectrolytes diluted by plasticizers other than

water, since this study has found that water interacts with the polymers in a different manner than that of other plasticizers in dynamical mechanical studies.

(1) The torsional braid method has been introduced as a dynamic mechanical technique for samples which are difficult to prepare. By employing this technique, un-plasticized DMDAAC could be studied; however, the difficulty of testing un-plasticized AMPS and AMBTAC still remains because of the brittleness of these materials.